

# PULSATING AURORA AND MAGNETIC $P_1(c)$ PULSATIONS

by

Trevor Michael Craven, B.Sc.(Chem.) Melb.Univ.  
B.Sc.(Hons., Phys.) Qld Univ.

This thesis is submitted in fulfilment of  
the requirements of the degree of  
Master of Science

UNIVERSITY OF TASMANIA

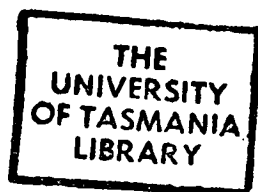
HOBART

October, 1984

*graduating  
1986*



Thesis  
Physics  
M.Sc  
CRAVEN



238744

DECLARATION

Except as stated therein, this thesis contains no material which has been accepted for the award of any other degree or diploma in any university, and that, to the best of my knowledge and belief, the thesis contains no copy or paraphrase of material previously published or written by another person, except when due reference is made in the text of the thesis.

Signed:

A handwritten signature in black ink, appearing to be 'T.M. Craven', written in a cursive style.

T.M. Craven  
September, 1984

## ACKNOWLEDGEMENTS

This completed thesis has been made possible only by the kind assistance of many individuals. Any inaccuracies present are however, the sole responsibility of the author, and result from shooting off the mouth before loading the brain.

Initial thanks must be extended to the Commonwealth Government of Australia for their funding of research in the field of Upper Atmospheric Physics (UAP), via the Antarctic Division branch of the Department of Science and Technology. It is hoped that such provision will be further increased, in order to develop and continue the excellent research effort, that has become a characteristic of the UAP group over many years.

To the Head Office staff of the Antarctic Division for their logistic support in operating expeditions, to the crew members of the Nella Dan for transit to and from Macquarie Island, and to my fellow 1983 expeditioners I offer my heartfelt gratitude for your assistance, companionship, and support, all of which made my experience a most satisfying and fruitful one.

I am indebted to Dr. Gary Burns (Officer in Charge, UAP, Antarctic Division) for his vast realm of ideas and enthusiastic involvement in all facets of this research. The entire project has been built upon the strong foundations he has laid down in this field, and his encouragement and willingness to assist, has been the major stimulus towards the prompt completion of this thesis.

Particular thanks also to Mr. Chris Eavis (1983 Macquarie Island electronics engineer) for his ability to repair and maintain the multiplicity of instruments required in this program. The volume of data collected is evidence itself of his efficiency in this respect.



Similar praise must be directed at the trade and technical staff, Mr. Henry Weiss (Senior electrical fitter and Mechanic), Mr. Ivan Porteus (Senior diesel mechanic), Mr. Graeme Currie (Radio technical officer), Mr. Peter McLennan (Technical Officer, Meteorology) and Mr. Mark Haste (Carpenter). To them, and other fellow expeditioners I am eternally grateful also for the lifelong bonds of friendship that were so easily established.

My meagre computing "expertise" proved no barrier to the diligence and excellent guidance of Mr. Howard Burton (Computer Systems Operator, Antarctic Division), who not only wrote the "EARS" (Auroral listening) data collection programs, but also proved that "action at a distance" is alive and well with his deadly accurate troubleshooting suggestions from Head Office. Howard and Gary also braved a week of dreaded seasickness to see my programs safely resident on the Macquarie Island system. Mr. Stanley Malachowski (1983 Davis UAP expeditioner) managed somehow to disentangle me from my DO loops with no IFS or BUTS, and I gratefully acknowledge his wizardry in helping to rewrite various plotting routines. These gentlemen saved me from becoming another poor innocent victim of this confounded computer age.

To the Bureau of Mineral Resources (BMR) and their representatives at Macquarie, Mr. Barry Page, and Miss Peta Kelsey, thank you for access to the magnetograms and assistance in their interpretation and reduction. I would also not have been able to enjoy my "jollies" around the island were not the laboratory left in such capable hands as those of Barry, Peta and Chris. Thanks also to Mr. Pelham Williams (1984 Davis UAP expeditioner) for his summary of magnetogram quiet day curve effects. I am also indebted to the University of Alaska for use of their coils in obtaining the magnetic micropulsation data for this work.

Dr. P.M. McCullough (Physics Department, University of Tasmania) also interrupted a very busy year of his own research at Parkes Radio Telescope, to offer guidance with this work. Professor Keith Cole (LaTrobe University) too, contributed many thought provoking ideas to me indirectly, via discussions with Dr. Burns.

The manuscript itself is the result of many excellent contributions. The final draft typing was done by Mrs. Betty Golding (Mathematics Department, University of Tasmania) while the initial difficult task of deciphering my scrawl was due to Antarctic Division typists, Moira Beresford, Veronica Dickson, July Hall, Jenny Hinden, Irene Wanless, and Betty Willemer (that's in alphabetical order girls!). Diagrams and figures were very capably handled by the Photographics section through Bob Reeves, Steven Brookes, and Glen Jacobsen, and the Drafting section through John Cox and Werner Bachmeyer. Final copy reductions were handled through the Tasmanian University Printers.

To Mother Nature and her marvellous Macquarie Island and delightful auroras, thank you for the experience.

Permission to present this thesis has been granted by the Antarctic Division via the Director, Mr. Jim Bleasel.

## ABSTRACT

This thesis is the result of a year spent at Macquarie Island (54°30'S, 158°57'E) on the 1983 Australian National Antarctic Research Expedition, collecting data pertaining to pulsating aurora and geomagnetic Pi(c) micropulsations.

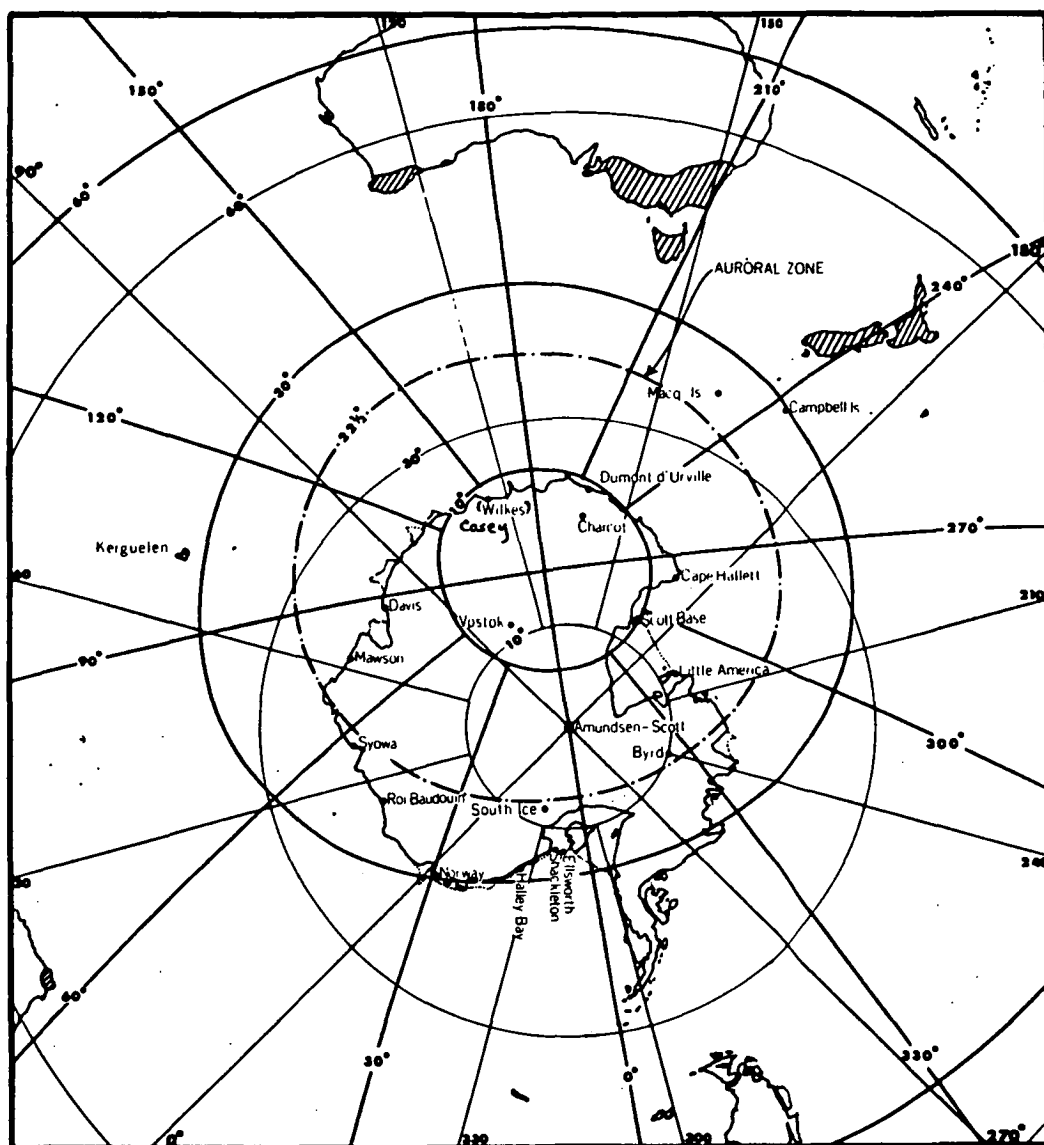
Data was collected with a 0.2s sampling period and stored by an LSI-11 microcomputer on floppy disks for the bulk of the year, then on RL02 hard disk for the final months. Strong peak-to-peak correlations were observed between the optical pulsating aurora, measured at the  $N_2^+$  4278Å band head emission, and the micropulsations. Average time delays were determined to be 0.6s and 0.3s for the D and H Pi(c) micropulsations respectively, trailing the optical fluctuations.

The H component Pi(c) micropulsations will be shown to be consistent with a precipitation induced Hall conductivity enhancement of the westward E-region auroral electrojet during the greater part of this activity. The sign, or phase, of the 4278Å/H micropulsation correlation function was in close agreement with the large scale magnetogram H component perturbation.

The D component Pi(c) have in the past been interpreted as either an E-region Pedersen conductivity induced variation, or a direct field aligned current effect. Their correlation sign, or phase, is shown to be not in accord with the large scale D component magnetograms which are known to be effected by other than E-region currents, namely the field aligned fluxes. The D micropulsations are more frequently correlated at an acceptable level with the optical emission, and their correlations are in general of greater magnitude than those of the H Pi(c).

Experimentally observed lack of a frequency doubling in the micropulsations with respect to the optical trace, occasional phase reversals of the correlations, and the delay sequence, wherein the optical pulses predominantly lead the H micropulsations, which in turn generally lead the D component, can all be reasonably explained in terms of the above theories.

A model has been developed, involving rotations of the total ionospheric electric field, which makes basic predictions concerning the phases of the correlations, and the lead-lag relationship between the micropulsation components. These predictions are borne out by the data set, specifically during phase reversals, and strongly indicate that the H and D Pi(c) micropulsations result from precipitation induced conductivity fluctuations in E-region current systems.



Relative location of Macquarie Island with respect to the auroral zone (courtesy Bond, Antarctic Division, internal publication).

CONTENTS

Title Page	<i>i</i>
Declaration	<i>ii</i>
Acknowledgements	<i>iii</i>
Abstract	<i>vi</i>
Relative location of Macquarie Island	<i>viii</i>
Table of Contents	<i>ix</i>
INTRODUCTION	1
1. <u>REVIEW OF LITERATURE</u>	
1.1 Introduction	6
1.2 Geomagnetic Pulsations	6
1.3 Pulsating Aurora	14
1.4 E-Region Currents	20
1.5 Incoherent Backscatter Radar	25
1.6 Existing Theories	31
2. <u>INSTRUMENTATION</u>	
2.1 The Wide Angle Photometer	41
2.2 The Micropulsation Coils	48
2.3 Data Collection - The LSI-II Microcomputer	54
2.4 Subsidiary Instrumentation	60
3. <u>PULSATING AURORA AND GEOMAGNETIC FIELD MICROPULSATIONS</u>	
3.1 Introduction	63
3.2 The Data Set	64
3.3 Mathematics of the Correlations	79
3.4 Correlation Analysis	103
3.5 Comparison with Magnetic Bays	119
3.6 Summary of Results	137

4.	<u>EXPERIMENTAL OBSERVATIONS AND THE <math>P_1(c)</math> MICROPULSATION THEORIES</u>	
4.1	Introduction	139
4.2	E-Region Conductivity Theories	140
4.3	Field-Aligned Current Theories	157
4.4	Current Models for Phase Reversals	178
4.5	Current Models and Other Observations	200
4.6	Conclusions and Future Research	208
	Appendix	210
	References	216

## INTRODUCTION

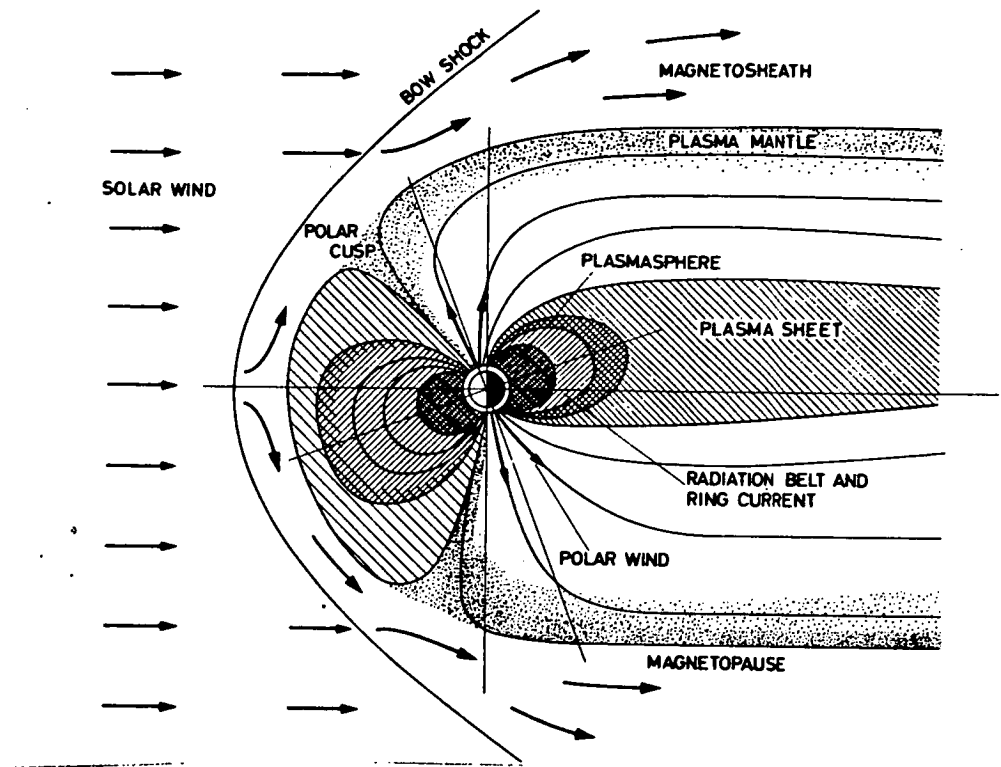
In essence, the Earth's intrinsic magnetic field configuration is that of an ordinary dipole, situated near its centre, and oriented slightly off-axis (by about  $15^\circ$ ). This field is generated predominantly by turbulent current flow within the Earth's molten iron core regions.

Continuous expansion of the hot solar corona produces a steady flow of charged particles, the solar wind, past the Earth. It suffers deflection by the dipole field generating a current sheet which effectively cancels the geomagnetic field on the windward side, compresses and enhances it on the earthward side (Ratcliffe, 1972). Called the magnetopause, this current sheet, situated at a distance of approximately ten Earth radii ( $10R_E$ ), forms a boundary confining the Earth's field within a cometshaped cavity known as the magnetosphere. Due to the supersonic nature of the solar wind, a bow shock is formed approximately  $4R_E$  sunward of the magnetopause, and the magnetosheath contained therein is a region of high magnetic turbulence (see Figure 1).

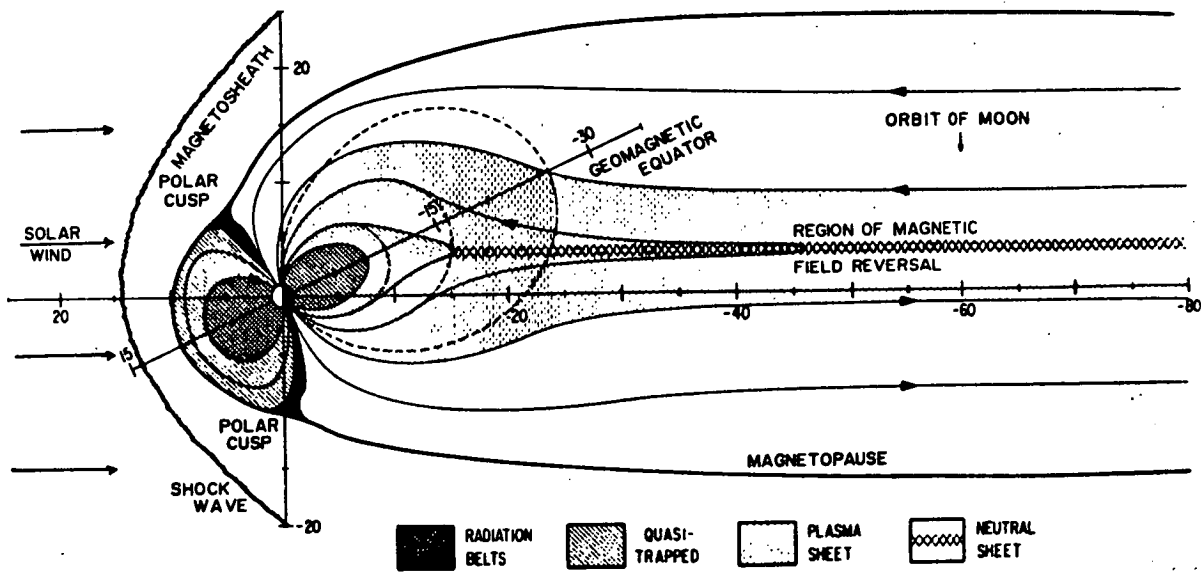
On the nightside the tangential force exerted by the solar wind streaming past, carries the Earth's magnetic field to distances in excess of  $1000R_E$  (Walker et al, 1975). Field lines above approximately  $78^\circ$  geomagnetic latitude in the noon meridian, and  $69^\circ$  in the midnight meridian, are swept away into the geomagnetic tail field (Fairfield, 1970). Oppositely directed lines of force from the two hemispheres are separated in the tail by the neutral, or current sheet, either side of which, a region of warm plasma, the plasma sheet, extends for several  $R_E$ .

On the sunward hemisphere, the region between where the geomagnetic field lines are closed, or drawn across the Earth and out into the tail, is known as the polar or magnetospheric cusp. It is here that the solar wind particles, having penetrated the shock front, may enter the

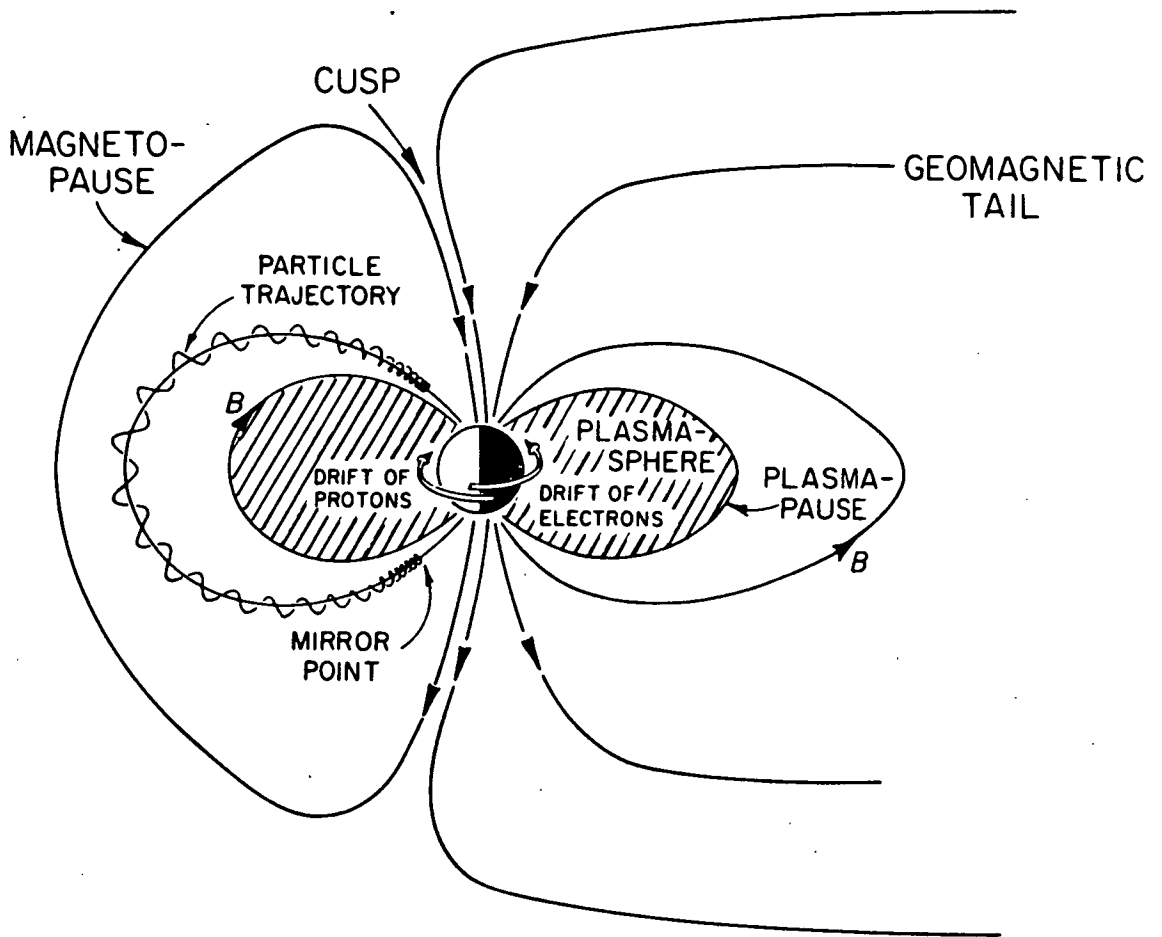




(a) from Bosenbaur et al., 1975



(b) from Ness, 1969



(c) from Kennel et al., 1982

**Figure 1** Schematic representations of the regions of the magnetosphere depicting some of the particle processes involved:

- (a) general flow of particles from the solar wind, and the magnetospheric regions
- (b) summary view of the magnetosphere and geomagnetic tail as deduced from spacecraft measurements
- (c) three components of trapped particle motion.

magnetosphere, or be convected towards the nightside of the Earth through the plasma sheet. The charged particles can then be guided down magnetic field lines towards the ionosphere.

Due to the low collision cross-sections existing at great heights on the field lines, the charged particles become easily trapped, and mirror back and forth between hemispheres with bounce periods of the order of seconds. This helical motion is accompanied by a magnetic field gradient drift which carries protons westward, electrons eastward, with circumnavigation times of the order of several hours, yielding an overall westward ring current (Ratcliffe, 1972).

Collision frequencies increase in the low altitude regions near the mirror points, so particles with small enough pitch angles (defined as the angle between the particles velocity vector as it crosses the geomagnetic equator, and the direction of the magnetic field vector) can result in the deposition of energy into the polar regions. Incoming electrons with energies of 10 keV or more, penetrate to altitudes around 100 km, where they rapidly energize multitudes of atmospheric oxygen atoms and nitrogen molecule-ions. De-excitation of these, results in the emission of visible light, known as the optical aurora. This occurs predominantly in a band called the auroral zone surrounding the geomagnetic poles at approximately  $67^{\circ}$  invariant latitude, lying near the feet of the field lines that are closed, and those that stream deep into the tail (Johnstone, 1978).

Such deposition of energy occurs with increasing probability during magnetically disturbed periods, accompanied by equatorward expansion of the auroral oval. These periods of disturbance are often produced by activity on the sun, such as solar flares, and prominence or filament eruption, whereby the solar wind flux is suddenly enhanced. The impact

of this increased solar wind on the magnetopause can typically compress it to within  $6R_E$ , resulting in an increased magnetic field at the Earth's surface by tens of gammas (1 gamma =  $10^{-9}$  tesla), constituting the "initial phase" of the storm (McPherron, 1970).

Within a few hours of this sudden commencement, the increased populations of protons and electrons enhance the normal ring current, causing depression of the field at the Earth's surface by hundreds of gammas. This "main phase" of the storm is followed by a "recovery phase" that may last one to two days, as the increased charged particle concentrations decay gradually.

Superimposed on this main magnetic storm may also be found several polar substorms, and auroral substorms. Polar substorms are considered to be a result of an increase in the quiet time polar current system.

Auroral substorms have similar development characteristics to the main magnetic storms, but with typical duration times of a few hours. Complexity is often introduced into the interpretation of their magnetic signature, by the superposition of several such substorms. The auroral substorm is a consequence of westward currents in the E-region ionosphere, flowing at heights near 100 km around the auroral oval (Rostoker, 1972).

This thesis is concerned with two particular aspects of the auroral substorm and the close correlation that exists between them - the geomagnetic field effect known as micropulsations, and the optical auroral intensity variations resulting from associated electron precipitation. An attempt is made to reconcile observations of these phenomena with the various mechanisms proposed for their generation.

# CHAPTER 1

## REVIEW OF LITERATURE

### 1.1 INTRODUCTION

This chapter reviews the vast body of literature that has sprung up concerning the relationship between simultaneous rapid variations in the geomagnetic field, and the auroral luminosity. The concurrent temporal and spatial incidence of these phenomena has led to various proposals concerning their origins and interdependence.

Auroral intensity fluctuations have been found to exhibit an extremely close correspondence with a particular type of geomagnetic field fluctuation known as Pi(c) (see Section 1.2). The general characteristics of these phenomena will be described here, together with a discussion of the various proposed theories on the possible generation mechanisms.

The remainder of this thesis, presents experimental evidence obtained from data gathered at Macquarie Island, from October 1982 to early October 1983, and examines how it fits with the theories.

### 1.2 GEOMAGNETIC MICROPULSATIONS

During an auroral substorm various large scale magnetic effects occur due to intensification of currents (known as the auroral electrojets) flowing in the E-region of the Earth's ionosphere. An equivalent current system responsible for these geomagnetic disturbance bays has been proposed by Sugiura and Heppner (1965), involving an eastward electrojet in the pre-midnight sector, and a strong westward electrojet in morning hours (see Figure 1.1).

The formation and intensification of these current systems and their predicted ground effects has been described by Rostoker (1972).

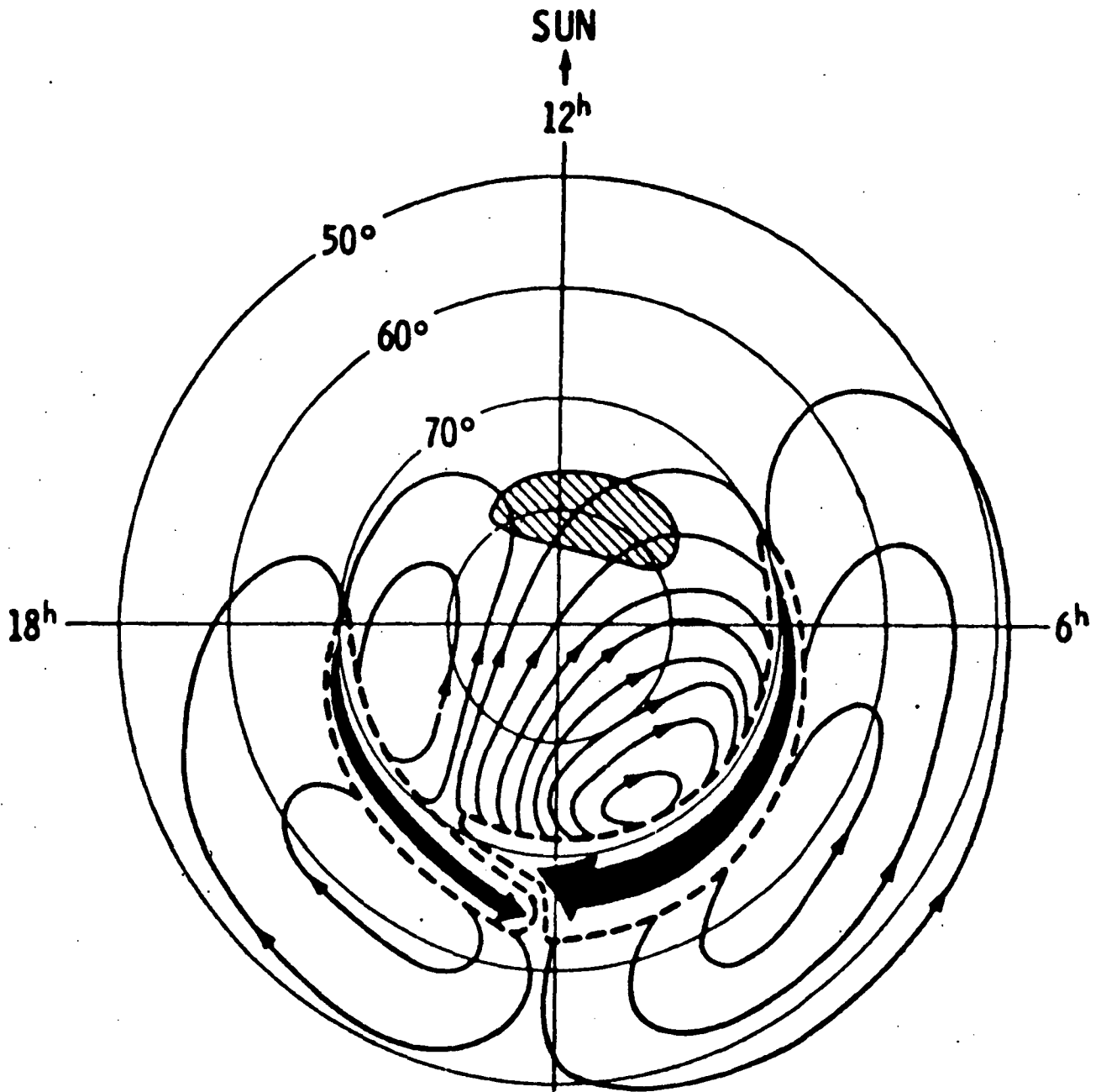


Figure 1.1      Equivalent current system for geomagnetic bays proposed by Sugiura and Heppner (1965) involving a strong eastward electrojet in the pre-midnight sector.

Magnetic bays in the regime of hundreds of gamma intensity result, and take several hours to recover.

Geomagnetic micropulsations, as the name suggests, are small scale fluctuations with amplitudes in the range 0.01 - 10 gamma (only 1 in 10,000 of the main field), with periods from 0.1 - 600 seconds, often superimposed on the larger bay disturbances. They have been divided into two major classes (Jacobs et al., 1964) according to their appearance. Pc are those exhibiting a continuous, regular, pattern, whilst Pi are so designated because of their irregular wave form character.

It is the quasi-sinusoidal Pi oscillations, generally associated with auroral substorm activity involving magnetic bays and optical pulsations (see Section 1.3), which will be of major concern to the present thesis (Reviews: Campbell, 1967, Saito, 1969; Rostoker, 1972; Heacock and Hunsucker, 1981).

Pi activity has been observed to concur in time and space with active aurora, and not generally with the pre-breakup quiescent, homogeneous arcs (Troitskaya, 1961). Heacock and Hunsucker (1981) using hundreds of observations from their Alaskan site records, report that they '... have never observed an instance of a midnight-morning sector substorm onset where the level of Pi activity did not increase at the onset ...'. Figure 1.2 readily depicts this particular relationship.

More recent discoveries have indicated that Pi activity also occurs at the feet of the dayside cleft (or cusp) field lines, and in the dayside sector of the polar cap (Heacock and Hunsucker, 1977b; Heacock and Chao, 1980). A prestorm enhancement of Pi activity with an average lead-time of  $1\frac{1}{2}$  hours has also been determined (Heacock and Chao, 1980).

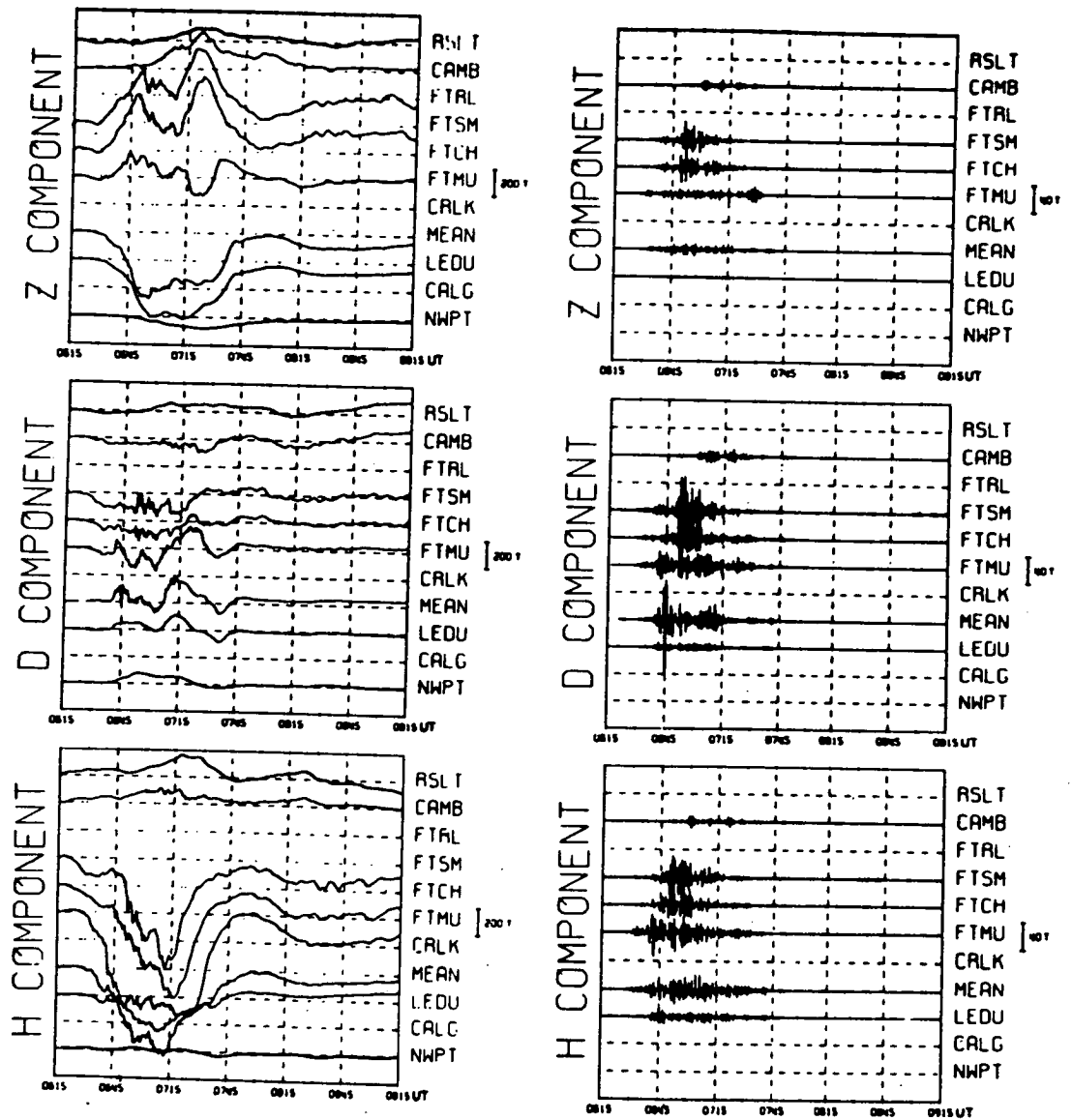


Figure 1.2 Magnetograms (left) and micropulsation records (right) from a latitudinal array of stations in Canada. Good correlation is seen between Pi micropulsations and magnetic bay activity (from Kisabeth and Rostoker, 1971).



These observations suggest that a Pi micropulsation generation mechanism exists that doesn't depend upon a closed field line condition. However, the entire gamut of Pi activity is sufficiently diverse that it may not be due to a single discrete mechanism. Field line closure may in fact be a necessary requisite in some cases.

Classification of Pi micropulsations has seen further subdivision into two spectral ranges, Pi1 with periods from 1-40 seconds, and Pi2 with periods from 40-150 seconds (Jacobs et al., 1964). Good correlation has been noted between Pi1 activity and negative bays in the H (north-south geomagnetic field direction) component of the magnetic field measured at College, Alaska, by Campbell and Matsushita (1962). Using a chain of auroral zone magnetometers, Olson and Rostoker (1975, 1977) observed that maximum Pi2 activity occurs whenever the E-region electrojet is directly overhead a particular site.

Thus, Pi activity appears to be strongly linked to E-region current systems, and Heacock and Hunsucker (1981) report from Alaskan site data that they '... have never observed a single case of large amplitude Pi activity occurring where there was no E-region...' present in the local ionosphere at that time.

From a study of continuous magnetic tape and chart recordings made at College, Heacock (1967a) devised a more useful working classification of Pi micropulsations. He designated as Pi(b), those impulsive broadband bursts of short duration lasting for 1-20 minutes, which have a sharply peaked occurrence distribution, centred around local geomagnetic midnight. These bursts were found to accompany the onset of auroral substorms (see Figure 1.3).

Saito (1969) has shown that whenever a low latitude station witnesses a Pi(b) event, then a substorm has erupted somewhere in the auroral zone. This makes them a viable indicator of substorm onset times (Rostoker, 1972).

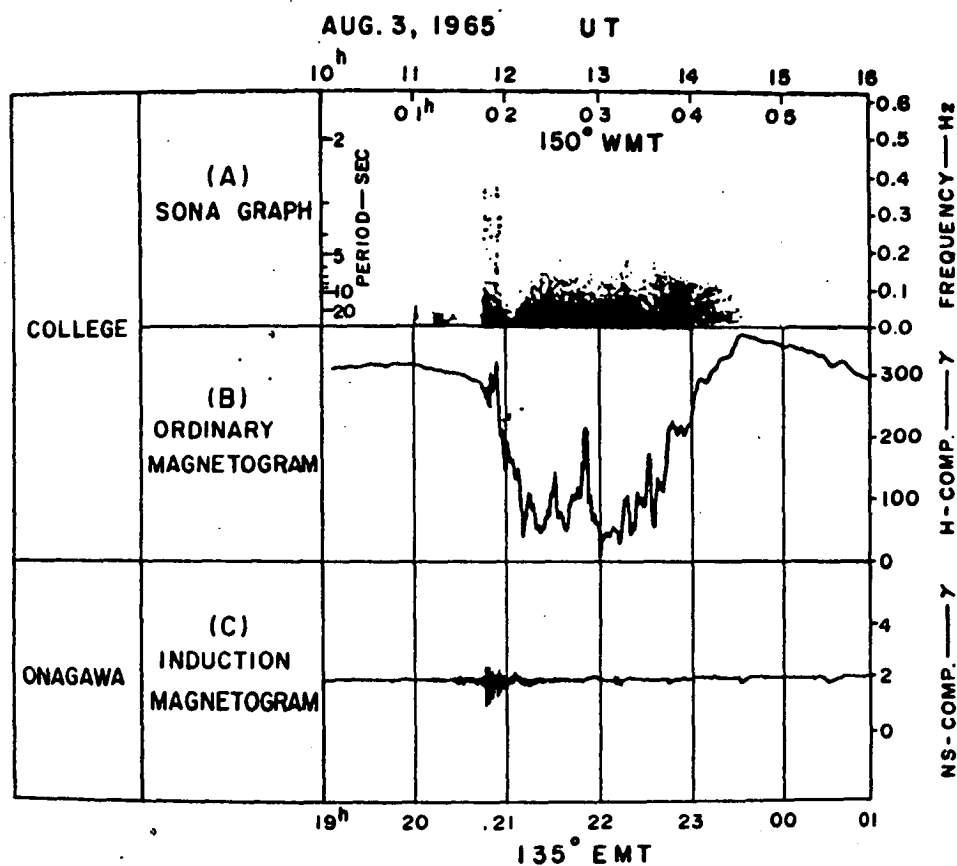


Figure 1.3 Magnetogram and sonagraph data depicting the association of Pi(b) (broadband) micropulsation activity with the magnetic bay commencement, and Pi(c) activity during the recovery phase (from Saito, 1969).

The other form of activity described by Heacock (1967a) displays a '... continuous, non-impulsive character...', and has been labelled Pi(c). These events have a longer duration, up to several hours, and are associated with the recovery phase of the geomagnetic bay (Saito, 1969; Kisabeth and Rostoker, 1971; Rostoker, 1972; Kan and Heacock, 1976). He also found a high correlation between the intensities of Pi(c) activity and the auroral electrojet responsible for the magnetic bay disturbance.

The range of frequencies present in Pi(b) burst spectra usually contain both higher and lower components than in Pi(c) events (Heacock, 1967a). In the auroral zone they exhibit Pi1 and Pi2, whilst at lower latitudes the higher frequencies are not recorded (Saito, 1969). Saito's report further highlights the close association of Pi2 with Pi(b) events, by noting that Pi2 occurs only during the substorm expansive phase, and upon its disappearance the bay commences recovery. The relationship is more firmly established by the fact that Pi(b) and Pi2 both have distinct midnight sector maxima (Heacock, 1967a). Sakurai and Saito (1976) have also found that low latitude Pi2 is simultaneous with the brightening of an arc at the onset of an auroral substorm. Haldoupis et al., (1982) have shown that Pi(b) activity is associated with a region of intense FAC (field aligned current) systems known to be a common feature of the Harang discontinuity (see Section 4.3), an evening-midnight phenomenon.

From College riometer records Parthasarathy and Berkey (1965) showed that Pi(b) events are strongly associated temporally with downcoming bursts of charged particles, whilst the existence of Pi2 at low latitudes is considered as evidence that Pi(b) micropulsations can propagate at large angles to geomagnetic field lines (Tepley et al., 1965).

As mentioned, Pi(b) events are strongly maximized around local geomagnetic midnight and according to Heacock (1967a) tend to be followed by Pi(c) micropulsations. These then persist for several hours until the associated magnetic bay has recovered. This relationship is immediately evident from Figure 1.3. It follows then, that Pi(c) exhibit a broad diurnal distribution with a morning hour peak, in the auroral oval (Heacock, 1967a; Heacock and Hunsucker, 1981). This is coincident with the similarly broad diurnal morning hour peak of the pulsating aurora (Royrvik and Davis, 1977; see Section 1.3), and Pi(c) have been observed simultaneously with auroral luminosity oscillations (review: Campbell, 1978).

Data gathered by Burns (1983) at Macquarie Island often displays peak-to-peak correspondence of auroral fluctuations and micropulsations. His work, which had a faster resolution time, compliments the earlier work of Campbell (1970) who observed that the micropulsations were delayed of the order of 1.3 seconds on average, with respect to the optical variations. Burns found shorter delay times, 0.2 - 0.6 seconds, indicating a close correspondence between the two phenomena at low (ionospheric) altitudes, and this has been confirmed by Oguti et al., (1984).

Subsequent work, which is the subject of this thesis, has gathered together a large volume of data supporting these observations. Excellent correlations (some with magnitude > 0.80) have been determined between the auroral optical emission fluctuations and irregular geomagnetic micropulsations, with periods predominantly in the range 6-20 seconds. Together with the broad morning hour peak in the distribution of these correlations, and their obvious association with geomagnetic bay recovery, the micropulsations involved exhibit the basic characteristics of Pi(c) as described by Heacock (1967a).

### 1.3 PULSATING AURORA

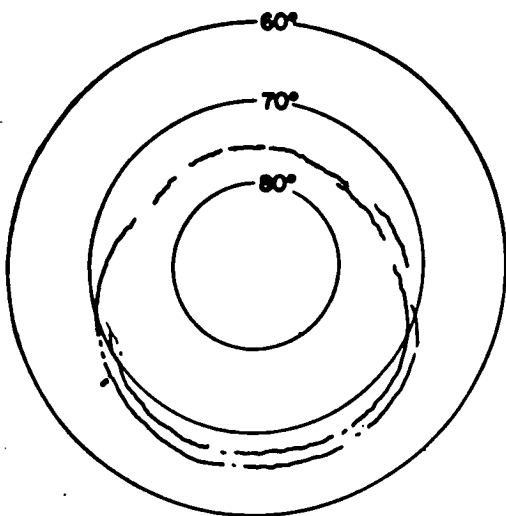
The introduction briefly described the auroral substorm phenomenon. Here it will be examined in closer detail with particular reference to the pulsating auroral forms that actually develop later in the course of the disturbance.

Akasofu (1968) has given excellent discussion on auroral substorm morphology, and the changes that take place in the auroral oval itself. He defines two main phases of the storm. The expansive phase commences with the brightening, or sudden formation, of an auroral arc in the midnight sector of the oval. Rapid spatial motions ensue as the arc bulges poleward and expands longitudinally, with the development of a westward travelling surge in the evening sector. The overhead passage of the surge defines the reversal from a positive to a negative perturbation bay in the large scale H-component magnetic field (Bond, private discussion). This plethora of spectacular activity takes typically 30 minutes to evolve.

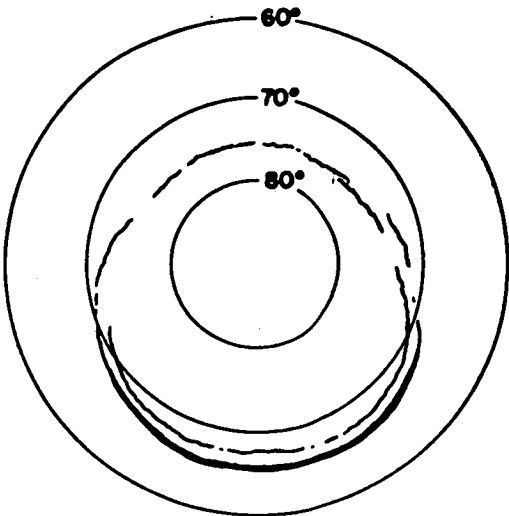
Towards the morning sector the display disintegrates into patches superimposed on a low level background diffuse aurora. These pulsating patches manifest themselves over the next hour or so, as quiet arcs once more re-establish themselves in the midnight sector. This delineates the recovery stage of the substorm, and the entire process, as described by Akasofu, is depicted in Figure 1.4.

Great difficulty can be incurred disentangling the stages of individual auroral substorms, as they tend to repeat, and often overlap during active periods (Akasofu; 1968, Ratcliffe, 1972).

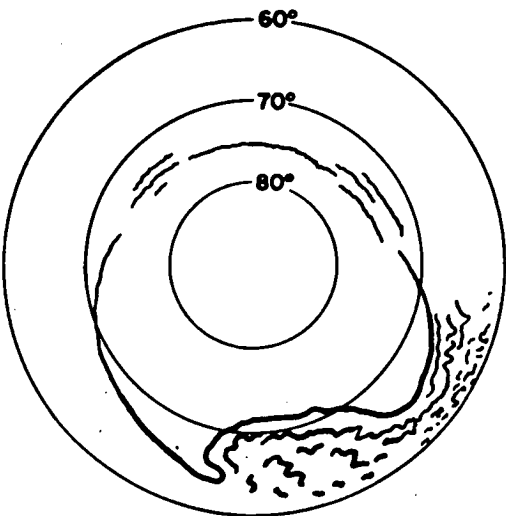
The International Auroral Atlas (1963) identifies a number of different auroral forms with time-dependent intensity fluctuations. Their period can range from fractions of a second to a few minutes,



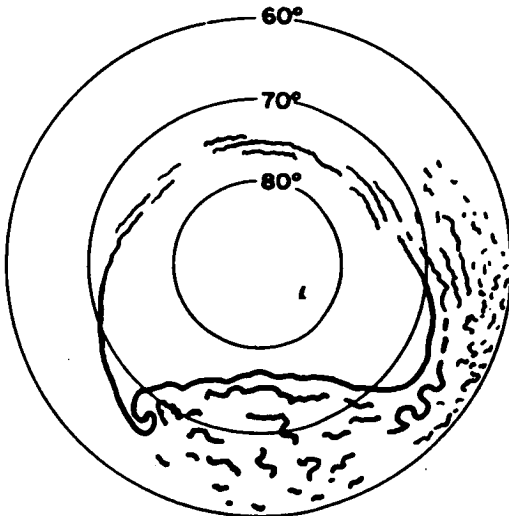
A.  $T=0$



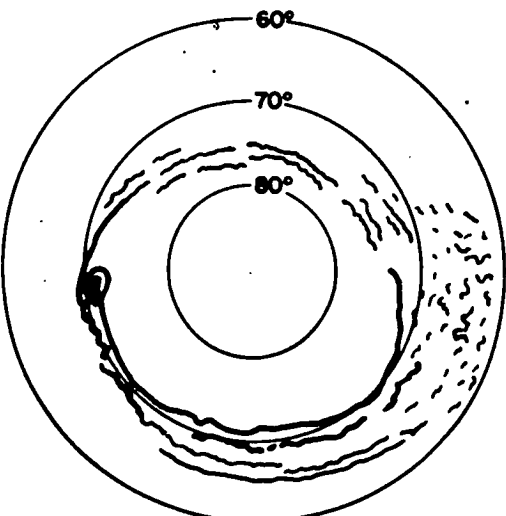
B.  $T=0\sim 5\text{ MIN}$



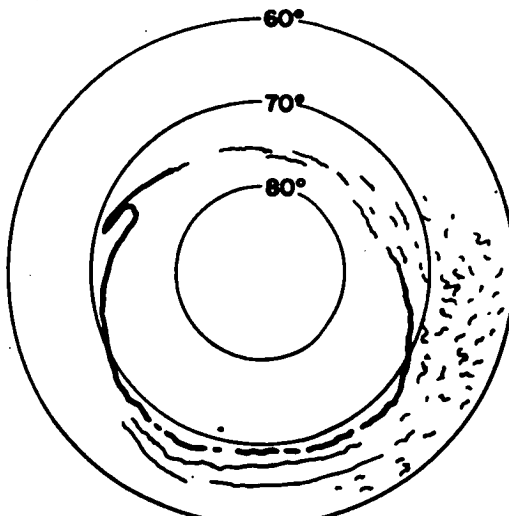
C.  $T=5-10\text{ MIN}$



D.  $T=10-30\text{ MIN}$



E.  $T=30\text{ MIN}-1\text{ HR}$



F.  $T=1-2\text{ HR}$

Figure 1.4 Schematic diagrams for the development of an auroral substorm (from Akasofu, 1968).

and the considerations here will centre largely on the  $P_1$ , pulsating aurora, category.  $P_1$  is there defined as aurora exhibiting a uniform brightness variation throughout the form.

The Macquarie Island instrumentation employs a wide angle photometer,  $30^\circ$  half-beam width (see Section 2.1), with which it is not possible to determine if the form actually brightens coherently. Hence, it was not possible to distinguish  $P_1$  from another form defined as  $P_2$ , called flaming aurora. In this case, surges of luminosity sweep upwards through the form, towards the zenith. This is not considered to be of any particular concern, since  $P_1$  and  $P_2$  may well be the same phenomenon viewed at different angles (Burns, 1983).

Two other forms,  $P_3$  which consists of very rapid flickering, and  $P_4$  known as streaming, will also not be a major problem, as the very nature of the wide angle photometer makes them difficult to detect. They will not show up as appreciable fluctuations, as they might, on a narrow field of view photometer system.

The wide angle nature of the photometer also ensures that physical drift motions of auroral forms will be less of a contaminant than for narrow angle systems. Such drifts are of the order  $100\text{--}1000\text{ ms}^{-1}$ , easterly in the morning, westerly in the evening sector (Royrvik and Davis, 1977; Oguti et al., 1981).

The general term, pulsating aurora, will be used in the above context, to cover the events to be examined in the remainder of this thesis.

Observations have shown that pulsating aurora appear generally at the equatorward edge of the auroral oval (Heppner, 1954, 1958; Cresswell and Davis, 1966), largely in the morning hours (Kvifte and Petterson, 1969; Brekke, 1971), and are associated with the recovery phase of geomagnetic bays (Cresswell and Davis, 1966). The auroral

oval expands equatorwards with increasing geomagnetic activity and the pulsating aurora are then observed at lower latitudes (Brekke, 1971). Pulsations can occur in all auroral forms, and it is found that arcs and arc segments dominate the activity during the evening, whilst patches are the major form in the morning hours (Royrvik and Davis, 1977).

Pulsating aurora are characteristically a low intensity phenomenon, of brightness less than 10 kR, compared with quiescent arcs and brilliant break-up aurora which can approach 100 kR (Johnstone, 1978). Evening sector pulsations are found to be of smaller amplitude in general than those in morning hours (Pemberton and Shepherd, 1975). They generally are superimposed on small intensity background diffuse aurora, with various values being quoted for the total amount of light that is fluctuating, from 10-30% Kvifte and Petterson (1969), 40% Campbell (1970), 70% on a 1 kR background Whalen et al., (1971), and even 100% by Miller and Zeitz (1971).

The light intensity does not vary in a smooth sinusoidal fashion, but appears to alternate rapidly between on/off states with non-uniform delays between successive pulses (Scourfield and Parsons, 1968; Oguti, 1971). Sometimes the switching appears to originate from a point within a patch and then spread out (Johnstone, 1978), and this was also the personal experience of the author, from Macquarie Island observations.

The shapes too may also be extremely varied, and can tend to persist for many pulsations (Cresswell and Davis, 1966), with neighbouring patches often found to be pulsating independently of each other in phase and period (Oguti, 1976). These particular points have proven extremely difficult to incorporate into any physically viable mechanism for their generation. Johnstone (1978)



points out that even in the train of pulsations from a single patch the period may vary, concluding that the mean period is not related geometrically to the magnetosphere, although the bounce period of trapped electrons is comparable to the period of pulsations.

Pulsating aurora are the result of excitation of atmospheric constituents by the electrons impinging on them. Very little contribution is considered to be due to protons or precipitating hydrogen atoms (Eather, 1968; Miller and Zeitz, 1971), though some structured hydrogen atom fluxes have been detected (Smith et al., 1980).

Occurrence of pulsating aurora on the equatorward edge of the auroral oval indicates that they are a closed field line phenomenon. Further evidence that a trapped flux is involved comes from the measurement of electron pitch angle distributions. These are found to contain a loss-cone at the minimum of the pulsation (Whalen et al., 1971; Bryant et al., 1971), and the distribution increases monotonically as the pitch-angle increases (Johnstone, 1978). Television image observations of simultaneous conjugate fluctuations in northern and southern hemispheres offer further conclusive testimony (Belon et al., 1968).

A low altitude for pulsating auroral emissions is suggested from their close association with cosmic noise absorption (Reid, 1967), and X-ray (Scourfield et al., 1970) pulsations, both of which are indicators of high energy fluxes. Triangulation studies have indicated a lower border typically around 80-100 km (Brown et al., 1976) though a higher range 83-140 km with a median altitude of 98 km has been reported (Stenbaek-Nielsen and Hallinan, 1979).

Stenbaek-Nielsen and Hallinan (1979) produced the extremely surprising result that the vertical extent is limited to around 2 km.

This is far shorter than that expected even from theoretical calculations of a monoenergetic uni-directional flux (Rees, 1963). Such a result, though disconcerting, may not be typical of all pulsing forms, as the measurements were carried out on irregular patches, or arc segments of only 10 km width, and a few seconds period. Rocket measurements of Yau et al., (1981) do not support the existence of such thin pulsating structures.

Typical pulsation altitudes tend to be lower than that of the general diffuse background (median altitude near 150 km, Brown et al., 1976), which suggests they are due to precipitation of higher energy electrons, rather than merely a flux increase (Davis, 1978). Not all measurements are in total agreement with this, as Stenbaek-Nielsen and Hallinan (1979) report no height change of emission for on/off states.

An essentially Maxwellian distribution of energies for the precipitating electrons is reported by Bryant et al., (1975)

$$N(E) = AE \exp \left( -E/E_0 \right)$$

with e-folding energy (most probable energy of the distribution)  $E_0$ , hardening by as much as 25% during optical peaks (similarly McEwen et al., 1981a). The distribution tends to diverge from Maxwellian behaviour at energies  $> 20$  keV, the fluxes being somewhat higher than those expected from a Maxwellian (Johnstone, 1978). Doppler line-width measurements have indicated a temperature decrease at the peaks of the auroral pulsations (Hilliard and Shepherd, 1966). Reductions in peak height emission of the order of 15 km have been estimated, and spectral hardening of the precipitating electrons is inferred. Back-scatter radar measured Hall conductivity increases, indicating harder precipitation within the maxima, have been recorded by Senior et al., (1982).

Measured hardening of the spectrum indicates  $E_0$  values ranging from 2.2 to 4.0 keV (McEwen et al., 1981a; Bryant et al., 1978), and even more intense from 5.6 to 9.0 keV (Sears and Vondrak, 1981). Note that an e-folding energy  $E_0$ , has an average energy of  $2E_0$  for a Maxwellian distribution, which will be biased higher by the divergent behaviour above 20 keV. Thus there appears to be sufficient flux at energies around 20 keV, which penetrate to around 95-100 km for the pulsating aurora to occur.

#### 1.4 E-REGION CURRENTS

Evidence has been presented that certain geomagnetic micropulsations Pi(c), and rapid auroral intensity variations are spatially and temporally related. Lag times less than one second as reported by Burns (1983), Oguti et al., (1984) and determined during this research (see Section 3.2), are indicative of an ionospheric origin for Pi(c) micropulsations, within auroral regions.

As a lead-in to the various theoretical generation mechanism proposals, consider the current systems that exist in the auroral zone ionosphere during a substorm. On a global scale the electric current system of an auroral substorm is rather locally confined (Rostoker, 1972), see Figure 1.1. An important point to note is that an auroral substorm involves a marked intensification of only a restricted part of the westward electrojet near geomagnetic midnight. Typically this covers a latitudinal width of only about  $5^\circ$ , extending longitudinally from less than  $10^\circ$  up to approximately  $90^\circ$  (Rostoker, 1972). Consequently, a marked latitudinal difference in the recorded storm signatures is expected at various stations (see Figure 1.5).

Difficulty may then be experienced in assigning substorm onset times at different latitudes, were it not for the fact that Pi(b) activity provides a singularly powerful tool at all locations (Saito, 1961; Rostoker, 1972):

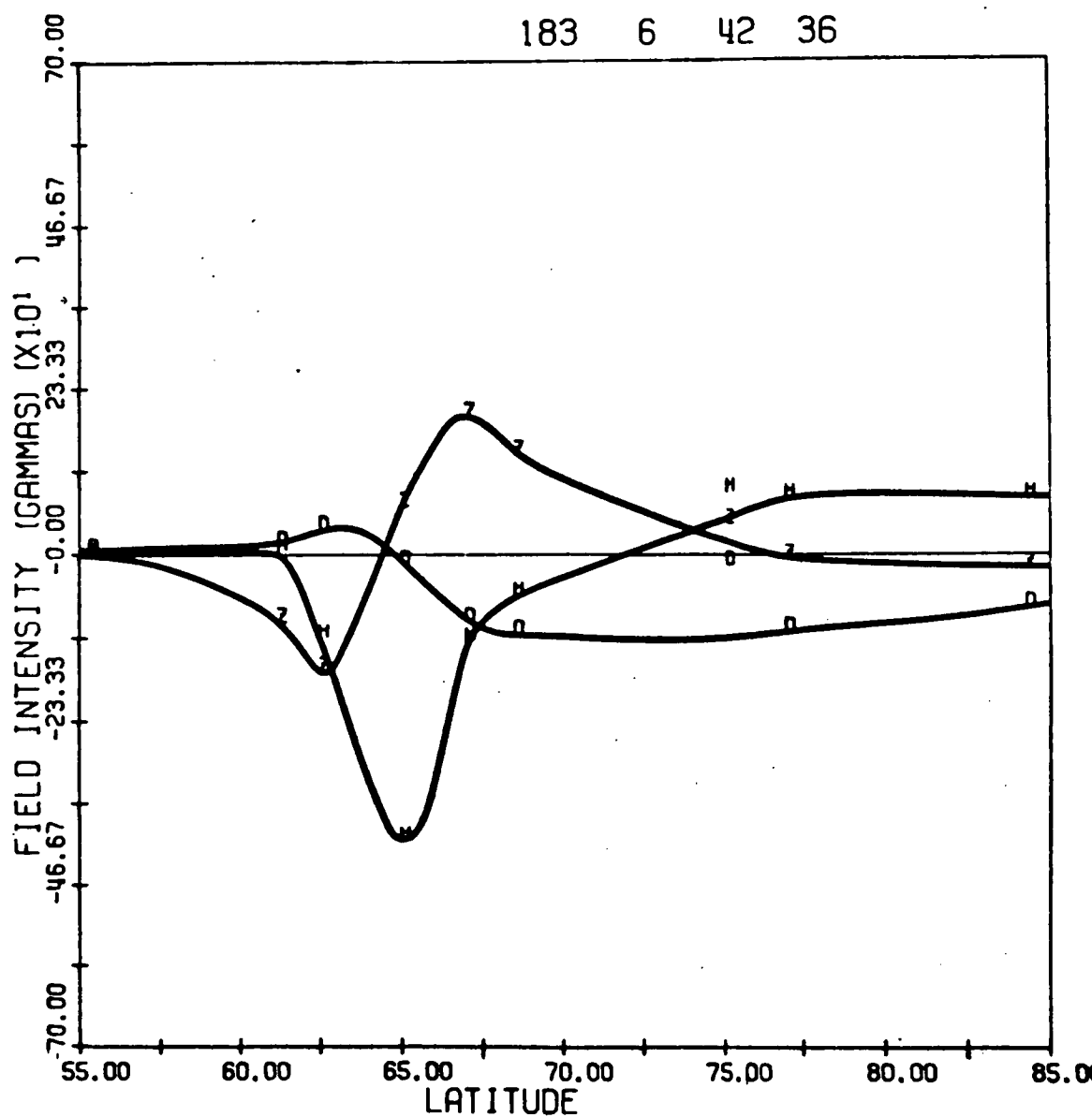


Figure 1.5. Magnetic perturbation pattern along a geomagnetic meridian recorded in Western Canada, 1970, during a polar magnetic substorm. Numbers at the top give the day, hour, minute and second for the time the profiles were calculated (from Kisabeth and Rostoker, 1971).

For stations within the auroral zone near local magnetic midnight the substorm is characterized by a negative excursion in the H magnetic field component. This is to be expected on the basis of an intensification of westward current above the station, the details of which have been comprehensively described by Kisabeth and Rostoker (1971), using data from a closely spaced latitudinal chain of stations across Canada.

Their study indicates that the current enhances first at the southern (equatorward) border of the electrojet, followed by quasi-periodic intensifications at the northern (poleward) border. It is the overall magnitude and stability of the equatorward portion of the electrojet which defines the nature of the substorm (Kisabeth and Rostoker, 1971).

Using a spherical harmonic analysis of the magnetic disturbance field (Chapman and Bartels, 1940) it is always possible to derive a two-dimensional equivalent current system, flowing in a spherical shell at some distance above the surface of the Earth, that can produce the perturbation pattern (Bonnevier et al., 1979) witnessed at any particular station. Some workers have actually argued the reality of such systems (Vestine and Chapman, 1938; Silsbee and Vestine, 1942). It has been shown, however, that to cover the energy losses within the electrojet, unreasonably high neutral wind velocities and/or electron densities are required for purely ionospheric sources to be able to maintain these systems (Böstrom, 1964; Bonnevier et al., 1970).

The required energy source must therefore reside in the outer magnetosphere, and so the real circuit must be some three-dimensional current system. This idea of current flowing down from the

magnetosphere was first proposed by Birkeland (1908, 1913) as a system of vertical line currents linking the westward electrojet to the magnetosphere (c.f. Böstrom, 1968). Böstrom (1964, 1968) extended the work of Birkeland by proposing two possible current systems. The first of these involves currents flowing along the curved geomagnetic field lines as field-aligned currents (FAC's), very much as in Birkeland's original postulate (see Figure 1.6a), whilst the second system invokes field-aligned current sheets at the poleward and equatorward borders of the auroral electrojet (see Figure 1.6b).

At auroral zone stations the proximity of currents that can vary in intensity, is responsible for appreciable magnetic perturbation effects. Transverse to the auroral zone, the integrated effect of these currents is seen to fall off quite sharply (Böstrom, 1968).

The reality of direct observation of these FAC's has been possible since the advent of rockets and satellites as data gathering devices. Cummings and Dessler (1967) were the first to show that FAC's had been unambiguously detected by Zmuda et al., (1966). Sounding rocket data (Whalen and McDiarmid, 1972) has shown that the field aligned fluxes are concentrated in the night-time hours in an oval shaped region in close relation to the visual auroral oval, and this has been further substantiated by satellite observations (Hoffman and Evans; 1968, Berko, 1973). This field has been reviewed by Arnoldy (1974).

It is the Böstrom-Birkeland current system postulates that have provided valuable clues as to the cause of the Pi(c) micropulsations which accompany the pulsating aurora. In the dual current-sheet model (Figure 1.6b) closure is effected in the ionosphere by an equatorward Pedersen current (Senior et al., 1982) while the westward auroral

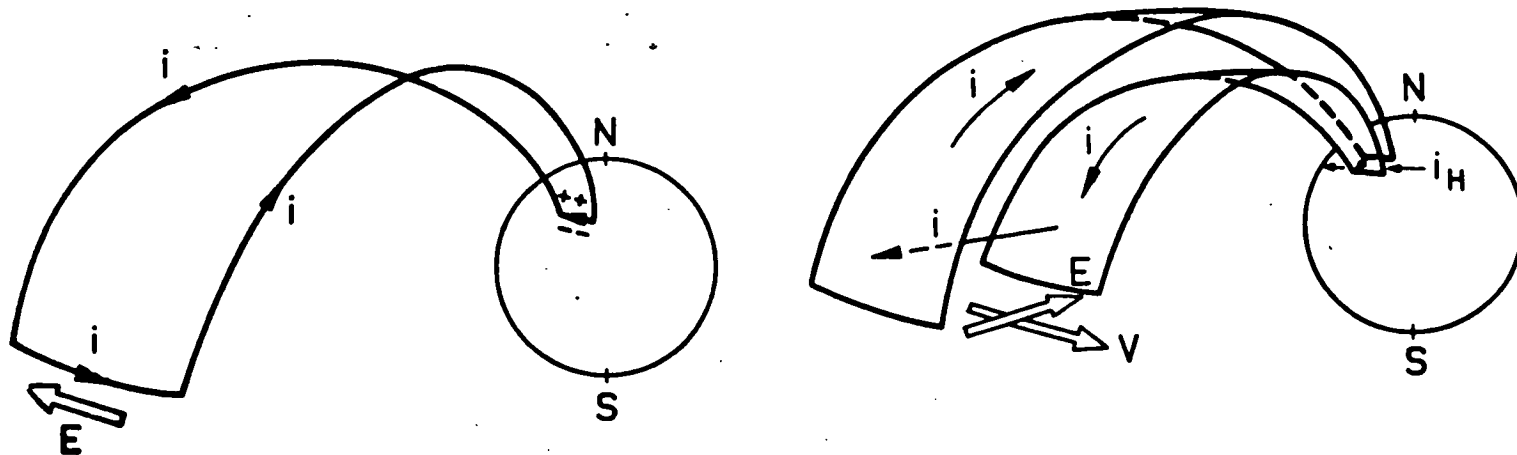


Figure 1.6 (a) Similar current system to Birkeland's suggestion but with the magnetospheric currents actually flowing along the curved field lines.

(b) Current system driven by plasma motions in the magnetosphere. Field aligned sheet currents at the poleward and equatorward edges of electrojet (Hall current) effect closure of the Pedersen current in the ionosphere.

(from Böstrom, 1964).

electrojet enhancement is an induced Hall current flow. It will be seen later (Section 1.5) that the altitudes of the Hall and Pedersen conductivity maxima has significant consequences for the optical correlation with the H (north-south) and D (east-west) magnetic field micropulsations.

### 1.5 INCOHERENT BACKSCATTER RADAR

For a more complete discussion of ionospheric current systems and their magnetic effects on the ground, an understanding is required of ionospheric electric fields, conductivities and neutral winds. It is possible to determine these quantities, together with the E-region currents themselves, using incoherent backscatter radar techniques (review: Banks and Doupnik, 1975).

Various ionospheric parameters - electron densities, electron and ion temperatures, and line-of-sight components of plasma drift velocities - are measured simultaneously. These are collected by a systematic sequencing of azimuth, elevation, and range gate of the radar antenna. This enables electron concentration, current density, conductivity profiles, electric fields perpendicular to the magnetic field, and neutral winds, to be inferred (Banks and Doupnik, 1975).

The altitude-dependent E-region current density is given by Brekke et al., (1974) as:

$$\underline{j} = \sigma_O \underline{E}'_{\parallel} + \sigma_P \underline{E}'_{\perp} + \sigma_H \underline{E}'_{\perp} \times \underline{B}/B \quad 1.1$$

where:

$\sigma_O$  = direct, or parallel conductivity

$\sigma_P$  = Pedersen conductivity

$\sigma_H$  = Hall conductivity

$\underline{E}'_{\parallel}$  = effective electric-field parallel to magnetic field

$\underline{E}'_{\perp}$  = effective electric-field perpendicular to magnetic field.



that is:

$$\underline{E}' = \underline{E} + \underline{\mu} \times \underline{B} \quad 1.2$$

where

$\underline{E}$  = electrostatic field

$\underline{\mu}$  = neutral wind velocity.

Radar measurements by Brekke et al., (1974) relate to current flow perpendicular to the magnetic field, and they present the altitude-dependent Hall and Pedersen conductivities as:

$$\sigma_H = \frac{n_e \bar{e}}{B} \left[ \frac{\Omega_i^2}{\Omega_i^2 + \nu_i^2} - \frac{\Omega_e^2}{\Omega_e^2 + \nu_e^2} \right] \quad 1.3$$

$$\sigma_P = \frac{n_e e}{B} \left[ \frac{\Omega_i \nu_i}{\Omega_i^2 + \nu_i^2} - \frac{\Omega_e \nu_e}{\Omega_e^2 + \nu_e^2} \right] \quad 1.4$$

where:

$n_e$  = electron density

$e$  = electronic charge

$\nu_i, \nu_e$  = ion-neutral, electron-neutral collision frequencies

$\Omega_i, \Omega_e$  = ion, electron gyrofrequencies  $\left( \frac{eB}{m_{i,e}} \right)$ .

These expressions follow from the collision transfer momentum equations for ions and electrons, without regard for pressure gradients or gravitational forces. Typical profiles for the radar measured electron concentrations, and derived conductivities are shown in Figure 1.7 from Brekke et al., (1974).

Brekke et al., (1974) adopted an ion-neutral collision frequency of  $7.5 \times 10^{-10} N(n) \text{ s}^{-1}$ , where  $N(n)$  represents the neutral air density (Dalgarno, 1964; Rishbeth and Garriott, 1969), making use of Banks and Kockarts (1975) static atmosphere model for  $N(n)$ .

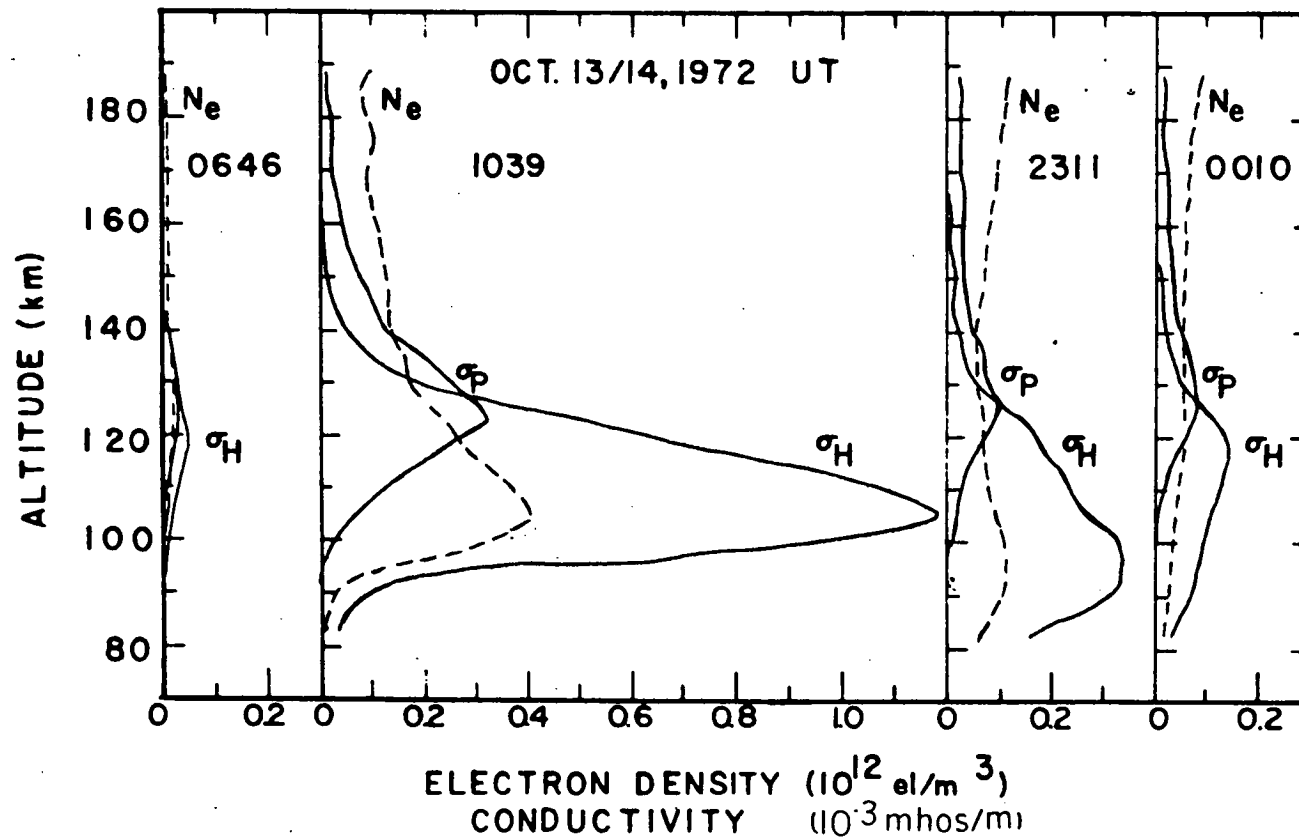


Figure 1.7 Electron density  $N_e$ , Pedersen conductivity  $\sigma_p$ , and Hall conductivity  $\sigma_H$ , altitude profiles for quiet evening (0646 UT), disturbed night (1039 UT), disturbed daytime (2311 UT), and quiet daytime (0010 UT).

(From Brekke et al., 1974).

For collisions between electrons and neutrals, the expression  $5.4 \times 10^{-10} N(n) T_e^{\frac{1}{2}} s^{-1}$ , where  $T_e$  is the electron gas temperature, was adopted from Nicolet (1953).

As regards the gyrofrequencies,  $\Omega_i$  is of the order of  $1 \times 10^2 s^{-1}$ ,  $\Omega_e \sim 7 \times 10^6 s^{-1}$ , with  $NO^+$ ,  $O_2^+$  being the dominant ionic species of the E-region (Jones and Rees, 1973). With increasing atmospheric density, the collision frequencies  $\nu_e, \nu_i$  increase to the effect that  $\nu_e, \Omega_e$  become equal at heights around 70 km, while this occurs around 140 km for  $\nu_i, \Omega_i$ . The Pedersen conductivity peaks near 125 km, whereas the Hall conductivity peaks close to 105 km where:

$$\nu_i > \Omega_i$$

$$\nu_e < \Omega_e$$

- so the following approximations have useful validity:

$$\sigma_p \sim \frac{n_e e}{B} \left[ \frac{\Omega_i}{\nu_i} - \frac{\Omega_e}{\nu_e} \right] \quad 1.5$$

$$\sigma_H \sim \frac{n_e e}{B} \quad 1.6$$

Since  $\nu_e$  is dependent on electron temperature,  $T_e$ , its variation has been investigated for auroral precipitation conditions. Maximum energy deposition occurs near 112 km, with negligible temperature increases below 170 km (Rees and Jones, 1973), implying that  $\nu_e$  suffers little temperature consequences of a precipitation burst. Since  $\nu_i, \Omega_e$ , and  $\Omega_i$  are even less variable, this means that the Hall and Pedersen conductivities are directly proportional to electron density changes in the region of their maxima (Burns, 1983).

Burns points out that, if the theory connecting H-micropulsations to Hall conductivity fluctuations, and D-micropulsations to Pedersen conductivity effects (see Section 1.6) is valid, then the H-micropulsations are an indicator of electron density variations around 105 km, the D-component providing a yardstick near 125 km.

Further to this, Figure 1.7 indicates that disturbed magnetic conditions cause the Hall and Pedersen conductivities to increase. The penetration depths of electrons into the Earth's atmosphere will be a function of their energy. Particles with 1-5 keV precipitate around 125-150 km, and those with energies greater than 5 keV reach regions below 125 km (Rees, 1963). So the ratio of Hall to Pedersen conductivities gives a crude measure of the energy of the precipitating electrons. The harder the electron energy spectrum the greater will be the Hall conductivity enhancement with respect to the Pedersen. Brekke et al., (1974) report observations to support this interpretation.

Other measurements made with the Chatanika, Alaskan radar facility by Brekke et al., have indicated that the neutral wind induced electric field,  $\underline{u} \times \underline{B}$ , is of little significance compared to the electrostatic field during disturbed ionospheric conditions. They also show that the electrostatic field has a magnetic meridional plane aspect during these disturbances, and that the appearance of negative bays on H-magnetograms is related to a north-to-south electric field reversal with accompanying conductivity increases. This implies that the westward auroral electrojet is predominantly a Hall current.

Fluctuations in the large-scale H-component magnetic field at the Earth's surface are often in close agreement with that expected from height-integrated E-region east-west current densities. The association is usually poor for the D-component and north-south currents (Brekke et al., 1977, see Figure 1.8). Although the magnetometer integrates

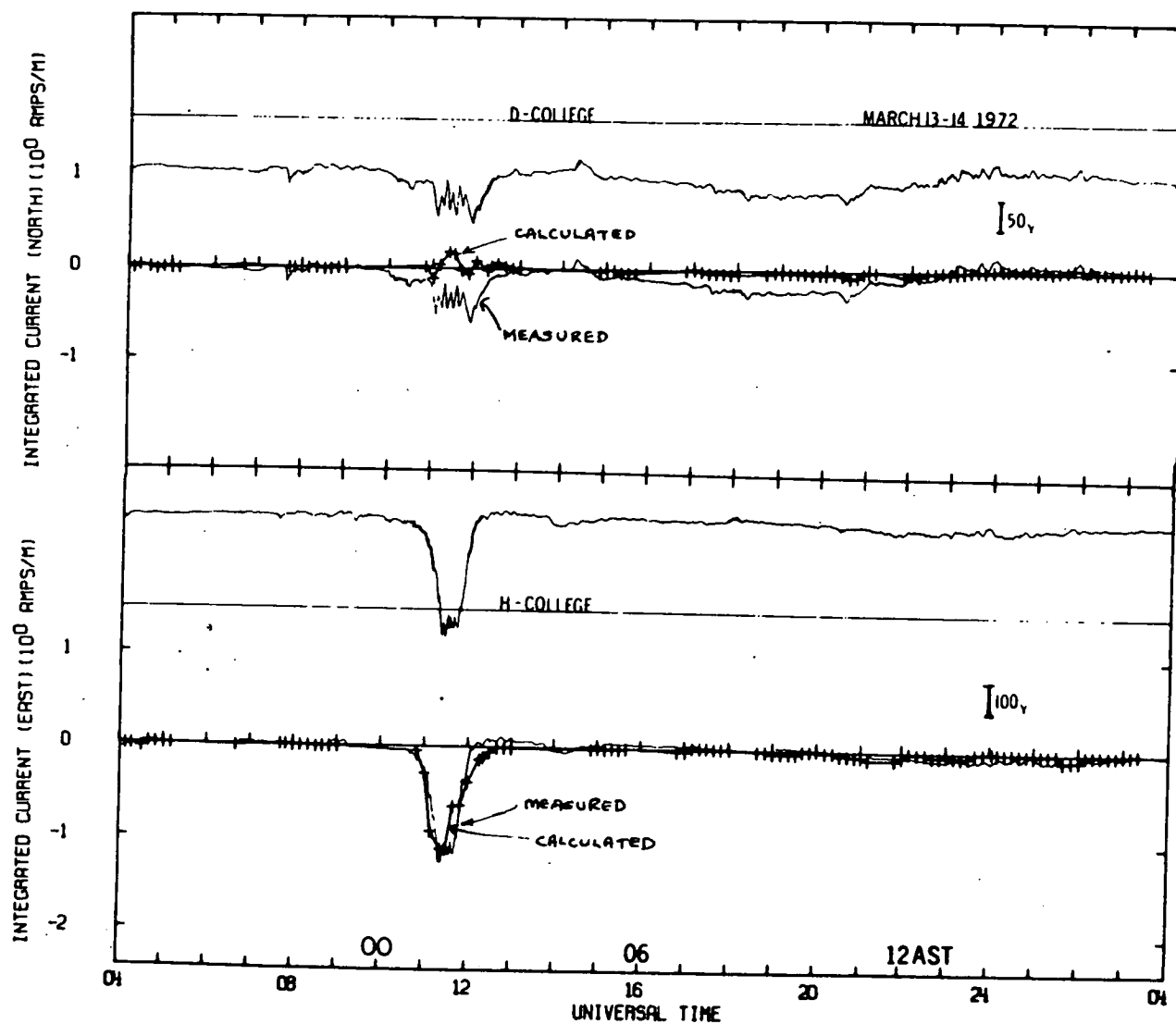


Figure 1.8 Comparison of inferred and measured magnetic variations. Note that the large-scale H component agrees well with the expected perturbation calculated from E-region currents and fields, whilst the D component does not.

ionospheric currents with a much broader field-of-view than the radar, and is sensitive to currents induced in the ground, one cannot always reconcile the D-component discrepancies without recourse to other currents that must be flowing, in particular, the FAC's.

The E-region currents depend, not only on the Hall and Pedersen conductivities, but also on the electric fields present at any particular time. Most back-scatter radar measurements have suffered from an insufficiently rapid sampling rate to monitor the electric field variations effectively. For example, Brekke et al., (1974) has a 30s sampling interval compared to the most common Pi(c) periods of 6-20s.

Haldoupis and Nielsen (1983) improved things slightly to a 20s sample rate, and showed the electric field strength actually decreases during Pi(c) enhancements. However, they also report rapid fluctuations of up to 15-20% of the average field strength, during these times. They found that long term electric field trends did not correlate all that well with large-scale variations in the magnetic field components, and hence the conductivity modifications were dominant in the observed magnetogram variations.

Leoninen et al., (1983) report on electric field measurements with a time resolution of 0.5-1.0s. They showed that the electric field fluctuations were basically in phase with the Hall conductivity.

#### 1.6 EXISTING THEORIES

The complex variety of geomagnetic and auroral activity has led to a number of proposals for their generation. One major difficulty rests with the question of whether the micropulsations are directly responsible for the auroral fluctuations or vice-versa, or if both are the result of some other mechanism. Pi(c) (or similarly Pil) micropulsations have been reported to have a close temporal and spatial relationship with auroral

optical pulsations (Campbell, 1970; Burns, 1983; Oguti et al., 1984). This particular section evaluates the major theories regarding these phenomena in the light of previous observational evidence.

A useful idea is to classify the theories according to the proposed region of origin of the pulsations. The two major regimes being the equatorial plasma sheet (Nishida, 1964; Coroniti and Kennel, 1970 a,b; Kan and Heacock, 1976; Davidson, 1979), and the local ionosphere (Cole, 1961; Campbell and Matsushita, 1962; Böstrom, 1964; Maehlum and O'Brien, 1968; Reid, 1976; Wilhem et al., 1977; Heacock and Chao, 1980; Chao and Heacock, 1980; Heacock and Hunsucker, 1981). A further intermediate region has also been considered (Petelski et al., 1978).

Nishida (1964) models a system whereby a stream of high energy electrons passing through the magnetospheric plasma, injects energy into a growing hydromagnetic (HM) wave. The calculated wave frequency has a similar range to that of the observed irregular pulsations. Subsequent bombardment of the electron beam onto the ionosphere increases the local conductivity so that the downcoming HM waves are increasingly shielded.

This could explain the observed association of Pi(b) with substorm onset (Saito, 1961), and the detection of Pi2 at low latitude stations (Tepley et al., 1965) may be due to Landau resonance of the electron beam with the HM waves, producing oblique propagation (Fejer and Kan, 1969).

Kan and Heacock (1976) question the likelihood of the instability producing observable amplitudes at the Earth's surface, because of the long Alfvén wavelength compared to magnetospheric dimensions.

An auroral precipitation mechanism based on the electron cyclotron wave-particle interaction, leading to pitch-angle diffusion of trapped electrons into the loss cone (particles with a directional motion close enough to that of the field lines are more likely to be precipitated due

to their lower magnetic mirror points, so that those particles with small enough pitch angles are said to define a loss-cone) was investigated by Kennel and Petschek (1966). Wave-particle resonances will become significant near a given particle's gyrofrequency, so this immediately suggests high-frequency fluctuations in the whistler mode for electrons. The whistler mode noise can be generated by the anisotropy in the electron distribution created by the existence of a loss-cone (Johnstone, 1978).

Coroniti and Kennel (1970a) extend the theory to embrace the associated micropulsations. They propose that the whistler mode noise (also known as auroral chorus or hiss) growth rate, is modulated by the magnetic field of HM waves, by an amount that depends exponentially on the HM wave amplitude. The HM waves themselves are, in turn, responsible for the micropulsations. They show that micropulsations as small as 2% of the ambient field strength can produce significant modulation.

Following up this approach, Coroniti and Kennel (1970b) argue that the HM waves themselves are generated as a drift instability of Alfvén waves, driven by a sharp electron thermal gradient at the inner edge of the plasma sheet. These drift waves have a small wavelength (10-100 km) perpendicular to the magnetic field, comparable with the size of pulsating auroral patches (D'Angelo, 1969), and a wavelength parallel to the field of similar dimension to the length of the field lines.

The predicted modulation region for this trapped electron distribution, which is responsible for the auroral pulsations, is determined to be in the vicinity of the geomagnetic equator. This part of the theory agrees well with observations of simultaneous pulsations at conjugate points in the northern and southern hemispheres (Davis, 1969) and ground/rocket co-ordinated observations of modulated particle fluxes (Bryant et al., 1971).



Further considerations by Chance et al., (1973) include conditions where the plasma pressure is of significant amplitude in comparison with the magnetic pressure. A drift-wave growth time from 5-30 minutes is predicted.

Assuming negligible rotation of the micropulsation polarization along the field lines from the geomagnetic equator to the top of the ionosphere, Coroniti and Kennel (1970b) predict a north-south linear polarization. Subsequent traversal of the ionosphere produces a rotation, of the order of  $90^\circ$  to a first approximation (Hughes, 1974). Predominantly east-west polarizations have been observed on the ground by Arthur et al., (1973) and Kan and Heacock (1976). The true extent of ionospheric rotation of HM wave polarization is still in doubt (review: Hasegawa and Lanzerotti, 1978).

Kan and Heacock (1976) outline a theory wherein  $P_i(c)$  micropulsations result from electrons streaming along plasma sheet field lines. The observed streaming is attributed to enhanced magnetotail reconnection (Vasyliunas, 1975) producing an anisotropic plasma pressure, with a greater pressure parallel to the field lines than orthogonal to them. Alfvén (MHD) waves are thus generated in the plasma sheet, at a distance of approximately  $15R_E$ , by the 'garden-hose-instability', and these then propagate towards the ionosphere. This theory predicts an east-west polarization above the ionosphere, and does not account for any rotation in passage to the ground.

Finally, Davidson (1979) models a self-modulated pulsation process in the outer trapped electron belts without the co-operation of HM waves, based on the limits of stably trapped particle fluxes discussed by Kennel and Petschek (1966). Removal of trapped electrons results from VLF wave interaction following an electron injection event. A cyclic wave growth and particle loss pattern can develop, analogous to a highly non-linear

relaxation oscillator. Davidson argues that the spatial extent of auroral pulsations is determined by wave ducting, since the observed drift velocities of pulsating aurora and cold plasma in the upper ionosphere are comparable,  $100\text{--}1,000\text{ ms}^{-1}$  (Johnstone, 1978).

Most of these theories predict that the micropulsations observed to be associated with the pulsating aurora, also have a geomagnetic equatorial region of origin. This involves propagation of the MHD waves responsible for the micropulsations at the Alfvén speed (approximately  $5 \times 10^5\text{ ms}^{-1}$  in the outer magnetosphere), from the equatorial region of auroral zone field lines. Transit times are of the order of a few minutes, whereas the electrons that produce the auroral pulsations (typically  $> 10\text{ keV}$ ) spend only a matter of seconds covering this distance.

This predicted lag-time has proven to be the major obstacle in the acceptance of the micropulsation part of such theories. Many instances of temporally intimate micropulsations and pulsating aurora exist throughout the literature, and the peak-to-peak correspondence has become abundantly clear with measurements that involve more rapid sampling rates (Campbell, 1970; Burns, 1983, Oguti et al., 1984).

Vestine (1943) originally noted the close correspondence between auroral luminosity pulsations and geomagnetic micropulsations. Campbell (1970) measured delays of only 1.2 sec. and this has been confirmed by Kazak et al., (1972) to within an accuracy of 3 sec. Fast response riometer cosmic noise absorptions, indicative of energetic downcoming electron bursts and hence, optical pulsations, have been shown to be coincident (approx. 1 sec. lag) with P11 (essentially P1(c)) measured at Macquarie Island by Reid (1976). Standard riometer variations in the range 20–100 sec. were noted at zero lag (sample time 2 secs.) with micropulsations by Lanzerotti et al., (1978).

Heacock and Hunsucker (1977a) have observed simultaneity of micropulsations and electron precipitation pulsations.

Despite all this, some doubt has remained as to the temporal relationship between auroral optical intensity fluctuations and Pi(c) micropulsations. Burns (1983) goes a long way to putting this issue beyond such doubt. His results and interpretations are supported by Oguti et al., (1984), and are strongly confirmed by this thesis which is an extension of Burns' research.

A near-zero time lag, does not preclude the pitch angle diffusion modulation mechanism, at the geomagnetic equator, being responsible for the structuring of the electron precipitation that is responsible for the pulsating aurora. If the Coroniti and Kennel (1970a) micropulsations are involved in this modulation, then they are not the same ones detected as Pi(c) on the ground, which must originate somewhere in the local ionosphere (Burns, 1983). This is substantiated by the absence of Pi(c) at geostationary orbits, although Pi(b) were often present, as measured by Gendrin et al., (1978), McPherron (1980).

Parks and Winckler (1969) have demonstrated the mutual existence of 5-15 sec energetic electron fluxes in the equatorial plane, and at the connecting conjugate points in both hemispheres. Further evidence has come from Tsurutani and Smith (1974), Ward et al., (1982), for the appearance of ELF hiss and auroral electron pulsations in the vicinity of the geomagnetic equator.

The first major theory linking the origin of Pi(c) micropulsations with ionospheric E-region current sources, was devised by Campbell and Matsushita (1962). Their work, based upon observations of 5-30s period micropulsations measured at College, Alaska, indicated that conductivity changes in the auroral electrojet, caused by precipitating electrons, could generate Pi micropulsations observable on the ground.

Cole (1961) has postulated that the H-component micropulsations are due to a current increase in the westward electrojet, and the D-component to an increase in an equatorward current. A model for these current systems linking the outer magnetosphere to the ionosphere has been presented by Böstrom (1964). This mechanism has received much attention in a number of related papers (Reid, 1976; Wilhelm *et al.*, 1977; Heacock and Chao, 1980; Chao and Heacock 1980; Heacock, 1980).

Reid (1976) found, from his Macquarie Island data, that P1 micropulsations were coincident with cosmic noise absorption pulsations. He proposed that the impulse in particle precipitation gives rise to a much larger number of secondary electrons. Ionospheric conductivity is thus enhanced, in turn increasing the electrojet current manifesting itself as a small magnetic bay intensification, that is, as a micropulsation. Reid indicates that the structured particle precipitation may achieve its modulation via the Coroniti and Kennel (1970a) pitch angle diffusion mechanism.

Most models argue for a precipitating auroral source of electrons with temporal variations embedded in it. Maehlum and O'Brien, (1968) model an ionospheric feedback system, originally postulated by Cole (1962), that can introduce significant temporal structure into an initially time-invariant electron precipitation event.

The first stage in this cycle involves ionization from the particle precipitation increasing the westward electrojet conductivity. The magnetic field above the electrojet is thus increased, and so the effective mirror point of bouncing, trapped electrons is raised. Due now to a reduction in flux of particles at the electrojet altitude, the ionization, conductivity, and therefore current, all decrease, reducing the magnetic field strength above the electrojet altitude.

Electrons can once more penetrate to this depth. This feedback loop simply repeats, and Maehlum and O'Brien calculate that periodic variations in the range 50-200s will ensue.

However, this entire process depends heavily on the presence of large magnetic disturbance fields, of nearly  $1000\gamma$ , and the requirement of a steep pitch angle distribution of electrons near the boundary of the loss-cone. Nearly isotropic pitch angle distributions in precipitating electron fluxes have been measured during peaks in pulsation activity (Whalen et al., 1971), and the most abundantly occurring auroral pulsations have periods of 6-20s, which this model has great difficulty in generating.

Birkeland's (1908, 1913) pioneering work has led to a far greater understanding of auroral zone phenomena. Three-dimensional current systems (Böstrom, 1964, 1968; Bonnevier et al., 1970; see Section 1.4) based upon his work have led to investigations of field aligned currents (FAC's or Birkeland currents) as Pi micropulsation sources. Wilhelm et al., (1977) explain their observations by interpreting H-component micropulsations as the magnetic effect of fluctuations in the auroral electrojet, and the D-component as a consequence of variations within Birkeland current sheets (as in Figure 1.6b). Their work confirmed the suspicion that the auroral electrojets show internal microstructure (Kamide et al., 1969) and they found the sheet currents to be fluctuating independently of each other, and decoupled from the electrojet fluctuations. Most of these results relate specifically to the substorm expansive phase, but they are consistent with the pulsating aurora data of Burns (1983), gathered at Macquarie Island.

Petelski et al., (1978) attributes micropulsation activity to Birkeland current chopping, stimulating HM waves, by an unstable

potential double layer, located at approximately 1Re altitude on auroral zone field lines. This double layer also accelerates the electrons whose flux variations are then due, either to inherent fluctuations of the double layer, or interaction with the micropulsations generated. Evidence for an electric field component parallel to the field lines has come from Evans (1975). This mechanism seems better related to 'inverted-V' events associated with auroral arcs, and so is not of great consequence in this study of pulsating auroral patches.

These represent the major theoretical arguments used to tackle the problem of pulsating aurora and their associated geomagnetic micropulsations. The picture that has most consistently emerged is one of pitch-angle diffusion of trapped electrons into the loss cone within a diffusion region near the geomagnetic equator (Bryant, 1982). Evidence for this has come from the extrapolation of velocity dispersal measurements of electron fluxes pointing to an equatorial source (Bryant et al., 1969, 1971, 1975; Yau et al., 1981).

The Kennel and Petschek (1966) mechanism for pitch angle diffusion by whistler mode turbulence has received further support, with the correlations observed between the occurrence of 40 keV electron precipitation and VLF chorus (Oliver and Gurnett, 1968). They argued that the anisotropic electron pitch angle distribution (due to the presence of a loss cone) can itself generate the whistler mode noise if the absolute flux of trapped particles exceeds some critical value. Sufficient turbulence is generated to make the electron loss rate (into the loss cone) equal to the injection rate of any sources acting. Some evidence exists for outer zone 40 keV electrons being held at or near limiting fluxes, which for L=5 is approximately  $10^8 \text{ cm}^{-2} \text{ s}^{-1}$  (Roberts, 1969).

The H-component of the Pi(c) micropulsations that are concurrently witnessed with the auroral optical fluctuations, are believed to be due to induced ionospheric Hall conductivity changes (producing enhancements of the westward electrojet), resulting from the structured particle precipitation. D-component micropulsations are either due to similar variations in the equatorward Pedersen conductivity, or directly from the modulations within the FAC's themselves.

Arnoldy et al., (1982) argues that the equatorward current responsible for the D-micropulsations is in fact a Cowling current. The auroral precipitation induced enhancement of ionization results in an eastward polarization electric field producing Cowling conductivity. This interpretation results from obstruction to the westward current flow perpendicular to the applied electric field. The presence of strong auroral electrojets seems to oppose this argument.

In this thesis, data gathered at Macquarie Island is presented and examined to evaluate its consistency with the ideas put forward in this chapter. The predicted effects of the three-dimensional model current loops, proposed by Böstrom, (1964, see Figure 1.6), are critically compared with the observations in an effort to determine which of the above processes is responsible for the phenomena.

## CHAPTER 2

### INSTRUMENTATION

#### 2.1 THE WIDE ANGLE PHOTOMETER

This research adopted the twin-channel wide angle photometer system developed for the use of Dr. Gary Burns during his studies of pulsating aurora, cosmic noise absorption, and geomagnetic micropulsations. Refer to his Ph.D. thesis (La Trobe University, Melbourne, 1983) for the practical considerations involved in the design of this instrument. It was determined that such a unit would be more compatible with the field of view of micropulsation coils (see Section 2.2), and less susceptible to auroral drifts and luminosity surges which could contaminate detection of the true pulsating aurora.

The photometer unit is mounted, zenith oriented, in the roof of the UAP (Upper Atmospheric Physics) laboratory. A schematic of the photometer system taken from Burns (1983) is shown in Figure 2.1. It has a dual section optical system: a telescope in front of the filter, and a condenser behind it. The purpose of the telescope is to focus the wide angle field of view from  $30^\circ$  down to a maximum acceptable deviation of  $2.75^\circ$  (within the limits of  $2^\circ$ - $3^\circ$ ) perpendicular incidence, upon the filter. Once filtered, the condenser then spreads the light uniformly on to the photocathode of a photomultiplier tube. These were 9658B tubes with a 27% quantum efficiency at  $4278\text{\AA}$ , and response times less than 100ns.

The  $30^\circ$  half-angle vertical incidence photometer system is used to detect both the  $5577\text{\AA}$  O('S) line, and the  $N_2^+$  1NG band. Only the  $N_2^+$  emission, with a band head at  $4278\text{\AA}$  was retained by the computer system for subsequent analysis. Interference filters were used to separate the two light sources.



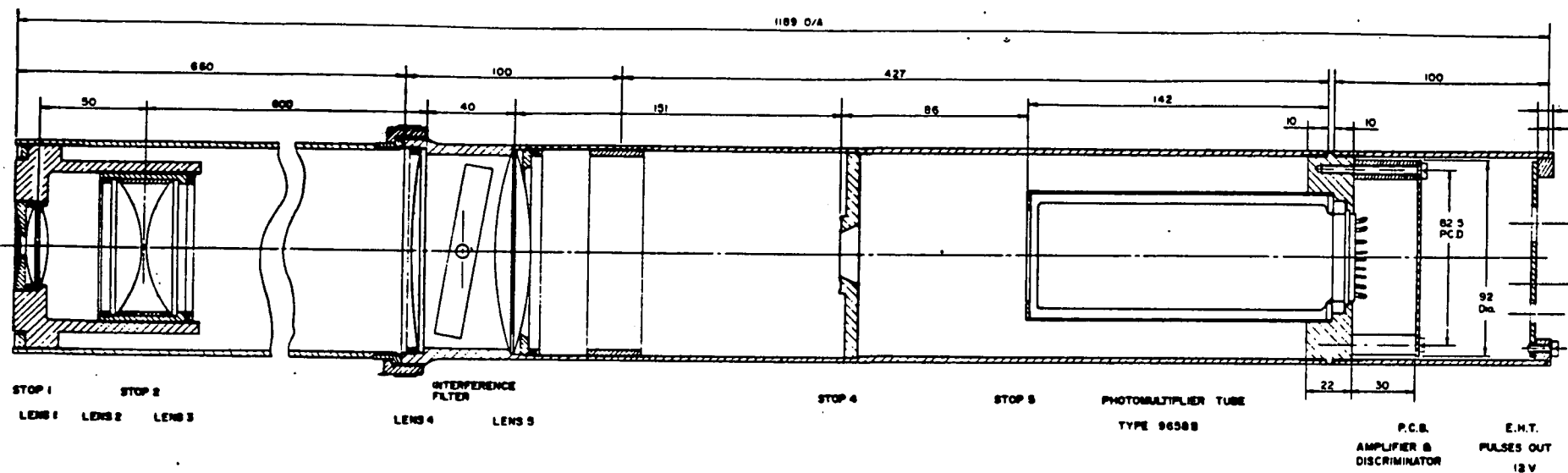


Figure 2.1 Schematic of the wide angle photometer optics

Stop 1	6.25 mm (diam.)	Lens 1	40 mm
Stop 2	58 mm	Lens 2,3	90 mm
Stop 3	19.25 mm	Lens 4	600 mm
Stop 5	46 mm	Lens 5	150 mm

(from Burns, 1983)

Use of the  $N_2^+$  first negative emission in the cross-correlation analysis with the geomagnetic micropulsations (see Section 3.3), was selected because of the near instantaneous response to high energy electron precipitation at auroral heights (Rees, 1963; Rees and Jones, 1973), and its proportionality to total incident energy (see Omholt, 1971).  $N_2^+$  emissions with band heads at  $3914\text{\AA}$ ,  $4278\text{\AA}$  and  $4709\text{\AA}$ , arise from excited state decay to the zero, first, and second, vibrational levels respectively, of the  $N_2^+$  ground state (Chamberlain, 1961).

Arnoldy and Lewis (1977) have shown that these emissions can be explained by direct excitation, using measured electron profiles, and a direct impact excitation model. The 'Precede' artificial aurora experiment dramatically illustrates the instantaneous response of this emission to electron impact upon the upper atmosphere.

O'Neil et al., (1979) using a pulsing rocket-borne electron accelerator, detected the ground-based response to the  $3914\text{\AA}$  band system. The results, shown in Figure 2.2, indicate an immediate response by the  $3914\text{\AA}$  band, and a much slower  $0(^1S)$   $5577\text{\AA}$  reaction. The closely related  $4278\text{\AA}$   $N_2^+$  1NG emission, was adopted as the measure of auroral activity here, due to its clear spectral displacement from other emissions that may contaminate the signal.

The incoming  $4278\text{\AA}$  emission, having traversed the optics of the detection system, is then converted by a photomultiplier tube into electrical pulses, which are sent to a rapid response amplifier, and pulse height discriminator unit, located immediately below the photomultiplier tube. Accepted pulses are then fed, via 50 ohm shielded coaxial cable, to a Photometer Control Unit which also generates the 1000V EHT for the photomultiplier, and the 12V for the discriminator circuitry. The EHT is applied continuously to the photomultiplier

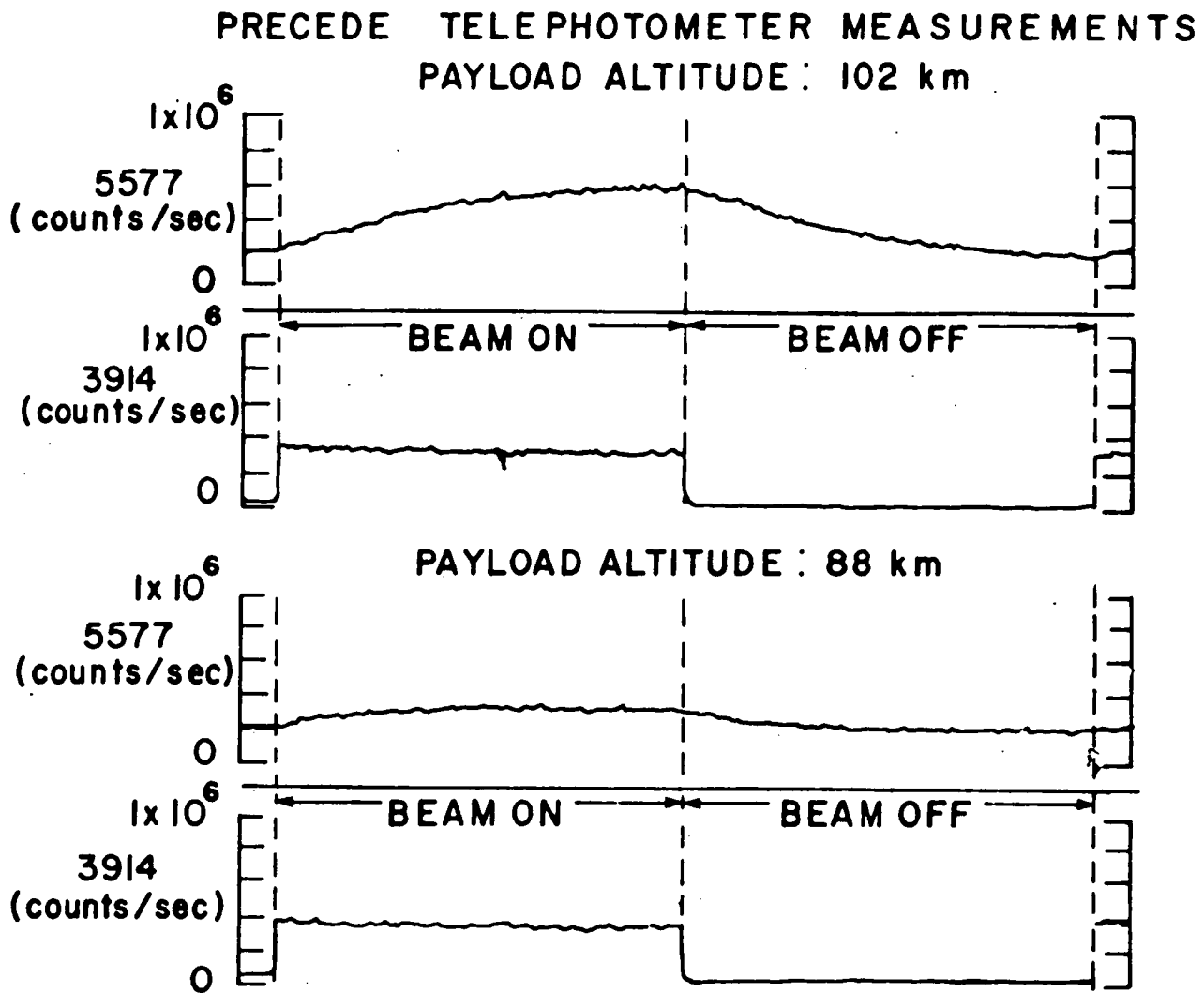


Figure 2.2 Measured intensity variation in the 3914Å band and the 5577Å oxygen line resulting from a pulsed electron accelerator at 88km and 102km. The 'beam-on' time is 2 seconds. Note the sharp response of the 3914Å intensity (from O'Niel et al., 1979).

to prevent any warm-up idiosyncrasies. Occasional tripping-out of this supply occurred due to voltage transients on the station mains. Such events were minimal, the EHT being reset within minutes of any mishaps.

Electronic processing then presents the squared-up pulses, via a Buffer, to an Interface Unit, which effectively counts the pulses over a 0.2s interval. These results are fed as binary numbers to a Parallel Interface Card controlled by an LSI-11 computer. An integrator system, run in parallel, also presents a voltage proportional to the pulse rate, to a Rikadenki chart recorder for visual inspection of the signal. Photometer electronics (after Burns, 1983) is shown in block diagram in Figure 2.3.

Photometer operation times were run slave to local nautical twilight to prevent saturation and subsequent damage to the photomultipliers. An automatic shutter system was controlled by a Venner Time Clock which was preset for on-off times every seven days.

Calibrator units were attached to each of the photometer tubes. These resided in a swinging arm mechanism, which brought the bulbs over the field of view of the photometers, for the first minute of every hour during operation. This uniform diffuse light source was not intended in any way as an absolute calibration of the system. Its function was to enable rapid regular checks of the stability of the electronics, and photomultiplier tubes every night.

Early in the year it was noted, particularly in the 5577Å channel, that the calibration occasionally failed to appear. This fault was found to be due to badly corroded and frayed wiring and was quickly remedied. These units then operated, with new equivalent bulbs, fault-free for the remainder of the year.

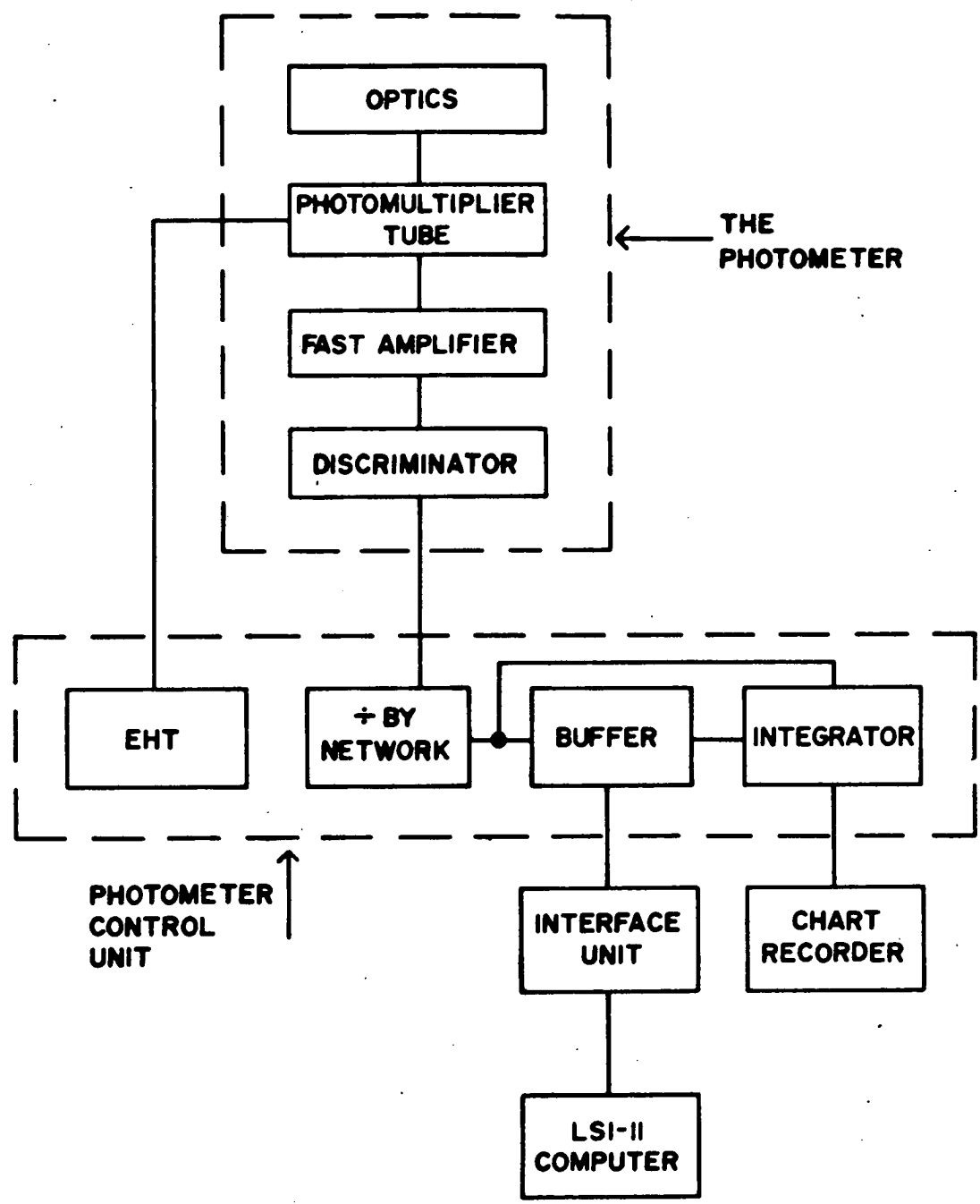


Figure 2.3 Schematic block diagram of the photometer electronics (from Burns, 1983).

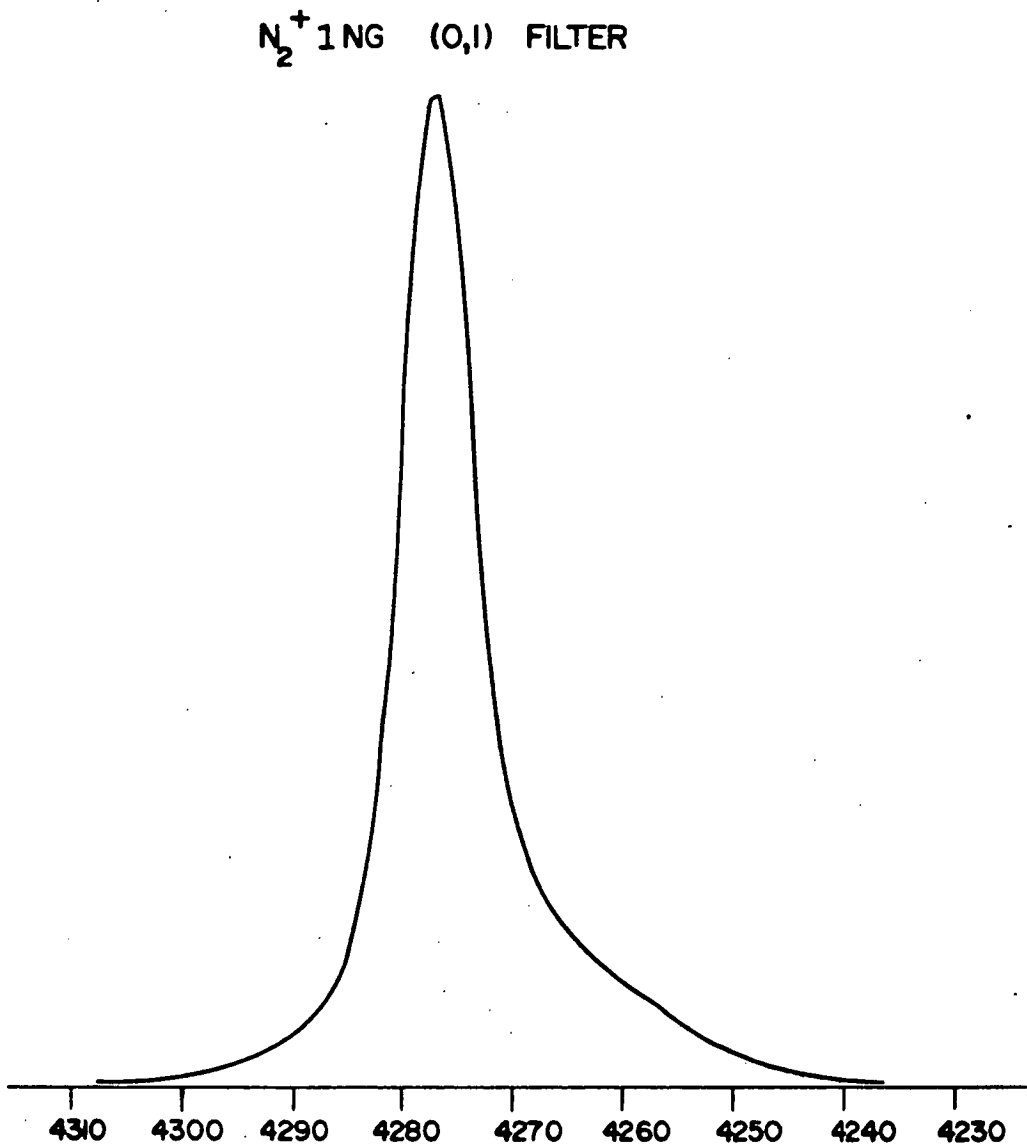


Figure 2.4 Wide angle photometer filter response with peak at 4276Å, and f.w.h.m. of 8.5Å (after Burns, 1983).

Burns (1983) measured the wavelength response of the filters. The relevant one for this thesis, that of the  $N_2^+$  1NG 4278Å band, is depicted in Figure 2.4. It has its peak at 4276Å, with a full width at half maximum of 8.5Å. Temperature sensitivity is not expected to have been a significant problem with the system housed in an air-conditioned laboratory at around 15°C. Occasional failure of the Ferrol furnace allowed this temperature to drop to around 5-10°C, but this problem was kept to a minimum by the station tradesmen (Mr. Mark Haste, carpenter/plumber; Mr. Henry Weiss, electrician; and Mr. Ivan Porteus, senior diesel mechanic).

In general, the photometers operated very successfully for practically the entire year, causing very few headaches, and requiring precious little maintenance.

## 2.2 THE MICROPULSATION COILS

The three component geomagnetic coil system was provided by the University of Alaska. They receive data annually in the form of reel-to-reel FM magnetic tape records. Operation of the equipment is by the Antarctic Division UAP (Upper Atmospheric Physics) personnel, and data access is made available to their various recording units.

A three coil system is maintained, in what was originally a true geomagnetic, H, D, Z arrangement. This orientation involves the H component increasing northward, D component increasing eastward, and Z component increasing downwards (thus forming a right-handed cartesian co-ordinate system). Having been installed and oriented in the summer of 1967-68, the coils now suffer a small but significant misalignment due to the slow eastward drift (approximately 9' of arc per year) of the magnetic pole. The 1984 resident physicist and electronics engineer expeditioners, Mr. Malcolm Lambert and Mr. David Rasch

respectively, have measured the angular misalignment in orientation to be presently nearly  $2^{\circ}$  west of north, for the H component, and  $1\frac{1}{2}^{\circ}$  north of east for the D component coils.

The last major overhaul to the micropulsation coils themselves was carried out by Mr. Dave Barrett (electronics engineer) and Dr. Gary Burns (physicist) during 1980. The coils are housed in perspex tubing and protected from the weather by inner and outer wooden boxes. In the case of the H and D coils (horizontal field), the outer boxes can be firmly bolted to horizontal concrete blocks for added stability. The vertical Z coil is much more difficult to stabilize and is thus susceptible to wind induced vibrations (not exactly a rarity at Macquarie Island). However, as it was not used in this analysis it is of little consequence for this thesis. All housings were found to be in excellent condition, and the coils were operated successfully throughout 1982-83.

Some other minor sources of interference were also intrinsic to Macquarie Island. Elephant seal pups can occasionally infiltrate the "seal-proof" fences erected around the coils, removal is as "delicate" as possible. The larger bulls can engage in territorial disputes across that part of the isthmus where the coils are situated. These all result in vibrational disturbances, but proved to be extremely rare during hours of darkness, and so have little or no effect on important data for this research. The same may be said about the spikes to the H coil trace whenever "Nuggets", the resident Ferguson tractor, previously known by a less salubrious name, was taken on its regular rubbish run.

From the coils, the signal is passed to an array of three Medistor amplifiers inside the UAP laboratory. Here is where the real troubles



began. These microvoltmeters were in desperate need of repair, and the back-up supply of replacement components, in an equally desperate need of replenishment. Initially only one of the three Medistors was operating to any degree of satisfaction on arrival in late October 1982. Mr. Chris Eavis, the 1983 electronics engineer was soon able to have all three instruments in working order. One Medistor however continued to give persistent trouble, displaying significant drift in the weekly calibration. Consequently, this unit was used to amplify the Z coil signal, as this was not required in the current research. My personal thanks are extended to Chris for the many frustrating hours he spent overhauling the Medistors, and keeping them up and running for the entire year.

The Medistor amplifiers are set up to give a  $\pm 2.5V$  output for a full-scale input of  $\pm 100$  microvolts. Calibration checks were made weekly and a test signal is applied every twelve hours for rapid visual inspection, on a chart recorder. An annual absolute calibration is performed to determine the coil and microvoltmeter frequency and phase responses.

Combined micropulsation coil and Medistor amplifier circuit frequency response, was obtained by applying a constant amplitude signal, at a range of frequencies, to the internal calibration windings of the coils. The corresponding output was then measured on the normal daily chart recorder, with appropriate adjustment of chart speed and gain, for easier more accurate determination. The frequency was varied from 0.1-7Hz and the normalized system response for each component is listed in Table 2.1, the curves being plotted in Figure 2.5.

The peak response for both the H and D component detection systems is close to 1.3Hz, and is roughly linear at frequencies below 1.0Hz.

Frequency (Hz)	H	D	Z
0.1	11.3	8.5	8.8
0.2	22.9	17.2	17.9
0.3	32.3	24.9	25.8
0.4	43.5	34.8	35.9
0.5	54.6	43.5	45.0
0.6	65.2	52.6	52.8
0.7	74.8	64.2	64.0
0.8	80.3	72.4	70.8
0.9	88.8	80.1	78.6
1.0	95.0	89.4	87.8
1.2	100.0	100.0	98.4
1.4	97.5	99.8	100.0
1.6	85.0	91.2	94.1
1.8	69.6	78.7	83.0
2.0	56.1	63.9	70.7
2.25	40.2	49.3	54.4
2.5	29.4	37.7	42.3
2.75	23.5	30.0	32.6
3.0	17.9	24.5	25.9
3.5	11.3	15.9	17.1
4.0	6.9	9.9	9.4
5.0	3.3	5.1	5.3
6.0	1.9	2.8	2.7
7.0	Signal too distorted		

Table 2.1      Normalized frequency response of micro-  
pulsation coils and their associated  
Medistor amplifier microvoltmeters

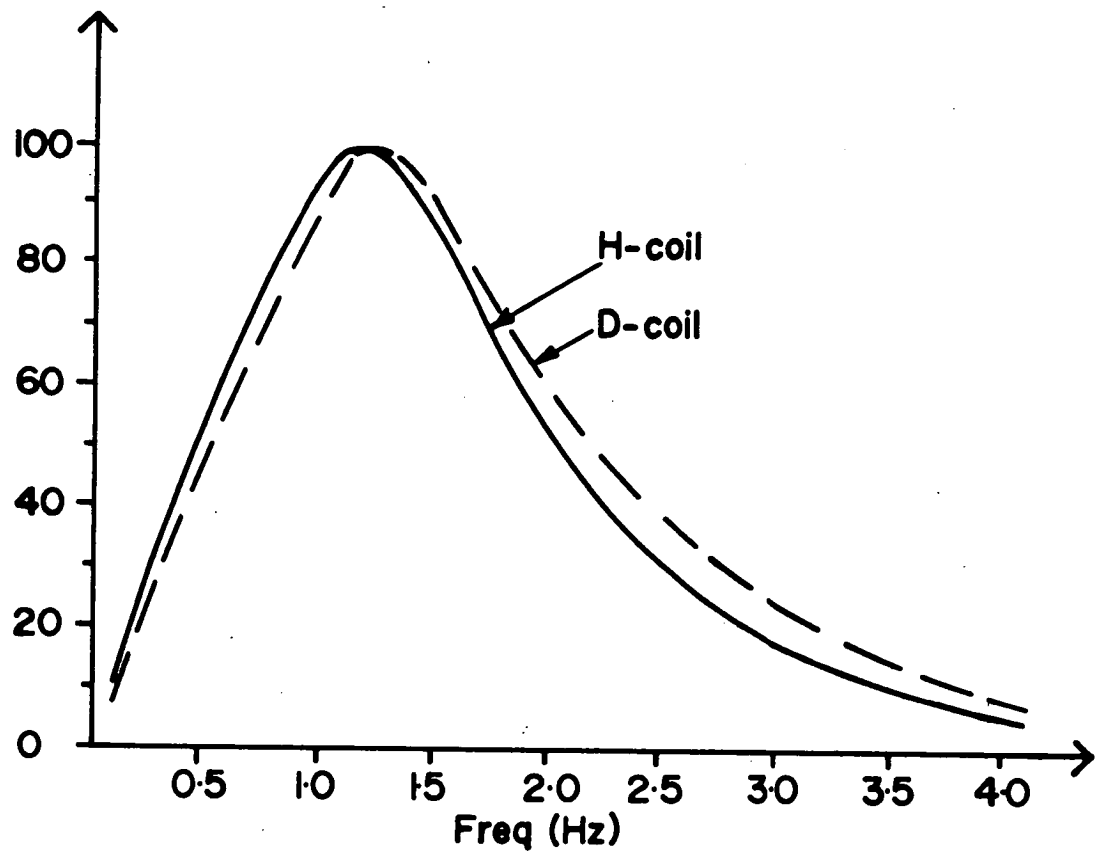


Figure 2.5 Normalized frequency response curves for the H and D component detection systems.

Period(s)	Distance (cm)	$\gamma_{p-p}$	$V_{p-p}(H)$	$V_{p-p}(D)$
6	632	6	0.58	0.58
12	502	12	0.60	0.61
15	432	15	0.60	0.59
60	370	30	0.30	0.30

Table 2.2 Results of the "gamma-slinger" rotating magnet test for the H and D detection systems.

This will have important consequences for the cross-correlation analysis of the micropulsations with the optical auroral pulsations (see Section 3.4).

Both the H and D coils were further subjected to an absolute calibration using a rotating bar magnet, affectionately dubbed the "gamma-slinger", placed at various distances from the coils. The value of the magnetic moment for this bar magnet has been determined to be  $7595 \pm 50$  dyne cm oersted<sup>-1</sup>. Distances were measured from the centre of the micropulsation coil to the centre of the rotating magnet.

Throughout this test the Medistors were operated on the 1mV range. Since normal operation involves the 100 $\mu$ V range, then an amplification factor of 10 times must be taken into account for scaling these results. Table 2.2 lists the results obtained from this particular test.

So with the Medistor amplifiers on their normal 100 $\mu$ V operating range, in the linear region of detector response (for frequencies less than 1.0Hz), a 1V output arises from a field change of approximately 0.17 gamma per second, for both the H and D coils.

Coil peak response can then be calculated using the results of the gamma slinger and frequency response calibrations. A one gamma amplitude field, fluctuating at the optimum response frequency (around 1.3Hz for both H and D systems) of the detectors, will produce an output of approximately 300 $\mu$ V.

Next it remained to determine the phase response of the system. This was done for the Medistors alone, and the combined coils and amplifier systems. Mr. Chris. Eavis again deserves the credit here for these measurements.

For the combined coil and amplifier circuit, a current is fed from a Feedback Function Generator, to the internal calibration windings of the coils. This signal is detected by the main coils and passed back, via the amplifiers, to an HP1742A cathode ray oscilloscope operated in X-Y mode, for comparison with the initial test signal. Results of the overall phase response at various frequencies are given in Table 2.3, and are in good general agreement with those measured by Burns (1983).

The normal daily signal is recorded in a variety of forms. Initially as an FM audio signal on magnetic tape for the University of Alaska, then as paper chart trace, for visual inspection, on a three channel Rikadenki recorder, and finally the H and D responses were passed, via Analog-to-Digital channels, to the LSI-11 microcomputer system for disk storage.

### 2.3 DATA COLLECTION - THE LSI-11 MICROCOMPUTER

For a more complete description of the LSI-11 microcomputer system and its installation at Macquarie Island in 1980, refer to Burns' Ph.D. thesis (1983). This section summarizes his report on the unit, and outlines the subsequent changes and improvements.

Data was presented to the LSI-11 Microcomputer by means of a Parallel Interface board, for the photometer channels, and an Analog-to-Digital board, for the H and D micropulsations. A floppy disk storage system was used to collect the data directly in digital form. Together with the availability of an omnigraphic plotter, the microcomputer system made it possible to analyse all the data on site. All the initial plots of the  $4278\text{\AA}$  auroral emission with the H and D micropulsations and the subsequent cross-correlation analyses were carried out directly at Macquarie Island.

<u>Phase Response (degrees)</u>		
<u>Frequency (Hz)</u>	H	D
0.1	84 ± 0.5	85 ± 0.5
0.2	80 ± 0.5	79 ± 0.5
0.5	66 ± 0.5	63 ± 0.5
1.0	43 ± 0.5	39 ± 0.5

0° shift at      2.0 ± 0.05 Hz for H  
                     1.90 ± 0.05 Hz for D

-90° shift at    5.70 ± 0.05 Hz for H  
                     5.40 ± 0.05 Hz for D

Table 2.3      Combined coil and medister amplifier  
                     phase response measurements.

Limited storage capacity on the floppy disks was found to be the only disadvantage with this arrangement. As will be described later, this particular problem has been removed by the addition of an RL02 hard disk facility. Floppy disks present 26 storage sectors with a capacity of 128 bytes per sector per track on each side of the disk. With 72 tracks per sector this amounts to around 0.25 megabytes per single side. The RX01 disk drives used were single density units which can record on only one side of the disk. This means, with a 5Hz sample frequency, the three data channels can be recorded simultaneously for a total of 130 minutes. At this point in time the Sampling Program terminates the writing of data to the disk, or the operator intervenes to halt the process.

Photometric data is processed by an Interface Unit which presents the pulse counts as binary numbers to the Parallel Interface Board. This is then sampled by a data acquisition program run on the computer.

Timing sequences are provided by the Interface Unit deriving its signal from a Systron Donner Chronometer. The Systron Donner is self-consistent to within 2ms over a period of a week, and accurate to within the 7-8ms propagation time of radio transmissions from VNG Lyndhurst, Victoria, to Macquarie Island. Such an accuracy is more than adequate for the 0.2s sampling rate adopted in this research.

The Interface Unit takes of the order of nanoseconds to exchange the data presented to the output from 5577Å data to 4278Å data. The sampling program, labelled "EARS" takes approximately 5μs before the second photometer value is accessed, so that no timing problem arises there. Both optical channels were recorded in Burns (1983) research, and it proved more convenient to retain existing interfacing, then simply ignore the 5577Å data channel from the software side of affairs. Mr. Howard Burton, from the Antarctic Division, is the man responsible for

providing such excellent programming and invaluable assistance, in trouble-shooting the various problems that arose (see later).

The photometric data number presented to the Parallel Interface board lies in the range 0-4095. Numbers in excess of this, within the sample time, are reduced by 4096 before being passed on. Data overflow figures are thus recoverable in the optical channel.

This is not the case for the micropulsation coil data. Medistor outputs are input to the computer via Analog-to-Digital channels. This converter is voltage limited, so that overflow data is set at saturation and cannot be recovered. The board is sampled at the end of each 0.2s period, and the digitized value at this instant is presented for storage. In contrast, the photometer channel results from a count over an approximate 0.2s period, and thus is an estimate of the emission intensity for the middle of the sample period. This introduces a delay of nearly 0.1s between the photometer and micropulsation values, a figure which must be taken into account when examining lead-lag delay times between the optical and magnetic pulsations (see Section 3.4).

Data collection is formatted into 5 minute segments stored sequentially on floppy disks. The initial entry for each file is the start time of the sample period, followed by the 1500 data points. Each file name has a letter designating the channel: B for 4278Å, C for H micropulsations, and D for D micropulsations (A is reserved for the 5577Å data which was not retained). Next, a four number array indicates the UT day and month, followed by a three figure extension denoting the UT time as a number of 5 minute segments. As an example, the three files for 03-Nov-82 from 1510-1515Z would be labelled B0311.182, C0311.182, and D0311.182, for the optical, H and D files respectively.



The RT-11 operating system used on the LSI-11 microcomputer is too slow in its file handling procedures to take care of file labelling. The sampling program (EARS) overcomes this by writing directory information upon termination of the data collection.

Due to the limited storage capacity of the floppy disks, a Fourier transform analysis is carried out on each photometer file before it is retained or discarded. This frees more space enabling the program to run for periods in excess of 130 minutes, by overwriting data that fails the Fourier examination. While the data for one five minute period is being collected, the sub-routine analyses the previous five minutes data.

This particular arrangement is not entirely foolproof, however, since the active breakup aurora, can undergo sufficient variation to yield appropriate co-efficients in its Fourier spectrum, to be retained. Since this activity precedes the pulsating aurora, the disk can be filled early in the evening, and the operator must be present to effect a changeover of the disk. Burns (1983) noted this difficulty in producing the subroutine to discriminate between the two phenomena.

Since the installation of an RL02 hard disk system with its 10-megabyte storage capacity, this is no longer of any consequence. No subroutine testing is required at all, for an entire night's data may be easily stored irrespective of the degree of auroral activity. Visual inspection of the chart records each morning indicate which periods need to be analysed for cross-correlations.

This also enables complete sequences to be obtained, whereas previously if the pulsating aurora happened to diminish for a short period those files were overwritten, and so the continuity of arguments based upon the neighbouring data was lost.

Unfortunately the RL02 installation was not finalized until after the arrival of the remaining software in the 25 August 1983 airdrop. September did provide some magnificent pulsating aurora however, and this data features strongly in the arguments presented in chapters three and four. Hard-working efforts by Howard Burton, Stan Malachowski, and Gary Burns at Antarctic Division, Kingston, and Chris Eavis at Macquarie Island, were responsible for the system being available for any use at all.

Only two major breakdowns occurred with the LSI-11 system during the year. The first of these was the failure of an RX01 disk drive unit, which was subsequently replaced. The diagnostic tests supplied by Howard Burton from Kingston ("action-at-a-distance" is alive and well!) enabled the problem to be rapidly diagnosed and treated.

The second breakdown involved the failure of a power supply for the RX01 Controller unit. The 5V rail had died, and due to lack of suitable replacement components, this problem persisted for nearly a month until new transistors arrived on the August airdrop.

Apart from these minor setbacks, the data collection and analysis proceeded very smoothly, and enabled all the data to have been examined before its return to Australia. This thesis examines the data which was collected from 29 October 1982 until 10 October 1983 at the ANARE (Australian National Antarctic Research Expedition) station on Macquarie Island. No data was collected during the final two weeks before departure on 25 October 1983 due to packing and preparations for return to the mainland, and handing over of the laboratory to the incoming researchers.

## 2.4 SUBSIDIARY INSTRUMENTATION

Various other scientific data collection is carried out at Macquarie Island, some of which is relevant to this particular research. These consist of a standard riometer aerial for the detection of cosmic noise absorption, an auroral all-sky camera, and a La Cour magnetometer (run by the Bureau of Mineral Resources, BMR) for detection of changes to the large-scale magnetic field of the Earth.

The standard riometer experiment runs continuously, with a visual chart recorder output within the UAP laboratory. Effectively it gives a measure of the free electron concentration in the ionospheric D-region, by monitoring the strength (at about 30MHz) of the cosmic radio noise signal. The diurnal signal is quasi-sinusoidal due to the overhead passage of the galactic centre.

Solar flare induced ionization increments appear during daylight hours causing increased noise absorption, whilst solar radio noise may appear as spikes or bursts superimposed upon the record. These can be of immense value as a guide to expected activity later that evening.

Auroral substorm activity is nearly always associated with increased opacity to cosmic noise, thus affecting the riometer signal level. Whether or not the degree of such absorption can be quantitatively related to some aspects of the pulsating aurora/micropulsations cross-correlation analysis is discussed in Section 4.3.

An all-sky camera (ASC) was operated throughout the year from an inset in the UAP laboratory roof. The mode of operation saw the shutter open for the initial 10s of every minute of observing time, whenever the sky was at least partially free of cloud, mist, or fog. Extremely rapid changes in weather, including sudden bursts of brief violent storms, make operation of such an instrument at Macquarie Island,

extremely wasteful of film. This necessary evil is magnified by the possibility of seemingly thick blankets of low level stratus cloud dispersing with great rapidity at times, revealing auroral activity. As a result the ASC was sometimes allowed to run, though the sky was cloud-bound. Tentative judgements were based on current auroral activity, and general meteorological conditions, as kindly supplied by the Bureau of Meteorology observers on the station.

Couple this with the huge volume of sea-spray that continually blows across the isthmus, and it is obvious that the film image quality is often most disappointing. Despite all this, a number of very beautiful auroral arc sequences containing turbulent breakup aurora, were obtained with a considerable degree of clarity.

Since the pulsating aurora is predominantly a low intensity phenomenon it is virtually impossible to use simple ASC photographs to detect it. Some hope was held that it may show up auroral contraction to the north of the station during 4278Å/D micropulsation positive cross-correlations (see Section 4.3). One particular evening, 23 August 1983, displayed predominant arcs over North Head (north of the observation site) in the early evening pre-breakup phase. Unfortunately, this was during a period of computer failure, and it was not possible to determine if any positive correlations occurred later that night.

As mentioned above, weather factors weigh heavily against ASC detection of aurora, and pulsating aurora even more decidedly so. With such a low level intensity, the presence of sea-spray, thin mists or fogs, or strong moonlight on thin haze or broken cloud are large contaminants to ASC detection of this elusive phenomenon.

The BMR 1a Cour magnetometer provides 24-hour continuous monitoring of the large-scale changes to the Earth's magnetic field. The resulting

magnetograms were used extensively to draw conclusions regarding the overhead current systems, which persist during the various phases of an auroral substorm. That this has particular validity for the H component has been demonstrated by Brekke et al., (1974) and Doupnik et al., (1977).

An annual check, and correction, is made on the orientation of the magnetometer system by the resident BMR geophysicist (Mr. Barry Page, summer 1982-83). This accounts for the slow drift of the geomagnetic pole, which is around 9' of arc, to the east, per year at Macquarie Island.

With the kind assistance of the geophysicists (Barry Page, and Miss Peta Kelsey, winter) the BMR magnetograms were made readily available for inspection. Reference to these chart records has been made regularly throughout this research, in particular, with regard to the latter stages of negative magnetic H bay recovery (see Section 3.5).

The provision of scaled mean hourly values (MHV's) is also very gratefully acknowledged. These have been used to check the author's estimate of the quiet daily curve (QDC) for each month. Such QDC's have been used to serve as a baseline for measuring the degree of disturbance on active days. The validity of this procedure is further discussed in Section 3.5.

## CHAPTER 3

### PULSATING AURORA AND GEOMAGNETIC FIELD MICROPULSATIONS

#### 3.1 INTRODUCTION

The simultaneous pulsating aurora and geomagnetic field micropulsations data, gathered at Macquarie Island (invariant latitude  $64.5^{\circ}\text{S}$ ) from 29.10.1982 to 12.10.1983, is presented here. The cross-correlation analysis is discussed, together with the results arising from it. In all, a total of 553 acceptable cross-correlations, of magnitude greater than 0.33, were obtained for the D-micropulsations and auroral pulsations, and 298 for the H-component.

The virtually instantaneous  $\text{N}_2^+$  1NG band at  $4278\text{\AA}$  was monitored using a zenith oriented, twin-channel, wide-angle photometer as the measure of auroral activity. A three component induction coil system recorded the micropulsations, the H and D channels being retained for the correlation analysis. Instrumentation has been discussed more fully in Chapter 2.

Data output was available in a variety of forms. Rikadenki chart recorders gave a continuous visual readout of each of the channels. For detailed analysis the data was collected in digital form on floppy disks, and in the latter part of the year on an RL02 hard disk storage system. H and D micropulsations, and the  $4278\text{\AA}$  optical emission were collected simultaneously in 5-minute data blocks at a 5Hz sample rate.

On site preliminary analysis of the data was performed, including the cross-correlations which are presented here. These have been examined statistically, to present a set of facts, with which to test the various theoretical mechanisms presented in Section 1.6.

### 3.2 THE DATA SET

As has been mentioned (Section 1.4), there is increasingly strong evidence that pulsating aurora and Pi(c) micropulsations are closely related both temporally and spatially (Campbell, 1970; Burns, 1983; Oguti et al., 1984). A brief examination of the excellent data profiles reproduced in Figures 3.1, will make it clear that the peak-to-peak matching of the optical and micropulsation fluctuations is a real phenomenon.

Figure 3.1(a) 18-April-1983: 1305-1310Z

This particular interval is typical of the bulk of the 4278Å data, with optical peaks approximately 100-150 units. This can be seen from the maximum and minimum values for the components in each 5-minute data segment which appears on the right of the plots. As mentioned in Section 2.1 no absolute calibration of the photometers has been carried out.

Here the D-micropulsations exhibit a larger disturbance than the H-component. This is a typical result, although it was not always found to be the case. Note that the deviation in the D-component is heavily weighted in the negative direction, a phenomenon apparent in the vast majority of files. The H-component also has a slightly more negative swing.

Both magnetic field component files are in excellent agreement with the relative peak heights of the 4278Å pulses. The D-micropulsations were, in general, found to be much better in this respect. This feature is evident in the group of four peaks between 13:08:30 and 13:09:10. The third pulse at 13:08:55 is diminished in the 4278Å and D-component files, but not so for the H. This phenomenon was also noted by Burns (1983) in his Macquarie Island research.

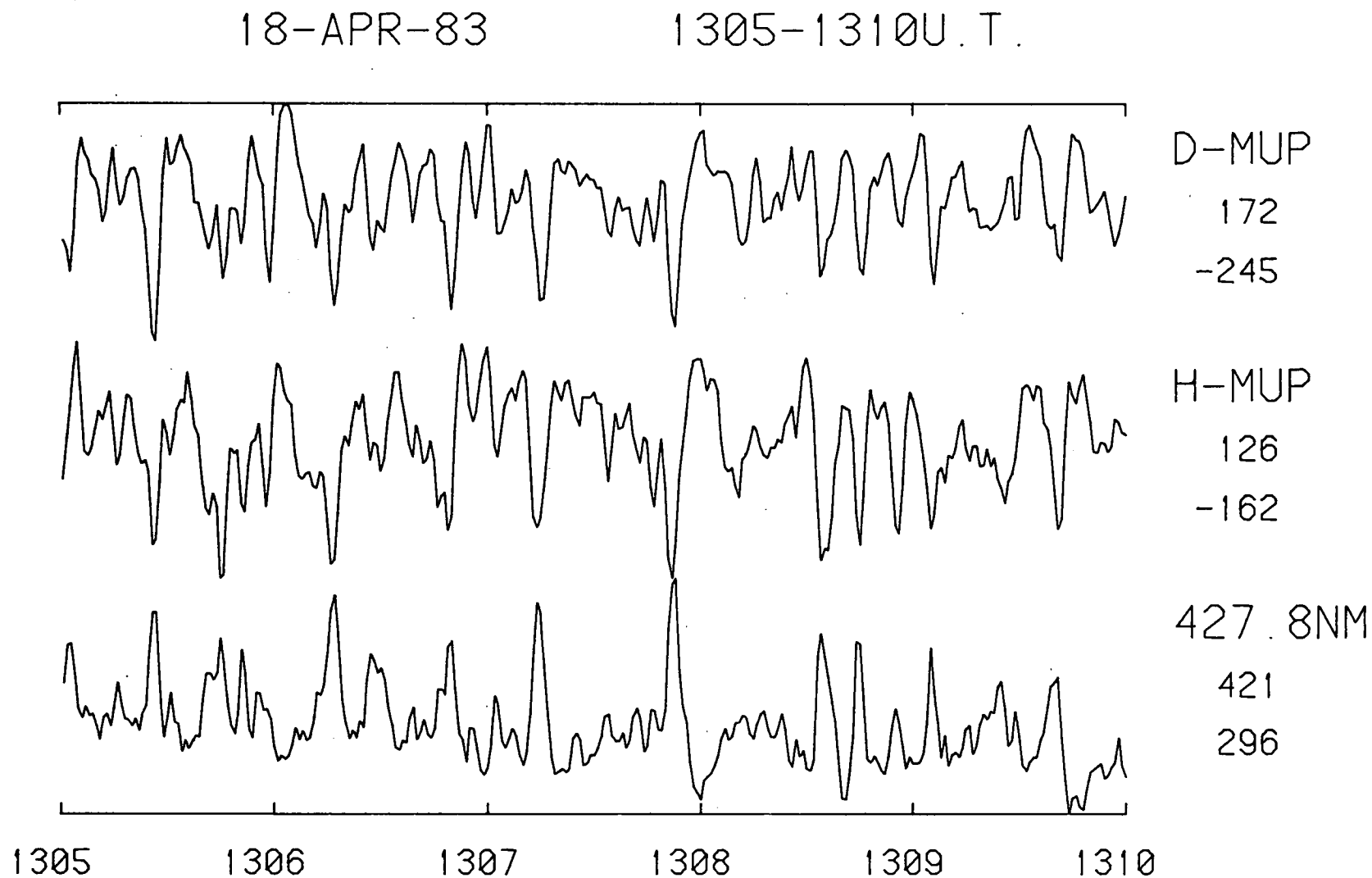


Figure 3.1(a) Plots of the 5-minute data files. Captions to the right indicate the file, and the maximum and minimum values for each block.



26-APR-83 1625-1630U.T.

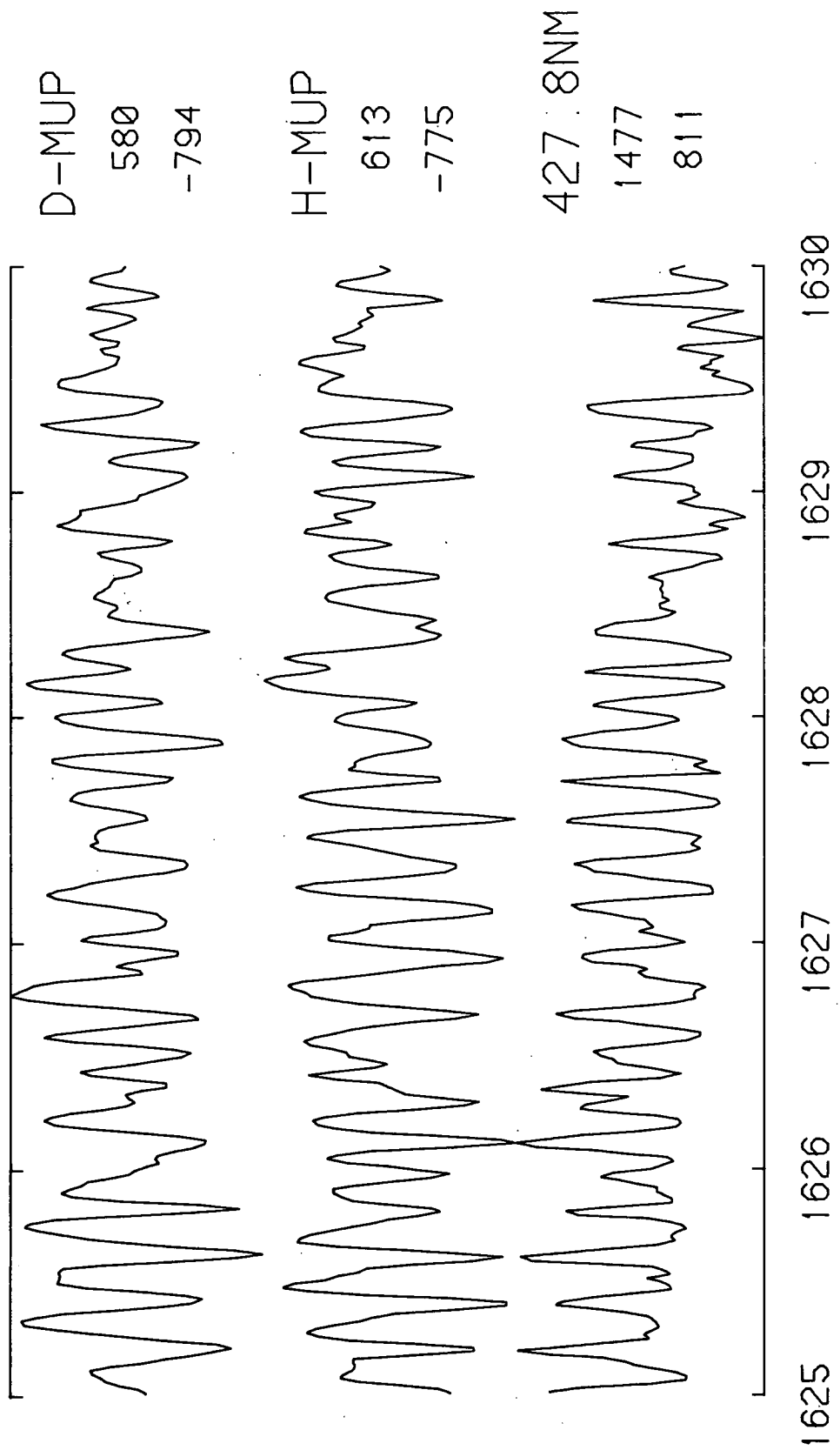


Figure 3.1(b)

28-APR-83

1350-1355U.T.

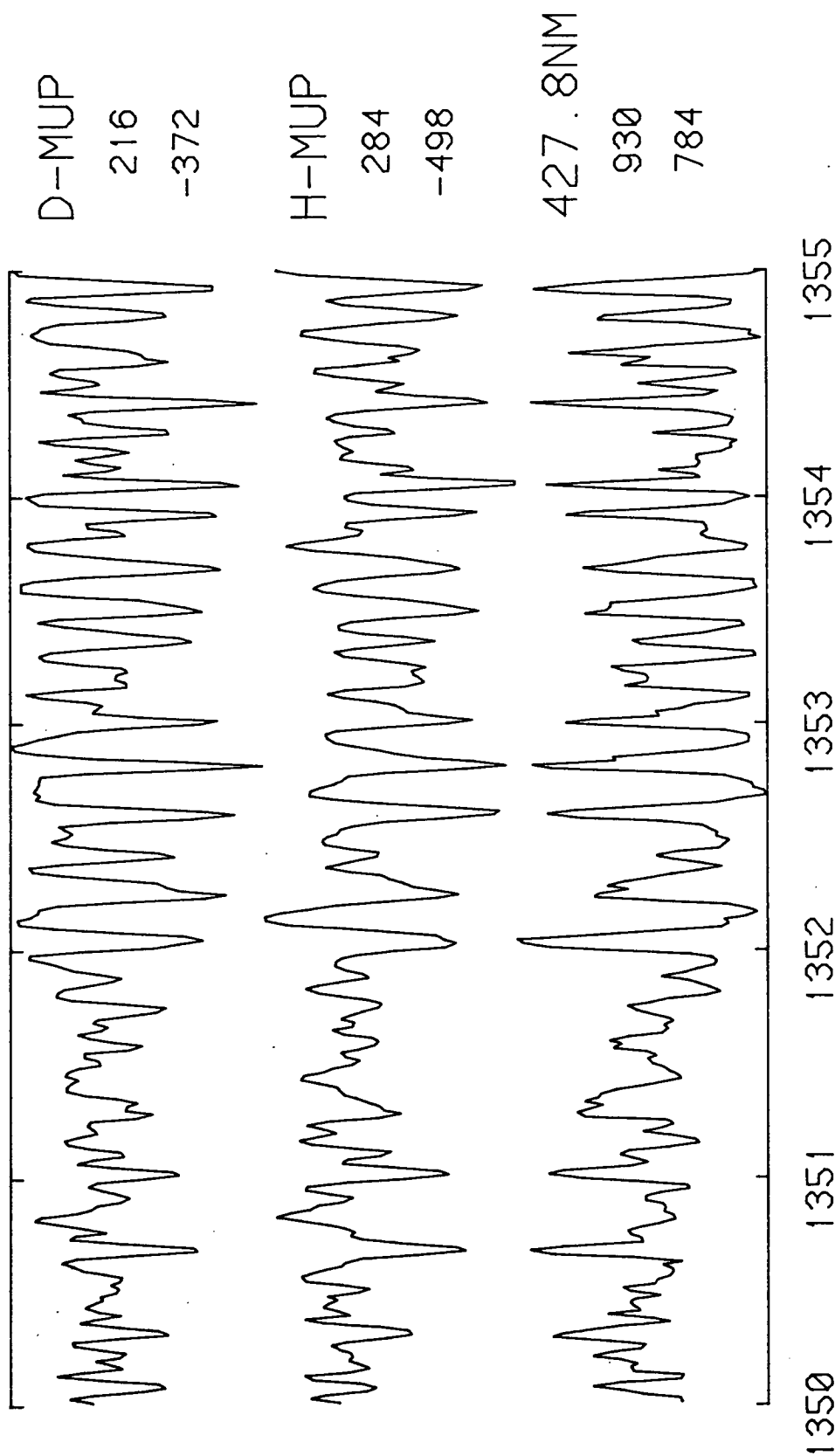


Figure 3.1(c)

28-APR-83 1355-1400U.T.

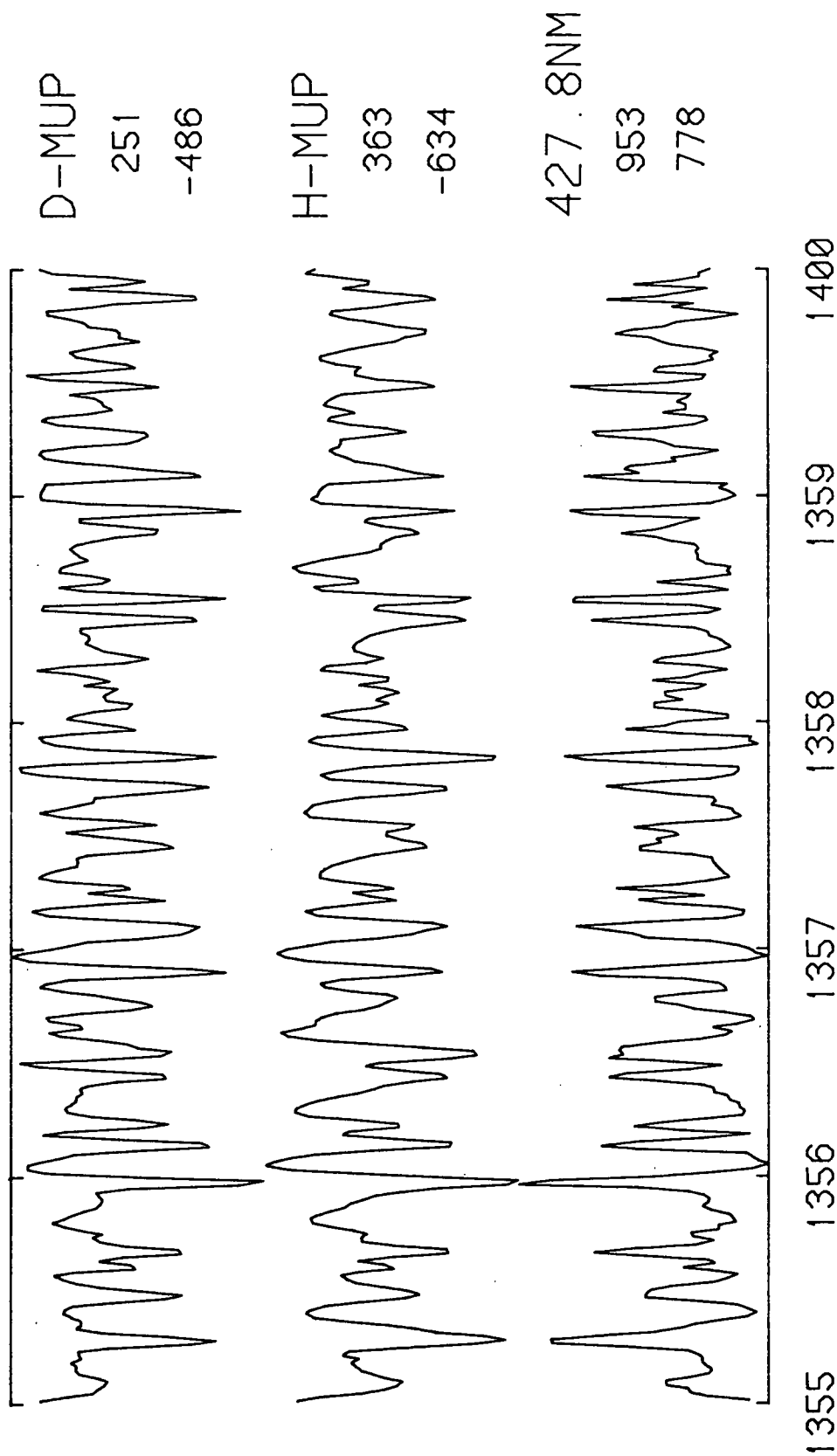


Figure 3.1(d)

23-MAY-83 1640-1645U.T.

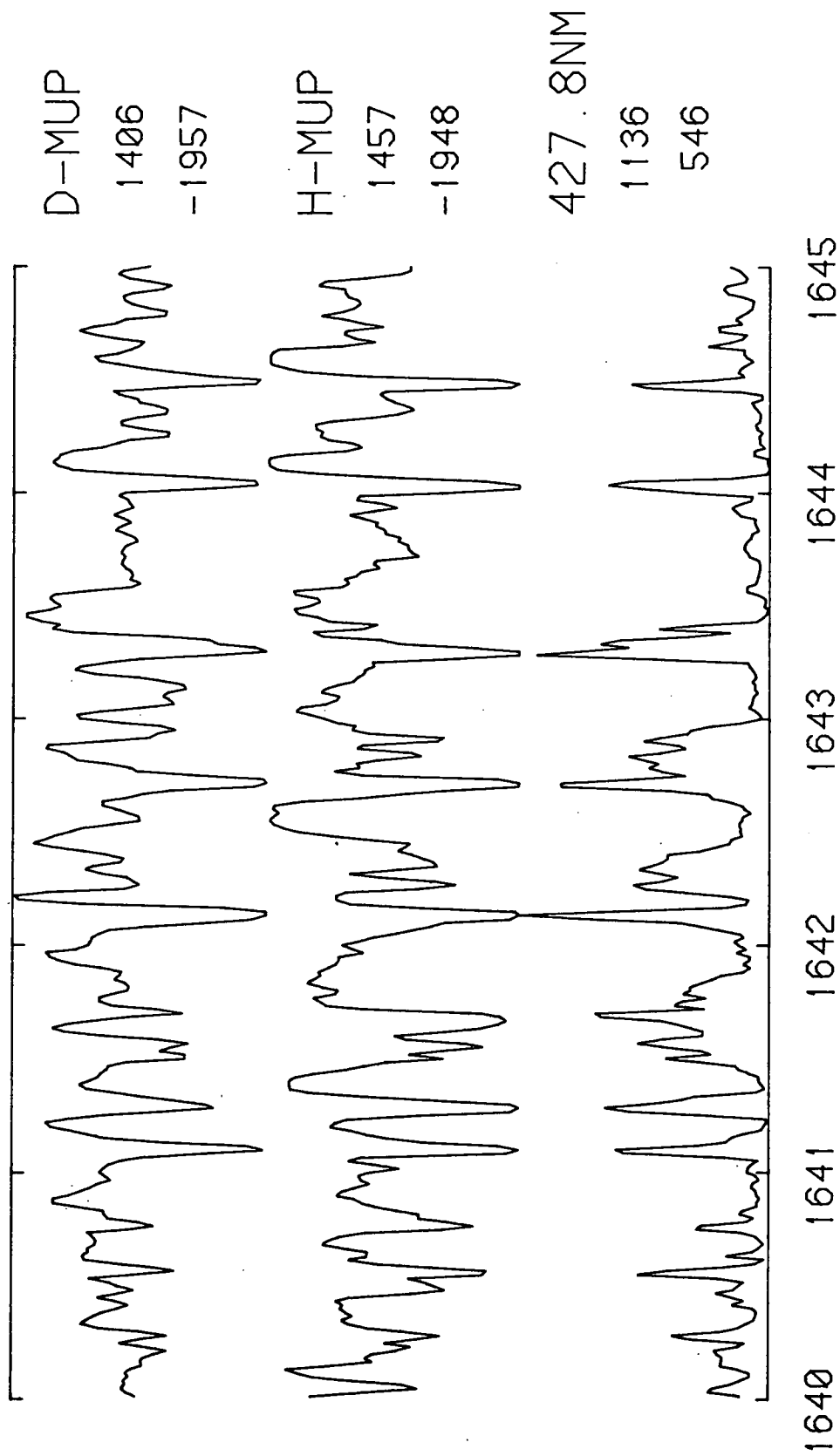


Figure 3.1(e)

07-SEP-83 1335-1340U.T.

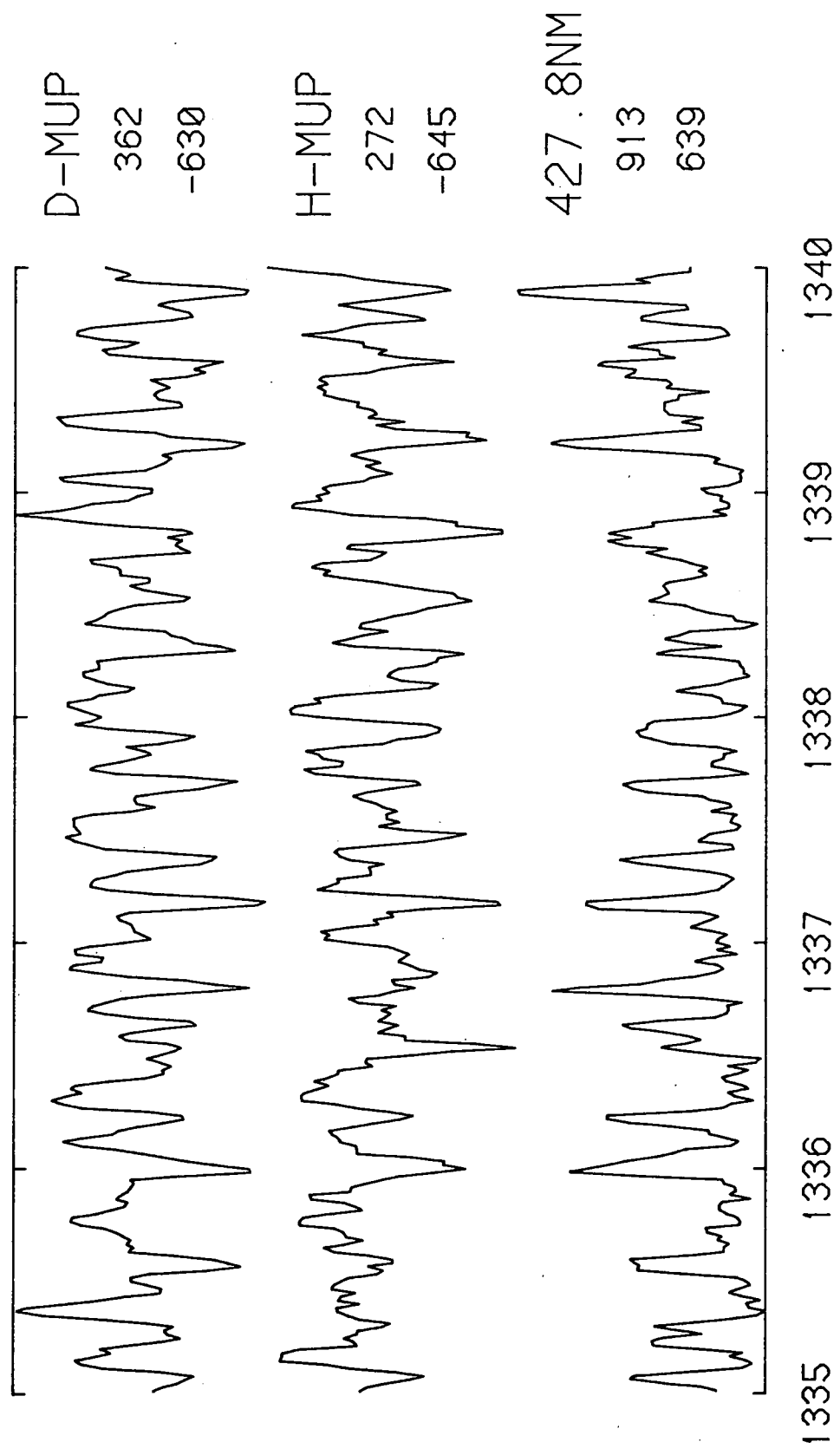


Figure 3.1(f)

Figure 3.1(b) 26-April-1983: 1625-1630Z

Excellent peaks of approximately 10-second period follow each other, with little time delay between pulses, in this data block. Pulse correspondence between the files is striking, with the smallest 4278Å variations being echoed by either or both of the H- or D-components. The minute peak at 16:25:30 even has an associated minor perturbation in the growing negative H-component pulse near 16:25:35.

This is in accord with Campbell (1970) who found from his Antarctic observations 'for every fluctuation of light in any part of the sky viewed by at least one of the photometers, there was a corresponding fluctuation of the magnetic field'. Oguti *et al.*, (1984) argue that 'the failure of previous studies to conclusively show the relationship between auroral and magnetic pulsations is due to inadequate coverage of the sky by single or multiple photometers'.

In this particular instance there are virtually no unmatched pulses in any of the three files. This indicates that the event was almost entirely confined to the local zenith (within the photometer field of view). The broader response zone of the coils, subjects them to variations outside the photometer region of observation, yet such extraneous fluctuations are absent here.

Optical peak heights reach nearly 400 units, somewhat greater than normal, with approximately 33% of the total light intensity fluctuating. A huge range of values has been reported on various occasions for this figure, from 10-30% (Kvifte and Petterson, 1969), to nearly 100% (Miller and Zeitz, 1971).

Figure 3.1(c),(d) 28-April-1983: 1350-1400Z

The second segment of this 10-minute block of data, 1355-1400Z, yielded the highest overall correlation for the year, -0.87 for both

components. As would be expected from this, the most intricate detail in the  $4278\text{\AA}$  emission is reflected in the micropulsation behaviour. Again, a strongly localized zenith event is postulated. Poor visibility and patchy cloud rendered the ASC photographs useless around this time.

All three channels,  $4278\text{\AA}$ , H- and D-micropulsations show a marked increase in activity from 13:52:00, with relative peak intensities and the asymmetry of pulse profiles being faithfully reproduced. Take for example the kinked peak at 13:53:00, and the split peak following immediately at 13:53:10, with further peak splitting at 13:56:10, 13:57:15, and 13:57:30. Running a ruler across the page quickly demonstrates the correspondence between the three data sets. This provides further evidence that the temporal near simultaneity is real, and not the chance result of a translation of a few minutes or so between files.

As discussed in Section 1.6, many researchers have reported this close temporal relationship between geomagnetic micropulsations and pulsating auroras (Vestine, 1943; Campbell 1970; Kazak, 1972; Reid, 1976; Lanzerotti et al., 1978; Heacock and Hunsucker, 1977a; Burns, 1983; Oguti et al., 1984). Despite this, the literature still occasionally contains arguments that this result can be used in support of the Coroniti and Kennel (1970a) theory (Scourfield et al., 1983). Coroniti and Kennel (1970a,b) postulated that geomagnetic micropulsations are indirectly responsible for the pitch angle diffusion of precipitating electrons at the geomagnetic equator. Detection of micropulsations on the ground cannot be used as such evidence. If equatorial micropulsations are responsible for structuring the electron fluxes, these must be different from those micropulsations measured in association with pulsating aurora in the auroral zone, which have been shown to be

closely correlated, within seconds, to the auroral fluctuations. Equatorial region micropulsations will require a travel time (at the Alfvén speed) of the order of a few minutes, compared to the few seconds taken by the auroral electrons.

Figure 3.1(e) 23-May-1983: 1640-1645Z

The data set here is characterised by the discrete nature of the pulsations present. Sharp, irregular pulses present powerful evidence of the close temporal connection between the optical auroral fluctuations and Pi(c) micropulsations, with definitive peak matching at 16:41:05, 16:41:15, 16:42:05, 16:42:40, 16:43:15, 16:44:00, and 16:44:30. Note also the magnitude of the variations, with 50% of the total light fluctuating, and the magnetic components nearing coil saturation.

Another important feature shows up clearly as a result of the sharpness of the pulses, and their wide separation. Both the H and D pulses are followed by a smaller magnitude, broader pulse in the positive direction after their original negative excursion. This is particularly evident when no other pulses follow immediately after, the peak at 16:44:00, being a classic example.

Figure 3.1(f) 07-September-1983: 1335-1340Z

The final set in this series of strongly correlated data again features sharp, short-period (5-6s) pulses at irregular intervals. D-component variations follow the  $4278\text{\AA}$  emission more closely than does the H-component. Apart from the initial major peak at 13:36:25, the relative peak height correspondence between the D-component and the optical trace, is extremely good. This early pulse receives a particularly strong echo in the H-micropulsation signal.



Figures 3.1(a-f) contain some of the best data obtained for the year. Both magnetic components provide definitive evidence for their association in time with auroral optical pulsations. However, almost twice as many closely correlated  $4278\text{\AA}/\text{D}$ -micropulsation files as  $4278\text{\AA}/\text{H}$ -micropulsation files, were obtained. It is clear that the D-component is in general, far more likely to yield a correlation than the H-component. This is in agreement with the numerically limited data set gathered by Burns (1983).

Examples where the D-component correlation is highly significant, whilst the H-micropulsations exhibit negligible correspondence with the optical trace, are shown in Figures 3.2(a,b). For the 19-February-1983, 1350-1355Z interval, the D-micropulsations follow the optical variations quite rigorously. Although a number of the optical peaks are matched by H-component pulses (13:50:02, 13:51:00, 13:51:40 and the major pulse at 13:52:08), the association is marred by many pulses that do not appear in either the D or  $4278\text{\AA}$  channels.

A similar situation exists in the data set for 31-March-1983, 1430-1435Z. In this case the D-component is very strongly correlated after 14:32:00, but the H trace has many discrepancies. Unmatched H-micropulsations are present at 14:31:00, 14:31:40, 14:31:55, 14:32:20, 14:33:25, and 14:33:40. Some H-micropulsations even appear to yield a positive correlation with respect to the optical fluctuations, for example at 14:30:05 and 14:34:10.

Alternatively, a few files were recorded wherein the H-micropulsations yielded excellent peak-to-peak correspondence, whilst the D-component displayed a much weaker association. Figures 3.3(a,b) illustrate this situation. Interestingly, the D-component diminished correlation does not generally arise from a presence of extra peaks in the D-file,

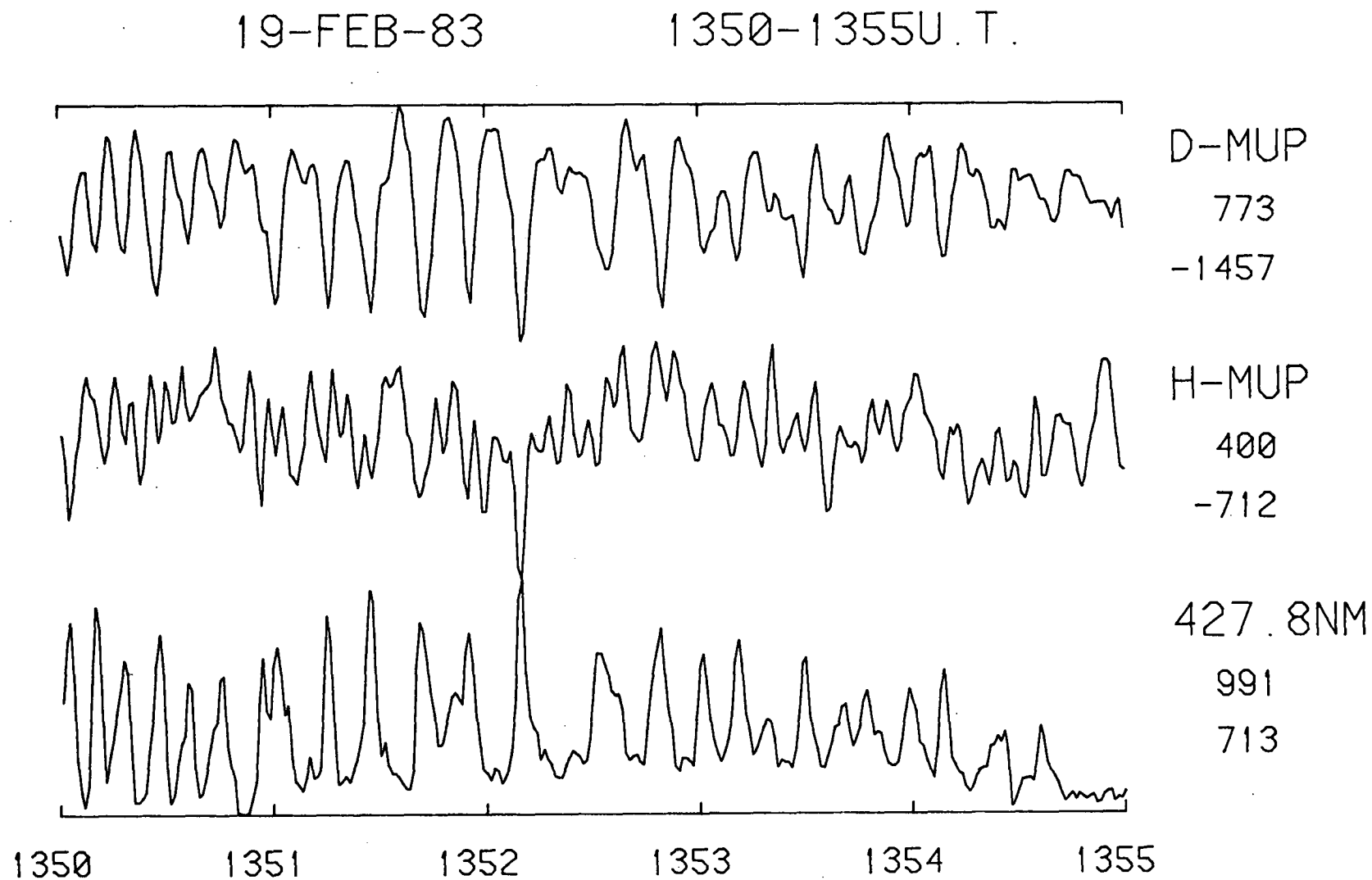


Figure 3.2(a) Example of data files for which the D component matches the optical variations well, whilst the H component suffers many poorly matched fluctuations.

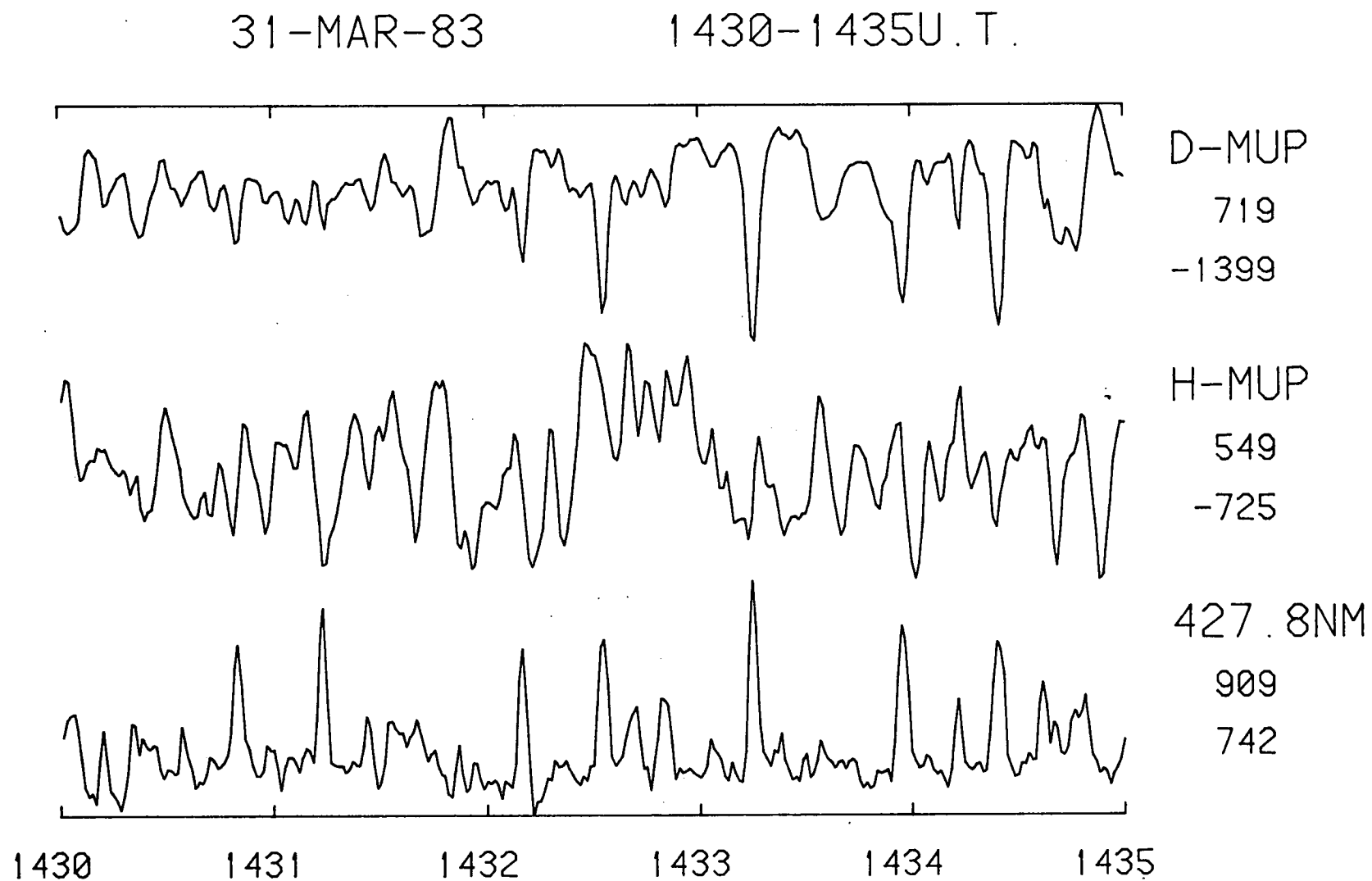


Figure 3.2(b) Again the H file exhibits many peaks with no echo in either the optical or D channels.

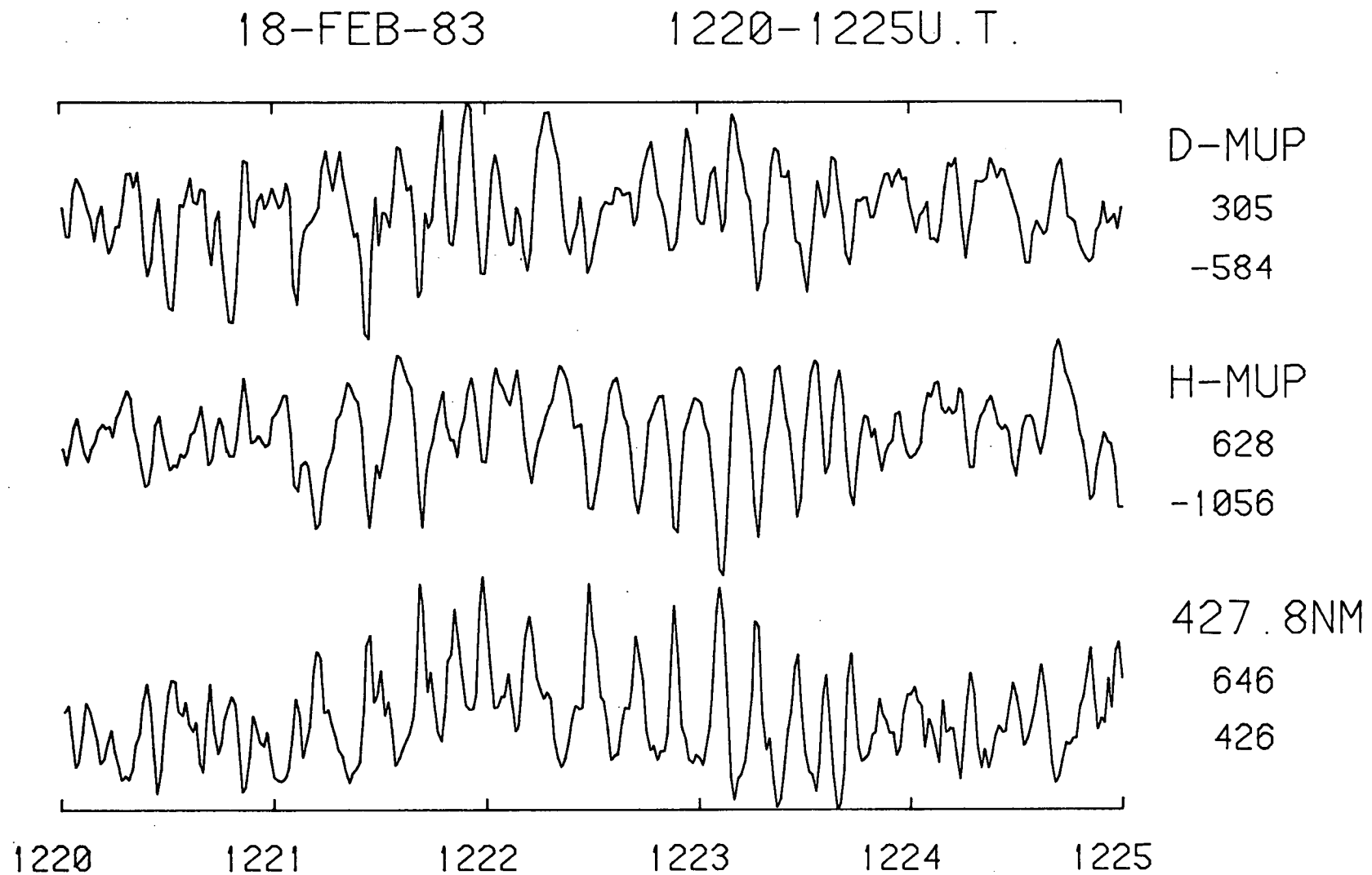


Figure 3.3(a) Weaker D correlation resulting from diminished response to optical peaks, rather than an over-abundance of unmatched pulses.

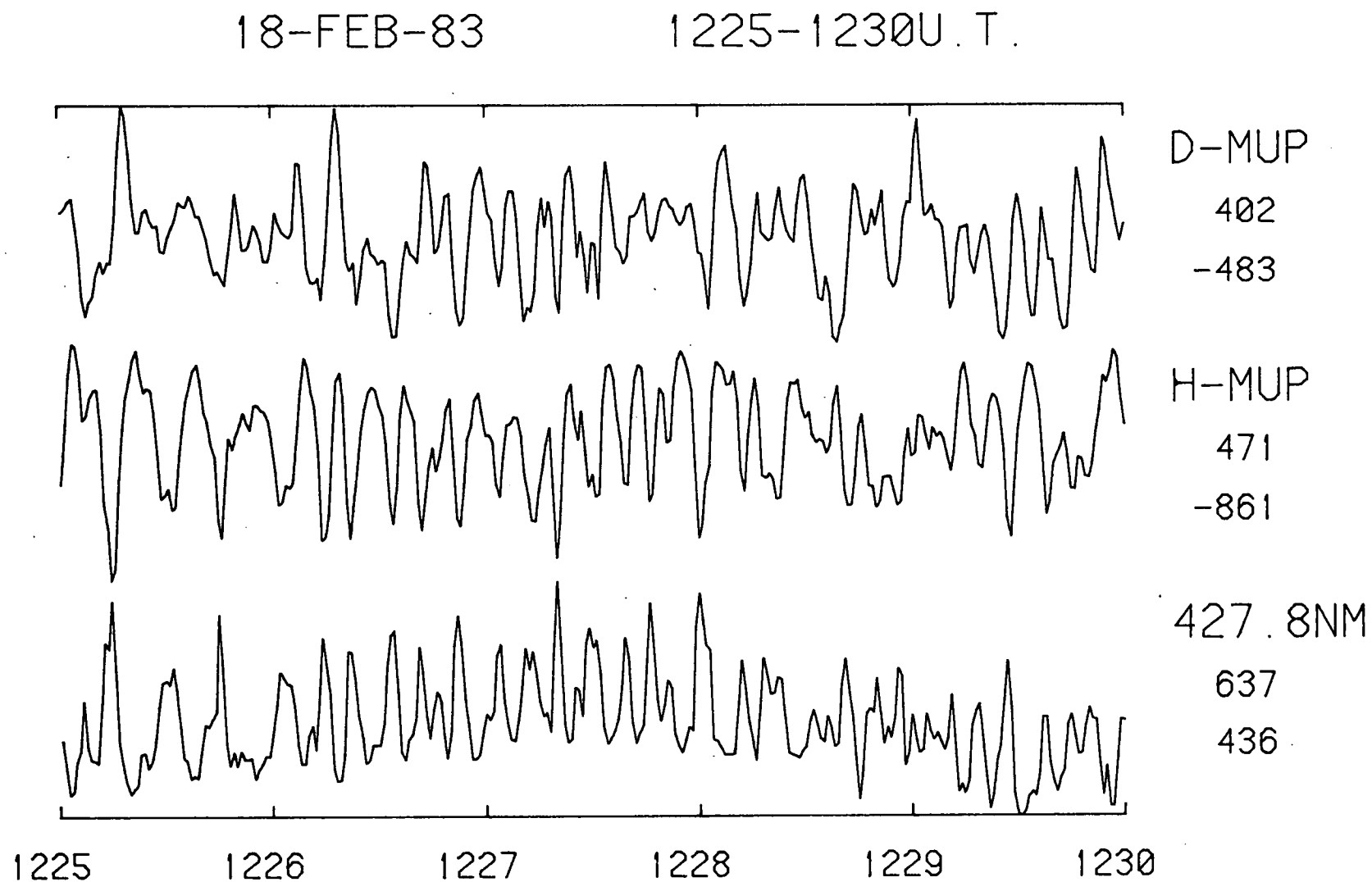


Figure 3.3(b) Further example of a smaller correlation for the D component with possible positive correlation of peaks at 12:25:15, 12:26:40, and 12:29:30.

but rather from the absence of, or weaker response to, major optical peaks. 18-February-1983: 1220-1225Z data block shows this quite clearly at 12:21:10, 12:22:45, 12:23:05, and 12:23:35. Occasionally a D-micropulsation is found to correlate positively with the optical emission, such as at 12:25:15, 12:26:40, and 12:29:30 in the second interval of this set.

### 3.3 MATHEMATICS OF THE CORRELATIONS

Prior to the installation of the RL02 hard-disk system, lack of data storage space necessitated the use of a Fourier analysis test program to determine if the  $4278\text{\AA}$  optical channel had an appropriate spectral range to warrant retention. In all successful cases, micropulsation activity was found to be present in the H and D files. The larger storage volume of the RL02 enabled all files to be saved for examination in the latter part of the year, 26-August-1983 until 10-October-1983.

The geomagnetic Z-component was not collected by the computer system for use in the subsequent data analysis. It has been shown to be very closely related to the H-component. Burns (1983) found the magnitude of this correlation to be typically of the order of 0.90, with the Z-micropulsations having a nominal lag of 0.3s with respect to the H-component. Burns (1983) also points out that even the large-scale Macquarie Island magnetograms display a strong correspondence between the H and Z components. The latter was also found to be the case for the data presented here, see Figure 3.4.

Initial data analysis consisted of plotting out the three files,  $4278\text{\AA}$  band emission, H and D micropulsations, in their 5-minute blocks for visual inspection. Immediately it was obvious that a large proportion of the files exhibit significant peak-to-peak

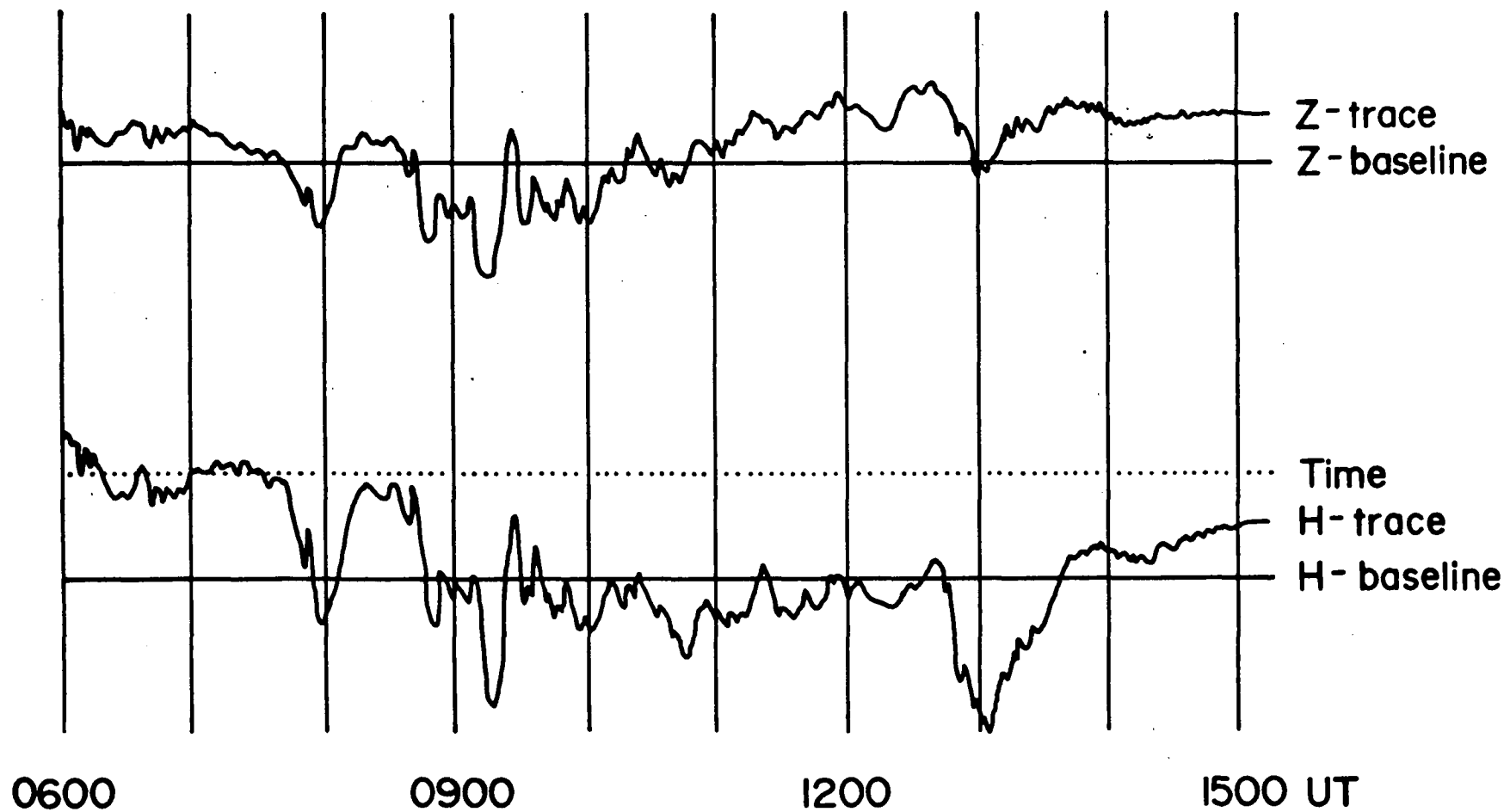


Figure 3.4(a) Portion of a BMR magnetogram depicting the close association between the H and Z components as determined at Macquarie Island, 26-September-1983.

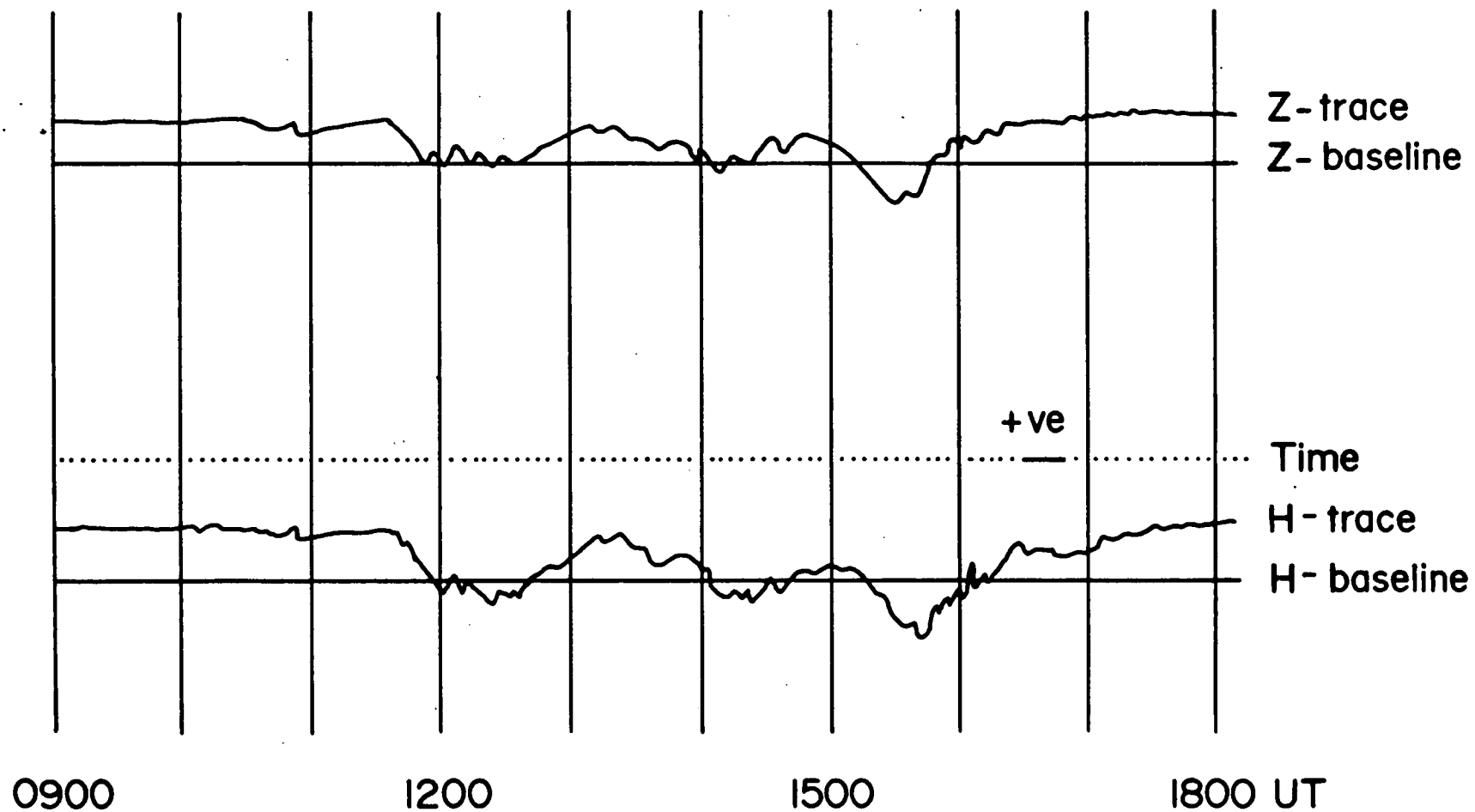


Figure 3.4(b) As for (a) measured during a less active period on 18-April-1983.



correspondence between the  $P_i(c)$  micropulsations and optical pulses. This was found to be particularly so for the D component.

Notice, in the files reproduced in Figures 3.1, 3.2, and 3.3, that the micropulsation values may be either positive or negative. Since the coils measure the time rate of change of the magnetic field, to a first approximation, then this is to be expected. A zero value corresponds to a stationary point of the field variations.

Subsequently the data was fed into a cross-correlation program that evaluates the correspondence, point-for-point, at a series of different lead-lag times. Let  $\{x(t)\}$  represent a 1500 point, 5-minute 4278Å file (sampled every 0.2s), and  $\{y(t)\}$  be the associated 1500 point, 5-minute micropulsation file. The cross-correlation function is then defined as:

$$v_{xy}(u) = \frac{1}{\sigma_x \sigma_y} \cdot \frac{1}{N-u} \cdot \sum_{t=1}^{N-u} [x(t+u) - \bar{x}] [y(t+u) - \bar{y}]$$

for  $u \geq 0$

$$= \frac{1}{\sigma_x \sigma_y} \cdot \frac{1}{N-|u|} \cdot \sum_{t=|u|+1}^N [x(t+u) - \bar{x}] [y(t+u) - \bar{y}]$$

for  $u \leq 0$

where:

$$N = 1500$$

$$\sigma_x, \sigma_y = \text{standard deviations}$$

$$\text{(e.g. } \sigma_x = \sqrt{\frac{\sum_{i=1}^N f_i (x_i - \bar{x})^2}{\sum_{i=1}^N f_i}} \text{ )}$$

$$\bar{x}, \bar{y} = \text{averages}$$

$$\text{(e.g. } \bar{x} = \frac{\sum_{i=1}^N f_i x_i}{\sum_{i=1}^N f_i} \text{ )}$$

18-APR-83

1305-1310U.T.

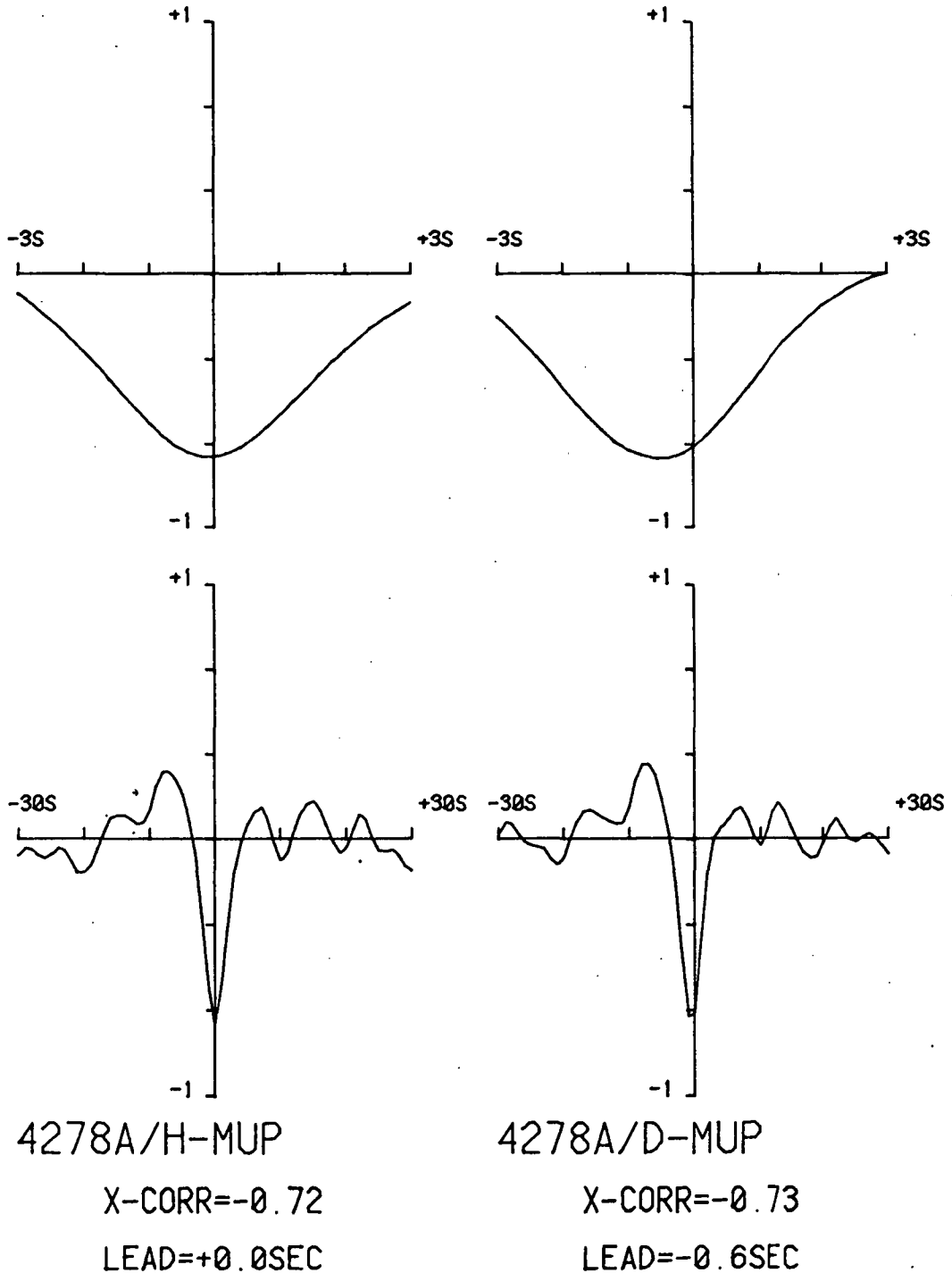


Figure 3.5(a) The optical-micropulsation cross-correlation functions plotted in two lead-lag ranges,  $\pm 30s$ , and in expanded form over  $\pm 3s$ . A negative value implies that the optical pulse leads the micropulsation. These functions correspond to the data files produced in Figure 3.1.

26-APR-83

1625-1630U.T.

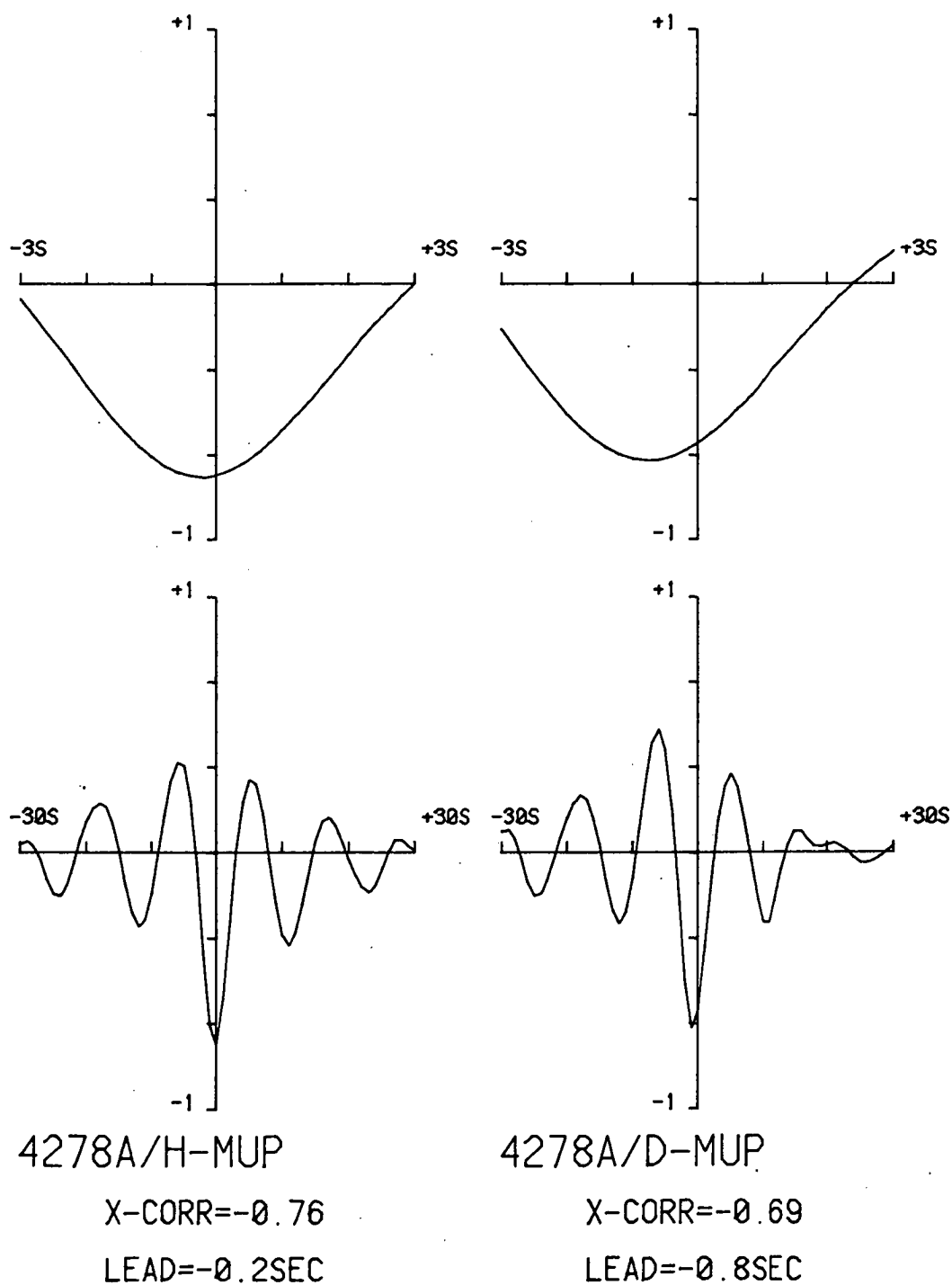
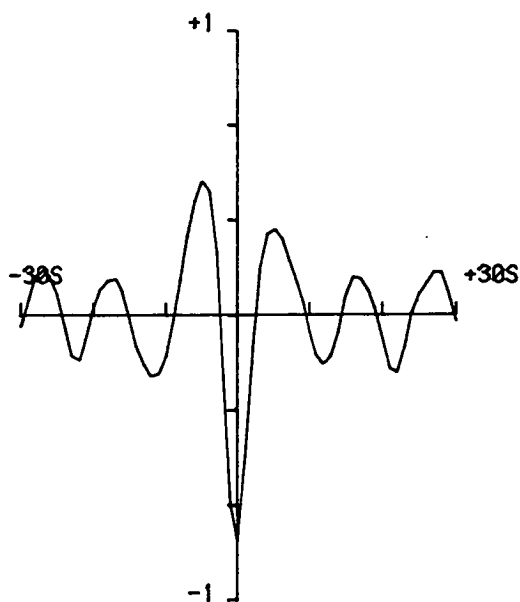
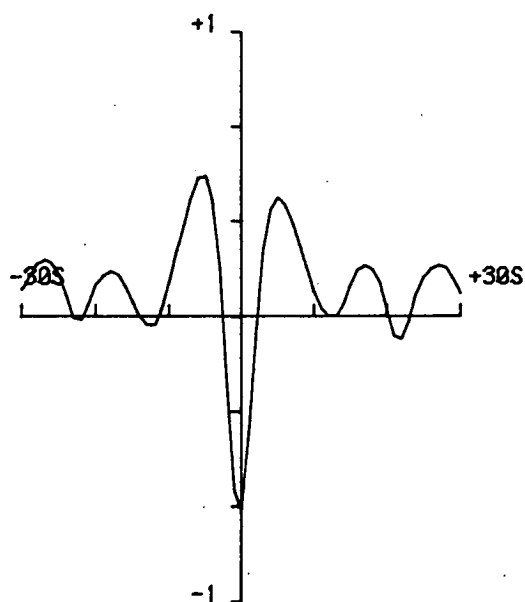
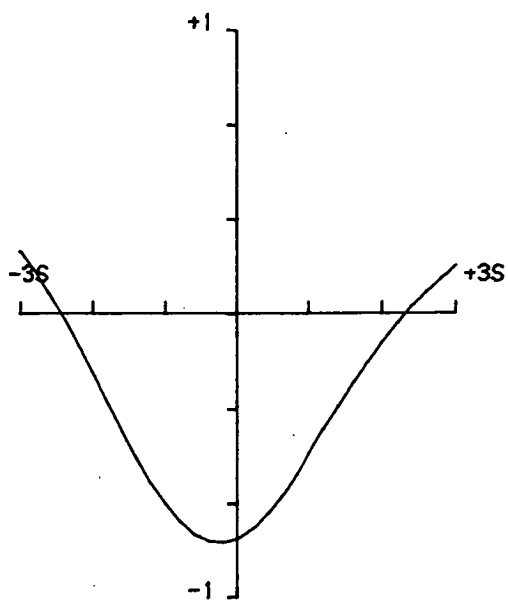
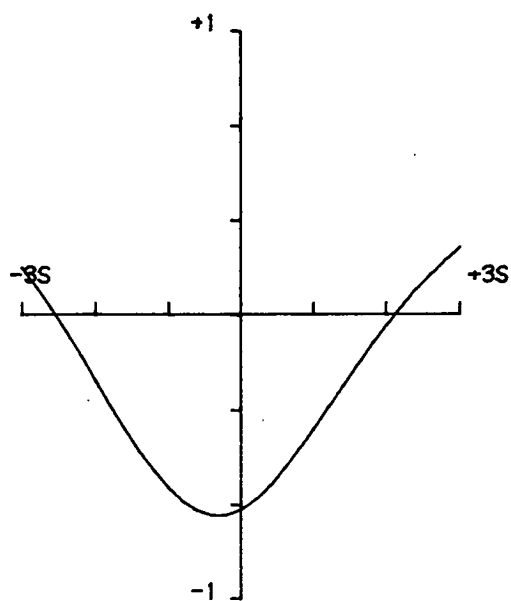


Figure 3.5(b)

28-APR-83

1350-1355U.T.



4278A/H-MUP

X-CORR=-0.71

LEAD=-0.4SEC

4278A/D-MUP

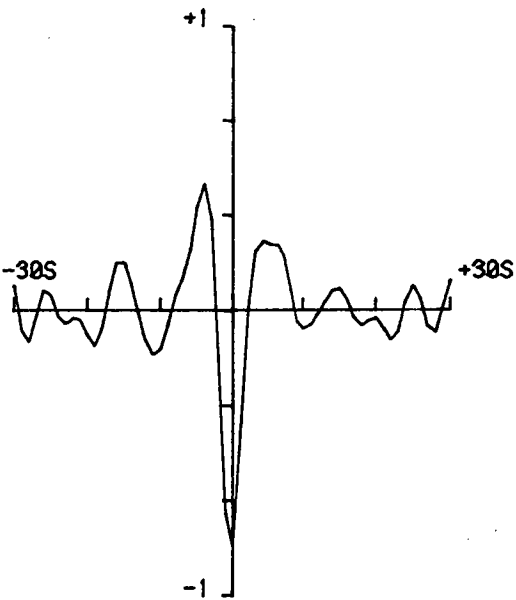
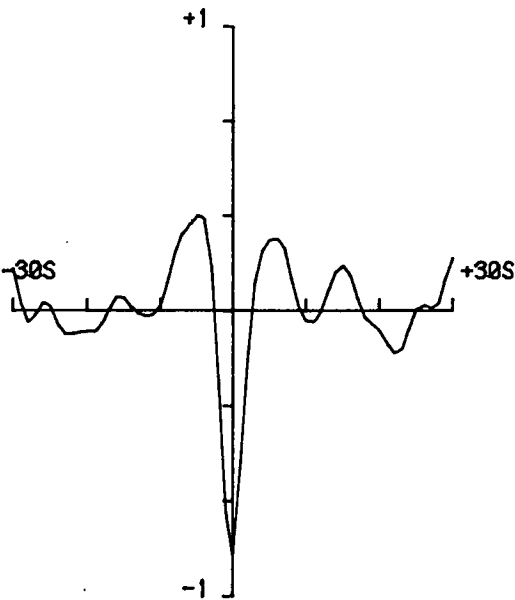
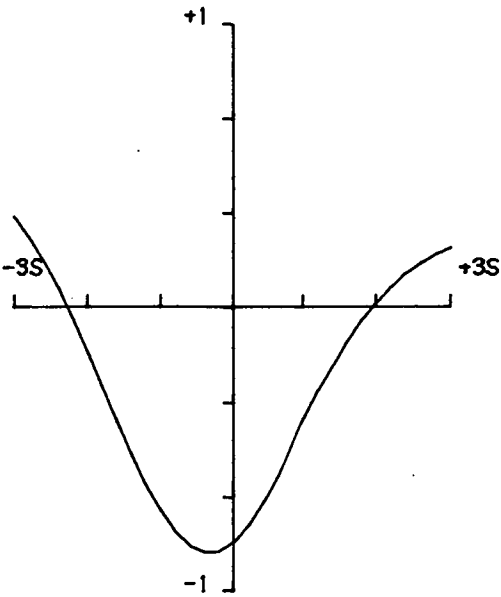
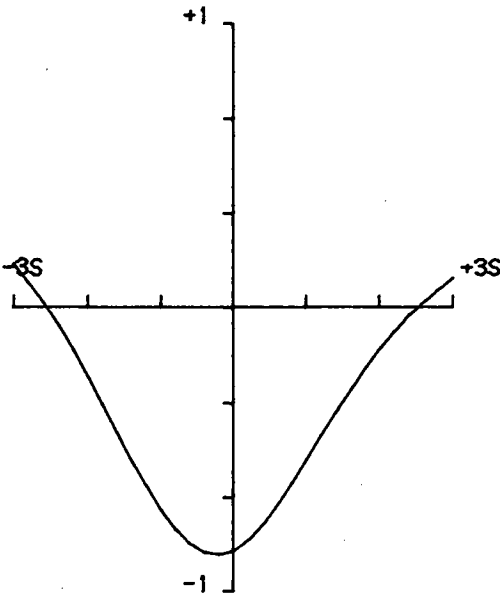
X-CORR=-0.81

LEAD=-0.2SEC

Figure 3.5(c)

28-APR-83

1355-1400U.T.



4278A/H-MUP

4278A/D-MUP

X-CORR=-0.87

X-CORR=-0.87

LEAD=-0.2SEC

LEAD=-0.4SEC

Figure 3.5(d)

23-MAY-83

1640-1645U.T.

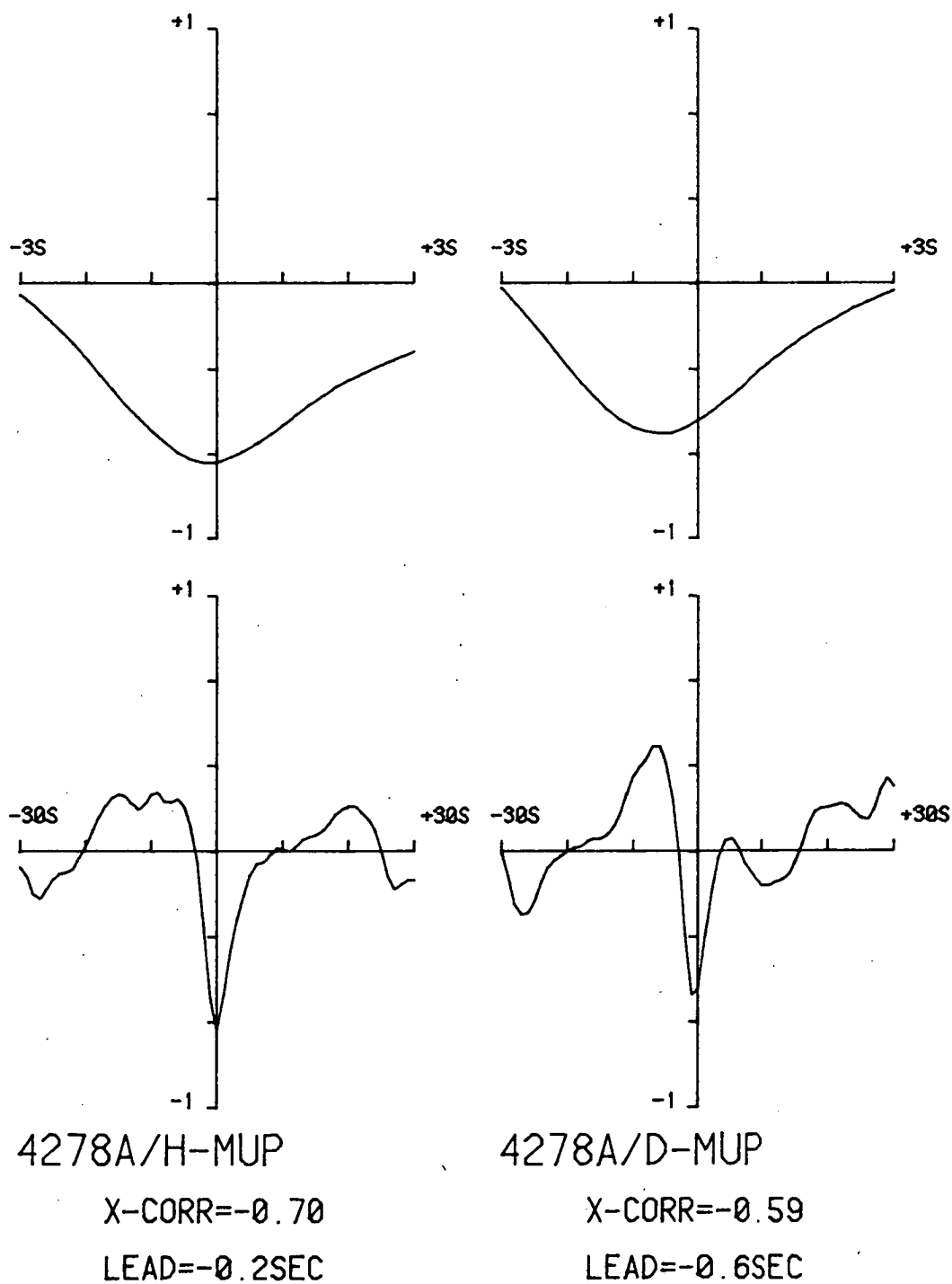
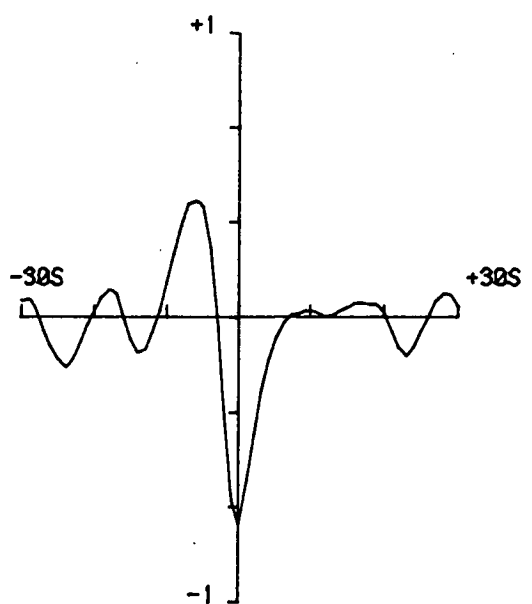
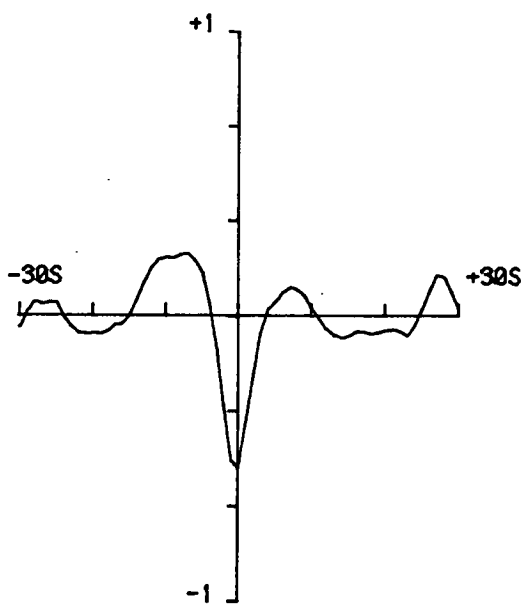
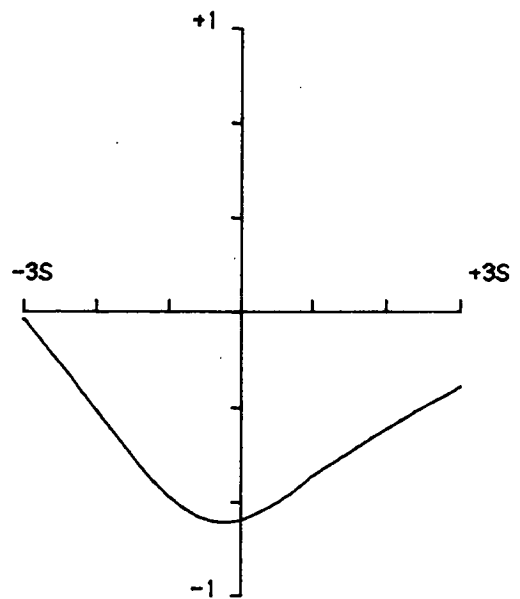
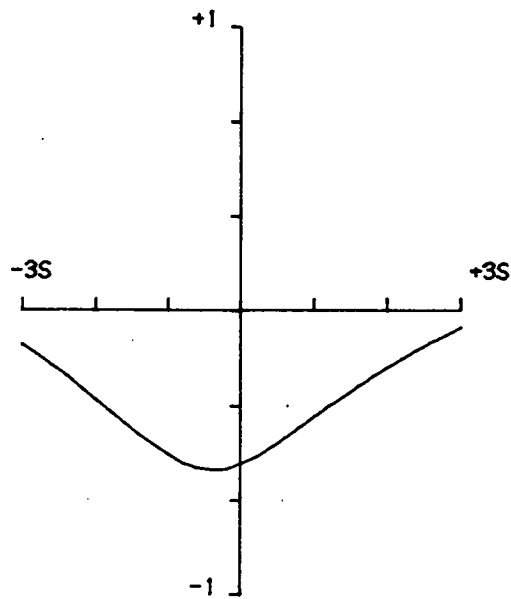


Figure 3.5(e)

07-SEP-83

1335-1340U.T.



4278A/H-MUP

X-CORR=-0.56

LEAD=-0.4SEC

4278A/D-MUP

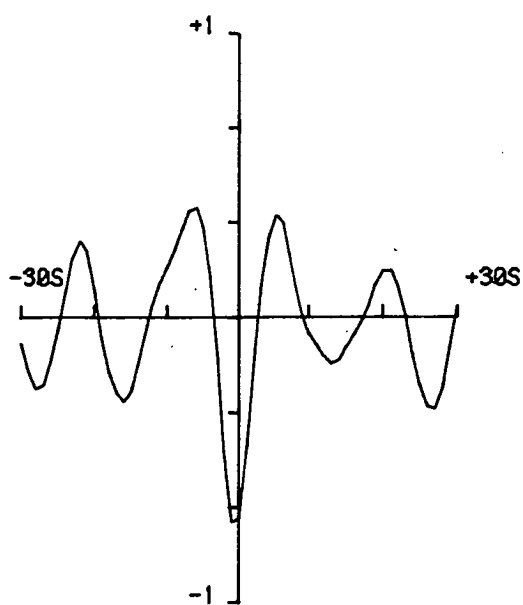
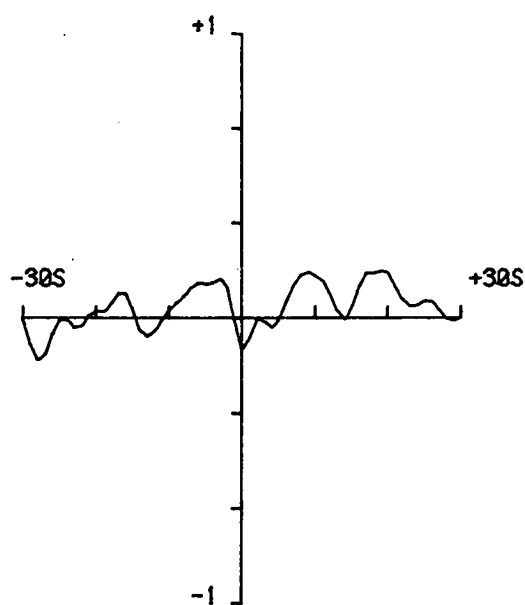
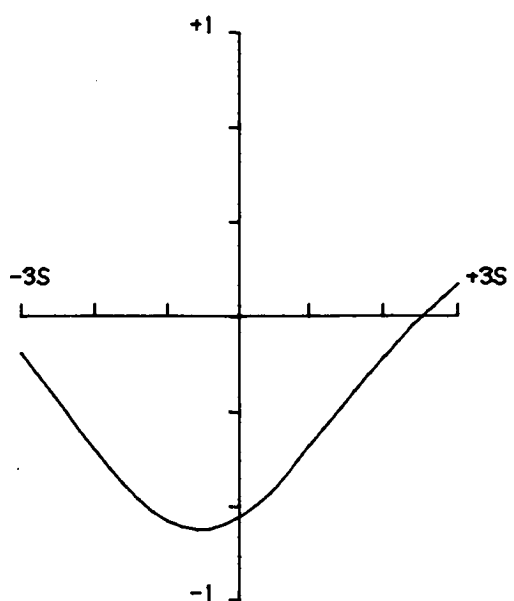
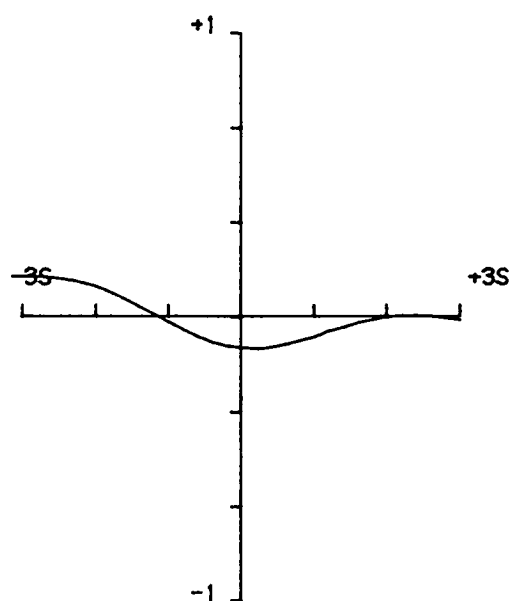
X-CORR=-0.74

LEAD=-0.2SEC

Figure 3.5(f)

19-FEB-83

1350-1355U.T.



4278A/H-MUP

4278A/D-MUP

X-CORR=-0.11

X-CORR=-0.75

LEAD=+0.2SEC

LEAD=-0.6SEC

Figure 3.6(a) Correlation functions for the data files of Figure 3.2.



31-MAR-83

1430-1435U.T.

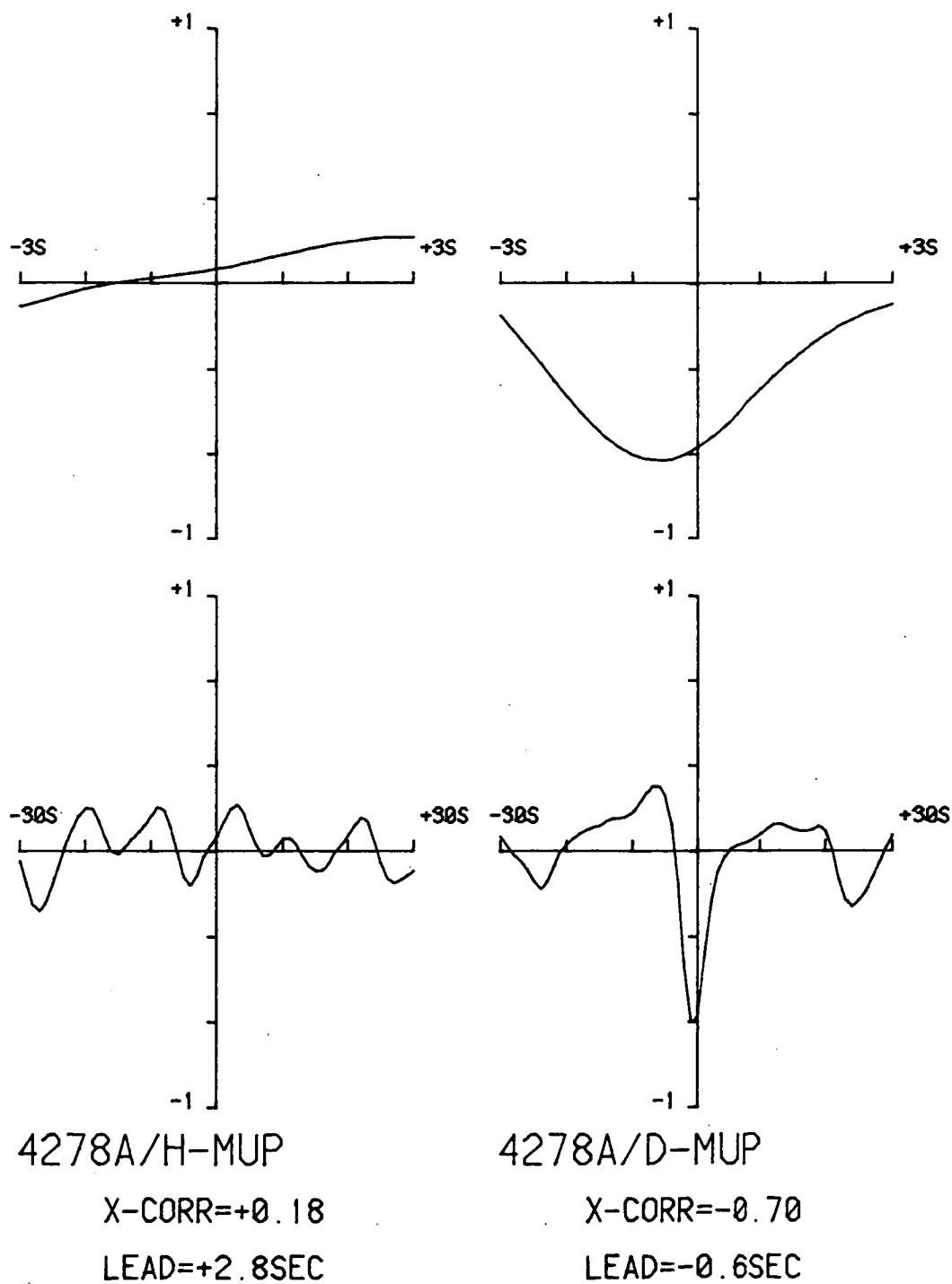


Figure 3.6(b)

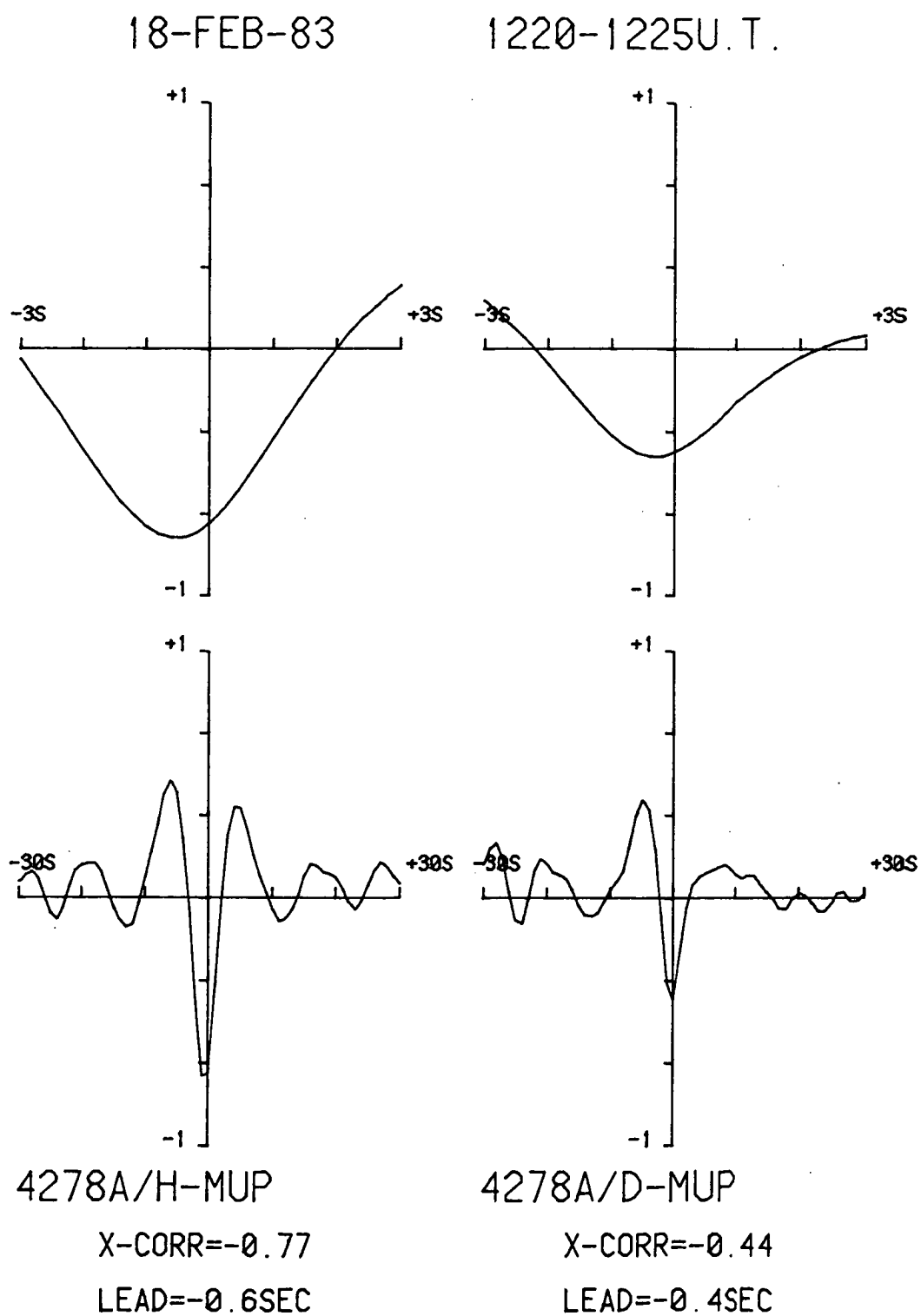
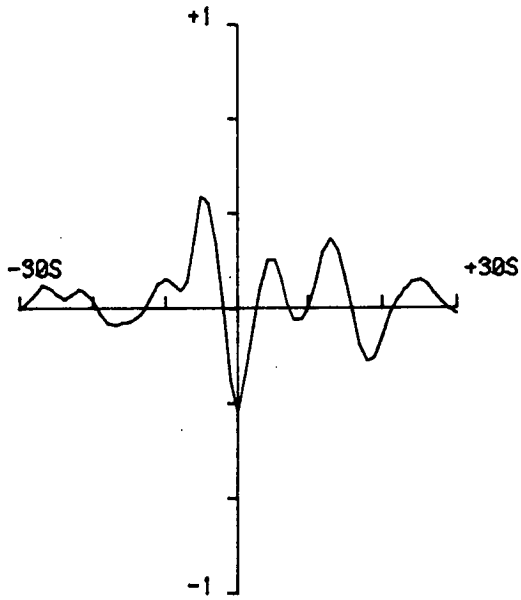
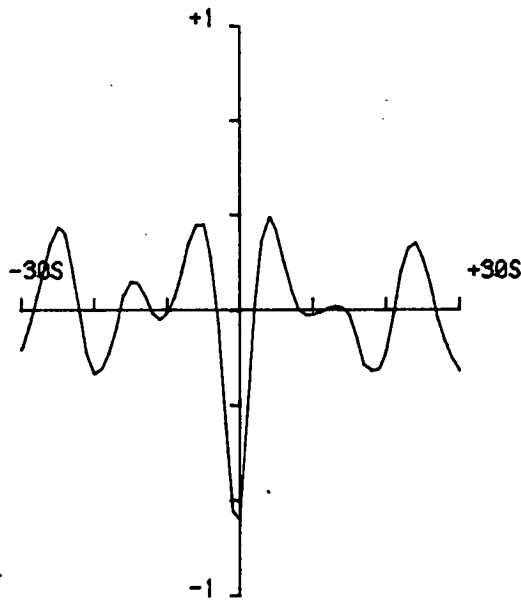
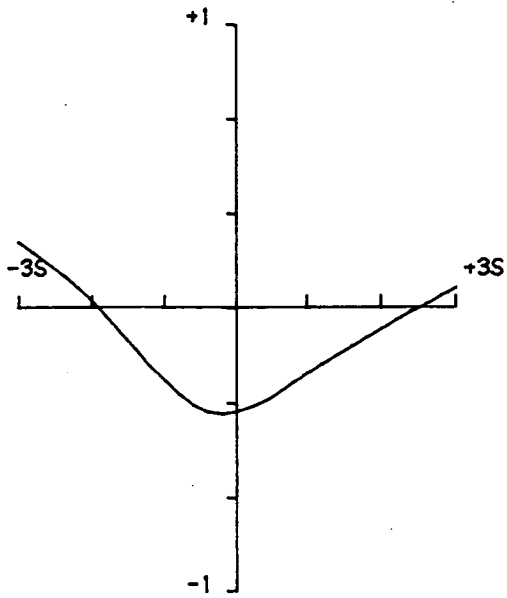
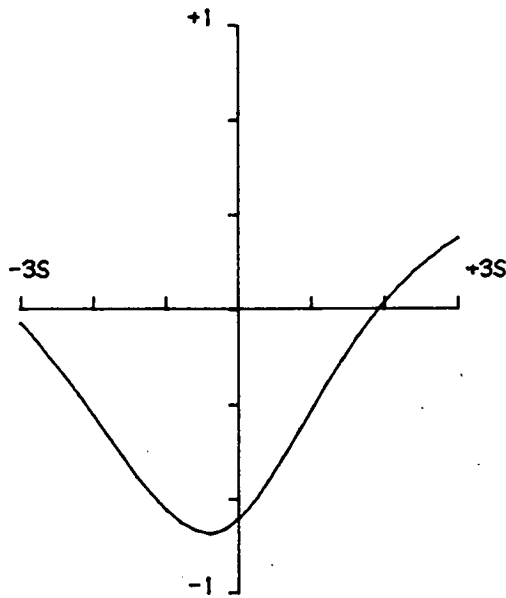


Figure 3.7(a) Correlation functions for the data files of Figure 3.3.

18-FEB-83

1225-1230U.T.



4278A/H-MUP

4278A/D-MUP

X-CORR=-0.79

X-CORR=-0.38

LEAD=-0.4SEC

LEAD=-0.2SEC

Figure 3.7(b)

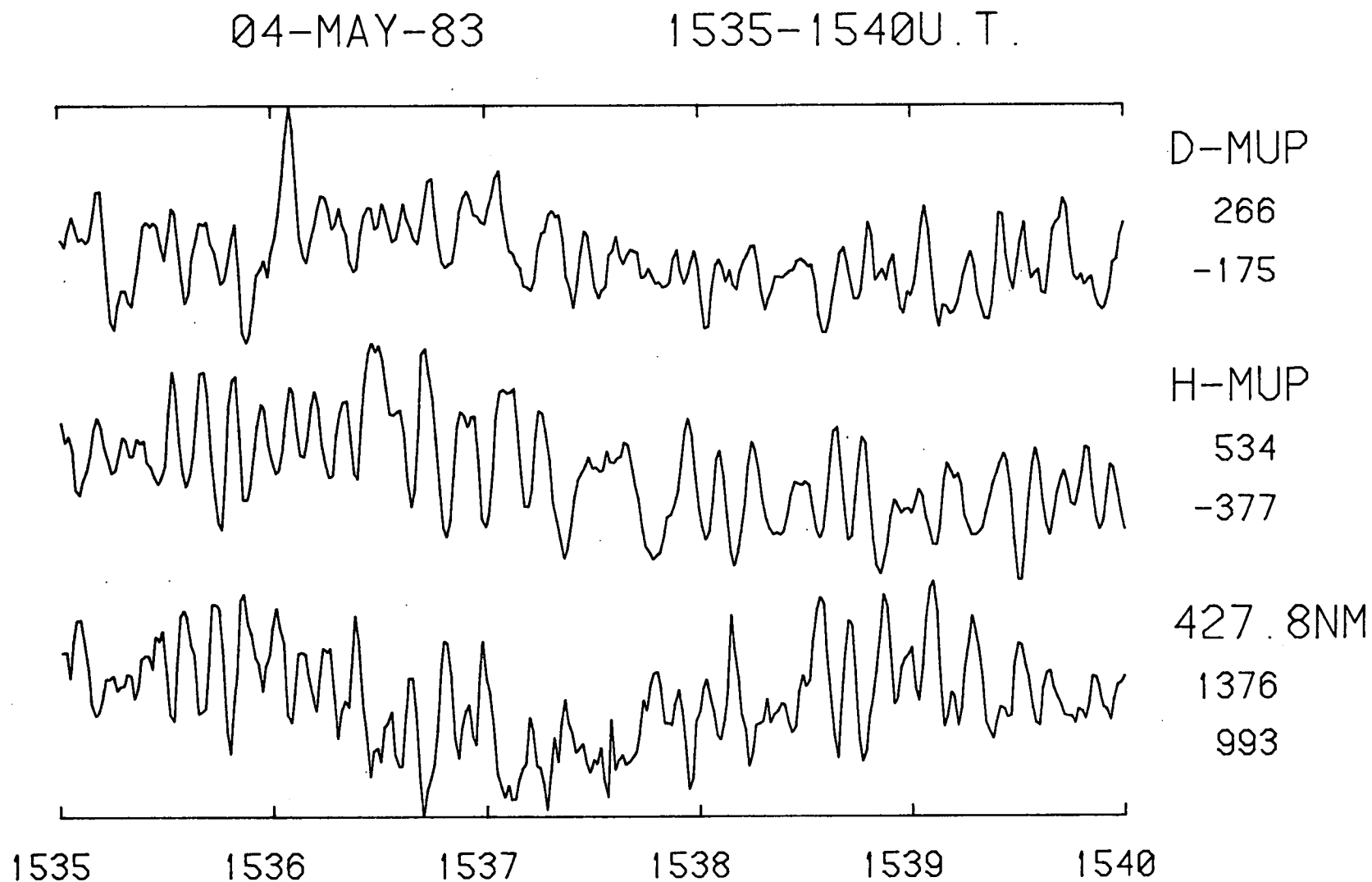


**Figure 3.8(a)** Data file in which the slow long term trend of the optical channel drifts in and out of phase with the micropulsation background variation.

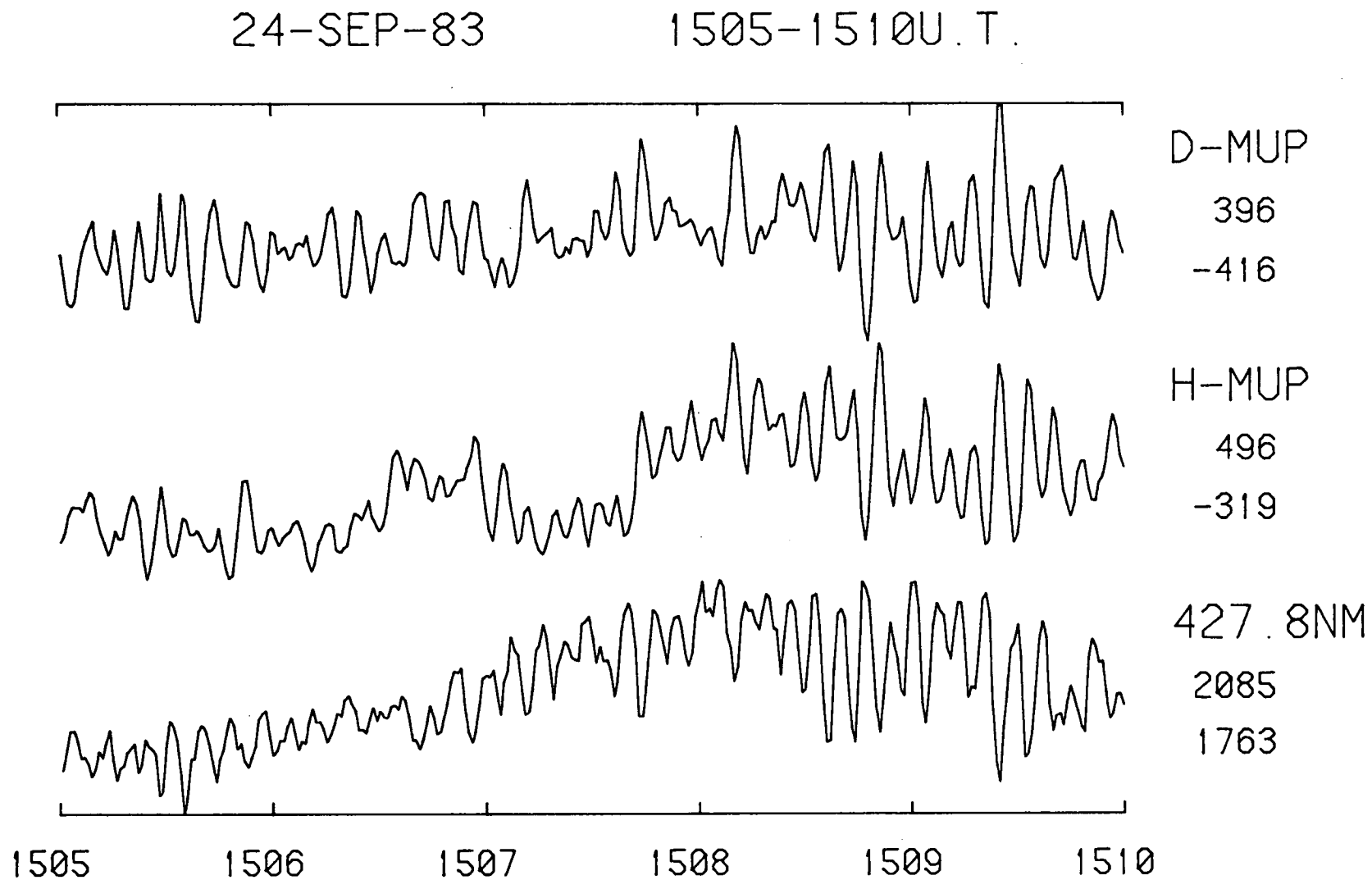


Figure 3.8(b) Here the background drifts remain relatively constant with respect to each file.

04-MAY-83

1535-1540U.T.

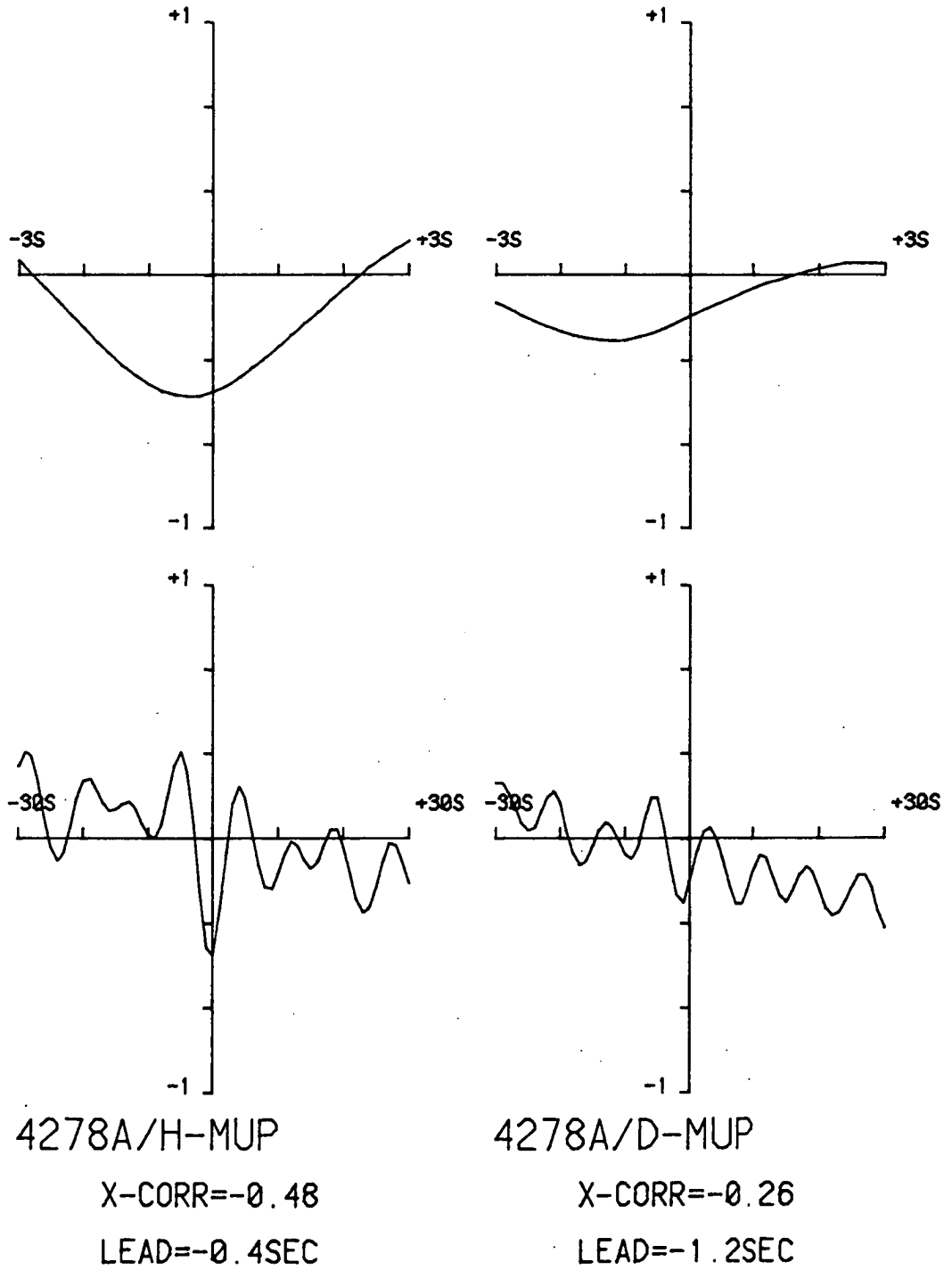


Figure 3.9(a) Gradient superimposed on normal correlation function due to long term trend in Figure 3.8(a).

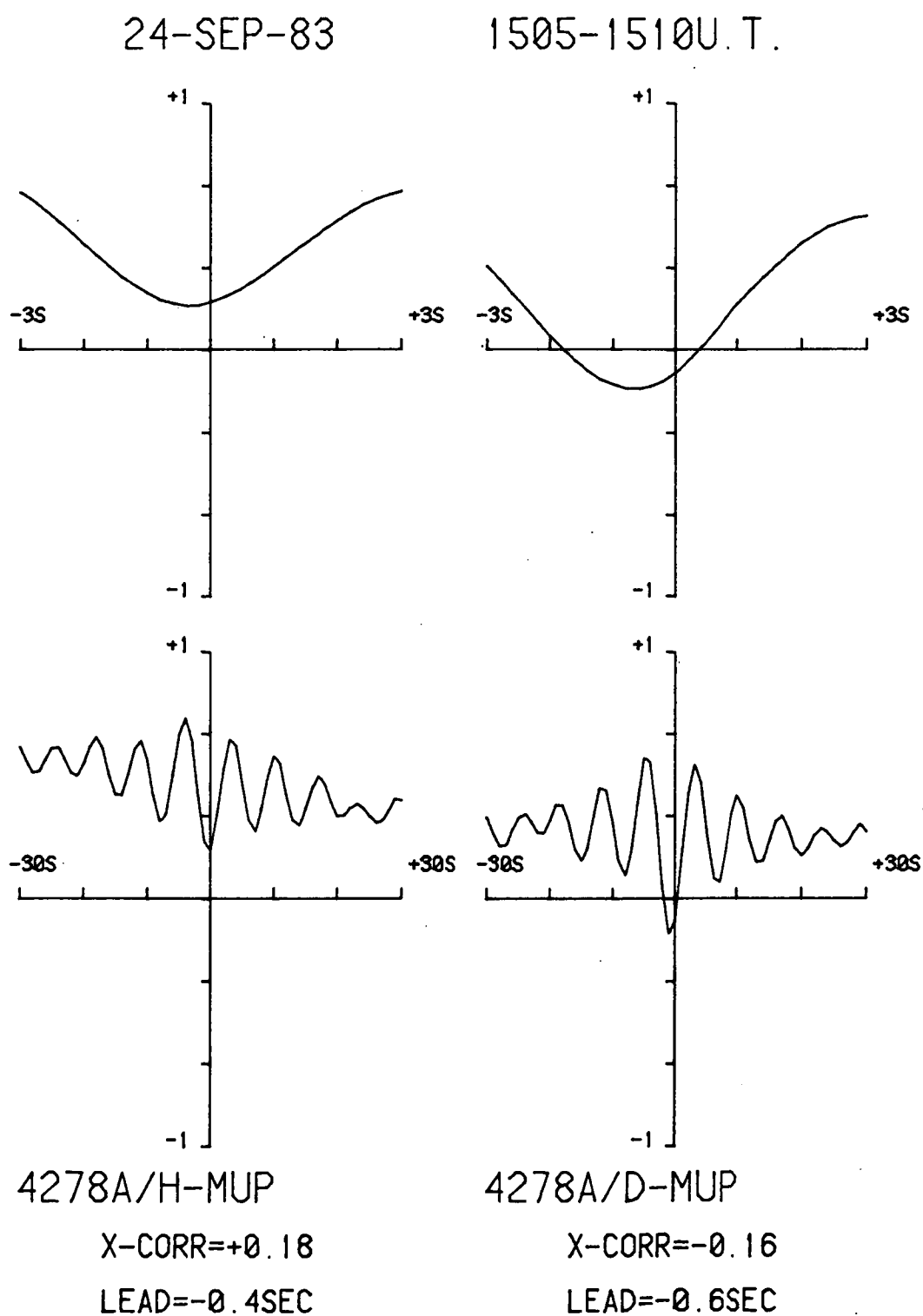


Figure 3.9(b) Vertical translation of correlation file due to coherent long term background drifts as shown in Figure 3.8(b).

This function was evaluated in increments of 5 units (i.e. 1s) for  $u = -150$  to  $u = +150$ , corresponding to a lead-lag of  $\pm 30$  seconds, then in increments of 0.2s (equal to the sample rate) in expanded form for  $u = -15$  to  $u = +15$ , corresponding to a lead-lag of  $\pm 3$  seconds. Cross-correlations for the data plots in Figures 3.1, 3.2, and 3.3 are shown in Figures 3.5, 3.6, and 3.7, respectively. The absolute maximum amplitude correlation value, together with its corresponding lead-lag time in seconds, is listed along with these plots. A negative value here implies that the optical emission leads the micropulsation.

In reference to the point made in Section 3.2 concerning a small broader positive swing of the micropulsation trace following a negative pulse, note that most of the correlation functions show a larger first positive lobe on the lag side. This was found to be the case for the vast majority of files.

Initially all files were saved that attained a cross-correlation co-efficient, for either micropulsation component with respect to the optical emission, of magnitude greater than or equal to 0.33. Some of the cross-correlation functions were found to slope with an overall positive or negative gradient, or be subject to an overall positive or negative vertical translation. Examples of such data files with computed cross-correlation co-efficients given, are depicted in Figures 3.8 and 3.9.

On 04-May-1983, 1535-1540Z, the data block shows how a long period (few minutes) trend in the optical emission can go in and out of phase with any slow drifts present in the micropulsation files. This causes the cross-correlation function to have an overall slope superimposed upon it.



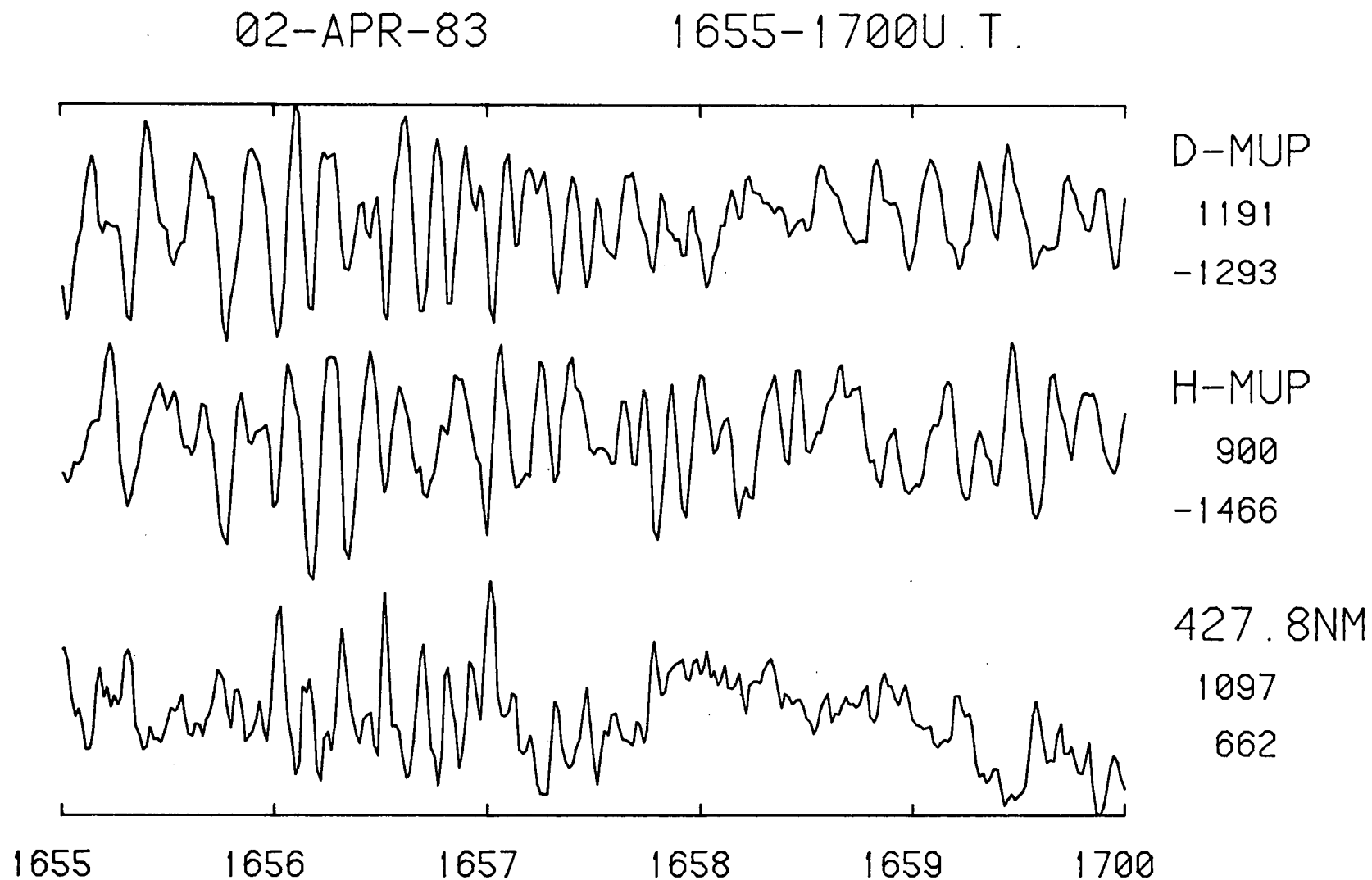


Figure 3.10(a) File for which the validity of the D correlation is suspect due to the presence of strong peaks between 1655:00 and 1656:30 which translate neatly into the 1656-1657:30 period of the optical trace.

02-APR-83

1655-1700U.T.

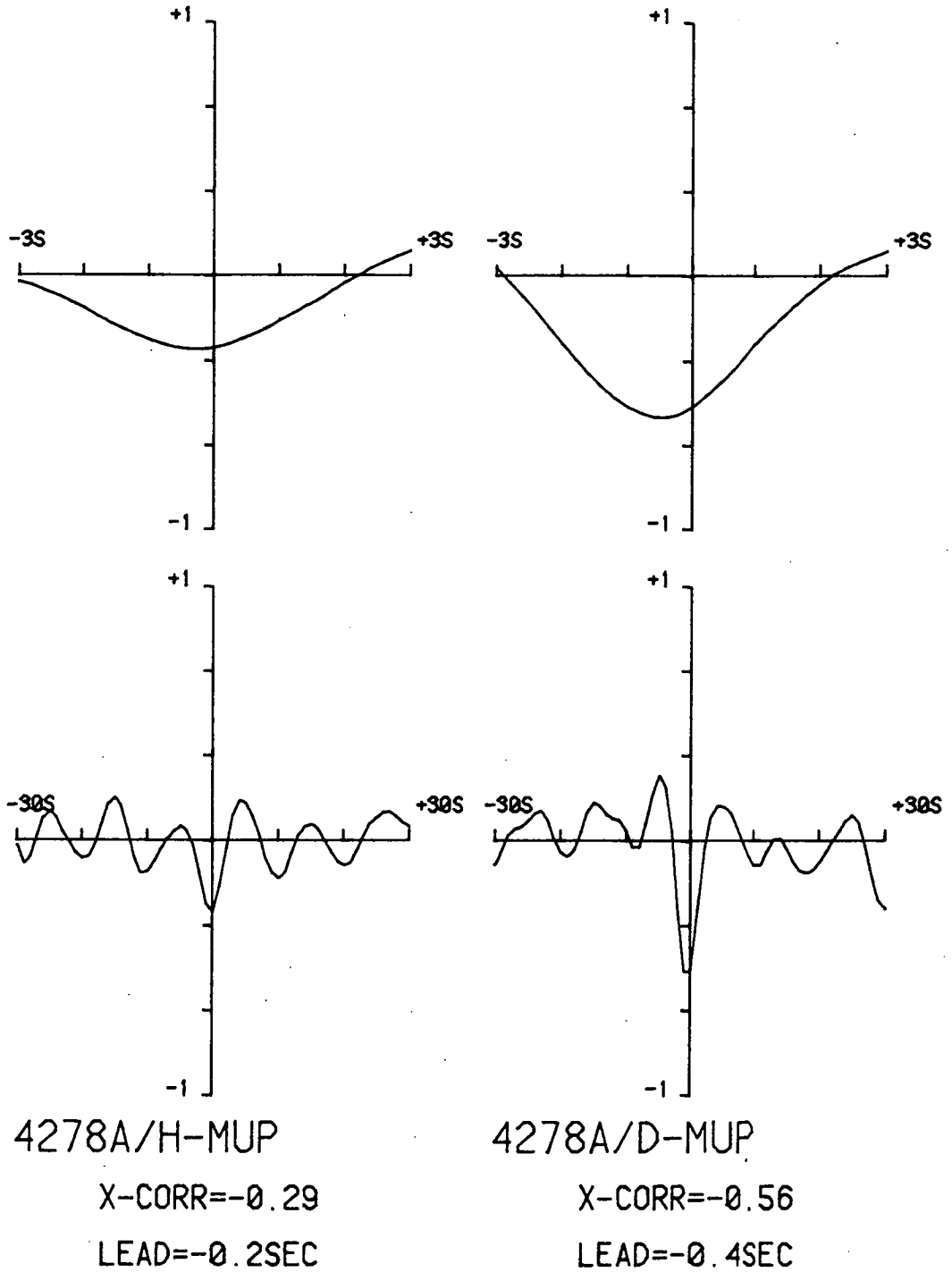


Figure 3.10(b) Cross correlation function depicting the bad behaviour at +30s in the D component.

For the time interval, 24-September-1983, 1505-1510Z, the long slow rise in auroral luminosity correlates positively with both micropulsation files. This is reflected in the cross-correlations, with the functions suffering a bulk positive shift.

Such data has been discarded from the final set retained for statistical analysis, because it invalidates any tests regarding the amplitude of the cross-correlations. The selection procedure adopted, was to omit all files for which an imposed gradient was present, and to eliminate those where the translated function did not cut the horizontal axis with its reverse side lobes. This effectively removes the problems caused by long period trends in the optical emission, which are not well detected by the coils, as was discussed in Section 2.2. This represented only a small amount of data removal, only 14 out of a total of 115 files in the D component, and 25 out of 90 for the H, the remainder falling victim to the contaminations described below.

A further small percentage of files yielded cross-correlation functions that were not "well-behaved" at their end-points,  $\pm 30$  seconds. Such an example is given in Figure 3.10 for the period 02-April-1983, 1655-1700Z. The value of the cross-correlation co-efficient dips dramatically around a lead-time of 30s. The phenomenon, in this case, is almost certainly due to the fact that the D-component has a number of large pulsations in the first minute and a half, that match quite neatly the prolific optical variations between 16:56:00 and 16:57:30. Despite the fact that this particular correlation appears visually honest, it was deleted from the final data set. This is because it falls midway between an unambiguous correlation, and extremes of the type, where a major spurious peak at a large displacement (within  $\pm 30$ s

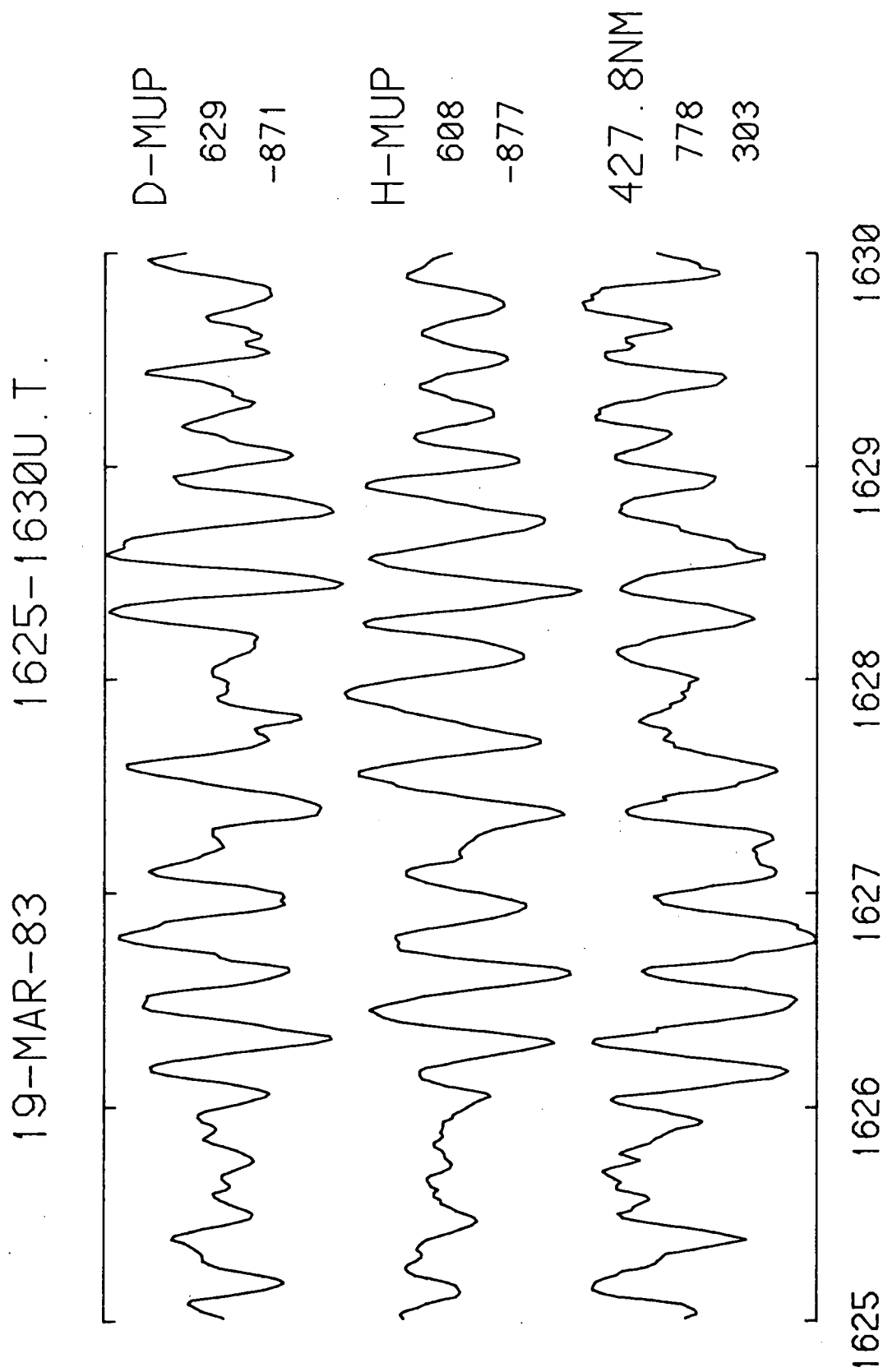


Figure 3.11(a) Longer period pulsations resulting in a broadening of the cross-correlation function.

19-MAR-83

1625-1630U.T.

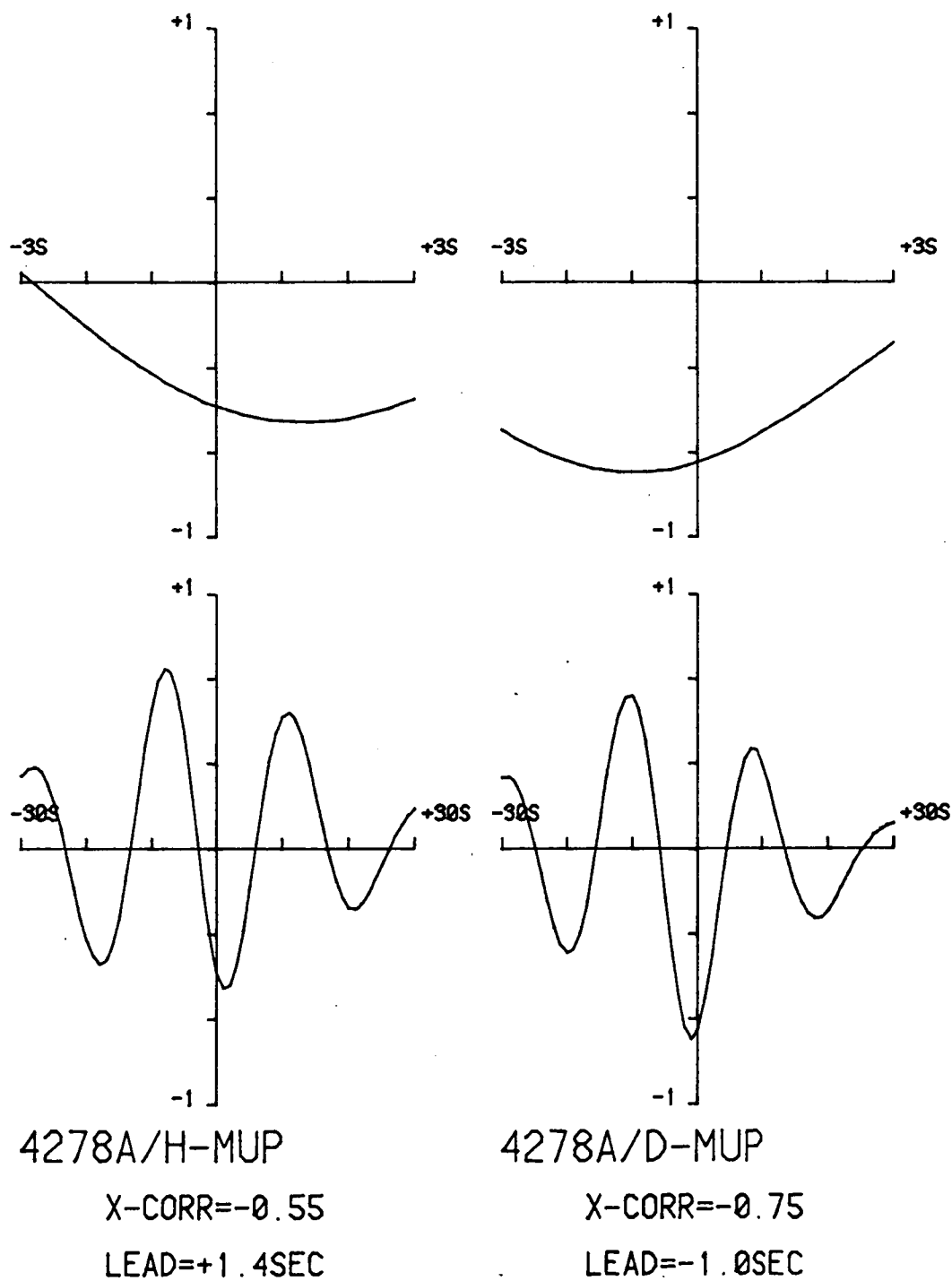


Figure 3.11(b)

of a major optical peak) contaminates the correlation by reducing faith in the lead-lag figure. The selection criteria chosen was to eliminate files of this type where the cross-correlation value was outside the limits  $\pm 0.15$  at the end points,  $\pm 30$ s.

However, some further files were retained which transgress the spirit of the data rejection criteria, but satisfy the objective selection standards. An example of this type appears in Figure 3.11 for the interval 19-March-1983, 1625-1630Z. Longer periods of pulsation have caused the correlation function to exhibit a broader pattern, with the initial side-lobes only just being completed within the 30s lead-lag limits. Such cases represent only a small percentage of the total retained set of data blocks.

These considerations serve to restrict the statistical arguments to a cleaner, uniform data set from which more reliable conclusions can be inferred.

### 3.4 CORRELATION ANALYSIS

All in all, a total of 553 cross-correlations between the geomagnetic D-micropulsations and optical auroral fluctuations, and 298 for the H-component with respect to  $4278\text{\AA}$  emission, satisfying the selection criteria, were obtained. Burns (1983) found a similar bias towards the D-component from his smaller data set.

A simple study of the times of occurrence of these events was conducted, the results being plotted in the histograms of Figure 3.12. The format consisted of grouping all the correlations into 15-minute intervals (i.e. three blocks per group). Note that the interval at the commencement of every hour (e.g. 0800-0815, 0900-0915, ...) has only two files, since the photometers applied a one minute calibration-bulb signal at the beginning of every hour. This removes the file

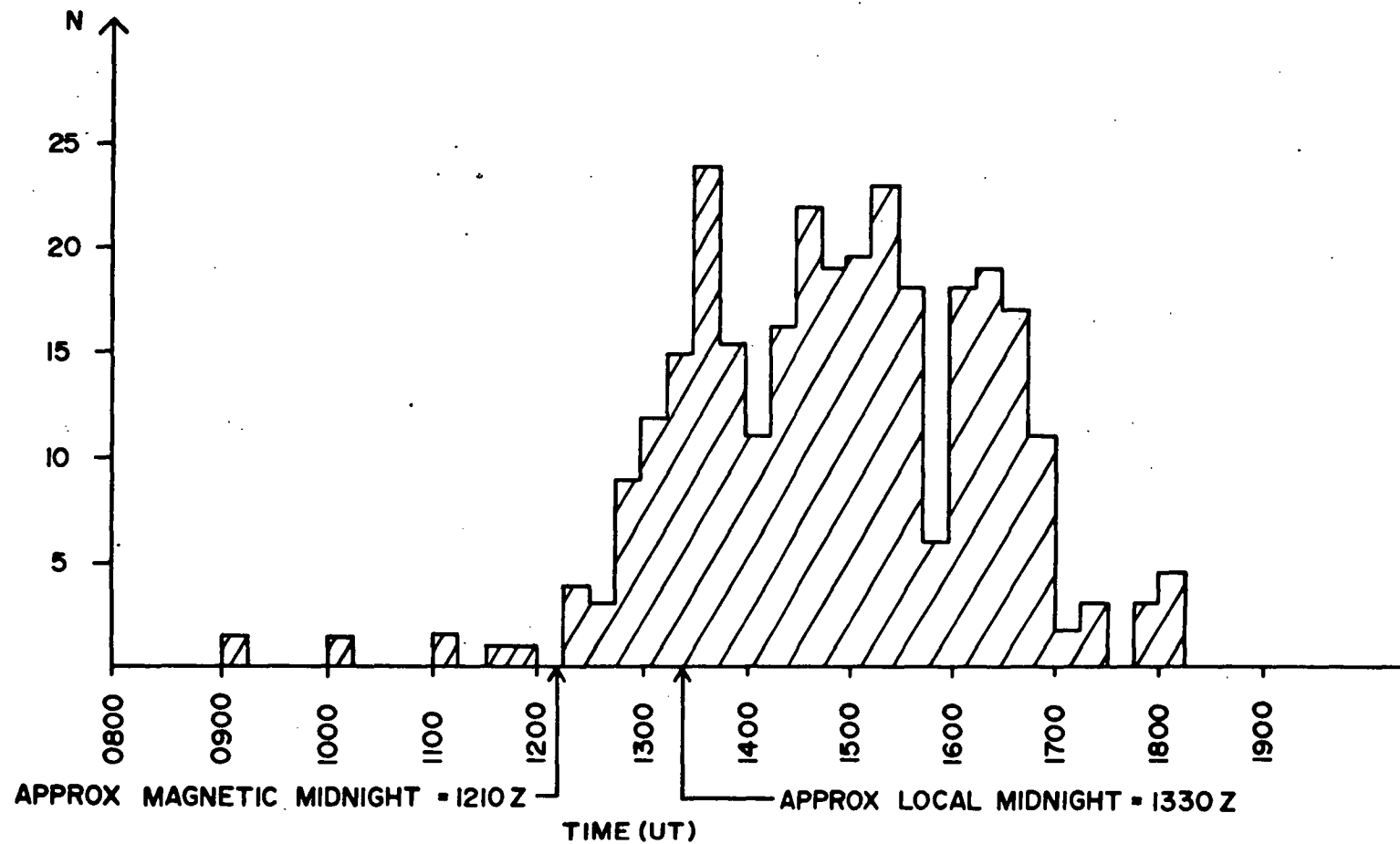


Figure 3.12(a) Histogram of the times of occurrence of all 4278Å/H micropulsation negative cross-correlations, compensated for the deletion of the first file in each hour. Note the broad morning hour maximum.

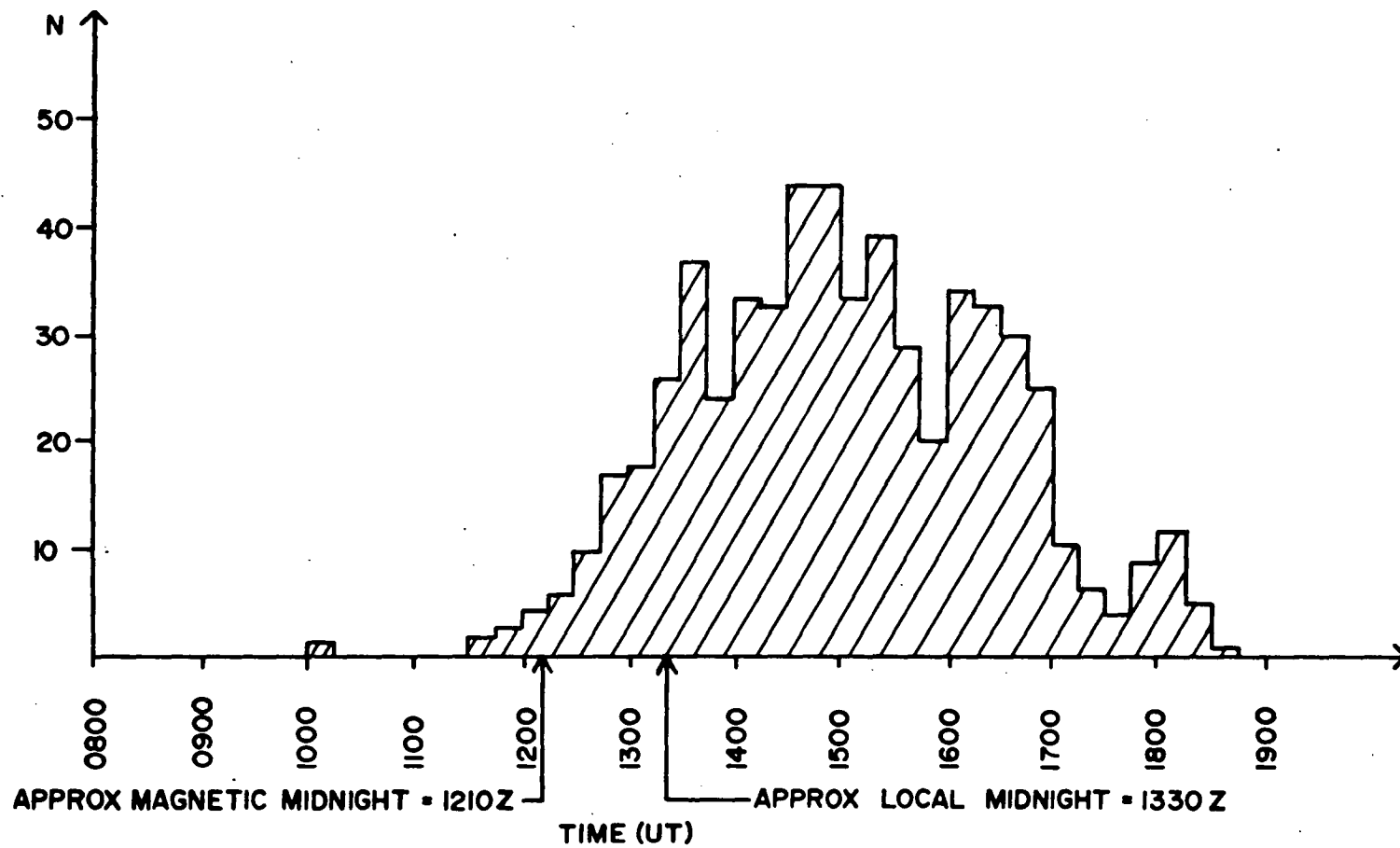


Figure 3.12(b) Similar histogram for the  $4278\text{\AA}/D$  micropulsation cross-correlations. Again note the broad morning hour maximum in occurrence.



from any analysis, reducing these intervals by one third. Such an effect has been compensated for in the histograms to increase the visual acceptability.

Both figures clearly exhibit a broad morning hour maximum frequency of occurrence, in accordance with other observations of pulsating aurora (Kvifte and Petterson, 1969; Brekke, 1971). Very few events were detected more than an hour in advance of local midnight (1324Z at Macquarie Island), magnetic midnight occurring at approximately 1210Z. Most of the data was collected between 1300 and 1700Z. Part of the reason for the data trailing off so rapidly after 1700Z is due to the photometers being slave to local nautical twilight, Macquarie Island being geographically only  $54^{\circ}30'S$ .

Next, the analysis moved to examine the values of the time delays of the micropulsation components with respect to the optical pulsations. Histograms for the lead-lag data appear in Figure 3.13, where statistical calculations reveal that, on average, the H-micropulsations trail the optical variations by 0.3s, with a standard deviation of 0.35s. For the D-micropulsations these figures are -0.6s (negative implies that the optical trace leads) average lag, with 0.28s standard deviation. These compare favourably with the values -0.2s, standard deviation 0.34s, for H-micropulsations and optical, and -0.6s, standard deviation 0.25s for the D-component from Burns (1983) data set, which was sampled at twice the present rate (i.e. 0.1s). The D-micropulsation lags are thus seen to be greater than those of the H-component with less variance in their magnitude.

Recall from Section 2.3 that the data collection process, via the microcomputer system, itself introduces approximately a 0.1s delay of the micropulsations with respect to the optical fluctuations.

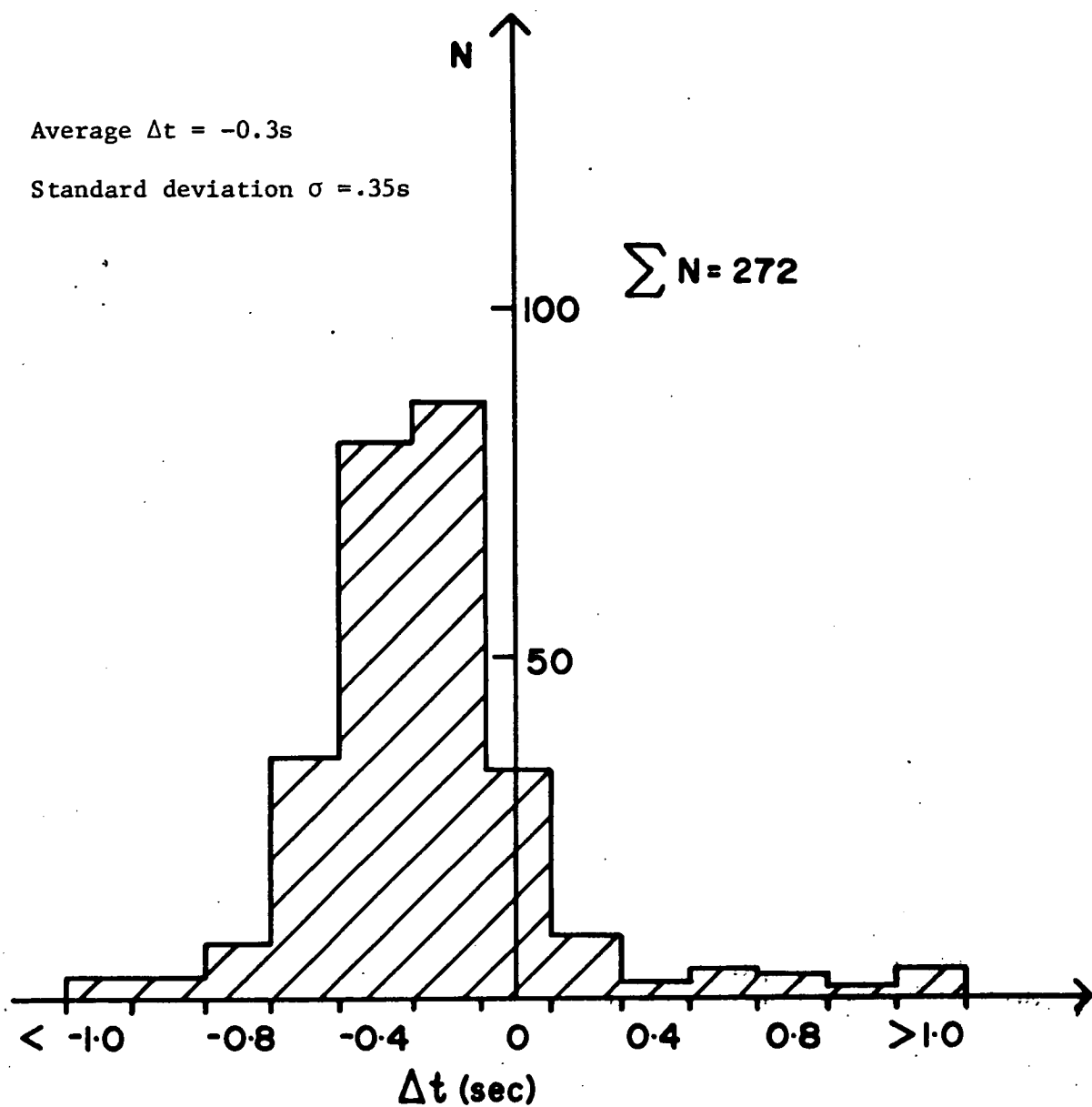


Figure 3.13(a) Histogram of the lead-lag delay relationship in all 4278Å/H micropulsation negative cross-correlation events. Note that a negative value implies the optical leads the micropulsation.

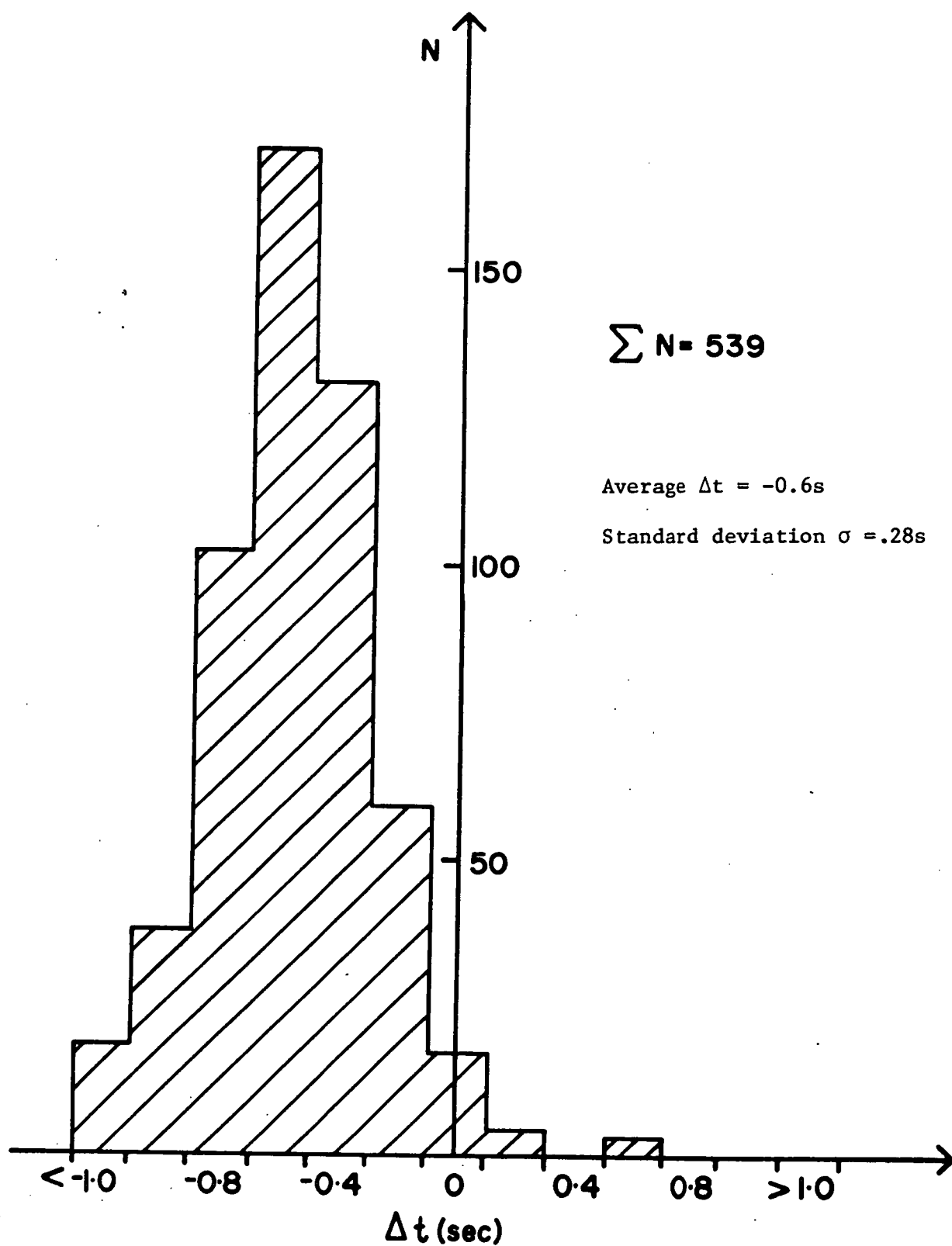


Figure 3.13(b) Histogram for 4278Å/D micropulsation cross-correlation lead-lag data. The optical generally leads by the order of 0.6s.

With Burns (1983) faster sample rate this figure is only 0.05s for the results presented in his thesis. This however does not adversely affect the following discussion, though it must be kept in mind.

As a further measure of the consistency of these results, the lead-lag differences between consecutive saved files were examined, and the outcome appears in Table 3.1(a).

Since this is only for the data that passed the selection criteria, both components yield good results, with relatively few instances of erratic lead-lag jumps from one file to the next. When the differences analysis is carried out for all pairs, where either of the magnetic field component correlations satisfies the selection criteria, it becomes obvious that the D-component gives a smoother variation. See Table 3.1(b).

The data was then analysed, in terms of the lag times, when both components had acceptable cross-correlation functions, in order to examine how often the H-micropulsations led the D, and vice versa. From 231 instances, the D-micropulsations were found to lead the H on only 37 occasions, there being 33 times when (on average) the fluctuations were simultaneous over the 5-minute periods. Figure 3.14 displays the histogram obtained from this study.

So, in general, the 4278<sup>0</sup>Å auroral optical emission leads the H-micropulsations, which in turn, lead the D-micropulsations. This is patently obvious from the lead-lag analysis just presented. The D-micropulsations have also been shown to correlate with the optical pulsations more frequently, and exhibit a greater coherency over longer periods of time.

The next logical extension is to break down the observations into various subdivisions, according to the magnitude of the correlations.

$\Delta t(s)$	0.0	0.2	0.4	0.6	0.8	1.0	>1.0
4278A/H	38	42	13	8	3	1	-
4278A/D	103	128	38	6	2	1	-

Table 3.1(a) Difference in lead-lag delay for consecutive pairs of well correlated data.

$\Delta t(s)$	0.0	0.2	0.4	0.6	0.8	1.0	>1.0	N.C
4278A/H	73	102	43	24	12	5	24	26
4278A/D	106	143	39	9	4	2	3	3

Table 3.1(b) Difference in lead-lag delay for all consecutive pairs where either the H or D component is well correlated. The D data is subject to considerably less random variations.

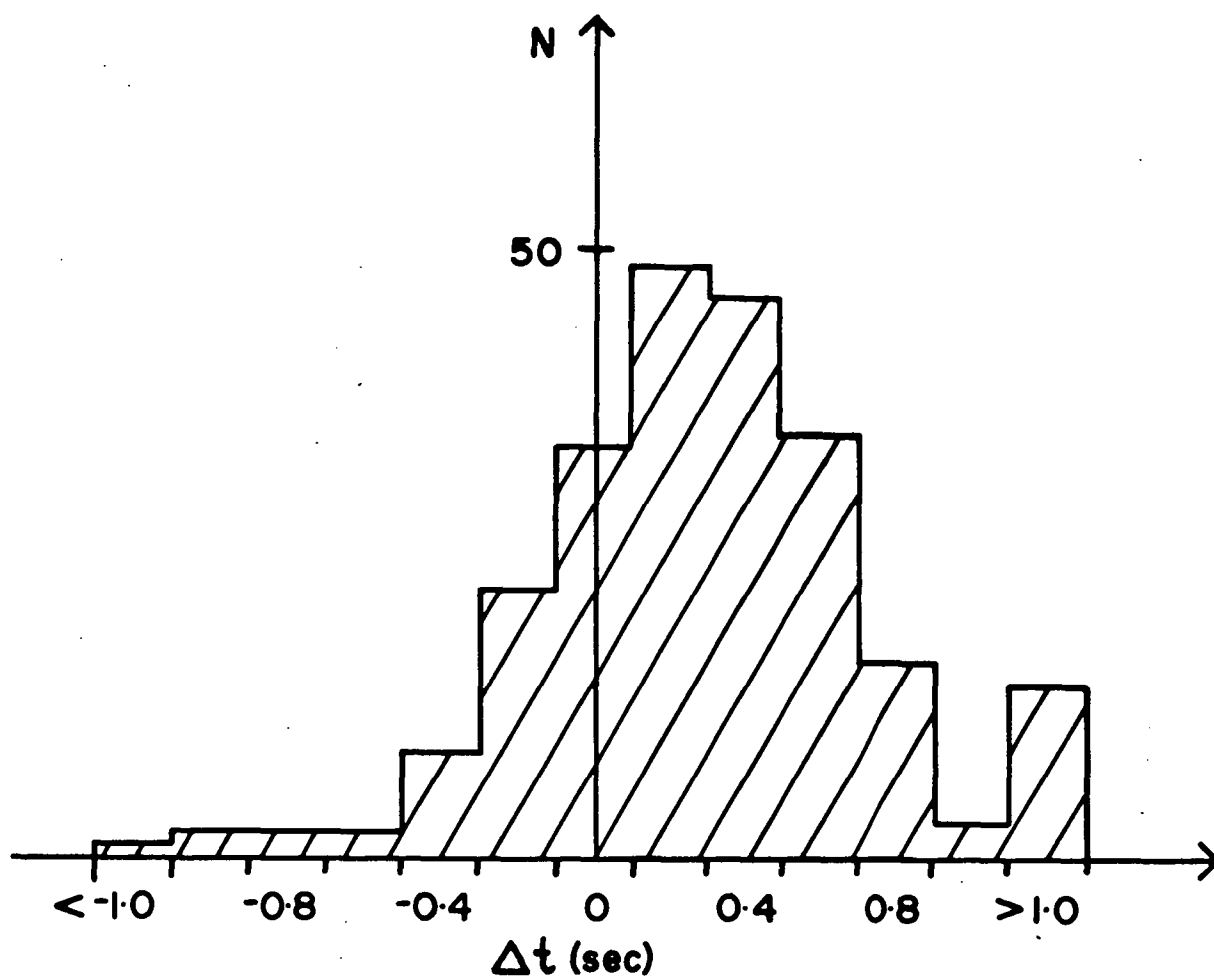


Figure 3.14 Histogram depicting the lead-lag relationship between the H and D micropulsation components. The H component leads the D on 161 occasions out of 231, trailing during only 37 of these 5-minute data blocks.

To facilitate a more complete analysis, this has been done on the basis of the lead-lag times of the micropulsations with respect to the 4278Å auroral fluctuations. A comprehensive documentation of these results appear in Tables 3.2. Not only does the D-component clearly yield a far greater number of events, as seen already, but the overall degree of correlation is considerably higher.

Examination of the last row in each of the tables reveals that the D-component has a correlation magnitude greater than 0.50 nearly 47% of the time. This figure drops to 40% in the case of the less abundant H micropulsations. This is in agreement with the concept of the D-micropulsations being more frequently correlated. If the correlation for the D component is larger in general, then it is to be expected that it will yield more correlations above a chosen magnitude.

On a relatively small number of occasions, the situation arose where the cross-correlation analysis lead to an in-phase arrangement, between the 4278Å optical pulsations and the geomagnetic micropulsations. That is, the correlation co-efficient returned a positive sign. An example of such an event is given in Figure 3.15 along with the correlation functions themselves. Note the excellent peak matching in both micropulsation channels, the low intensity diffuse auroral background, and the larger positive swing in the micropulsation data.

Table 3.3 enumerates the results of a complete consideration of all files which survived the selection processes previously described.

The D component is seen to yield 14 well correlated positive files, whilst the H component provides 26 such events. However, a number of other files, which failed to pass the stringent selection criteria, display quite obvious visual in-phase correspondence. Since the total number of positively correlated files is small, and the correlations generally weaker than the more more abundant negatively

Correlation Magnitude Delay (Secs)	0.33 to 0.40	0.41 to 0.50	0.51 to 0.60	0.61 to 0.70	0.71 to 0.80	>0.81	Totals
>1.0	1	1	1		1		4
1.0	1						1
0.8		1	1	1			3
0.6	1	2	1				4
0.4		1	1				2
0.2	3	2	2	1			8
0.0	11	8	7	6	1		33
-0.2	28	20	18	12	6	1	85
-0.4	20	30	16	19	6	2	83
-0.6	9	11	6	6	2	1	35
-0.8	2	5	1				8
-1.0	1	1	1				3
<-1.0	2	1					3
Totals	79	83	55	35	16	4	272
% Total	29.0	30.5	20.2	12.9	5.9	1.5	

Table 3.2(a) Complete diagnostics for correlation  
magnitude versus lead-lag time for 4278A/H  
micropulsation data.



Correlation Magnitude Delay (Sec)	0.33 to 0.40	0.41 to 0.50	0.51 to 0.60	0.61 to 0.70	0.71 to 0.80	>0.81	Totals
>1.0							
1.0							
0.8							
0.6		2			1		3
0.4							
0.2	2	2					4
0.0	3	6	4	2	1		16
-0.2	19	16	12	7	4	1	59
-0.4	18	40	46	20	5	1	130
-0.6	30	64	39	28	9	1	171
-0.8	20	31	26	17	6		100
-1.0	12	11	11	3	1		38
<-1.0	4	7	7				18
Totals	108	179	145	77	27	3	539
% Total	20.0	33.1	26.9	14.3	5.0	0.7	

Table 3.2(b) Details of 4278Å/D micropulsation cross-correlations.  
 Very few data files were obtained where the D  
 component actually led the optical pulsations.

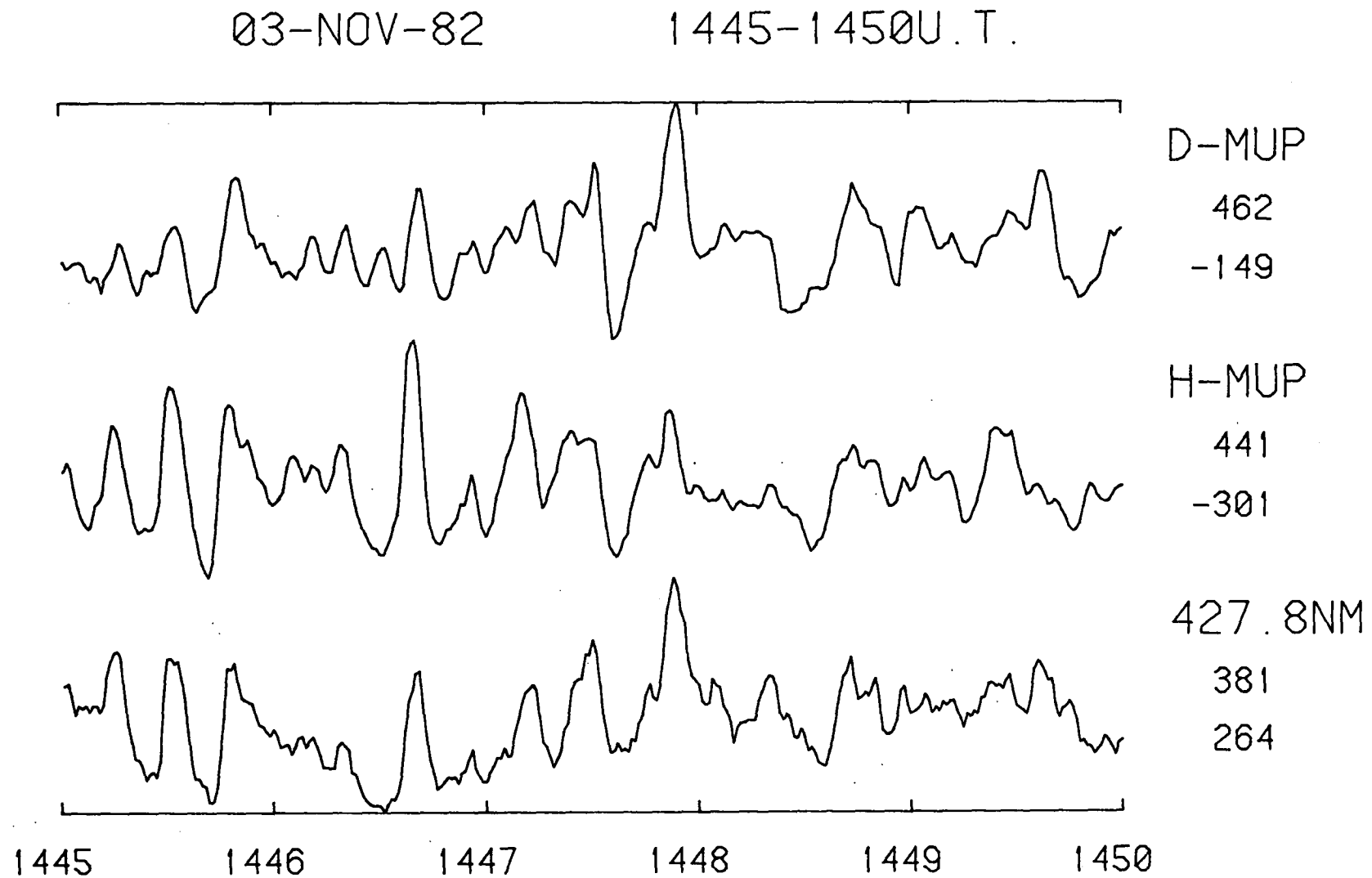


Figure 3.15(a) Example of strong positive correlation between the optical emission and micropulsations. Note the greater positive swing in the micropulsation channels (i.e. maximum value greater in magnitude than minimum value).

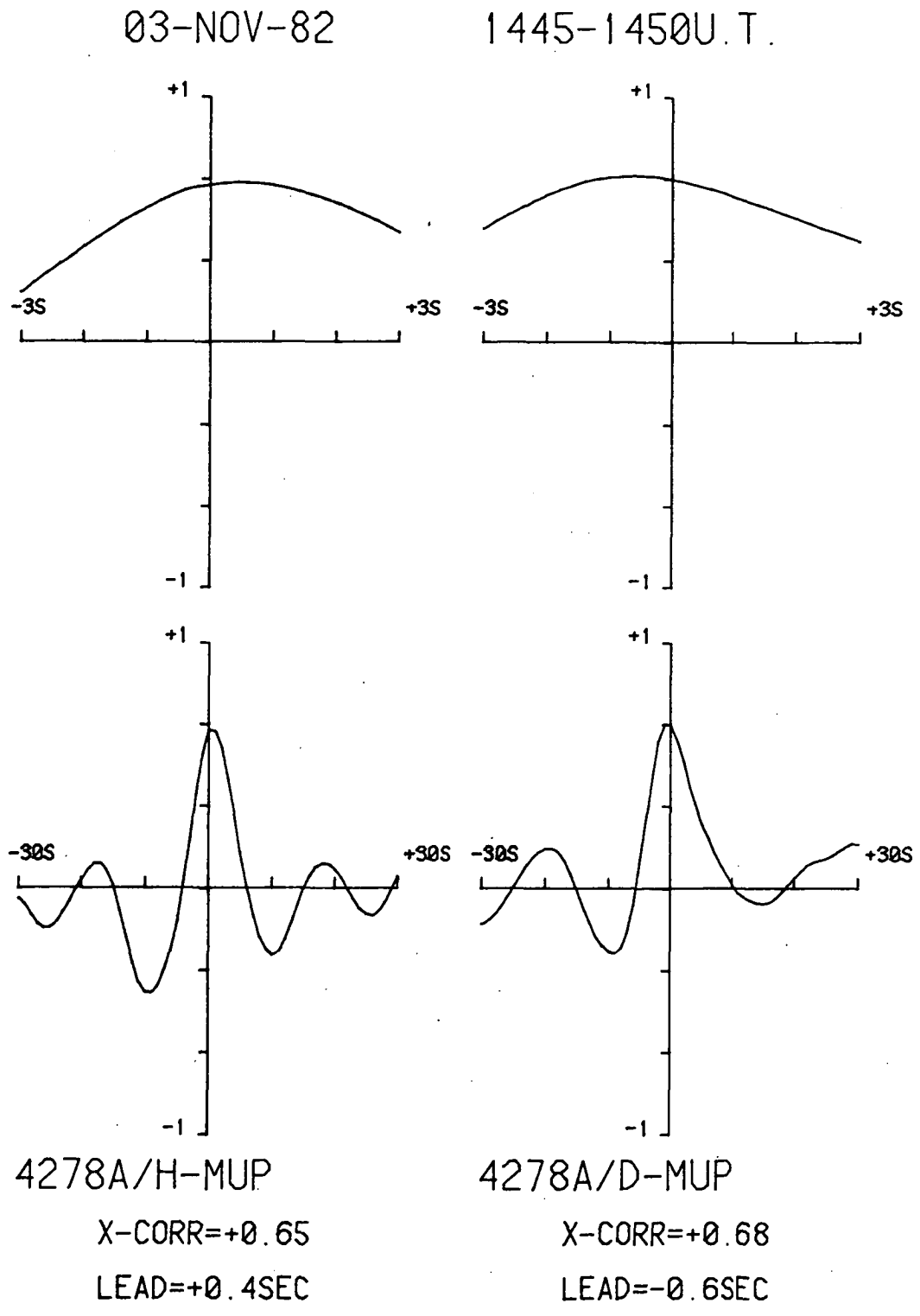


Figure 3.15(b) Cross-correlation functions for the in-phase arrangement of the pulsations.

4278A/H Micropulsations

4278A/D Micropulsations		Negative	Positive	Not Correlated	Totals
	Negative	222	6	310	539
	Positive	0	5	9	14
	Not Correlated	50	15		
	Totals	272	26		

Table 3.3 Statistics of all data files that survived the correlation criteria described in the text. Both components show a strong predominance towards negative correlations, and the D component produced nearly double the number of good files as H.

4278A/H Micropulsations				
4278A/D Micropulsations		Negative	Positive	Not Correlated
	Negative		23	
	Positive	3	20	10
	Not Correlated		11	
		$\Sigma = 54$		
		$\Sigma = 33$		

Table 3.4      Results of a more subjective study which counts all files that exhibit a pronounced positive correlation tendency, with the strict selection criteria waived.

correlated events, all files that appear to exhibit a phase reversal, were examined. Table 3.4 gives the results of this more subjective study.

Although this is still a relatively small sample set, it seems to indicate that the H-component is more likely to suffer a phase reversal than the D. A further conclusion is that the two micropulsation files do not necessarily undergo a phase reversal at the same time. One or other, or both components may yield a positive correlation - cases exist for all three possibilities.

Macquarie Island data displayed two main periods where these phase reversals were most likely to occur. Firstly, early in the evening, or alternatively in the later morning hours, often following a good sequence of negatively correlated files. Observation times of these events are depicted in the histograms of Figure 3.16.

Interestingly, these times of occurrence may contribute to the excessive bias of the data toward negatively correlated events. As previously mentioned the photometers were made slave to local nautical twilight and were only operative at times earlier than 1000Z, and later than 1700Z from March until September 1983. Slightly in excess of 70% of the data was obtained during this period, however, so that there must still be a strong, real leaning toward negative correlations.

### 3.5 COMPARISON WITH MAGNETIC BAYS

The positive correlations were usually observed at times when a negative geomagnetic H component bay was in its late recovery stages. This condition was sometimes disguised by the overlapping commencement of a new negative bay. However, in this situation, the files near the local maximum of the trace yielded a positive result, then returned

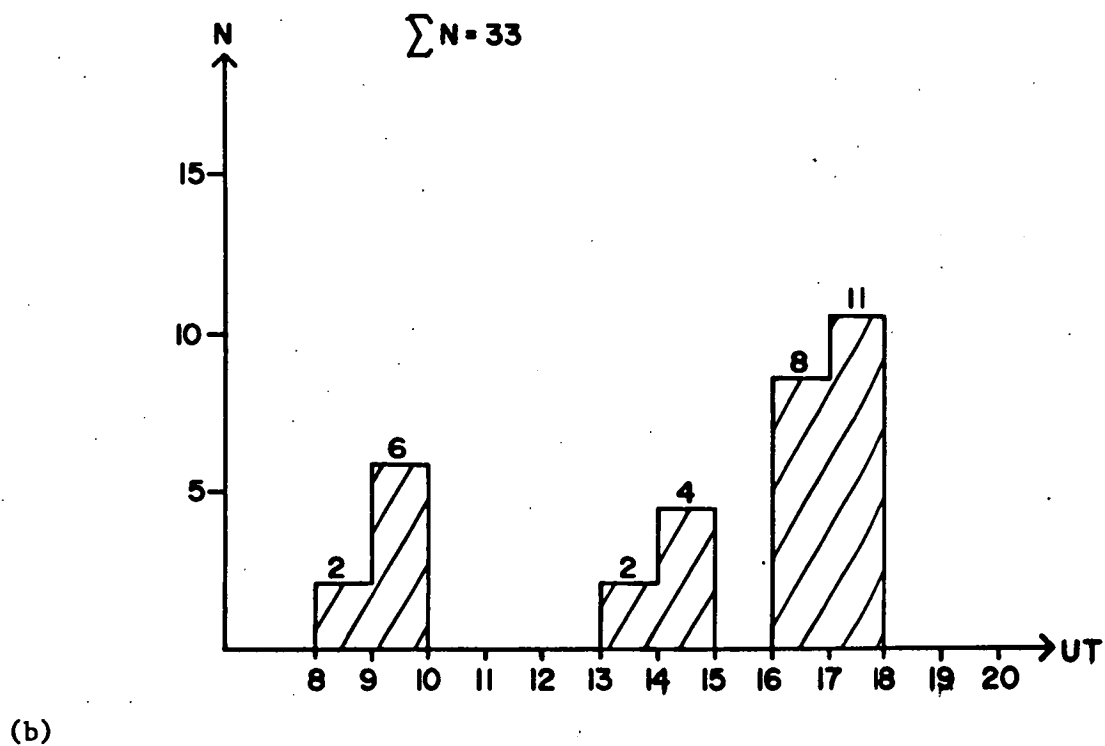
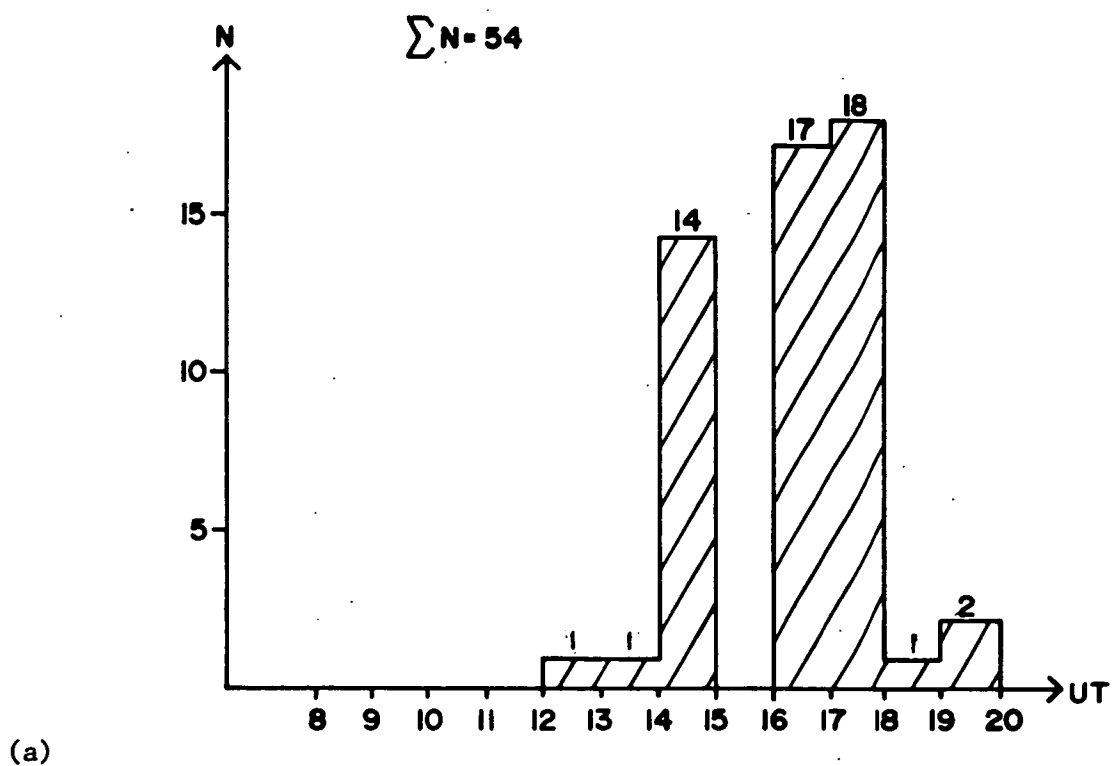


Figure 3.16 Time of occurrence of positively correlated files 4278Å/H (a), and 4278Å/D (b).

to negative correlations as the next bay gained control. Note that practically all negatively correlated files occurred whilst the H component magnetic bay was still significantly negative.

Examples of the large-scale magnetic field configuration during positively correlated files are given in Figure 3.17.

Clearly the D component magnetograms are subject to less systematic changes, and there appears to be very little connection between these and the sign of the micropulsation correlations. In fact, the D micropulsations tend to suffer their correlation phase reversals in the late recovery stages of negative H-bays as well. So it is essentially the H magnetogram which can be used as an indicator to possible phase reversed correlations.

A more detailed study was carried out on the large-scale magnetograms, to determine clearly the association of the various correlation phases with the overall magnetic field activity. To effect this, a QDC (quiet day curve) was determined for each month by taking hourly averages of the five or six magnetically quietest days for that month. This empirical curve could be used to estimate the deviation of the magnetic field, in magnitude and direction, at any other time during the given month.

Burns (private discussion) points out that the large-scale H component magnetograms may not be a totally reliable quantitative indicator of the overhead current system during substorms, particularly in the late decay phase. This is because an enhanced ring current system may cause the 'quiescent' level of the curve to be depressed with respect to the normal QDC, as measured on near neighbouring days of low magnetic activity. So the overhead E-region current system may actually have a minor easterly component (resulting in positive  $4278 \text{ Å/H}$  micropulsation correlations) despite the fact that the actual magnetogram trace still lies marginally below the QDC value.



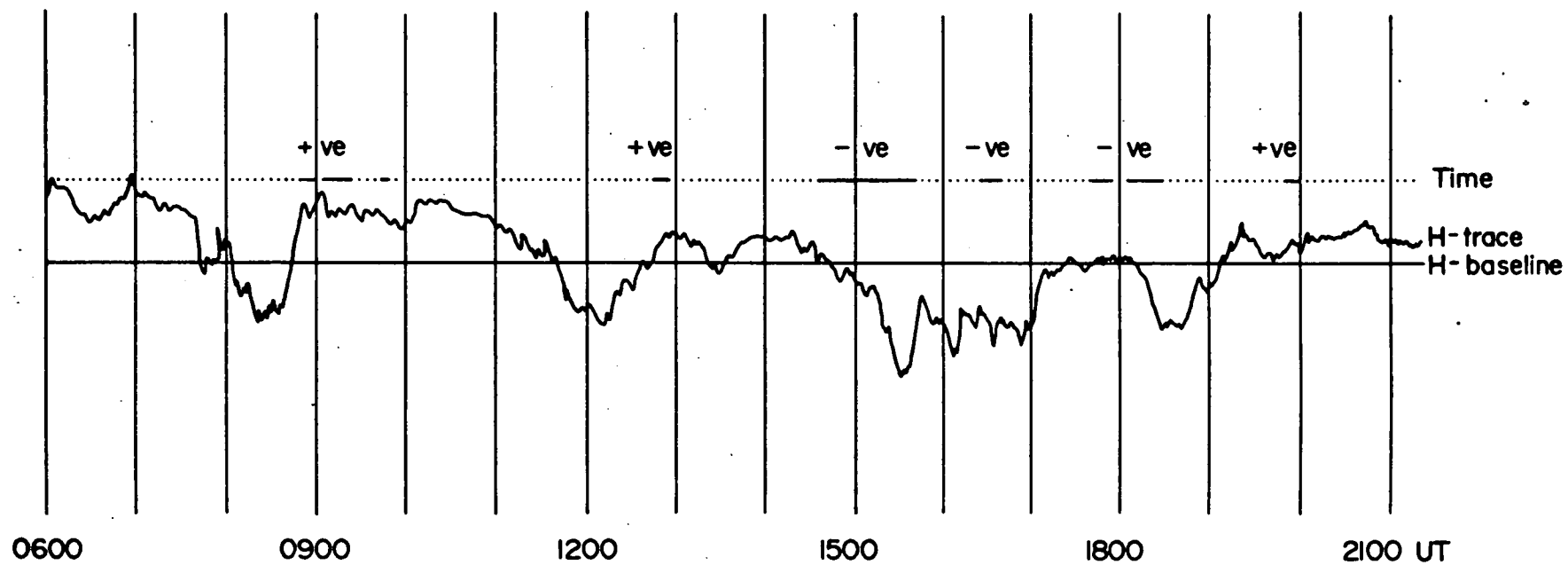


Figure 3.17(a) Macquarie Island BMR magnetogram for the very active day 23-May-1983. Pulsating aurora accompanied a number of magnetic bays, with positive correlations being returned in the latter stages of bay recovery.

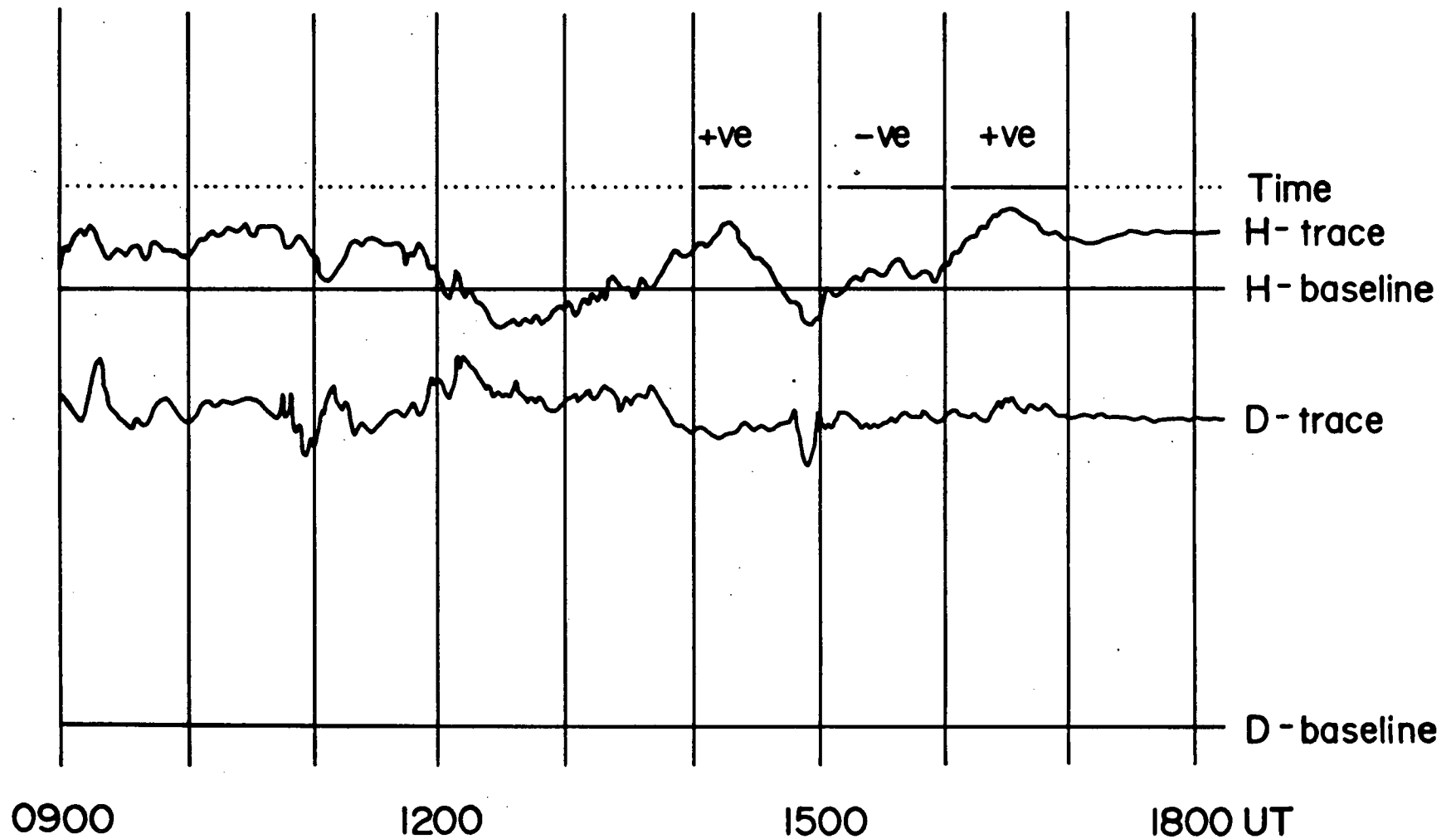


Figure 3.17(b) Magnetogram data for 02-October-1983. Note again that positively correlated files tend to occur near maxima in the large-scale H component at or around complete bay recovery.

Such use of an 'iron-curve' method has been severely criticised by Mayaud (1967) for similar reasons to those stated above, and he points out that the more magnetically active the period in question, the less reliable this method will be. What is important here, is that all the positive phase correlations occur in the late recovery stage of the bays, at or near positions of local maxima in the H component. Taking into account the above considerations, this may well be indicative of a significant degree of current reversal in the local overhead E-region system.

September 1983 was selected as an appropriate month to calculate QDC's for both the H and D field components. This was a most suitable period since the RL02 hard disk facility was then in operation saving all files for correlation analysis. Scaling of the magnetograms was performed in accordance with the method prescribed by the Bureau of Mineral Resources, as outlined below.

For this month the magnetically quietest days were found to be the 02, 03, 04, 05, 06 and 30th of September. This seems to represent an unfortunate bias toward the initial part of the month. However, such an unavoidable selection did not prove undesirable, as the final day of the month reflected the earlier trends extremely well.

The general format of the magnetograms is depicted in Figure 3.18, and this layout is referred to in the following discussion.

Shrinkage of the record during photochemical processing is determined first. Three sets of circled crosses, at 100mm spacing, are imprinted on the magnetogram before attaching the sheet to the La Cour magnetometer drum. Typically three readings are taken (as shown by the vertical lines on the diagram) and averaged, yielding shrinkage factors of the order 0.8 - 1%.

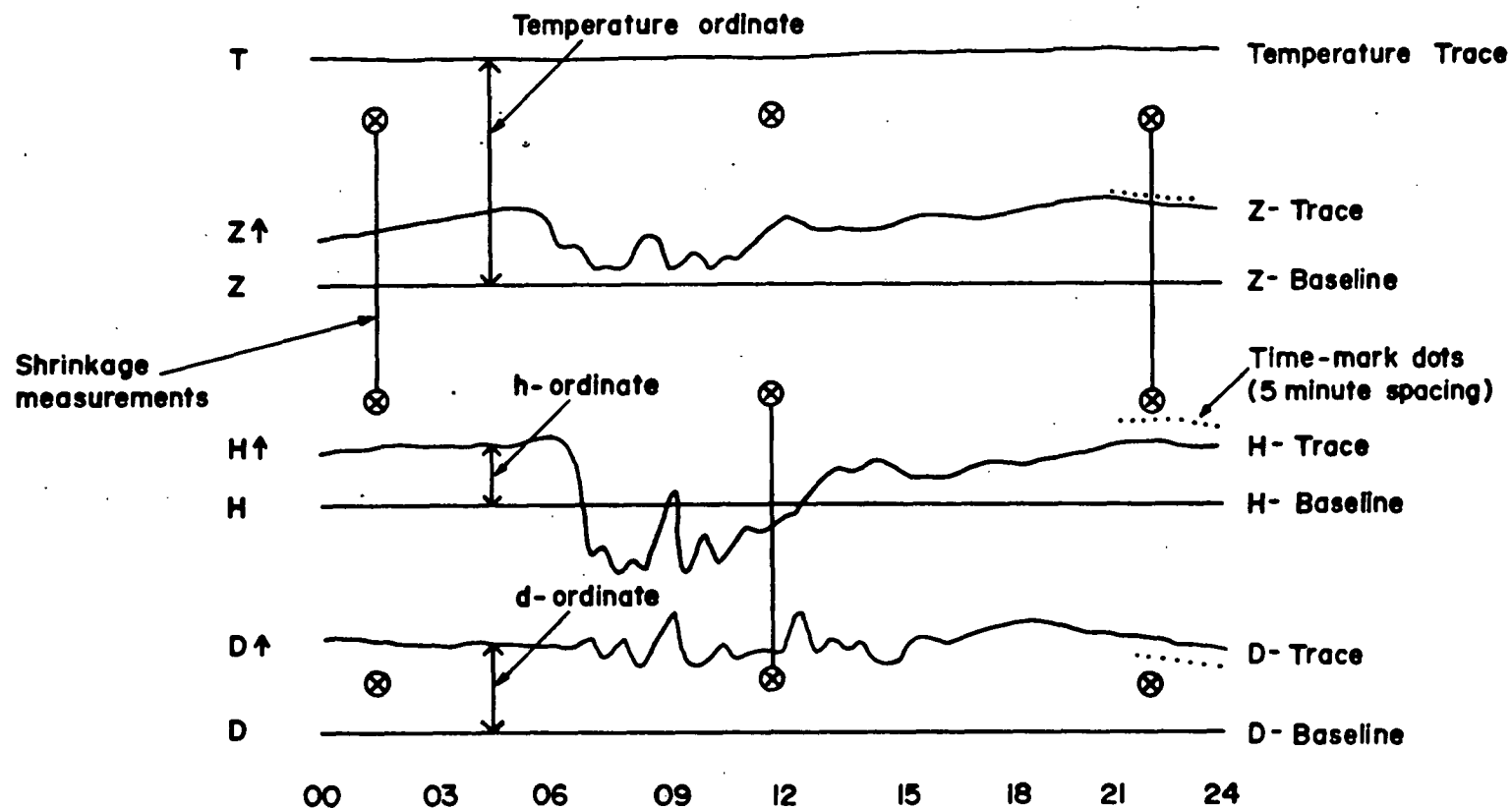


Figure 3.18 Format of the BMR Macquarie Island magnetograms depicting the three traces, a temperature ordinate, individual 5-minute timing marks for each trace, and the shrinkage markers.

For the H component, the H-ordinate is read as a difference in millimetres between the H-baseline and the H-trace, which then has the shrinkage correction factor applied. The H-baseline value is itself temperature dependent, and the temperature is determined from its own particular trace, thus:

$$t = B_t + (S_t \times T)$$

where:

$t$  = ambient temperature

$B_t$  = temperature baseline =  $-83.5^{\circ}\text{C}$  at Macquarie

$S_t$  = temperature scale value =  $-1.50^{\circ}\text{C/mm}$  at Macquarie

$T$  = temperature ordinate corrected for shrinkage

so in determining the value of the H component:

$$H = BH_s + Q_H (t - t_s) + (S_H + h)$$

where

$H$  = H component magnetic field value

$BH_s$  = H-baseline value at standard temperature  $t_s = 12492 \text{ nT}$

$Q_H$  = temperature co-efficient =  $2.0 \text{ nT}/^{\circ}\text{C}$

$t_s$  = standard temperature =  $5.0^{\circ}\text{C}$  at Macquarie

$S_H$  = H scale value =  $19.33 \text{ nT/mm}$

$h$  = H-ordinate corrected for shrinkage

Values for the D component are easier to extract from the magnetogram since the baseline value does not depend on the temperature:

$$D = B_D + (S_D \times d)$$

where:

$D$  = D component magnetic field value

$B_D$  = D-baseline value =  $26^{\circ}58.2'$

$S_D$  = D scale value =  $2.37 \text{ min/mm}$  at Macquarie

$d$  = D-ordinate corrected for shrinkage

These figures are determined every hour for each of the six days, the values averaged, and a QDC is thus established.

Matsushita and Campbell (1965) have published the expected QDC's, from an analysis of Sq magnetic variations, from a 'global' network of stations. Their curves are given as a function of dip latitude, where:

$$\text{dip latitude} = \arctan \frac{\tan (\text{dip angle})}{2}$$

with magnetic dip angle measured positive below the local horizontal plane. Macquarie Island has a dip latitude of approximately  $-67^{\circ}$ , somewhat outside the scope of the published figures.

Mr. Pelham Williams (Davis physicist, Antarctic Division, 1984) kindly extrapolated the data to obtain typical variations for Macquarie Island. September fits in as an E-month (equinoctal) in Matsushita and Campbell's analysis, and the extrapolation of their data is plotted against the empirically determined QDC's from Macquarie Island magnetograms in Figure 3.19.

For both the H and D component QDC's the maxima and minima occur slightly later than suggested by Matsushita and Campbell, and display a smaller range of variation. The general shapes, on this reduced scale, are in rather good agreement. It should be pointed out that the E-month curves are an average over 4 months, so that any minor fluctuations will be smoothed out. A similar analysis of Macquarie Island QDC's, conducted by Mr. Pelham Williams, for November, December 1982, and January 1983, again yielded considerable individual variation from the corresponding Matsushita and Campbell D-month curves. The average over these three months was, however, in much closer accord with their figures.

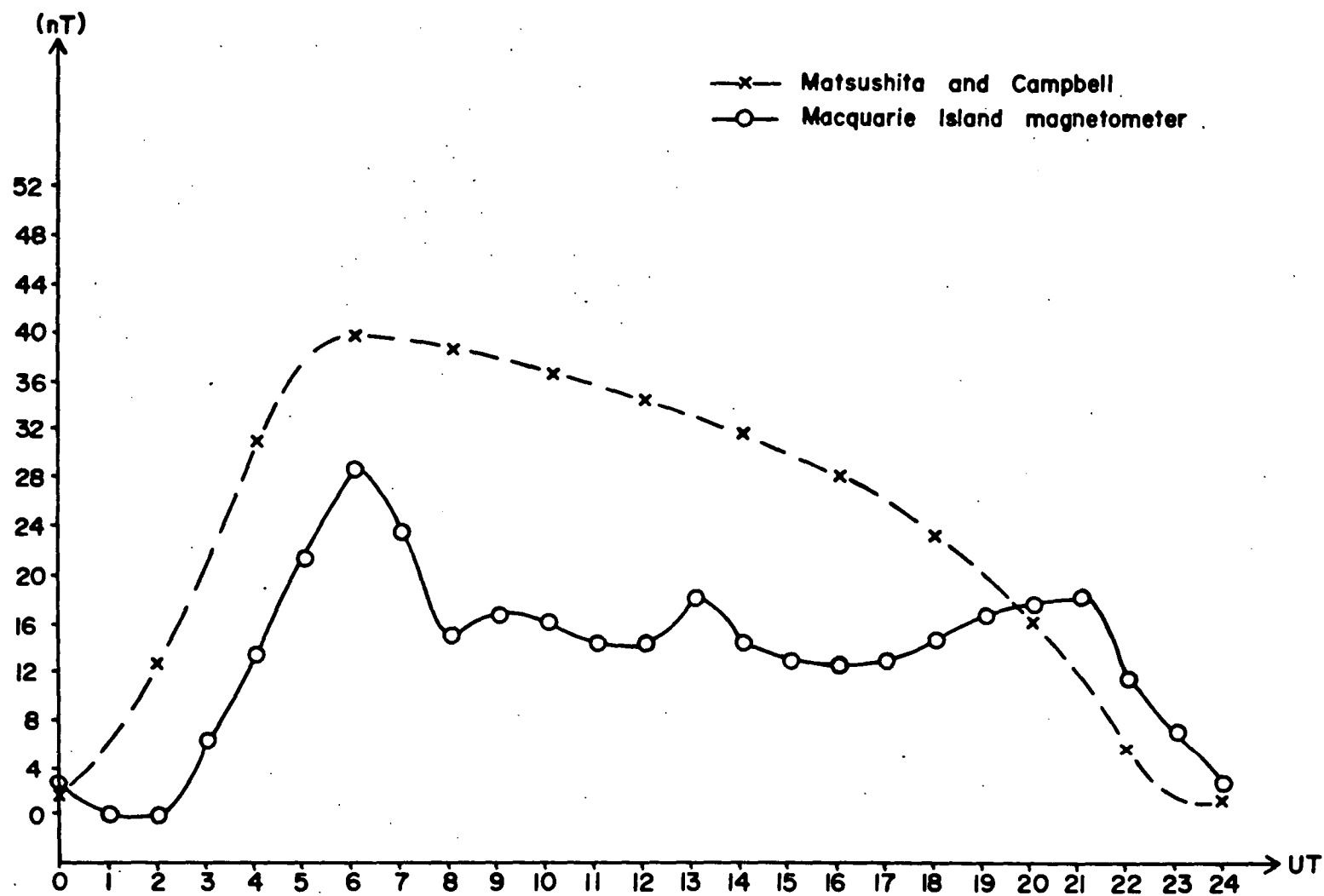


Figure 3.19(a) Large-scale H component Macquarie Island quiet day curve for September 1983 versus the extrapolated predictions of Matsushita and Campbell.

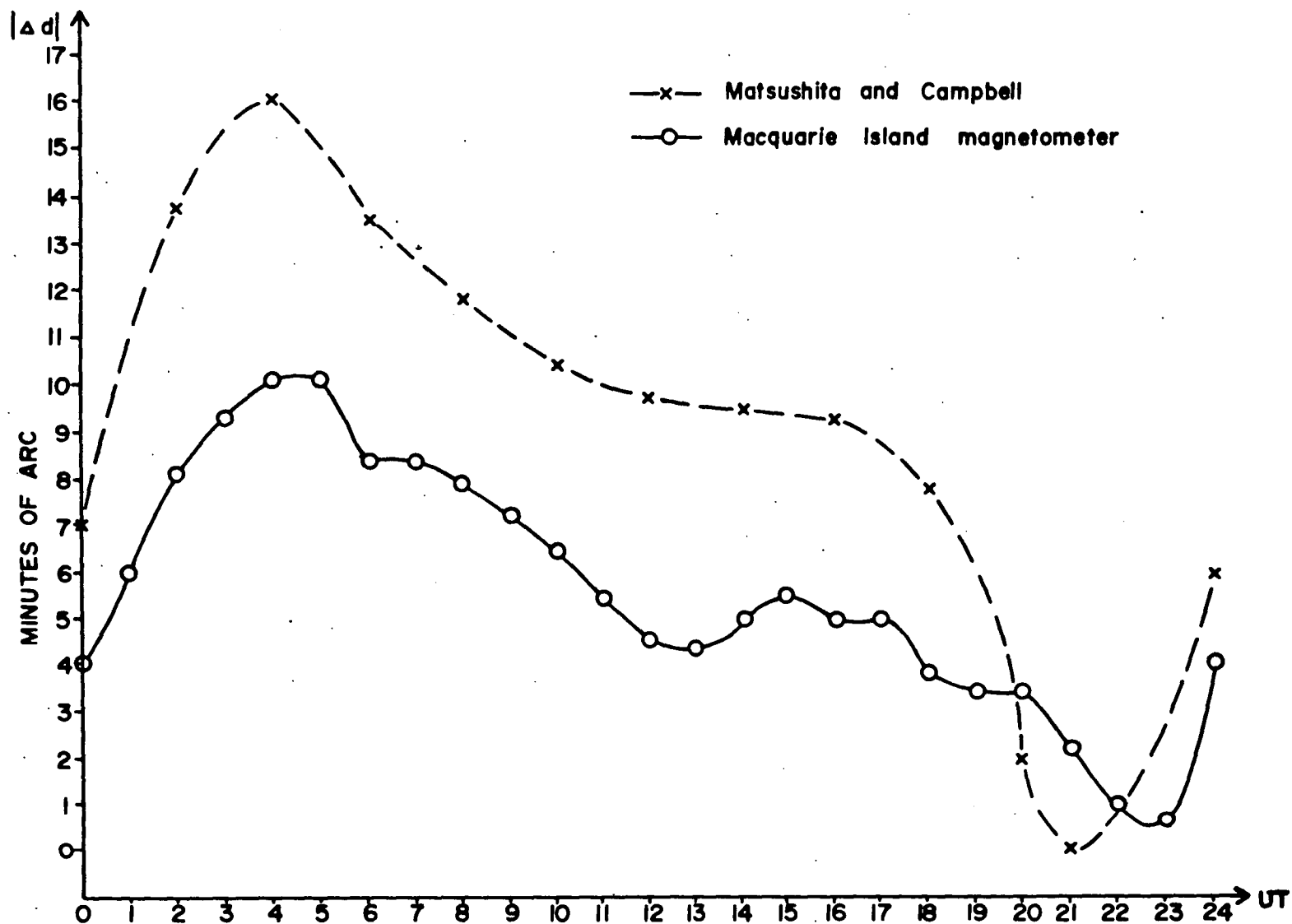
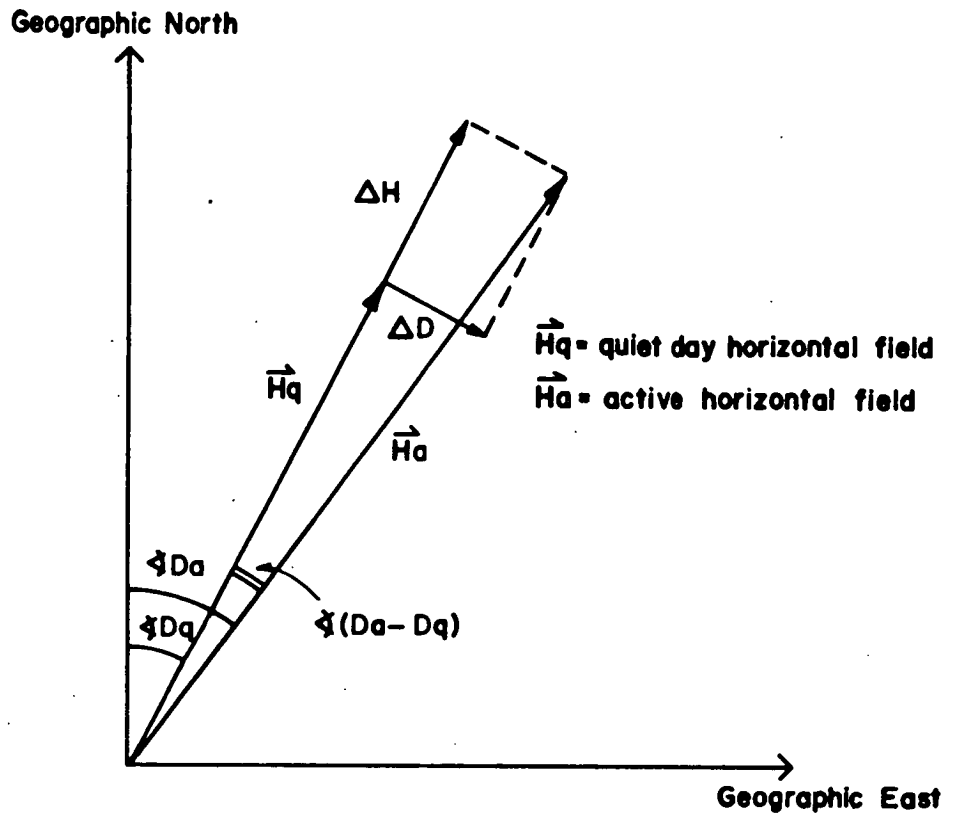


Figure 3.19(b): Similar plot for the D component.





Define:

$\Delta H \rightarrow$  positive along the direction of  $\vec{H}_q$

$\Delta D \rightarrow$  positive  $90^\circ$  east of direction of  $\vec{H}_q$

then:

$$\Delta H = |\vec{H}_a| \cos (D_a - D_q) - |\vec{H}_q|$$

$$\Delta D = |\vec{H}_a| \sin (D_a - D_q)$$

Figure 3.20 Schematic representation of the calculation required to derive the large-scale changes  $\Delta H$ , and  $\Delta D$ , from the H and D components of an actual magnetogram, via the 'iron-curve' QDC method.

Having determined a QDC for each of the H and D magnetic field components, the data was analysed to determine the departure of each of the components from their quiet day value during correlated pulsation files. A minor complication, involving a parallax error between the magnetic traces and their associated timing marks (see Figure 3.18), had to be accounted for here. For the H field component this amounted to a difference of only 20 seconds, whilst for the D component, the relevant timing dots occurred approximately 1.8 minutes ahead of the corresponding point on the D trace. This error was accounted for in reading the average ordinate over each 5-minute correlation file.

The La Cour magnetometer effectively measures the total horizontal magnetic intensity with the H trace, defining its direction by virtue of the D curve. It becomes a simple matter to calculate the change in the field components required to shift the horizontal vector from its quiet day position to that which it occupies on an active day (refer to Figure 3.20).  $\Delta H$  is defined as the increase in magnetic field component along the direction of the quiet day vector at any particular time. Correspondingly,  $\Delta D$  is defined as the increase in the direction perpendicular to this, positive variations toward the east.

A complete analysis of the September data yielded the histograms of Figure 3.21. These show quite clearly that the sense of the  $4278\text{\AA}/H$  micropulsation correlations agrees rather well with the idea of a dominant overhead east-west current. Positive correlations were found chiefly when the overall magnetic H component tended positive (recall the ring current effect) as expected from an E-region ionospheric eastward current. On the other hand the D component field changes were somewhat smaller and do not indicate as decisively the expected correlation phase.

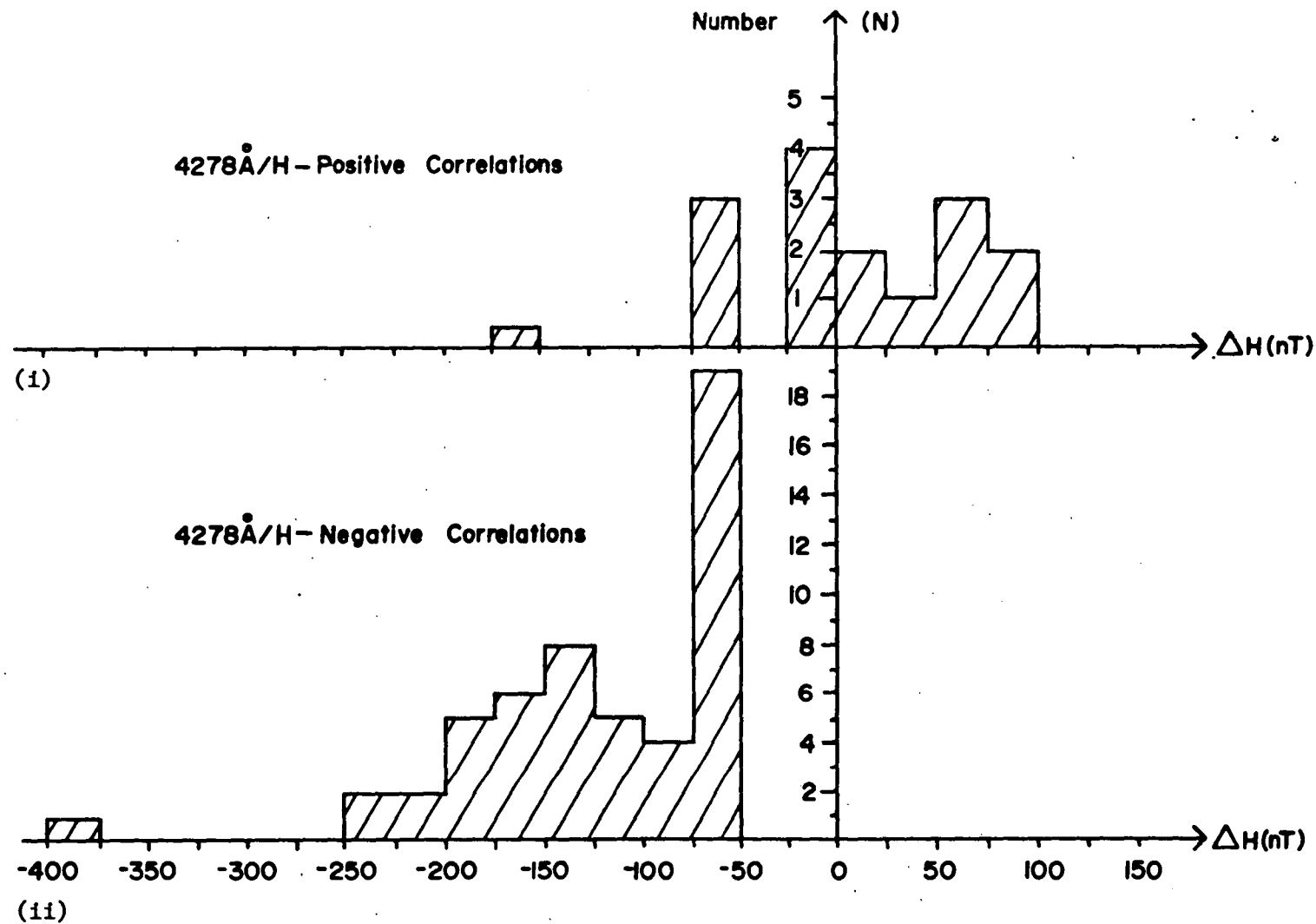


Figure 3.21(a) Histograms depicting the change in total H component versus the number of files that produced positive (i), or negative (ii), correlations of the H micropulsations with the optical emission.

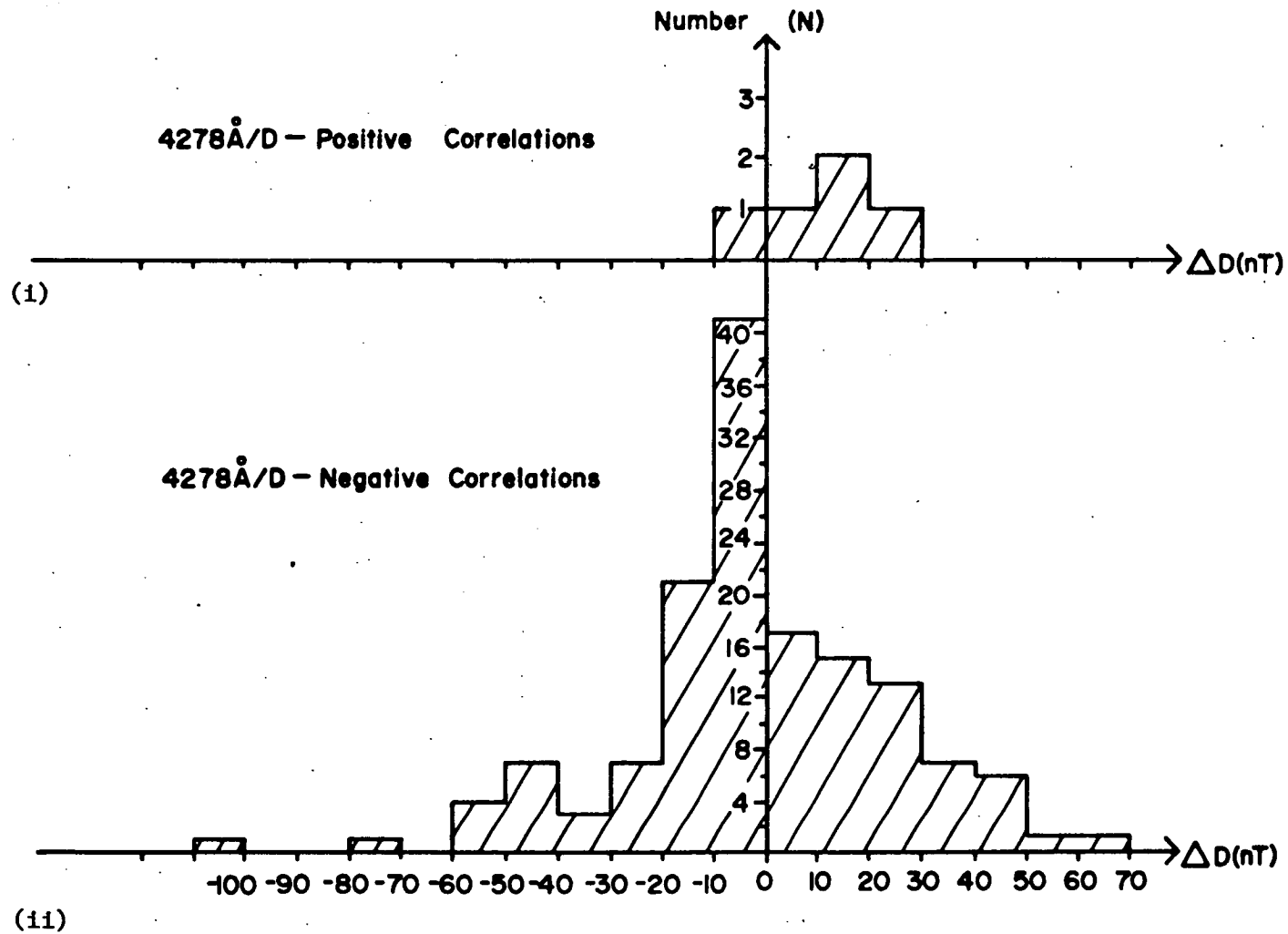


Figure 3.21(b) Similar histogram for the D micropulsation correlations and change in total D field. Note the more random changes in  $\Delta D$  versus correlation sign.

For the H component, a QDC was determined for each month of data collection, from November 1982 until September 1983 inclusive. Since the  $4278\text{\AA}/D$  component correlation phases did not fit well with the erratic variations of the large-scale D component magnetic field, they too were compared with the variations of the total H component. Figure 3.22 reproduces histograms of the two micropulsation components, with positive and negative optical correlation phases, versus the change in total H component magnetic field. These figures demonstrate a definite tendency for both the  $4278\text{\AA}/H$ , and the  $4278\text{\AA}/D$  micropulsation correlation phases, to become positive at times when the overall H magnetic field component is near or in excess of its QDC value. In the case of the H micropulsations this reflects the existence of a considerable local easterly E-region current distribution.

In conclusion then, this study of the large-scale magnetic field configuration during times of micropulsation occurrence yields the following results:

- (i) H component micropulsations and H magnetograms are affected by similar current systems. The bays in the H magnetograms are accepted as westward E-region auroral electrojet effects, and this implies a similar source for the H micropulsations.
- (ii) D component micropulsations and D magnetograms are affected by different current systems. Brekke et al., (1974) have shown that FAC's influence the D magnetogram, so this gives evidence that the D micropulsations may be unrelated to these FAC's.
- (iii) D micropulsations are associated with general trends in the H magnetograms. It is therefore likely that they are an ionospheric current system phenomenon.

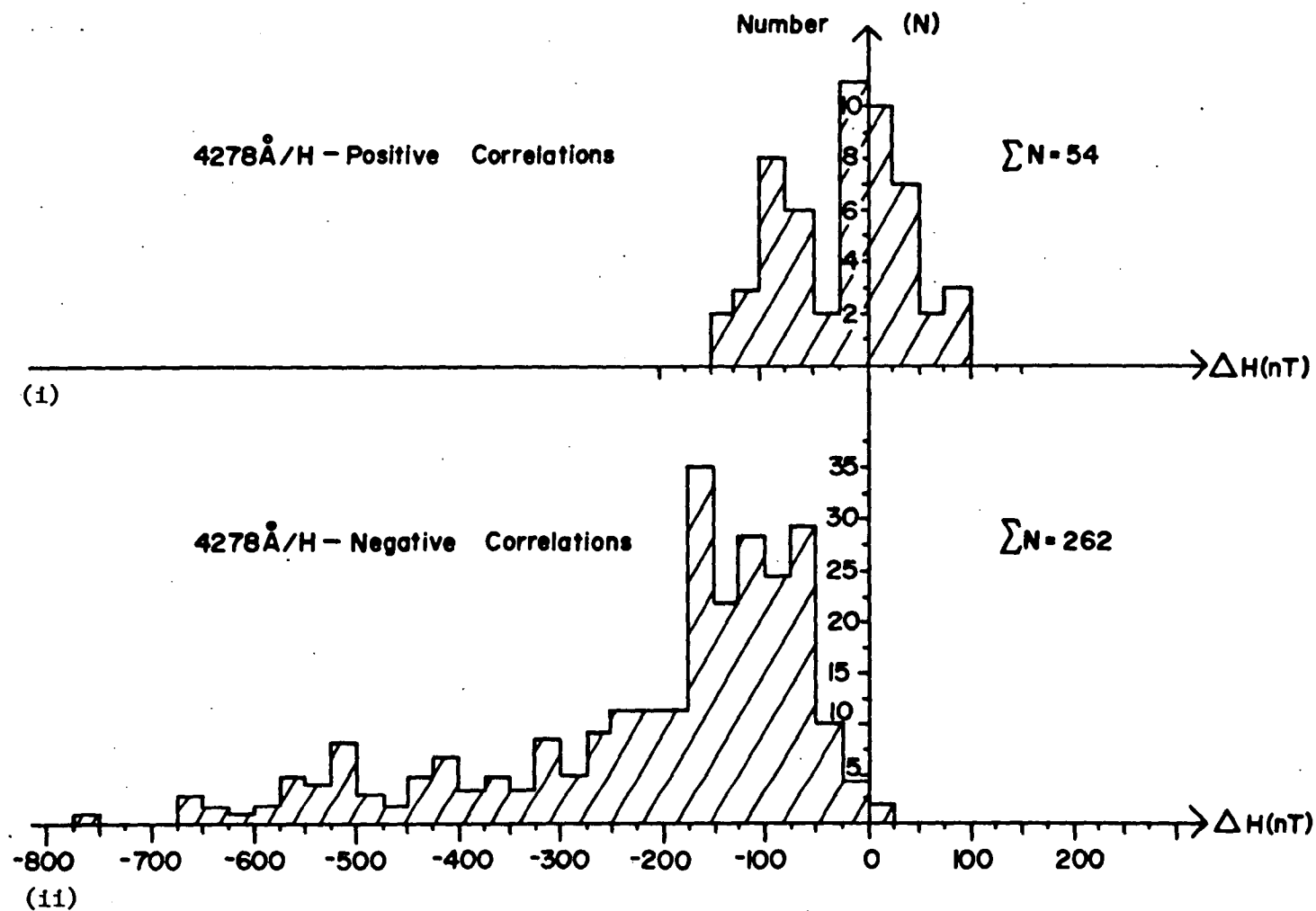


Figure 3.22(a) Full year's data indicating strong preference of negative H correlations for  $\Delta H$  negative.

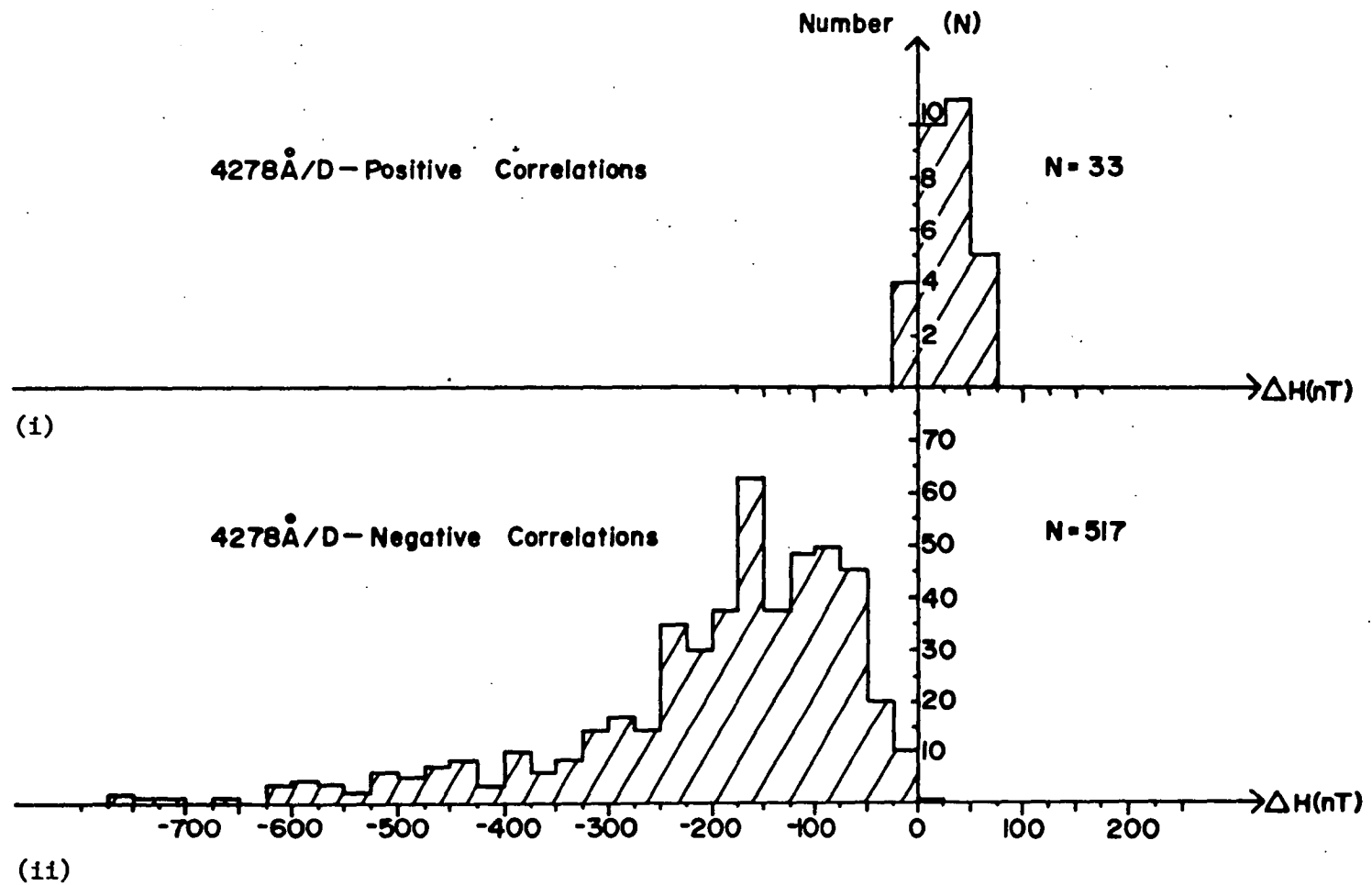


Figure 3.22(b) Full year's data for D correlations versus changes in  $\Delta H$ . The figure strongly points to an ionospheric current control of the D micropulsations as well.

### 3.6 SUMMARY OF RESULTS

Any realistic model or theory concerning the Pi(c) micropulsations must be able to explain the findings which have been presented in the preceding sections of this chapter. Many of the observations have been noted in part before (Burns, 1983; Oguti et al., 1984) but they are here based upon nearly a complete year's data collection.

The following summarised points are the major findings, and against them the theoretical predictions will be compared in chapter four:

- (i) The  $4278\text{\AA}$  optical auroral  $\text{N}_2^+$  1NG band emission generally leads the Pi(c) micropulsations by less than one second.
- (ii) The H-component micropulsations tend to lead the D-component by approximately 0.3s on average.
- (iii) The D-component micropulsations are more coherent over extended time periods, and are more likely to yield an acceptable correlation, than the H-component.
- (iv) The D-component micropulsations tend to yield higher magnitude cross-correlation co-efficients with the optical pulsations, than do the H-micropulsations.
- (v) The great majority of cross-correlations yield negative values, though phase reversals (not necessarily of both components together) do occur.
- (vi) The two major periods of occurrence of phase reversed files were early evening and late morning.
- (vii) The phase of the H-micropulsation cross-correlations is in basic accordance with the large-scale H-component magnetic bay signature.



- (viii) The D-micropulsations bear little phase resemblance with the more erratic D-component magnetograms, and in fact, follow more closely the large-scale H-component.
- (ix) The H-micropulsations are (marginally) more likely to yield a phase reversal correlation than the D-component.
- (x) During negatively correlated files, the negative swing of the micropulsation channels is usually far greater than the return positive pulse. The opposite is true for phase reversals.

## CHAPTER 4

### EXPERIMENTAL OBSERVATIONS AND THE $Pi(c)$ MICROPULSATION THEORIES

#### 4.1 INTRODUCTION

Observational evidence regarding the close association in time of the auroral optical pulsations and the  $Pi(c)$  micropulsations points strongly towards local ionospheric production of the  $Pi(c)$ . In this chapter the two major mechanisms for generation of  $Pi(c)$  micropulsations will be examined, in terms of the experimental observations summarized in Section 3.6.

The H component magnetic field will be affected by fluctuations in an east-west current system. Measurements indicate that this is predominantly a Hall current, and it is known as the auroral electrojet. The measured Hall conductivity maximizes at an altitude of 105km (Brekke et al., 1974) in the ionospheric E-region. The theory, to be critically examined here, proposes that it is the variations in this Hall conductivity which is responsible for the H micropulsations.

Similarly, north-south directed currents will influence the D component of the magnetic field. With a large-scale north-south electric field, these will essentially be due to the Pedersen conductivity, which peaks around 125km altitude (Brekke et al., 1974). One theory proposes the D component micropulsations to be under the control of these Pedersen conductivity fluctuations. An alternate argument considers the D micropulsations to originate directly from variations in the downcoming field aligned currents (FACs), which carry the structured electron precipitation responsible for the pulsating aurora.

With respect to the E-region conductivity argument being responsible for each of the  $P_i(c)$  components, it has been conjectured that the D micropulsations are in fact due to Cowling, and not Pedersen, conductivity changes (Arnoldy et al., 1982). Cowling conductivity is, in effect, an algebraic sum of Hall and Pedersen conductivities, which controls the current flow in the direction of the electric field, whenever flow perpendicular to the field is inhibited. With north-south electric fields being predominant (Brekke et al., 1974; Doupnik et al., 1977) this implies restricted flow in the east-west direction. Strong westward auroral electrojets decry this argument. An E-region conductivity cause of the D component  $P_i(c)$  will be considered here to be a Pedersen effect.

#### 4.2 E-REGION CONDUCTIVITY THEORIES

This section examines the data in terms of both the H and D micropulsations being related to E-region conductivity variations caused by the precipitating electron flux.

Auroral substorms have previously been described as specific enhancement of the westward auroral zone electrojet (Rostoker, 1972). Since the magnetic field H component is defined as positive northward, a westerly overhead current enhancement will result in a negative displacement of the north-south field with respect to the normal quiet day curve. This turns out to be the case, as determined by the Macquarie Island Bureau of Mineral Resources (BMR) magnetograms.

If the postulate that the H micropulsations are indeed a consequence of increased westerly E-region currents (Reid, 1976; Wilhelm et al., 1977; Burns, 1983; Oguti et al., 1984), then it is expected that the micropulsations will be negatively correlated with respect to the optical pulsations, at these times. This has been shown to be the case,

with negative optical/H micropulsations occurring always in association with a negative geomagnetic H bay.

The fact that, at these times, the dominant electric field is directed equatorward (Brekke et al., 1974; Banks and Doupnik, 1975) implies that the westward electrojet is a Hall current. Increased Pedersen conductivity, with an equatorwards electric field, results in enhanced equatorward current flow. This will produce an increased westward magnetic effect measured on the ground. Since the D component is defined as increasing eastward, a negative optical/D micropulsation cross-correlation will arise.

Due to the westward auroral electrojet and its associated equatorward leakage current dominating the morning hours (Rostoker, 1972), it is expected that the correlations of both Pi(c) components will usually be negative throughout this period. This is in agreement with the data presented in Section 3.4.

During evening hours, however, it is known that the auroral electrojet is largely directed toward the east (Rostoker, 1972). Brekke et al., (1974) have shown, from backscatter radar measurements in the northern hemisphere, that the electric field is then directed toward the pole. Hall and Pedersen conductivity enhancements, for this orientation, both result in increased H and D magnetic fields. So the pre-midnight correlations can be expected to yield positive inphase values for both components. This was found to be the case for the D component, whilst some of the rejected data contained examples of poorly correlated, but weakly positive, H component correlations during early evening hours.

Banks and Doupnik (1975) state that the transition, which is often abrupt, from poleward to equatorward near magnetic midnight,

is the most striking feature of the diurnal electric field pattern. Positive correlations, as expected, can be found before this time when the overall electric field vector is directed toward the pole.

For the H component to yield a positive correlation, it seems that a reversal of the E-region electric field is required, resulting in an eastward electrojet current. With the Pedersen current being in the direction of the electric field, this means the D component micropulsations will also switch to a positive correlation at effectively the same time. An example of this situation is depicted in Table 4.1, from 02-October-1983, where both components undergo a gradual ascendancy of positively correlated files after a period of confused not well correlated activity. The opposite change is seen to occur from about 1640Z, though slightly later for H, as both files revert to a negative response. A gradual, rather than sudden, electric field reversal appears to be responsible for the turnabout.

The more gradual transition, which appears to be a characteristic of the correlation phase reversal events in the late morning hours, has significant consequences for the E-region conductivity micropulsation mechanism. A closer look will be taken at this in Section 4.4, where a model is presented to account for phase reversals which do not necessarily occur simultaneously in both components.

Brekke et al., (1974) and Doupnik et al., (1977), could quite faithfully reproduce the H component magnetograms from their measurement of E-region currents and electric fields. At the same time they found that the D component magnetogram suffered many fluctuations which could not be explained in terms of their measurement. They attributed these to field aligned current effects, which tend to fluctuate incoherently even over small distances, say 100km (Wilhelm et al., 1977; Sato and

02 OCTOBER 1983

TIME (UT)	4278A/H MICROPULSATION		4278A/D MICROPULSATION	
	<u>Lead/Lag</u>	<u>X-Correlation</u>	<u>Lead/lag</u>	<u>X-Correlation</u>
1545-1550		N.C.	-0.4	-0.33
1550-1555		N.C.	-0.4	-0.61
1555-1600		N.C.	-0.6	-0.34
1600-1605	(calibration)		(calibration)	
1605-1610	0.0	+0.20	-0.6	+0.08
1610-1615	-0.2	+0.57	-0.8	+0.40
1615-1620	-0.4	+0.12	-0.8	+0.33
1620-1625	-0.8	+0.48	-0.2	+0.27
1625-1630	-0.8	+0.56	-0.8	+0.49
1630-1635	-0.2	+0.43	-0.4	+0.49
1635-1640	-0.4	+0.64	-0.8	+0.48
1640-1645	-0.6	+0.52	-1.4	+0.17
1645-1650	-0.4	+0.35	very weak negative	
1650-1655	-0.4	+0.45	weak negative	
1655-1700	-0.4	+0.42	-0.4	-0.17
1700-1705	(calibration)		(calibration)	
1705-1710	-4.0	-0.25	-0.2	-0.36
1710-1715	+1.2	-0.29	-0.2	-0.52
1715-1720	-0.4	-0.17	-0.2	-0.50

Table 4.1. Cross-correlation phase reversals occurring simultaneously in both micropulsation components. The D component appears to revert back to negative correlations slightly before the H.

Iijima, 1979). The fact that the D micropulsation positive correlations also tend to occur when the large-scale H magnetogram is at or near a local maximum, may be taken as evidence that it is the E-region current effects that are the controlling influence on their generation.

The east-west extent of the E-region current system has been shown to be continuous in the range  $10^{\circ}$ - $90^{\circ}$  of longitude (Rostoker, 1972). This is limited to a much smaller length, of the order of  $5^{\circ}$ , in the north-south latitudinal direction. Since the detection coils have a larger reception area than the photometer field of view, then the micropulsation files will be expected to record signals from regions unavailable to the photometer. Such a far greater longitudinal extent of the current systems will mean that the H coil should detect more unwanted fluctuations than the D. As a result, the D micropulsation files will be less contaminated, and as observed, are expected to yield more frequent and/or better cross-correlations with respect to the optical channel.

A greater coherency of the optical/D micropulsation cross-correlations over longer periods of time may also be incorporated within this explanation. Enhancements travelling along the electrojet, depending on the time of the observation, can contaminate the H component files both before and after they appear overhead of the station. Correlations of the H component, either side of the zenith observations, can be ruined by these far field effects.

It is time now to examine how the observed lead-lag time delays between the three phenomena fits with an E-region conductivity explanation. The data in Section 3.4 revealed that the optical pulsations tend to lead the H micropulsations by an average of 0.2s (taking into account the 0.1s delay introduced by the data collection

process, see Section 2.3), with the D component fluctuations following a further 0.3s behind.

Consider firstly the delay of the D micropulsations with respect to their north-south H component counterparts. With a geomagnetic equatorial region of origin for the electron bursts (Nishida, 1964; Coroniti and Kennel 1970a,b; Kan and Heacock 1976) responsible for the conductivity enhancements, velocity dispersal will mean that the more energetic electrons will arrive first in the local ionosphere (Bryant et al., 1975; Yau et al., 1981). Delay times between the various effects will depend upon the altitude of excitation of the individual phenomena, the time rate of change of the free electron concentrations responsible for the conductivity variations, and the conditions which exist along the ensuing path to the detection system. The last point of these has more particular relevance to a FAC mechanism (see Section 4.3).

Figure 1.7 (refer Section 1.5) from Brekke et al., (1974) showed that the Hall conductivity peaks at an altitude of approximately 105km, which is below the Pedersen conductivity peak at 125km. It was demonstrated in Section 1.5 that both conductivities are directly proportional to the free electron concentration in the vicinity of their maxima (Burns, 1983). It is the Hall conductivity, which dictates changes in the auroral electrojet (at near constant electric field strength), that is considered to be responsible for the H micropulsations. If the D micropulsations are a result of changes to the equatorward current arising from variations in the Pedersen conductivity, then it is expected that the H micropulsations will lead the D. This is because the more energetic electrons, which arrive first, are able to penetrate to greater depths in the ionosphere, so the Hall conductivity will be enhanced before the Pedersen.



Theoretical height-ionization rate profiles for monoenergetic unidirectional electron fluxes, assuming collisional thermalization processes, are reproduced in Figure 4.1, from Stenbaek-Nielsen and Hallinan (1979).

It can be seen that the electrons responsible for the Pedersen conductivity enhancements, around 125km, have energies of the order of 3keV. Those that penetrate to the peak Hall depth at 105km have higher energies close to 10keV. From the simplistic stance of monoenergetic fluxes the travel times have been computed for a geomagnetic equatorial origin some 50,000km distant. These figures appear in Table 4.2. They show that the H micropulsations can be activated approximately 0.7s in advance of the associated D component.

Though this figure is around twice the mean value obtained experimentally, it is of the desired order of magnitude required to fit with observation. Obviously some degree of activation of the D component occurs from the higher energy portion of the flux which is typically Maxwellian below 20keV (Bryant et al., 1975; Johnstone, 1978). So the expected delay of the D micropulsations with respect to the H, will on average, be somewhat less than monoenergetic, monodirectional flux calculation. The E-region conductivity mechanism therefore offers a feasible explanation for why the H micropulsations predominantly lead the D.

It is not valid to simply continue this argument to embrace the auroral optical pulsations, because the free electron concentration build-up (and hence the conductivity enhancement) is not expected to be an instantaneous process, which the  $N_2^+$  optical emission is generally considered to be (Omholt, 1971; Rees and Jones, 1973).

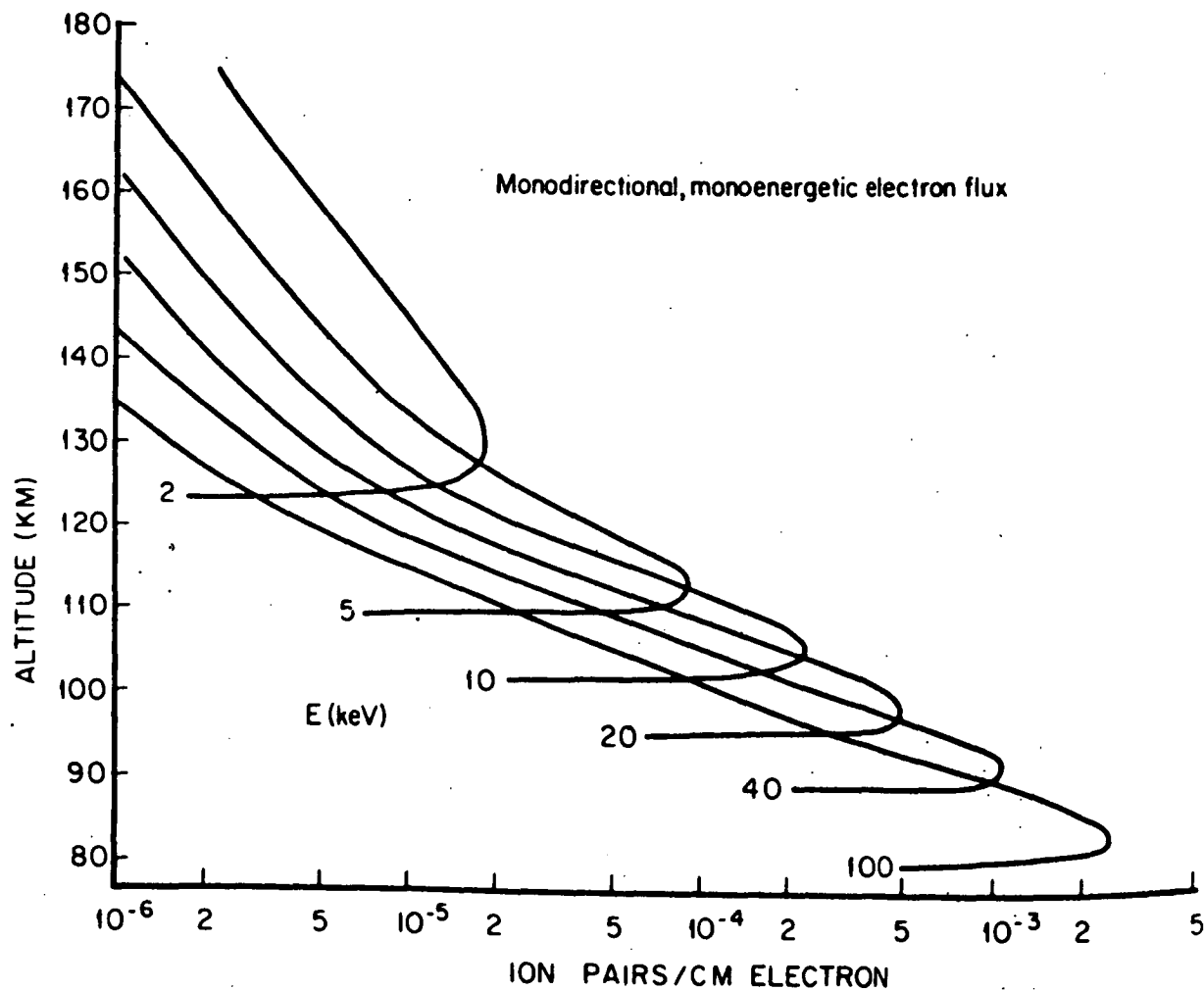


Figure 4.1 Theoretical height-ionization rate profiles for monoenergetic unidirectional electrons assuming collisional thermalization. Electrons with 2-3keV precipitate at the Pedersen conductivity peak (125km), those with 5-10keV reach the Hall peak (105km) and >10keV penetrate to pulsating auroral heights (80-100km) (after Rees, 1963).

Auroral optical emission has been determined to be generated at heights between 80-100km (Rees, 1963; Brown et al., 1976) and more recently with average lower borders between 83-140km at a median altitude of 98km (Stenbaek, Nielsen and Hallinan, 1979). In Section 2.1 it was shown in the experiment by O'Niel et al., (1979) that this auroral emission was coincident with the arrival of the precipitating electrons, the  $N_2^+$  1NG band being virtually instantaneous. The optical pulse detected on the ground is therefore an excellent reproduction of the primary electron flux incident on the ionosphere around 90-100km.

Consider a pulse of electrons arriving at the auroral altitude with a duration of approximately 6s, and for ease of calculation let it be a sinusoidal shape. Suppose also that the change in magnetic field closely follows this pulse, that is, the change in conductivity has the same immediate response. Table 4.2 indicates that the optical pulse, as a result of say 20keV electrons, will lead the change in the H magnetic component by nearly 0.25s, the D slightly further delayed. The micropulsation measured by the coils is, to a first approximation, the time rate of change of this magnetic variation, and is thus reflected in the differentiated conductivity pulse. Figure 4.2 shows that this implies the H micropulsation should lead the auroral optical peak by the order of approximately 1.25s, and by nearly a second for the D component.

The magnitude of the lead by the micropulsation over the optical pulse will be accentuated or alleviated by the shape of the pulse. Positioning of the micropulsation peak depends on the maximum rate of change of the conductivity pulse. The particular point emphasised here is that this situation predicts that the micropulsation will lead the optical pulsation.

E (keV)	Time(s)	Altitude (km)
3	1.54	125 (Pedersen peak)
5	1.19	
10	0.84	105 (Hall peak)
15	0.69	
20	0.59	100 (optical aurora)
25	0.53	
30	0.49	

Table 4.2     Calculated travel times for monoenergetic unidirectional electron fluxes from a geomagnetic equatorial source 50,000 km distant.

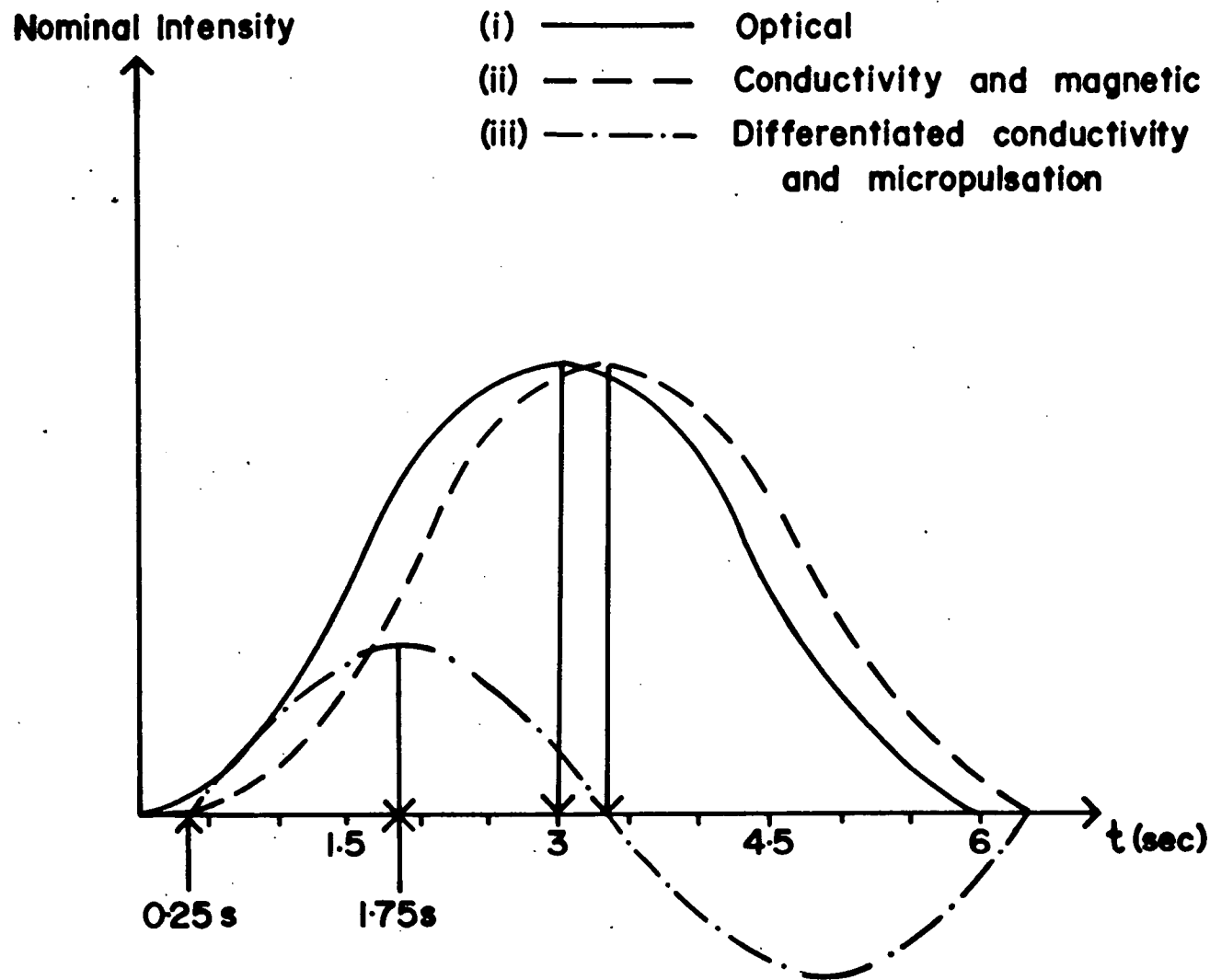


Figure 4.2 Schematic of a sinusoidal optical pulse, and assumed instantaneous conductivity pulse. The micropulsation, being proportional to the time rate of change of conductivity, should lead the optical and display an equal and opposite return pulse.

What salvages the conductivity theory from this predicament, is the fact that the production of free electrons, in the auroral ionosphere, is not likely to be such an instantaneous process. Jones and Rees (1973) have studied the temporal build-up of the free electron density, and their conclusions are summarized in the plots of Figure 4.3.

These indicate that the free electron concentration maximum is delayed of the order of 5-6s, at the heights of the Hall and Pedersen conductivity peaks, with respect to the peak flux of the ionizing precipitation. Recall from Section 1.5 that the Hall and Pedersen conductivities are directly proportional to the free electron density in the region of their maxima (Burns, 1983). The magnetic micropulsations depend on the time rate of change of this build-up, and so are not necessarily subject to delays of 5-6s magnitude. For the optical pulse to lead the micropulsations, as is generally observed, it is essential that the optical peak intensity is achieved before the maximum rate of change of conductivity occurs.

Note that these considerations are based on the assumption that the H and D micropulsations are overwhelmingly due to conductivity variations in the auroral ionosphere, and that any ionospheric electric field changes which occur, are dominated by them.

Figure 4.3(a) from Jones and Rees (1973), adopts a 10s period ionization function to produce theoretical plots of the ensuing variations in electron density. The most rapid time rate of change of these variations, is seen to be delayed of the order of a second with respect to the ionization function peak. An incident flux, typical of auroral precipitation, with maximum energy deposition at 112km, was adopted. The free electron density modulation came

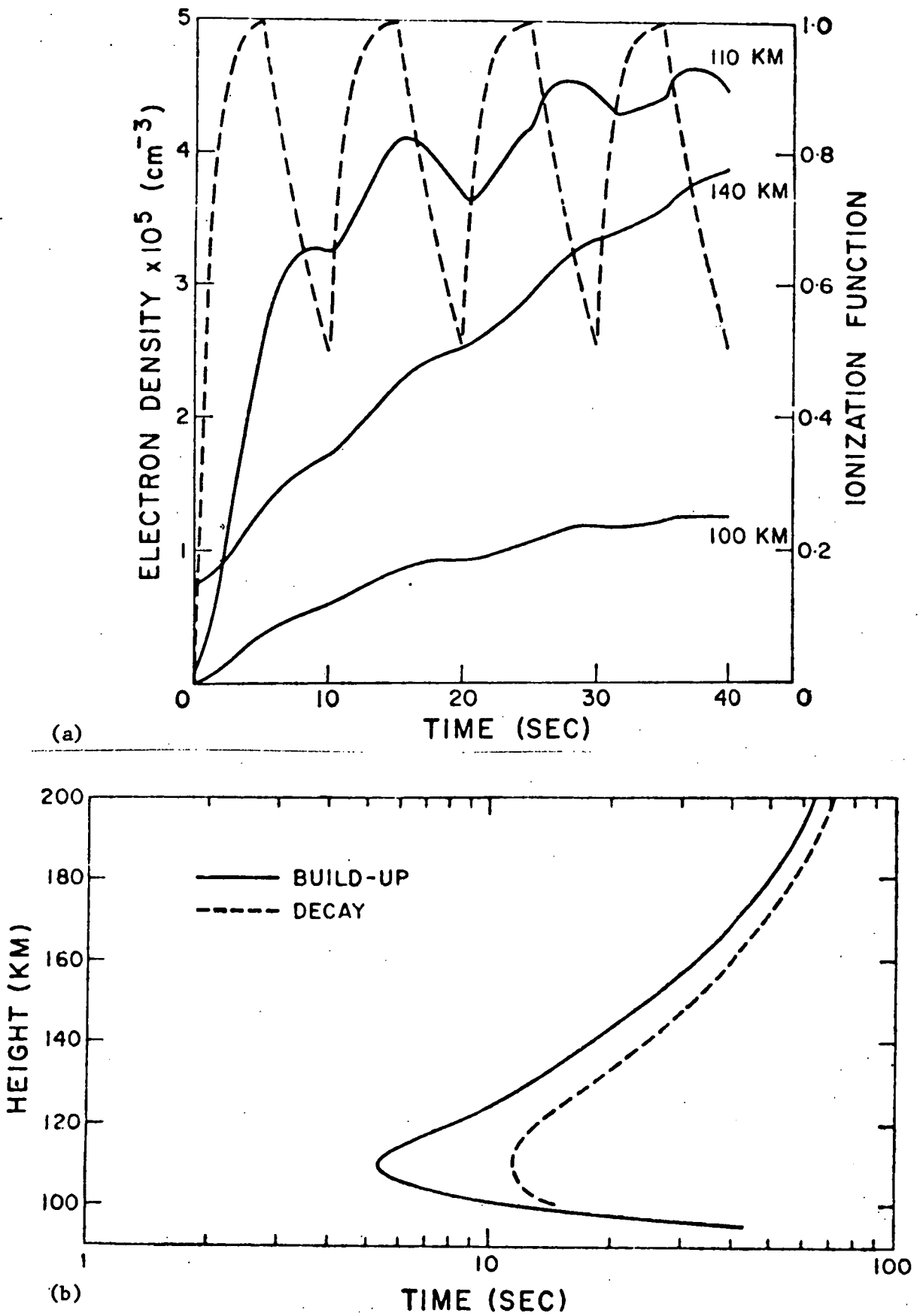


Figure 4.3 Variations in electron density from an applied ionization function (a), and the altitude dependence of the time required to achieve 63% of steady state electron density, in buildup and decay (from Jones and Rees, 1973).

out to be maximized in the vicinity of the Hall and Pedersen conductivity peaks, corresponding to the region of micropulsation production according to the theory under consideration.

Jones and Rees (1973) also showed that the higher the free electron concentration already present, the more rapidly does the increased electron density follow the incident energy. Burns and Cole (1984, private communication) point out, that since the Hall conductivity peaks in a region of higher electron density, this effect may contribute to the delay of the D with respect to the H micropulsations.

Therefore, according to an ionospheric conductivity controlled mechanism for micropulsation generation, the delay in the rate of electron density build-up with respect to the nearly instantaneous optical response to the precipitating flux, is responsible for the optical fluctuations leading the micropulsations. A velocity dispersal altitude effect causes the H micropulsations to marginally lead the D component.

Differentiation of the conductivity pulse showed that, for a symmetrical pulse, the micropulsation should respond with two equal and opposite peaks. Figure 4.2 displays a positive pulse followed by a negative echo, for convenience of comparison only. It has been shown that the vast majority of micropulsations correlate negatively with the optical peaks.

Observations made at Macquarie Island indicate that the initial pulse is of far greater magnitude than the subsequent opposite excursion. This situation can be explained quite neatly within the confines of a conductivity mechanism.

The  $N_2^+$  1NG band emission has been shown to be strongly related to the primary electron flux in a nearly instantaneous fashion (Rees, 1983;



Omholt, 1971; Rees and Jones, 1973). Only 18.7eV is required to excite the  $N_2^+$  ion to the 1NG band emission level. Electrons with energies of several keV can produce these excited ions at a rate of 3 ion pairs/100eV of initial energy (Dalgarno, 1961). Omholt (1971) has argued, that since the  $N_2^+$  emission is directly proportional to the ionization rate of  $N_2$ , then it is also directly related to the energy of the incident auroral electrons. The optical peak follows closely the precipitating flux in very rapid fashion.

Employing a typical auroral ionization function with a differential number flux:

$$n(e) dE = 3.3 \times 10^8 E \exp(-E/2.3) dE \text{ cm}^{-2} \text{ s}^{-1} \text{ keV}^{-1}$$

where the energy  $E$  is expressed in keV, e-folding energy  $E_0$  is 2.3keV (somewhat smaller than that measured for pulsating aurora, see Section 1.3), Jones and Rees (1973) considered an auroral event with a maximum energy deposition at 112km. They calculated the corresponding build-up of electron density at four different altitudes, and its subsequent decay profile. These results are displayed in Figure 4.4.

They show, that for an ionization function maximum achieved after 3s from onset, the peak rate of change of free electrons follows nearly 4s from onset, in agreement with the optical leading the micropulsations. The time for the free electron concentration to reach its maximum, is approximately 10s around 100-120km altitude, whilst the decay is considerably slower. So the ionization pulse is an asymmetric phenomenon with a much more rapid rise time, than decay time. This situation is also obvious from the altitude profiles of build-up and decay shown earlier in Figure 4.3(b). Here the decay time turns out to be of the order of three times the build-up period.

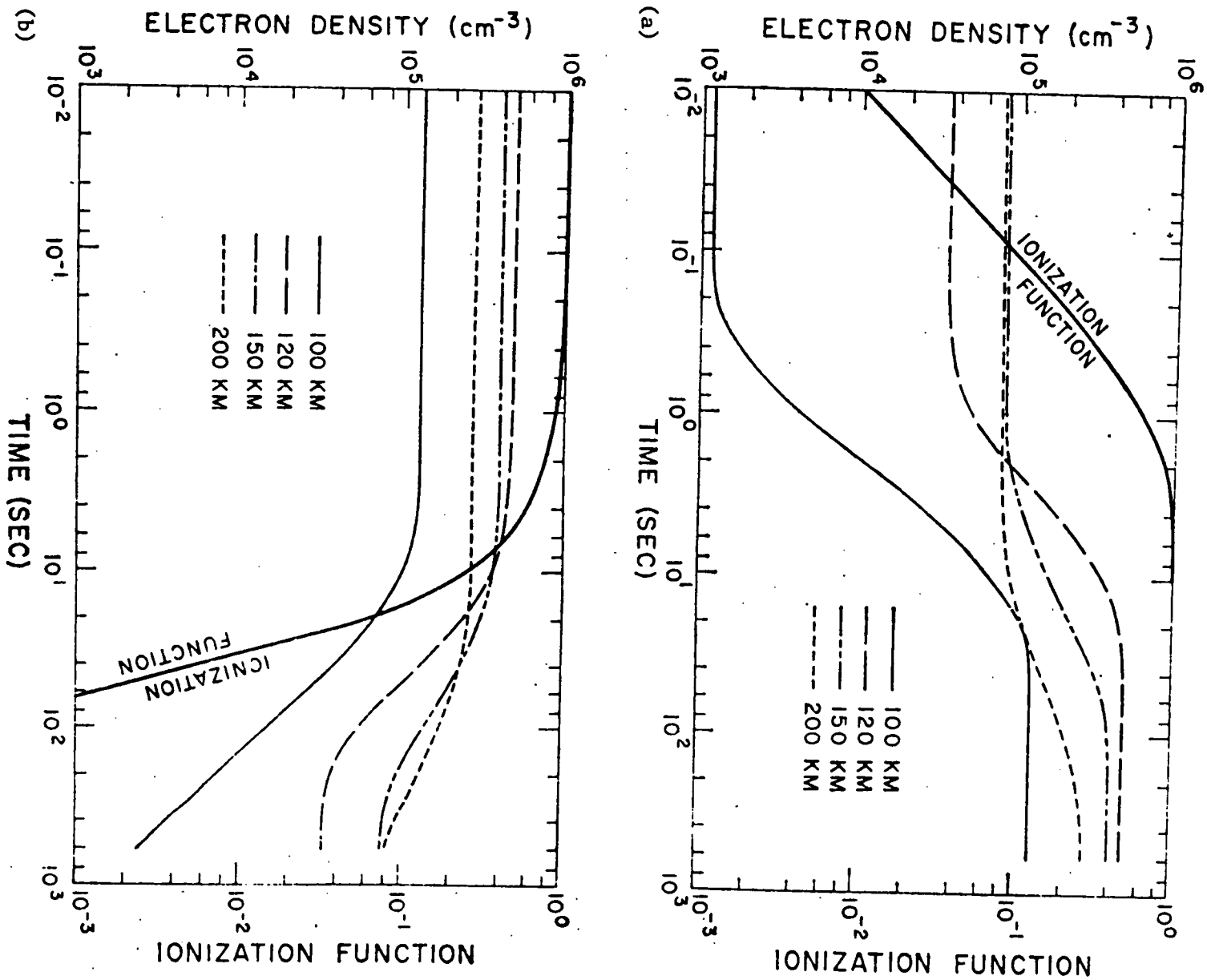


Figure 4.4 Buildup (a) and decay (b) of electron density at four altitudes resulting from ionization by electron bombardment of the given ionization function (from Jones and Rees, 1973).

A similar asymmetry has been observed in the shape of cosmic noise absorption (CNA) pulsations (Reid, 1971; Burns, 1983) which are also believed to be related directly to the free electron density.

Since the Hall and Pedersen conductivities are proportional to the free electron concentration in the vicinity of their maxima, the associated conductivity waveforms will be similarly asymmetric. Differentiation of this waveform will therefore yield a strong initial deflection, followed by a weaker return pulse. The diminution of the following reverse peak will be further accentuated by the reduced coil response to the slower decay of the pulse.

Thus, the free electron density considerations, clearly demonstrate, that an E-region conductivity controlled micropulsation mechanism can adequately explain lead-lag delays, and the lack of a pronounced frequency doubling effect in the micropulsation response. Large-scale magnetogram considerations have shown that predominant E-region currents can account for the sign of the  $4278\text{\AA}$ /micropulsation cross-correlations, and their association in time with phase reversals. The different extent of the auroral currents in east-west and north-south directions, provides some explanation for the predominance of better, more frequently correlated, D micropulsations with the optical fluctuations.

An E-region conductivity explanation for the H component tending to suffer more phase reversals than the D, will be presented in the light of the current model examined in Section 4.4.

Thus it seems that the observations can be comfortably accounted for in terms of the H micropulsations being a Hall conductivity effect, and the D micropulsations responding to Pedersen conductivity variations.

Note again that no particular recourse to E-region electric fields has been required in these arguments. Leoninen et al., (1983) have

presented electric field data (resolution time 0.5-1.0s) showing that it fluctuates essentially in phase with the Hall conductivity. The implication that can be drawn from the success of these conductivity arguments is that this finding is expected to be the case. Either the electric field fluctuations are largely in phase with the conductivity variations, or else they are not the dominant influence on the E-region current oscillations during pulsating aurora.

#### 4.3 FIELD ALIGNED CURRENT THEORIES

Here the results listed in Section 3.6 will be examined in order to test their consistency with a field aligned current (FAC) generation mechanism for the D component micropulsations. In the previous section it was demonstrated that E-region current effects could satisfy the experimental observations, and that the H micropulsations in particular, are now more generally accepted as being due to Hall current electrojet fluctuations (Burns, 1983; Oguti et al., 1984). However, very reasonable proposals can be submitted for the D micropulsations being produced by structured field aligned currents (Wilhelm et al., 1977), so these must be critically scrutinized here in terms of the current data.

Since the H component is still being considered as an E-region current phenomenon, then the majority of its cross-correlations with the optical emission will be negative. A whole new situation now exists for the D component however.

Burns (1983) has offered an explanation for the dependence of the correlation sign on the relative location of the FAC's with respect to Macquarie Island. The vertical photometer field of view will be a circle of 116km diameter at 100km altitude, taken as an approximate height of the auroral emission (Brown et al., 1976; Stenbaek-Nielsen

and Hallinan, 1979). Magnetic field lines incident at Macquarie Island form an angle of  $12^\circ$  with the vertical. Electrons impinging on the atmosphere, at 100km altitude, more than 21km north ( $100 \tan 12^\circ$ ) of the island, will result in a magnetic disturbance in an easterly direction, as measured on the ground (see Figure 4.5(a)). These will contribute towards a positive valued 4278Å/D micropulsation cross-correlation.

On this basis, approximately 72% of the field of view of the photometer system is biased towards negative correlations. As a result a greater abundance of negatively correlated files should be obtained in any data set collected.

Macquarie Island, invariant latitude  $64.5^\circ\text{S}$ , is situated marginally north of the equatorward edge of the southern auroral zone (Bond, Antarctic Division, internal publication). The observed region of pulsating aurora is a broad area extending over magnetic latitudes  $60^\circ$ - $75^\circ$ , usually on the equatorwards side of active auroral displays (Johnstone, 1978). It is generally spatially and temporally coincident with the diffuse aurora which typically stretches a few hundred kilometres wide (Swift, 1981). Consequently the photometer cone of reception should be quite symmetrically situated with respect to the pulsating aurora, and good positive correlations should be rather rare, as is observed.

A possible connection should therefore be expected between positive D micropulsation correlations and the  $K_p$  index, as a measure of geomagnetic activity. The more magnetically active the Earth's field, the greater the equatorward expansion of the auroral zone (Rostoker, 1972). This could in effect push the bulk of the pulsating aurora north of the station causing the D to correlate positively with the 4278Å emission. Such a connection is too tenuous from the limited suitable data collected in this research.

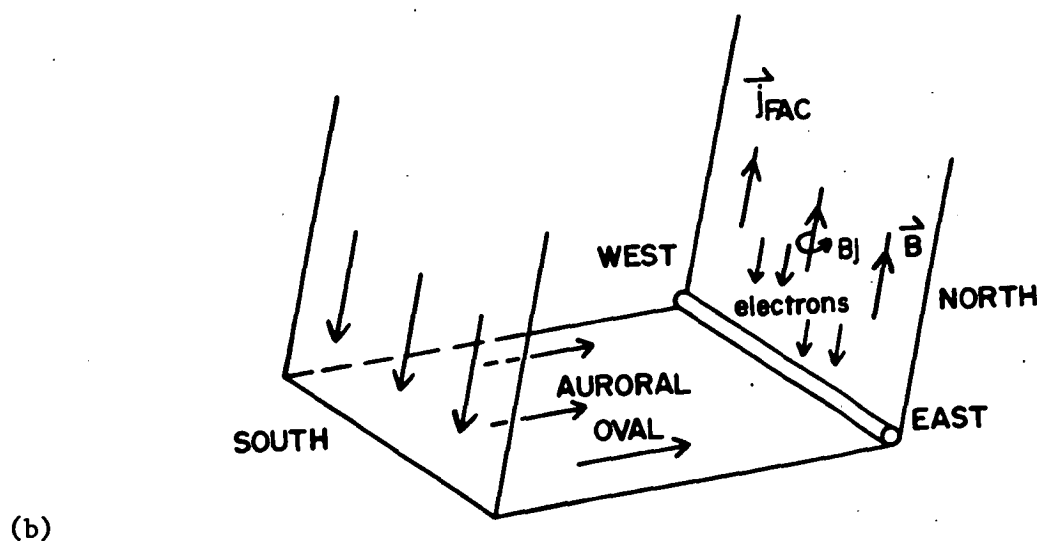
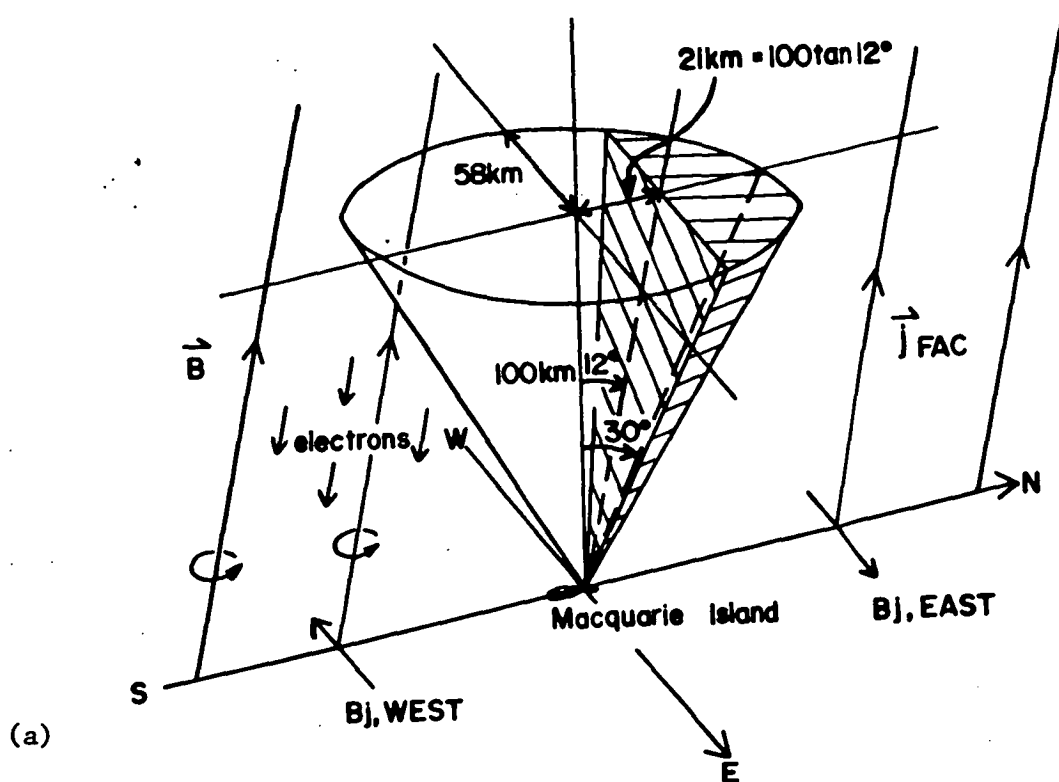


Figure 4.5 Field aligned current sheets showing the dependence on location with respect to Macquarie Island for the sign of the D component ground variation (a), and the pulsating aurora on equatorward edge of the auroral oval (b).

Other side effects should be noticeable as a result of this symmetry with respect to the observation site. D micropulsation files should be obtained which contain both in-phase and anti-phase responses to auroral pulses. Pulsating patches are typically 10-50km in width (Johnstone, 1978), so that some may appear to the north, the south, or may even overlap the reversal line. The overlapping situation can produce peaks that do not match the relative optical peak height ratios. An example of this possibility was depicted in Figure 3.3 for 18 February 1983, which also contains a mixture of positively and negatively correlated peaks.

The existence of occasional positively correlated pulses (patches greater than 21km north of the island) in the D component amid prolific negatively correlated peaks, can degrade the overall maximum correlation co-efficient. Figure 4.6, from 15 May 1983, 1325-1330Z, displays a file for which the  $4278\text{\AA}/D$  micropulsation correlation yielded the value -0.46. Neighbouring data blocks either side had the higher values -0.69, and -0.70 respectively. Minor peaks at 13:25:03, 13:25:20, 13:25:40, 13:27:20, 13:27:30 and 13:29:05, all appear to match in-phase with the corresponding optical pulses, causing the total correlation to diminish in amplitude.

However, it would seem to be expected that these phenomena should manifest themselves much more frequently than is the general observation. The relative peak-to-peak ratio in the D component is normally particularly good, much better than that for H. It would also seem doubtful that the D micropulsations should be so consistently better correlated than the H component under these circumstances. A symmetrical disposition of pulsating aurora about Macquarie Island, should yield many more cases where patches more than 21km north of the station degrade the negative correlations of those south of this location. If, on the other hand, the FAC mechanism is dominating

15-MAY-83

1325-1330U.T.

D-MUP  
316  
-597

H-MUP  
652  
-476

427.8NM  
877  
627

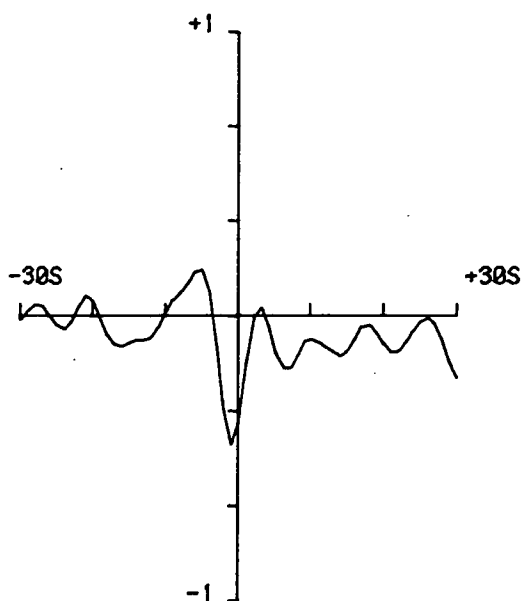
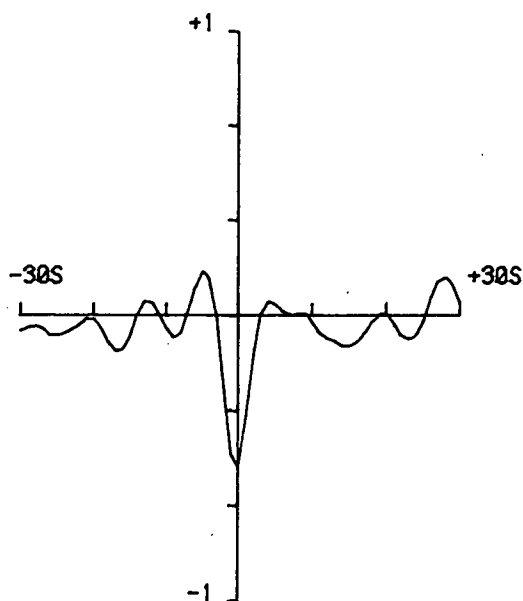
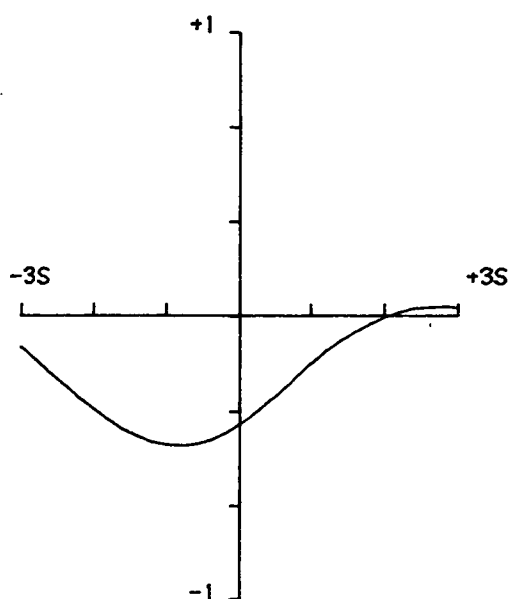
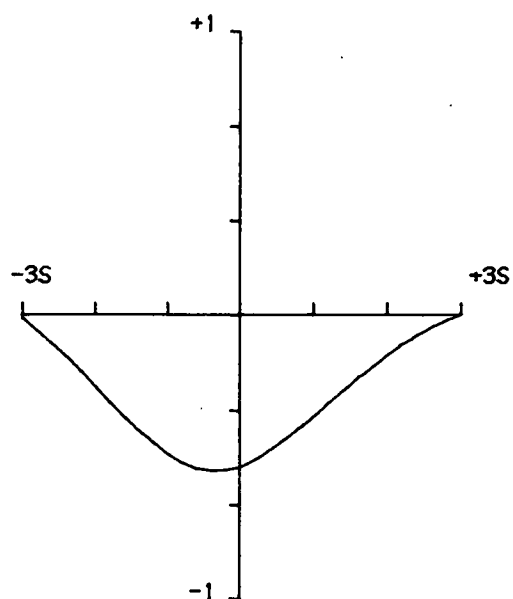
(a) 1325 1326 1327 1328 1329 1330

Figure 4.6 Possible degradation of 4278Å/D component correlation due to minor positive matching of some of the peaks.



15-MAY-83

1325-1330U.T.



(b)

4278A/H-MUP

X-CORR=-0.55

LEAD=-0.4SEC

4278A/D-MUP

X-CORR=-0.46

LEAD=-0.8SEC

production of the D micropulsations, then the parts of the electrojet outside the photometer window must exert a powerful influence on the H-coil, for its correlations to fall so consistently short of those for the D component.

FAC theory provides plausible arguments for the fact that both micropulsation channels do not necessarily switch in correlation phase at about the same time. The situation is easily envisaged where patches north of the station begin to dominate the event. This would result in the D component returning positive correlations with the optical fluctuations, the H component remaining negative.

Alternatively, reversal of the E-region auroral electrojet, via an electric field reversal, does not necessarily imply a change in location of the associated FAC as well. In this case it will be the H component alone that undergoes a change of sign to positive correlations.

In fact, it would appear highly fortuitous that both these phenomena should ever occur together to cause a synchronous reversal for both components. That such occasions do in fact arise, tends to arouse serious doubts about the validity of FAC's exerting a dominant influence on the D micropulsations.

Sato and Iijima (1979) used magnetometers carried on board polar orbiting satellites to determine the configuration of the Birkeland or FAC systems (see Figure 4.7). The FAC's are seen to flow away from the ionosphere (electron flux down) on the equatorward edge of the auroral oval in the morning sector, consistent with the observation of pulsating aurora at these times. These basic flow patterns are maintained during magnetically active periods, though the system broadens and shifts to lower latitudes.

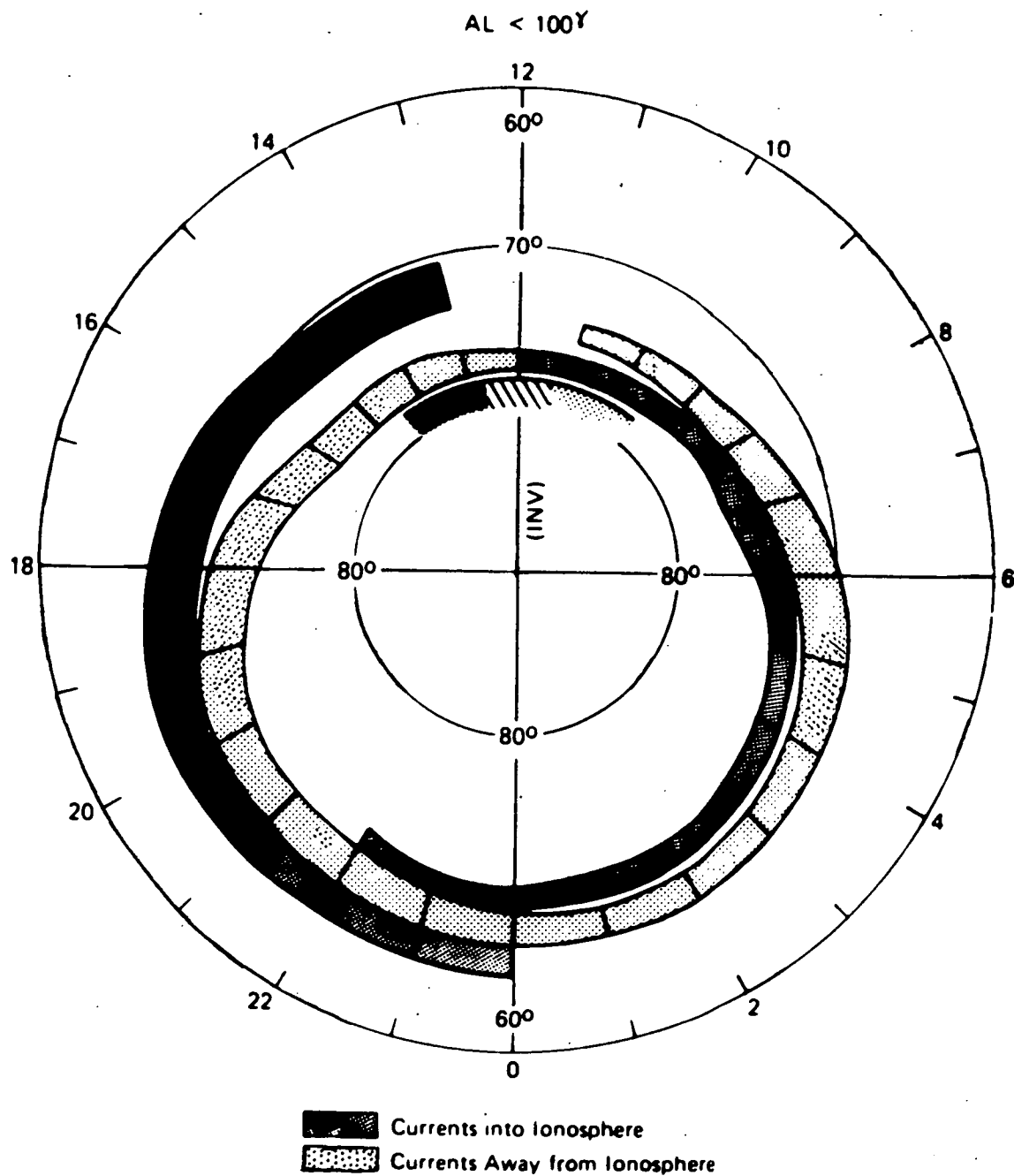


Figure 4.7 The normal position of the FAC system. Currents away from the ionosphere (electron precipitation) become more equatorward from 0000-0600 hours (after Saito and Iijima, 1979).

High variability and complex features appear whenever the westward auroral electrojet intrudes deeply into the evening sector. The late evening sector, 2000-2400 local time, contains a region of turbulent reverse FAC's known as the Harang discontinuity (Sato and Iijima, 1979). From the data it has been noted that positively correlated D micropulsations may occur during this pre-midnight activity. Since pulsating aurora are due to modulated deposition of electrons (current out of the ionosphere), then for a FAC explanation, the system must have expanded equatorward slightly, to push the upgoing FAC region to a position biased north of the station. This is because in the Harang discontinuity the electron precipitating FAC region is normally more poleward than in the later morning hours (see Figure 4.7).

On 23 May 1983, the D component yielded positive correlations in the pre-midnight period, H being rather poorly correlated but quite definitely negative apart from one dubious file. A deep westward electrojet intrusion caused a negative magnetic bay, 0740-0850Z, which upon recovery revealed positive optical/D micropulsation correlations. The figures for this event appear in Table 4.3.

ASC film of the event is unable to show conclusively the dominant position of the pulsating aurora with respect to the station. This is due to the problems intrinsic to Macquarie Island and low intensity pulsating aurora (see Section 2.4), and a near full moon shining on patchy cloud during the period concerned. The general appearance of the quiet arcs in the earlier evening were predominantly southward of the station however, a situation not favourable for a FAC mechanism.

TIME (UT)	4278A/H MICROPULSATION	4278A/D MICROPULSATION
	<u>Lead/Lag</u> <u>X-Correlation</u>	<u>Lead/Lag</u> <u>X-Correlation</u>
0850-0855	N.C.	-0.6   +0.33
0855-0900	N.C.	-0.6   Weak <u>positive</u>
0900-0905	(calibration)	(calibration)
0905-0910	-1.2   -0.26	-0.4   +0.43
0910-0915	-1.0   -0.58	-0.4   +0.37
0915-0920	Very weak, <u>positive</u> (?)	-0.4   +0.05
0920-0925	Very weak, negative	-0.4   +0.21
0945-0950	-0.8   -0.29	-0.4   +0.75

Table 4.3      Data for the event in the early evening of  
23 May 1983 with a deep intrusion of the  
westward electrojet into the premidnight  
sector.

It may, however, prove possible to test the FAC mechanism by examining the magnitude of the auroral emission at these times. When the D component correlation turns positive, then a contraction or translation of the pulsating region has occurred, and it might be expected that the magnitude of the auroral light emission should decrease. Burns (1983) found, for his one possible reverse phase file, that the total auroral luminosity had diminished by almost 50% on its earlier value during negative correlations. (Note that all components suffered the reversal to normal phasing for his event).

Conversely, no significant intensity level change is expected when the H component turns to positive correlations, the D component remaining negative, as this is effectively an electrojet reversal (local, at least).

What is required, essentially, are data sequences containing phase switches, measured on the recovery portion of a single magnetic bay. This ensures that no contamination creeps in from pulsating auroral regions associated with another bay. Such a requirement may in fact be unreasonable in view of the lifetimes of individual patches (Cresswell and Davis, 1966), but should be satisfied in terms of the same family of pulsating patches retaining a similar average intensity pattern. Oguti et al., (1984) have demonstrated the stability of the linear co-efficients relating luminosity variations to magnetic fluctuations, for periods in excess of 30 minutes. Note that the general level of magnitude of the individual pulses in the 5-minute files should gradually decrease. This is because a spatially drifting patch (towards the equator) will gradually depart the

photometer field of view. It is extremely difficult, without television imaging to tie individual peaks to particular patches, and arguments in this area suffer from the variety of parameters involved.

Two particular sequences, containing a D component phase reversal, were recorded which were candidates for the analysis outlined above. Tables 4.4 give the intensity changes associated with these events, and also estimates of the average pulse height throughout each 5-minute interval (measured in the same units as the overall intensity).

Unfortunately the results are rather inconclusive. For the 05-March-1983 event the individual mean pulse height appears to slowly diminish, with little change to the background intensity. On the 02-October-1983 the background intensity falls dramatically right through the observations. The average height of optical peaks decays too, but continues this process even as the D component files return to negatively phased correlations.

All these considerations here rest on rather shaky ground, due to the dependence upon the accompanying background diffuse aurora. If it is not anchored specifically to the pulsating patches, then it may or may not suffer a contraction or translation at the same time. On the limited amount of data available, considering the number of variable factors involved, no confident conclusions can be drawn either way on this subject.

The major period of occurrence of the positively correlated events turned out to be in the later morning hours. Again this, if anything, goes against a FAC system precipitating electrons into the ionosphere equatorward of the station. Later stages of pulsating aurora are associated with the gradual re-establishment of a quiet

OPTICAL LEVELS

TIME (UT)	4278A/H-M $\mu$ P		4278A/D-M $\mu$ P		MIN.	MAX.	AVERAGE PEAK HEIGHT
<u>05 MARCH 1983</u>							
1640-1645	+1.8	-0.42	-0.4	-0.44	408	677	100
1645-1650	+1.0	-0.39	-0.6	-0.55	458	648	100
1650-1655	+0.8	-0.63	-1.0	-0.69	430	594	75-100
1655-1700	0.0	-0.59	-4.0	-0.49	398	566	50-75
1705-1710	+1.8	-0.24	0.0	+0.16	423	618	75-100
1710-1715	+3.0	-0.26	-0.4	+0.41	401	602	50-75
1715-1720	+0.6	+0.52	-0.6	+0.16	367	470	50
<u>02 OCT. 1983</u>							
1530-1535	+0.6	-0.19	-0.2	-0.50	1353	1694	200-250
1535-1540	N.C.		-0.2	-0.43	1461	1875	200-250
1540-1545	N.C.		-0.4	-0.35	1318	1738	200
1545-1550	N.C.		-0.4	-0.33	1231	1630	200
1550-1555	N.C.		-0.4	-0.61	1170	1514	200-250
1555-1600	N.C.		-0.6	-0.34	1086	1603	200
1605-1610	0.0	+0.20	-0.6	+0.08	799	1226	200
1610-1615	-0.2	+0.57	-0.8	+0.40	712	1093	200
1615-1620	-0.4	+0.12	-0.8	+0.33	655	1060	150-200
1620-1625	-0.8	+0.48	-0.2	+0.27	572	899	150-200
1625-1630	-0.8	+0.56	-0.8	+0.49	546	976	200
1630-1635	-0.2	+0.43	-0.4	+0.49	472	1056	200-250
1635-1640	-0.4	+0.64	-0.8	+0.48	412	949	250
1640-1645	-0.6	+0.52	-1.4	+0.17	324	860	250
1645-1650	-0.4	+0.35	-0.6	-0.13	272	653	150-200
1650-1655	-0.4	+0.45	-0.4	-0.13			
1655-1700	-0.4	+0.42	-0.4	-0.33	303	530	150
1705-1710	-4.0	-0.25	-0.4	-0.36	246	408	100
1710-1715	+1.2	-0.29	-0.2	-0.52	240	391	100
1715-1720	-0.4	-0.17	-0.2	-0.50	223	325	50-75

Table 4.4 Auroral luminosity and peak height data.



arc system, as the region once again contracts toward the pole (Rostoker, 1972), and hence, southward of Macquarie Island.

How can a FAC effect account for the observed lead-lag relationship that exists between the three phenomena? The H micropulsations are still proposed as an E-region current effect, so that the argument predicting their small delay with respect to the optical is valid here.

Variations within a FAC will produce ULF electromagnetic waves, which must then travel down through the ionosphere with propagation near the Alfvén speed. In Figure 4.8 the basic geometry of the situation is outlined.

Production of the wave occurs continuously along the FAC, and a ground observer will receive the integrated effect of this emission, after it has traversed the ionosphere. Broadening of the D component pulses would be an expected consequence of this extended emission path length. Inspection of the data files reproduced in Chapter 3 would tend to indicate that this is not the case. Note however that some broadening is also expected in the H component pulses due to increased noise from its extended area of reception. The example of very rapid optical oscillations sharply echoed by the D component in particular, in Figure 4.9, is evidence against this extended path length from FAC emission.

The delay of the D component micropulsation over its optical and H component counterparts will now be due to the propagation time of the wave, as it traverses the auroral ionosphere. This will depend critically on the electron concentration - total electron content of the wavepath. Increased ionization should again provide an added D component delay.

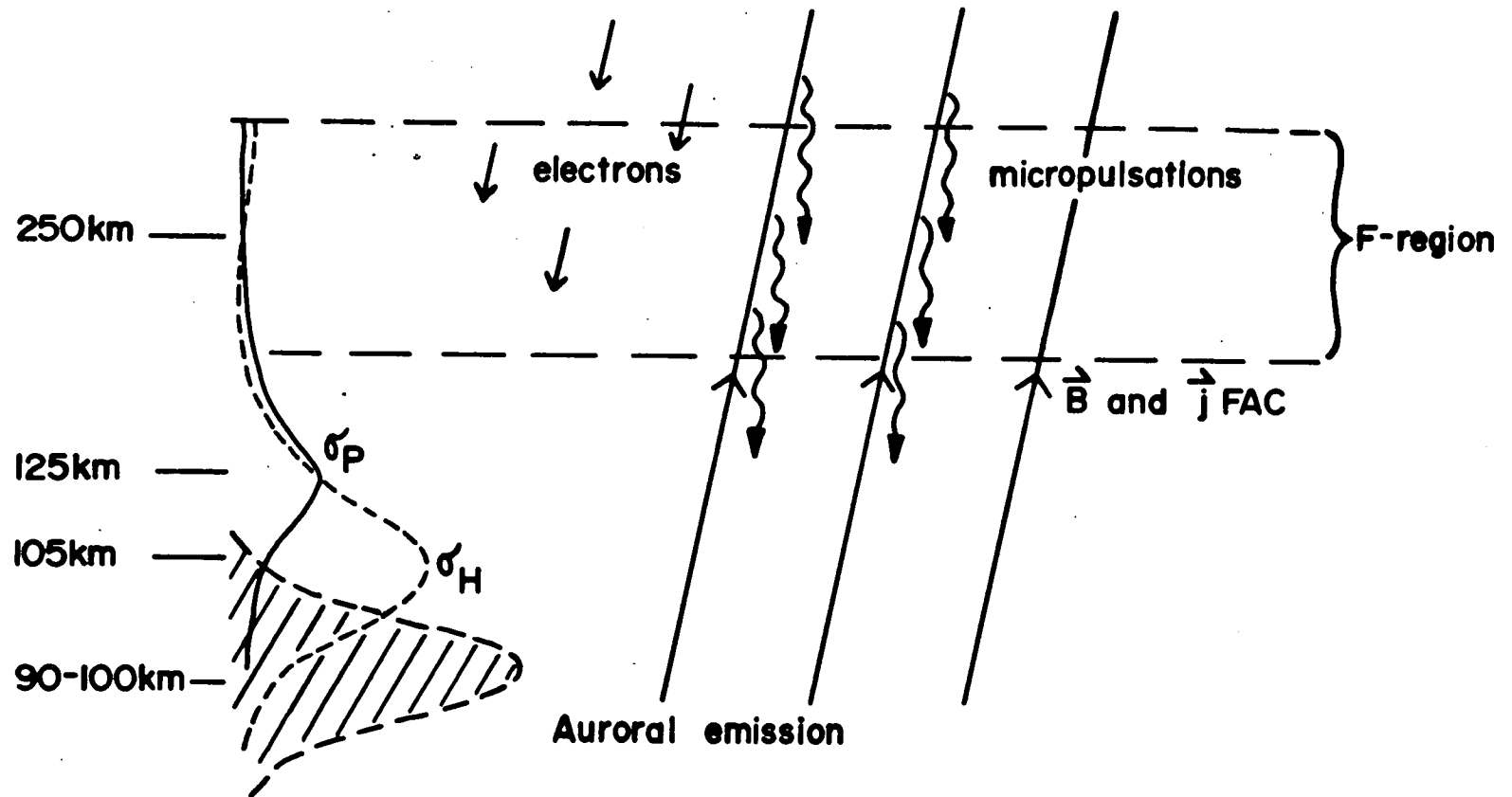


Figure 4.8 Schematic of ULF wave production along the extended path of the FAC and its propagation path through the auroral ionosphere.

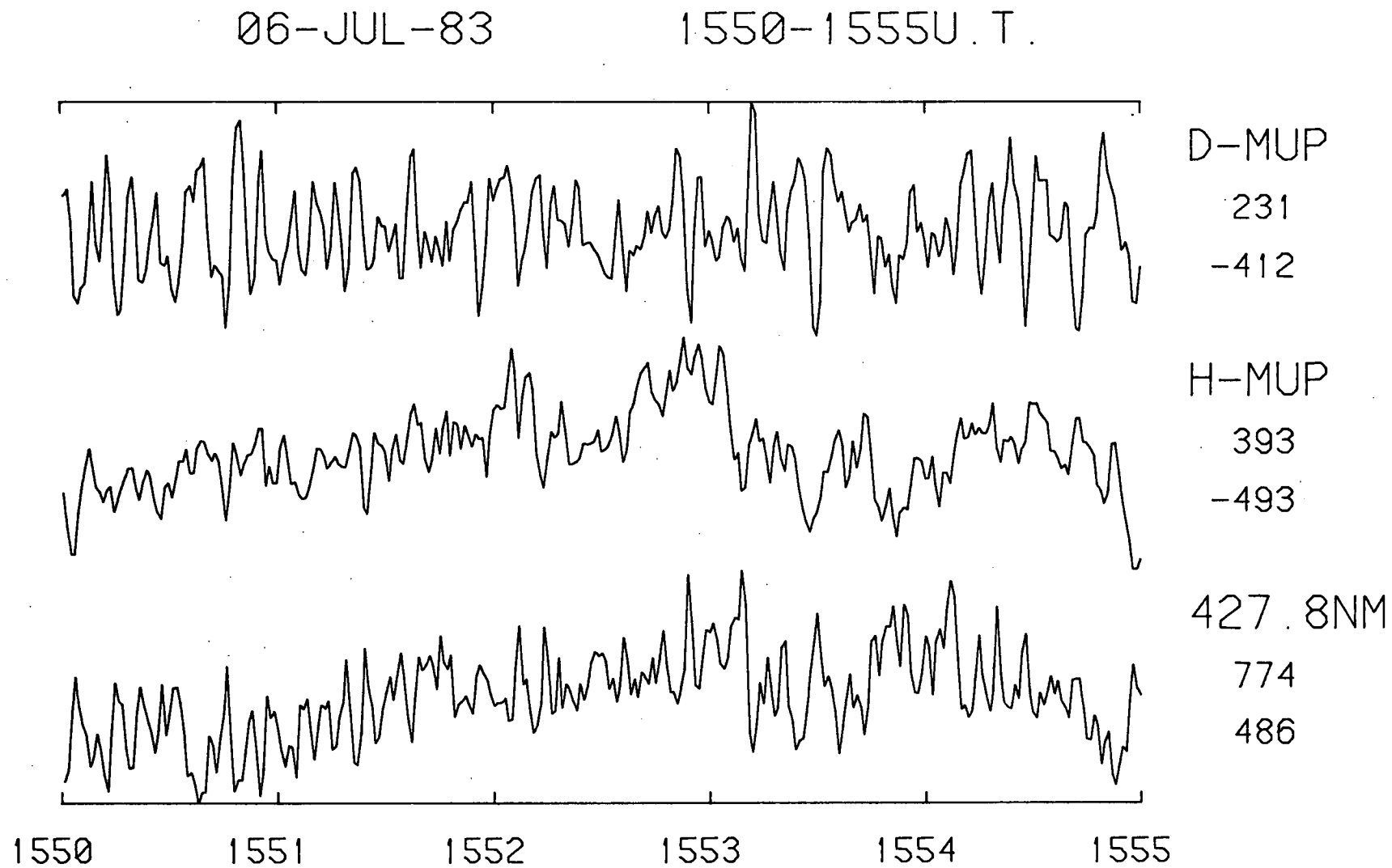
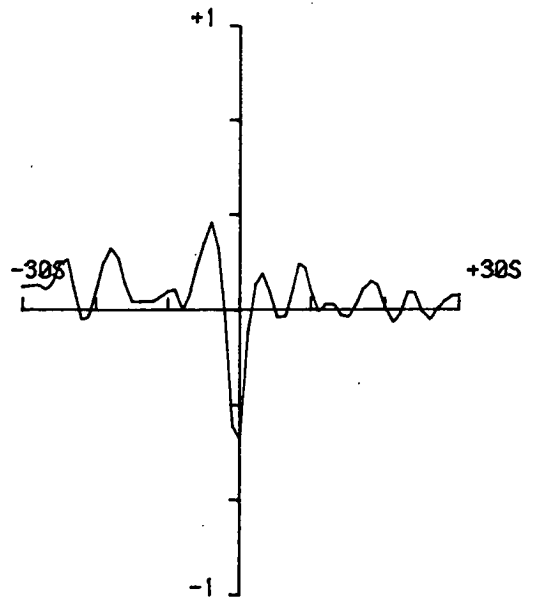
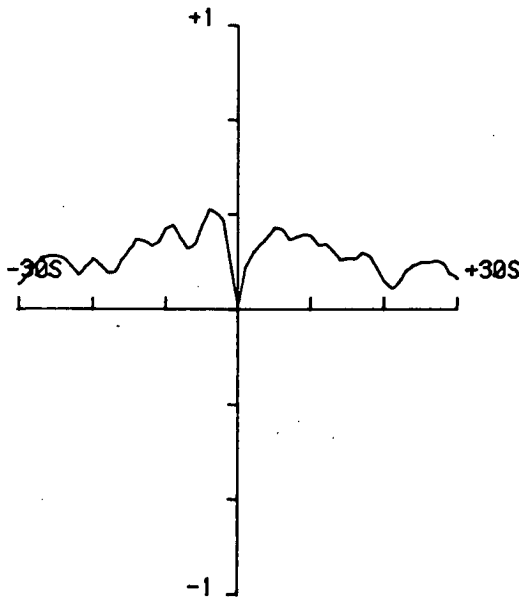
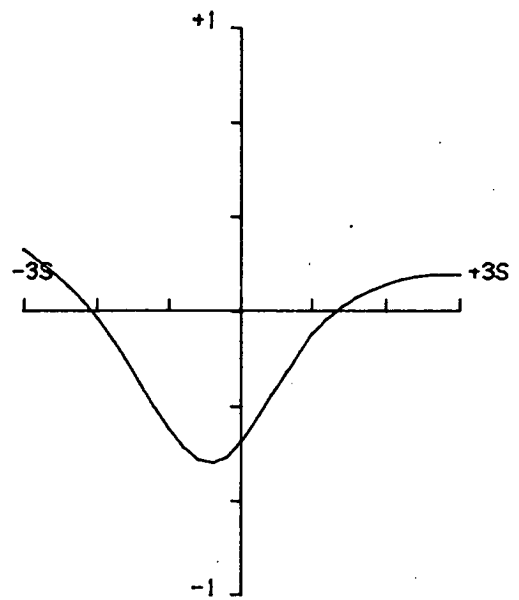
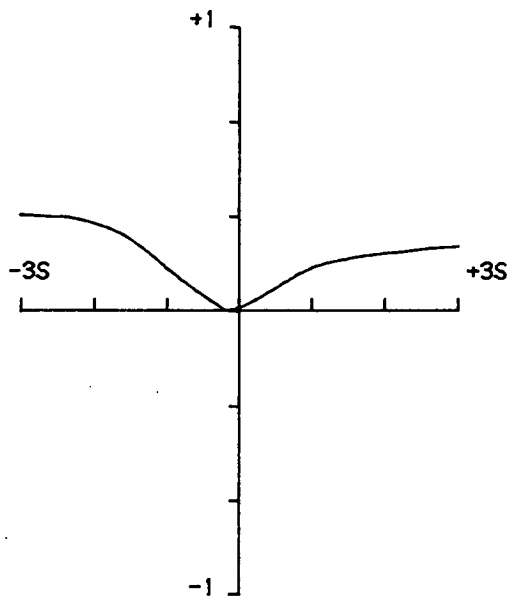


Figure 4.9(a) Example of rapidly pulsating optical file being closely accompanied by micropulsations, particularly in the D trace.

06-JUL-83

1550-1555U.T.



4278A/H-MUP

4278A/D-MUP

X-CORR=+0. 0

X-CORR=-0.54

LEAD=-0.2SEC

LEAD=-0.4SEC

Figure 4.9(b) Note the multiplicity of lobes in the D component cross-correlation function.

Francis and Karplus (1960) computed the time for an ULF wave to traverse the ionosphere, arriving at an answer of 1.4-1.6s, and rather insensitive to frequency. Field and Greifinger (1967) calculated delays of the order of 2s from studies of nuclear explosions. These delays increased with increasing ionization. Such delay times are necessary to meet the observed requirements that the optical emission leads the micropulsation. It appears that a FAC induced D component micropulsation mechanism could account for their observed lag with respect to optical aurora and the H component.

Maximum electron density in the ionosphere is at an altitude of 250km (Ratcliffe, 1972), and a measure of this is given by the parameter  $f_oF_2$  (the penetration frequency for the ordinary-mode wave in the ionosphere). A possible method of discrimination, between a Pedersen conductivity, or FAC effect, for generation of the D micropulsations, has arisen from discussion with Dr. Gary Burns (OIC, Antarctic Division, UAP Section) of an idea proposed by Professor K.D. Cole (Head of Physics Department, LaTrobe University). The suggestion is to examine the correlation between  $4278\text{\AA}/H$  micropulsation delays and  $f_oF_2$ , then repeat the study for  $4278\text{\AA}/D$  micropulsation delays for  $f_oF_2$ . The former is expected to simply yield noise, though a minor correlation may arise from an increased D-region ionization at times of increased  $f_oF_2$  (see below). For the D component delays, however, a strong correlation is expected if it is a FAC effect since the propagation time delay depends largely on the F-region ionization, and thus  $f_oF_2$ .

Unfortunately, it appears as if the D-region data available from the Macquarie Island standard riometer, cannot be used with any real confidence as a genuine  $f_oF_2$  indicator of any FAC mechanism.

Ranta and Ranta (1978) found the correlation between  $f_{O}F_2$  and standard riometer absorptions to be poor at high latitudes. Any association between the two arises only from a similarity between ionizing factors in the F- and D-layers, and not from a close dependence of electron densities. The D-region absorption occurs, despite low electron concentrations, because of the high local electron-neutral collision frequency. An ionosonde was erected at Macquarie Island during the 1983-84 station changeover so that local measurement of  $f_{O}F_2$  is now possible. Part of the 1985 UAP (Upper Atmospheric Physics) research program will be to make an  $f_{O}F_2$  (and probably  $fE_s$ ) micropulsation delay time study.

Campbell (1970) claims that the delay time of the micropulsations should increase with the total light emission of the aurora. This will be in response to the production of free electrons at auroral heights, and hence, along the micropulsation wavepaths. Both components should be similarly effected, but an added contribution is expected for the FAC generated D-component due to increased F-region ionization. Data collected at Macquarie Island was not generally supportive of Campbell's hypothesis. Wide spread of delays occurred more or less randomly over a large intensity range. Examples were shown in Table 4.4.

The final major consideration in this section is to determine whether or not a FAC mechanism can support the lack of a micropulsation frequency doubling phenomenon.

An electron burst will suffer a velocity dispersal as it traverses the distance, from its modulation source region at the geomagnetic equator, to the auroral ionosphere. Since the magnetic field variation depends upon the current flowing along the field line, the D component variation will be proportional to the number of electrons arriving at a particular time, multiplied by the velocity of the electrons (Burns, 1983):

$$B_D(t) \propto N_E(t) v_E(t) .$$

Since the velocity distribution is essentially Maxwellian, particular velow 20keV, then the number of electrons within a small velocity range  $dv_E$  is given by:

$$N(v_E)dv_E = \left(\frac{2}{\pi}\right)^{1/2} v_E^2 \left(\frac{m_e}{kT}\right)^{3/2} \exp\left(\frac{-m_e v_E^2}{2kT}\right) dv_E$$

where

$$kT = E_O = \text{the e-folding energy of the distribution,}$$

so that

$$N(v_E)v_E dv_E = A v_E^3 \exp\left(\frac{-\frac{1}{2} m_e v_E^2}{E_O}\right) dv_E$$

with:

$$A = \left(\frac{2}{\pi}\right)^{1/2} \left(\frac{m_e}{kT}\right)^{3/2} = \text{constant for a given e-folding energy.}$$

Then choose:

$$E_O = kT = 3\text{keV.}$$

So that:

$$N(v_E) v_E dv_E = A v_E^3 \exp(-9.49 \times 10^{-16} v_E^2) dv_E.$$

This quantity has been calculated for various values of the electron energy, and the results appear in Table 4.5. The time of travel-velocity dispersal effects, result in the product of an asymmetric magnetic pulse, with a more rapid rise time than decay (see Figure 4.10).

Differentiation of this pulse will again lead to a much larger amplitude initial peak followed by a weaker return pulse. The coil frequency response will further amplify this effect, and so the prediction here agrees well with observation.

E (keV)	1	2	3	5	10	20
$v_E(\text{ms}^{-1})$	$1.74 \times 10^7$	$2.46 \times 10^7$	$3.25 \times 10^7$	$3.89 \times 10^7$	$5.96 \times 10^7$	$8.38 \times 10^7$
$\Delta t(\text{s})$ [Traversal time over $5 \times 10^7 \text{m}$ ]	2.87	2.03	1.54	1.19	0.84	0.59
$N(v_E) \cdot v_E$	3.95A	8.38A	12.59A	14.00A	7.27A	0.75A

Table 4.5    Velocity dispersal of a Maxwellian distribution.

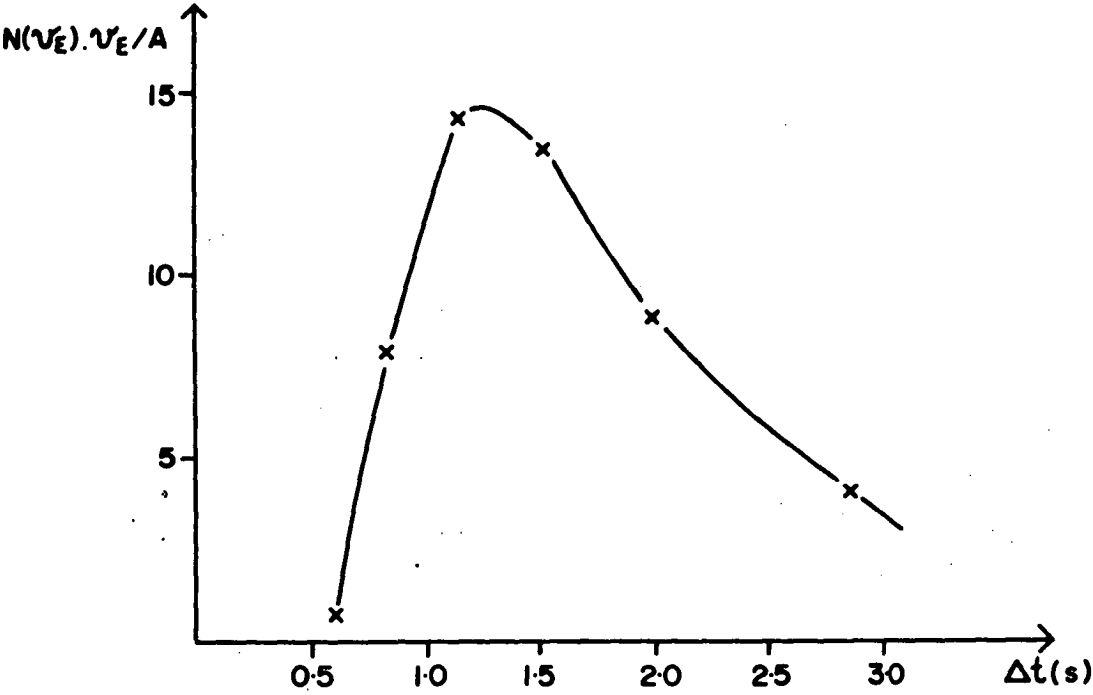


Figure 4.10    Profile of the asymmetric magnetic pulse in the ionosphere, due to the velocity dispersal of a clump of electrons commencing at the geomagnetic equator with a Maxwellian velocity distribution for an e-folding energy 3keV.



FAC's have been shown to be able to account for the more ostensible observations of the D micropulsations: predominance of negative phase correlations, lagging both the optical and H component, phase reversals of each component on their own, and the lack of a significant frequency doubling, are all basically encompassed by such an origin.

However more subtle effects, which are not so comfortably embraced, tend to generate a pervading feeling that the FAC's are not the major factor in D micropulsation production: late morning occurrence of positive correlations when the auroral zone is receding poleward, synchronous phase reversals with the H component, greater coherency of data strings with uniform relative peak amplitude echoes, consistently greater correlation values than for the H micropulsations, and the absence of pulse broadening, all contribute to the growing doubt regarding a FAC generation mechanism.

#### 4.4 CURRENT MODELS FOR PHASE REVERSALS

The occurrence of phase reversed correlations, almost exclusively during the late recovery stages of negative geomagnetic H bays, seems to indicate that the overhead current system suffers a reversal at these times. This may in fact be an electrojet microstructure effect (Kamide et al., 1969; Heacock, 1967a), and not indicative of the entire current system, since some bay recoveries were not accompanied by positive correlation events. At some of these times, of course, the commencement of a new bay over-rode any such possibility. The fact that the large-scale magnetogram sometimes remained weakly depressed on the occasion of positive correlations, presents no real problems, as the effects of an increased ring current have been discussed in Section 3.5.

The impetus for the simple current model about to be discussed, arose from collaboration with Dr. Gary Burns on the possible misalignment of the Macquarie Island micropulsation coils. Some degree of misalignment must inevitably creep into a fixed system due to the slow wandering of the Earth's magnetic poles. That such an error is very minor for the coils used in this research has been pointed out in Section 2.2.

It should be possible, by modelling the reversals in the overhead current system, to make basic predictions regarding the magnitude and relative phasing of the H and D micropulsations with respect to the  $N_2^+$  1NG emission. The model to be presented will consider firstly, the implications of small angular rotations in the direction of the auroral electrojet.

Encouragement to pursue this line of thought came from Banks and Doupnik (1975) report, which indicated that the midnight electric field poleward to equatorward reversal, may sometimes take place gradually. Figure 4.11, taken from that paper, shows a diminution of the north-south electric field component, and an enhanced east-west component as the transition proceeds. Effectively this means that the electric field rotates around from northward (poleward) to southward (equatorward), rather than jumping from one state directly to the other.

Banks and Doupnik (1975) also state that the electric field tended to have an eastward component whenever the point of observation was located equatorward of the auroral zone. This configuration can drive the H component into positive correlations, D remaining negative, if the eastward component of the electric field has sufficient magnitude. This may be expected to happen in the later morning hours, when the auroral oval is receding poleward, and quiet arcs are re-establishing themselves. This is in agreement with the data.

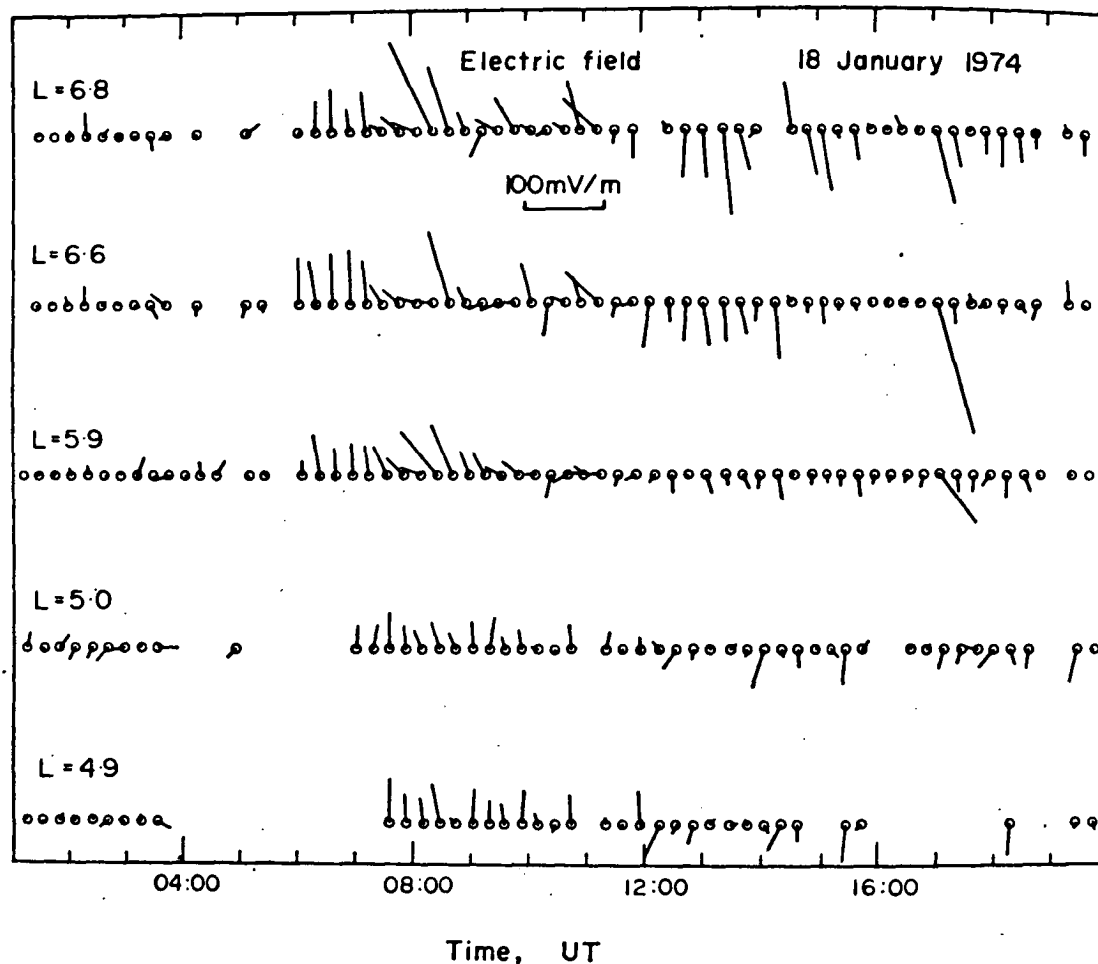


Figure 4.11 Experimental electric fields on 18-January-1974 for five different L-shells. Geomagnetic north is upward in the figure, east is to the right, gaps in the data are due to low signal strength (from Banks and Doupnik, 1975).

Consider initially, small angular variations in the electrojet system about the orientation of the detection coils, and also the result of a reversal of this electrojet current (see Figure 4.12). The electrojet has been shown to be predominantly south of west in the northern hemisphere (Senior et al., 1982), corresponding to somewhat north of west at Macquarie Island. Therefore configuration 1, is expected to be the major current system whose effects were observed in this research. It will produce negative correlations of the micropulsations with respect to the corresponding optical fluctuations, in both magnetic components.

Conversely, situation 4 dominates the evening sector, when the auroral electrojet is an easterly current. Both micropulsation components yield positive correlations for this configuration.

Orthogonality of the Hall and Pedersen currents dictates the overall magnetic effects of these configurations. The impact that the two vector currents will have on the cross-correlation figure, in phase and relative magnitude, is depicted in Table 4.6. Also given is a qualitative estimate of the combined effect of these Hall and Pedersen currents.

Immediately, a prediction borne out by the observations is made for situation 1, the most common configuration. The D component correlations are expected to be more strongly negative than the H. Coupled with the fact that the H component suffers more strongly from effects outside the photometer reception region, it is easier to see why the Macquarie Island data is biased so heavily toward D micropulsation correlations (to the tune of nearly two to one).

The prediction is also quite specific for the opposite extreme where the auroral electrojet has reversed from north of west, to south of east, situation 4. This time the D component correlations should

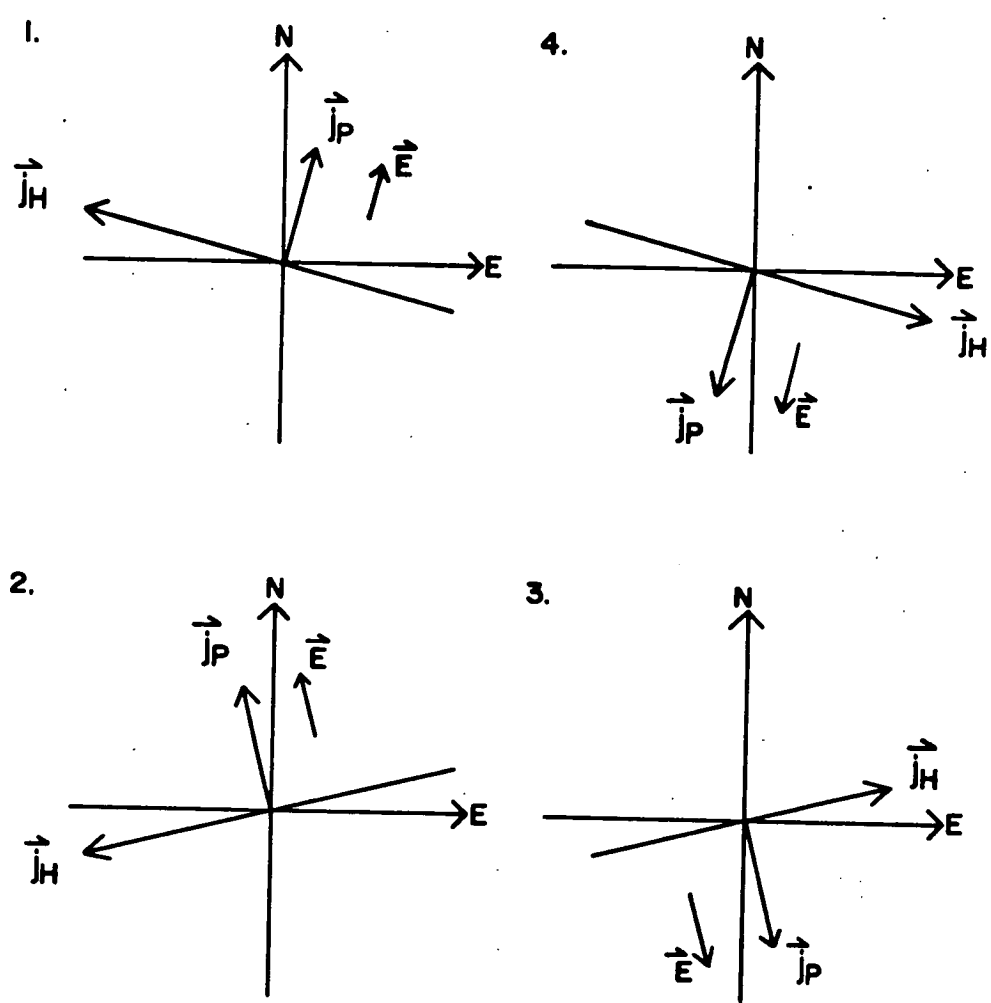


Figure 4.12 The ionospheric current effects of small angular rotations of the total electric field from its most common direction (slightly east of "coil" north, Figure 1), and the usual field reversal position (Figure 4).

Field in Figure 4.12	4278A/H Micropulsation			4278A/D Micropulsation		
	Hall	Pederson	Total	Hall	Pederson	Total
1	Strong -	Weak +	Medium -	Weak -	Strong -	Strong -
2	Strong -	Weak -	Strong -	Weak +	Strong -	Medium -
3	Strong +	Weak +	Strong +	Weak -	Strong +	Medium +
4	Strong +	Weak -	Medium +	Weak +	Strong +	Strong +

Table 4.6 Qualitative estimates of the Hall and Pedersen contributions to the sign of the H and D micropulsations/optical correlations, for the configurations depicted in Figure 4.12.

Time (UT)	4278A/H		4278A/D	
	<u>Lag</u>	<u>Correlation</u>	<u>Lag</u>	<u>Correlation</u>
1725-1730		N.C.		N.C.
1730-1735		v. weak positive		weak positive
1735-1740	-0.4	+0.48	-0.8	+0.52
1740-1745	-0.2	+0.26	-0.6	+0.66
1745-1750	-0.2	+0.33	-0.6	+0.37
1750-1755	-1.0	+0.25	-0.6	+0.40
1755-1800	-0.8	+0.30	-0.6	+0.56

Table 4.7 19 Apr. '83 event depicting a better correlated positive D component, as predicted for situation 4 from Figure 4.12.

turn out more strongly positive than the H, and this appears to be so in the data for 19-April-1983 shown in Table 4.7.

Referring back to Table 4.4 it is obvious that this circumstance is not always the case. However, with so few nights of positively correlated data no true statistical estimates can reasonably be made. It is also quite possible, with the occurrence of these type of events later in the morning hours, that the overhead current system may sometimes be more like situation 3. This is because the observation site has rotated to a point that may be approaching the limits of the electrojet current. Referring back to Figure 1.1 indicates that near 0600 hours, local time, a reversed electrojet could have a considerable equatorward component. Obviously, the degree of magnetic activity and extent of the electrojet system itself, will have profound effects on the currents operating at these times. A current reversal sees the electrojet pointing north of eastward, since Macquarie Island should be equatorward of the receding auroral zone. The H component can thus be more positively correlated than the D in this case.

Note that none of the current systems examined so far actually yield instances where the correlations are oppositely phased. These were, in fact, determined experimentally to be the most common occurrence. The final correlation outcome results from a balance between the Hall and Pedersen contributions. For only one of the files to alter phase, requires a major enhancement of just one or other of the currents, for the configurations in Figure 4.12. The very nature of the conductivity production virtually precludes this, though a specific spectral hardening, at 10-15keV for example, could cause greater dominance of the Hall current. Evidence does not appear in the literature to support such a requirement.

Assume for the moment that such a precise spectral hardening may somehow arise. In situations 2 and 3, this would mean that the Hall contribution to the D component correlation could dominate the Pedersen, enforcing a phase reversal for this component. It could only be expected to attain rather weak correlations however, whilst the H component would produce very powerful oppositely correlated files. This does not appear to be supported by the observational evidence.

Configurations 1-4 are the result of a very dominant north-south electric field, which is observationally determined to be the usual case (Brekke et al., 1974; Doupnik et al., 1977). Suppose however, that the transitions between equatorward and poleward fields (and subsequent electrojet reversal) involve an increase in east-west electric field (Banks and Doupnik, 1975). Effectively, this means that the electric field completes its reversal by rotating through a more complex variety of orientations.

Two fundamental changes (and their reverse) may occur, and these will be considered here. For each possibility the initial starting position will be taken as situation 1, the normal strong westward auroral electrojet, governed by its equatorward electric field.

The first case examines the effect of the westward electric field increasing, as the equatorward field diminishes, before switching to a poleward one. This is equivalent to an anticlockwise rotation of the electric field. The second case involves a clockwise rotation, or easterly electric field increase. The predictions which arise from this multiplicity of configurations are displayed in Table 4.8.

Notice now that case I, westerly increasing electric field, yields examples where the D component produces positive correlations, the H remaining negatively so. This happens in configurations C and D,



CASE I Anticlockwise (westward) rotating field	4278Å/H MICROPULSATION			4278Å/D MICROPULSATION		
	Hall	Pedersen	Total	Hall	Pedersen	Total
A. 	Strong -	Weak +	Medium -	Weak -	Strong -	Strong -
B. 	Strong -	Weak -	Strong -	Weak +	Strong -	Medium -
C. 	Weak -	Strong -	Strong -	Strong +	Weak -	Medium +
D. 	Weak +	Strong -	Medium -	Strong +	Weak +	Strong +
E. 	Strong +	Weak -	Medium +	Weak +	Strong +	Strong +

Table 4.8(a) Westerly increasing electric field and the relative contributions of the Hall and Pedersen currents to the H and D component correlations with the pulsating aurora.

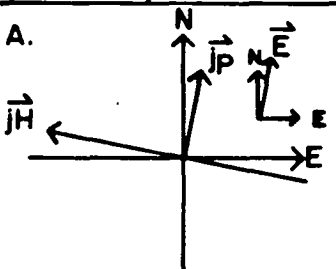
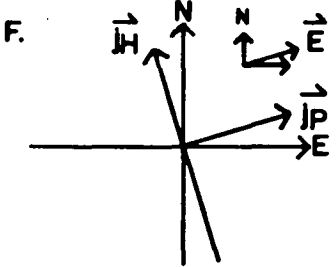
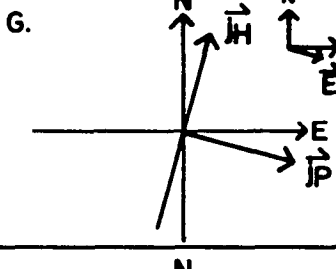
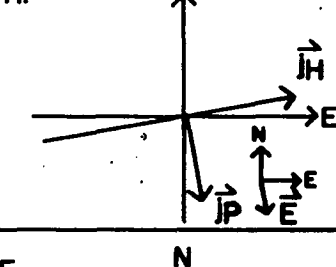
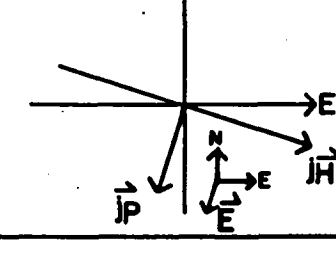
CASE II Clockwise (eastward) rotating field		4278Å/H MICROPULSATION			4278Å/D MICROPULSATION		
		Hall	Pedersen	Total	Hall	Pedersen	Total
A.		Strong	Weak	Medium	Weak	Strong	Strong
		-	+	-	-	-	-
F.		Weak	<u>Strong</u>	Medium	<u>Strong</u>	Weak	Strong
		-	+	+	-	-	-
G.		Weak	<u>Strong</u>	Strong	<u>Strong</u>	Weak	Medium
		+	+	+	-	+	-
H.		Strong	Weak	Strong	Weak	Strong	Medium
		+	+	+	-	+	+
E.		Strong	Weak	Medium	Weak	Strong	Strong
		+	-	+	+	+	+

Table 4.8 (b) Easterly increasing field, note that the Hall current dominates the D component in positions F, G, and the Pedersen current more powerfully controls the H at these times.

where the westward component of the electric field has become the dominant factor. Similarly, for case II, the easterly directed field attains superiority in configurations F and G. Here then, the H component turns to positive correlations while D maintains its negatively correlated character.

The important point to arise from this discussion, is that the east-west electric field must dominate the north-south contribution, for just one of the micropulsation components to yield a phase reversal.

Many factors can spoil the chance of observing a clean smooth transition through the stages of cases I and II. Not the least of these is the prospect of a new negative bay commencement, as has already been pointed out. Other disruptive influences include, the relative positioning of the observer to the auroral activity, the actual dimensions of the region of reversal, and the intrinsic nature of the changes to the electric field. It may, therefore, be a little too much to expect, in the rather limited volume of phase reversal data collected, to be able to clearly identify the predicted effects from a uniform evolvement through each of the stages A-E, via either path.

However, one particular facet of the activity lends itself as an unambiguous clear indicator of these phase reversals. Configurations C and D for case I, and F and G for case II, involve a switch in emphasis of the Hall and Pedersen currents. Here it is the D micropulsations which are more heavily influenced by the Hall current, whilst the Pedersen current becomes the major contributor to the H component. It is then expected, under these conditions, that the D micropulsations should now lead the H, due to the velocity dispersal altitude dependency effects discussed in Section 4.2. This is a precise and definite prediction which can very easily be checked.

Table 4.9 is a compilation of the cross-correlation figures for files which exhibit H and D components of opposite phase. Clearly, the D micropulsations are, in general, leading the H component. Of equal importance is the fact that the H micropulsations once again lead when both components have the same phase with respect to the optical fluctuations. For example, earlier in the evening of the 20-September-1983, both files were negatively correlated with the H micropulsations leading the D, as predicted. Similarly, on 02-October-1983 (refer to Table 4.1), the H and D micropulsations both returned positive correlations with respect to the optical auroral pulsations, with the H component leading the D.

Some of the lead-lag delay times of the micropulsations with respect to the optical, tend to jump somewhat erratically during periods of phase reversed activity. This is indicative of the very turbulent nature of the ionospheric activity at these times.

Note also that the case I and II qualifications of strong or medium correlation amplitude, are based on the total vector electric field rotating with constant magnitude. This is not expected to be true in reality, and was introduced merely for convenience and simplicity, so as not to disguise the basic arguments of interest. The fact that, despite any such complications, the temporal disposition of one micropulsation component to the other agrees so well with the predictions, is very strong evidence for the E-region current generation mechanism.

Further observational evidence that these events tend to occur in the later morning hours, and it is the H component which is seen to be more likely to go positive, is in agreement with the eastward electric field assuming control, i.e. case II. This is in line with Banks and Doupnik (1975) for stations equatorward of the pulsating aurora.

DAY	TIME (UT)	4278A/H-M $\mu$ P		4278A/D-M $\mu$ P	
30 OCT. 82	1520-1525	-1.0	+0.31	-0.6	-0.57
01 APR. 83	1705-1710	-0.6	+0.32		N.C.
	1710-1715	-0.4	+0.48	-0.2	-0.07
18 APR. 83	1630-1635	-0.4	+0.44	-0.4	-0.48
	1635-1640	-0.6	+0.39	-0.4	-0.32
	1640-1645	-0.4	+0.41	-0.6	-0.26
	1645-1650	-0.6	+0.14	-0.6	-0.14
14 MAY 83	1845-1850	-0.6	+0.45	-0.2	-0.37
23 MAY 83	0905-0910	-1.2	-0.26	-0.4	+0.43
	0910-0915	-1.0	-0.58	-0.4	+0.37
	0945-0950	-0.8	-0.29	-0.4	+0.75
	1950-1955	-0.6	+0.16	-0.2	-0.17
16 SEPT. 83	1420-1425	-1.2	+0.39	-0.4	-0.78
	1425-1430	-1.4	+0.22	-0.6	-0.38
	1430-1435	-1.4	+0.11	-0.4	-0.29
	1435-1440	-1.2	+0.34	-0.6	-0.57
	1440-1445	-1.2	+0.28	-0.6	-0.54
	1445-1450	-0.8	+0.29	-0.4	-0.52
	1450-1455	-0.6	+0.42	-0.6	-0.50
	1455-1500	-0.8	+0.44	-0.6	-0.55
19 SEPT. 83	1705-1710	-2.2	+0.28	+0.08	-0.43
	1710-1715	+0.2	+0.40	+0.6	-0.73
20 SEPT. 83	1655-1700	-0.4	+0.27	-0.4	-0.35
	1715-1720	-0.4	+0.10	-0.4	-0.21
	1720-1725	-0.4	+0.29	-0.2	-0.32
	1725-1730	-0.4	+0.41	-0.2	-0.30
	1730-1735	-0.8	+0.13	-0.4	-0.47
	1745-1750	-0.6	+0.17	-0.2	-0.48

Table 4.9 Oppositely phased correlations. Note that the D micropulsations tend strongly to lead to H component now.

Only one observation period is at large variance with the predictions as outlined above. This was for the 17-September-1983, between 1605-1645Z, and the cross-correlation analysis results appear in Table 4.10 for this event.

Between 1605-1630Z, the H micropulsation delay figures are quite randomly variable between consecutive files. This may be indicative of a complex microstructure in the auroral electrojet at this particular point in time. The two files covering the 10-minute sequence from 1610-1620Z, are reproduced in Figure 4.13, their corresponding cross-correlation functions appearing in Figure 4.14.

Firstly, during the 1610-1615Z file the overall average micropulsation lag with respect to the optical peaks is  $-0.6\text{s}$  for both components. Most of the positively correlated peaks in the H component data are either nearly synchronous with, or fractionally trail, the negatively correlated D micropulsations. However, the four labelled A, B, C and D in the H component, all serve to advance its final lag time to coincide with that of the D micropulsations. There exists the possibility that these are spurious peaks that form a chance correlation from outside the photometer field of view.

For the following data block, 1615-1620Z, the problem of assigning peaks is even more variable. Optical peaks at 16:15:55, 16:16:40, 16:16:50, 16:17:22, and 16:18:42 appear to lead the corresponding positively correlated H micropulsations. The converse is true for optical pulses at 16:15:18, 16:16:10, 16:18:20, 16:19:02, 16:19:15, and 16:19:45. These pulses tend to enhance the large negative swing of the cross-correlation function at a lag time near 5s.

These arguments apply to the entire data string for 17-September-1983, and are indicative of an unusual, highly variable period of activity. This is further highlighted by the condition of the

TIME	4278A/H MICROPULSATION		4278A/D MICROPULSATION	
	<u>Lead-Lag</u>	<u>X-Correlation</u>	<u>Lead-Lag</u>	<u>X-Correlation</u>
1605-1610	-0.2	+0.08	-0.6	-0.59
1610-1615	-0.6	+0.28	-0.6	-0.68
1615-1620	+1.2	+0.31	-1.0	-0.70
1620-1625	-0.2	+0.34	-1.0	-0.58
1625-1630	+1.4	+0.28	-0.8	-0.34
1630-1635		N.C.	-1.0	-0.22
1635-1640	-0.6	+0.43	-0.8	-0.17
1640-1645	-0.6	+0.25	-0.6	-0.23

Table 4.10    Cross-correlation and lead-lag times for  
the unusual H-component phase-reversal  
event of 17 September 1983.

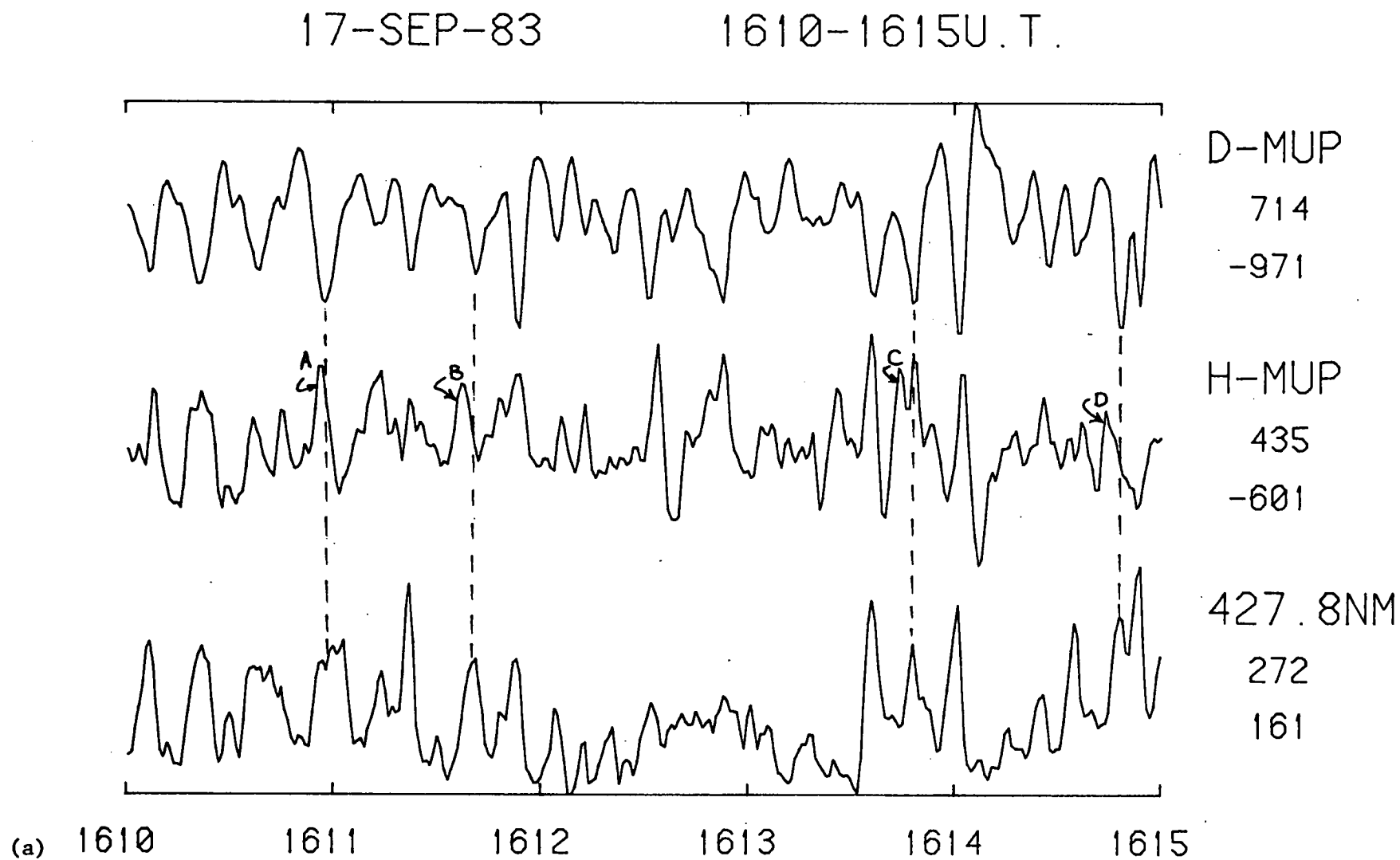
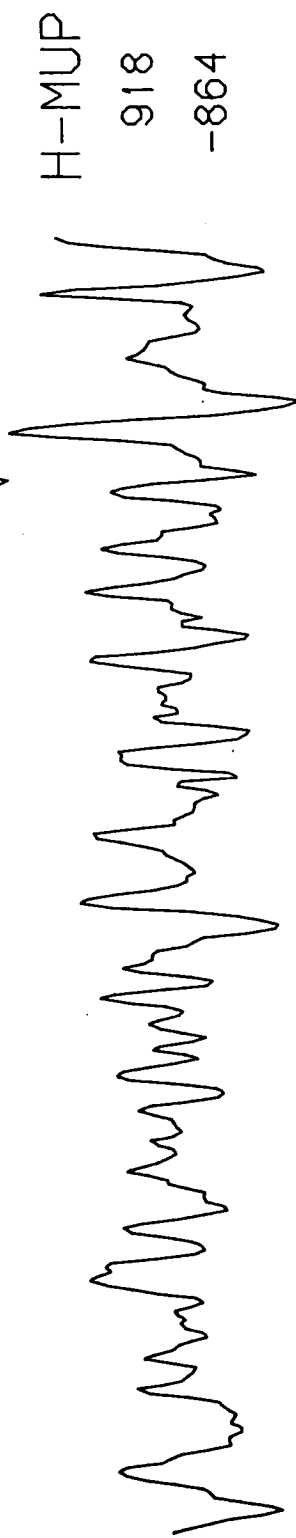
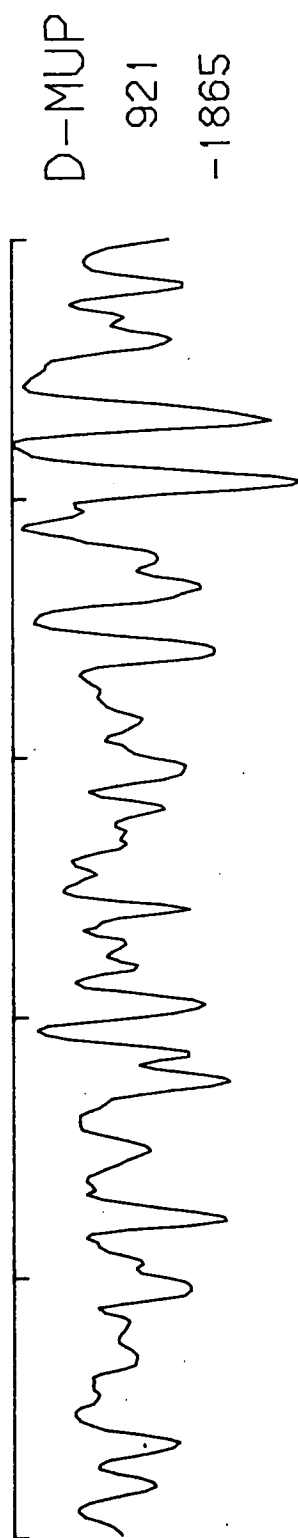


Figure 4.13 Data for unusual event for 17-September-1983.



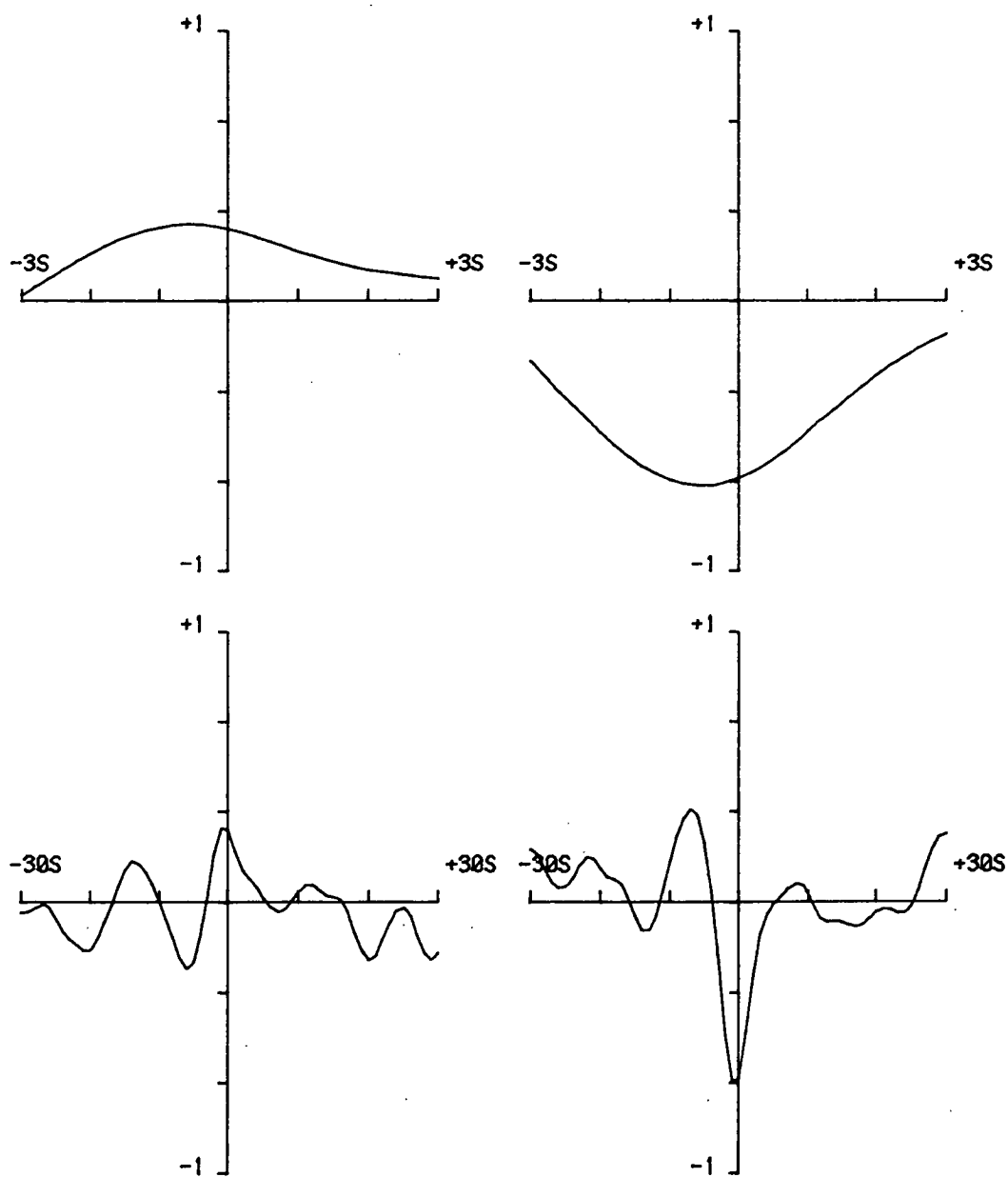
17-SEP-83 1615-1620U.T.



(b) 1615 1616 1617 1618 1619 1620

17-SEP-83

1610-1615U.T.



(a)

4278A/H-MUP

X-CORR=+0.28

LEAD=-0.6SEC

4278A/D-MUP

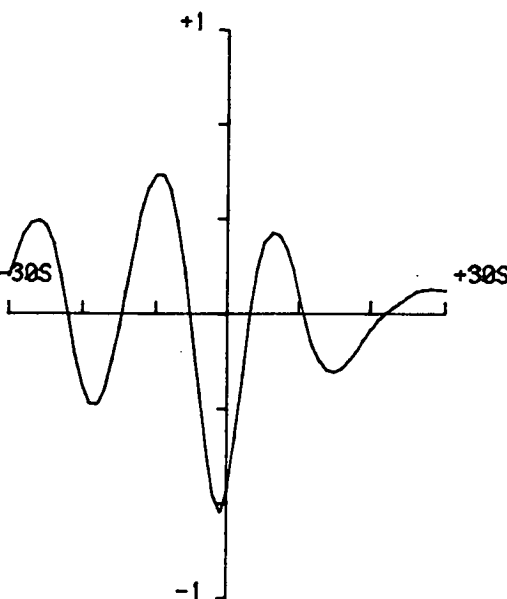
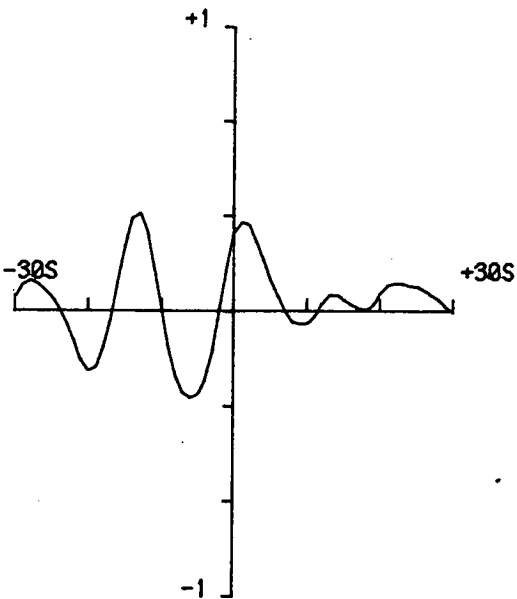
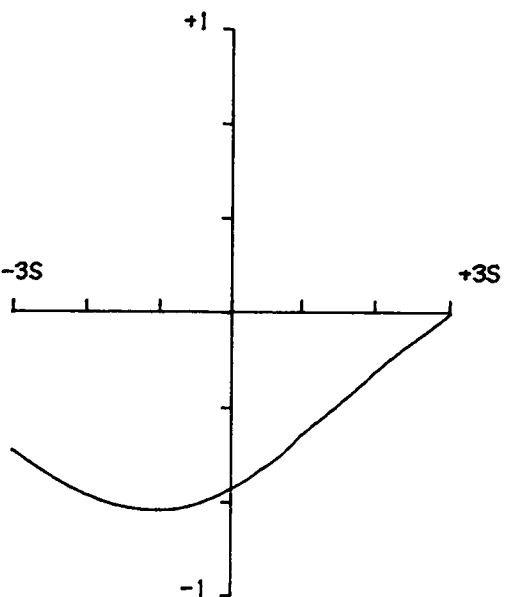
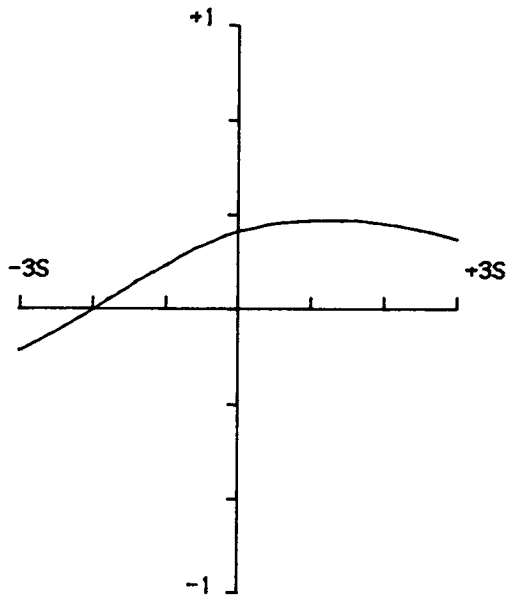
X-CORR=-0.68

LEAD=-0.6SEC

Figure 4.14 Cross-correlation for same event.

17-SEP-83

1615-1620U.T.



(b) 4278A/H-MUP  
X-CORR=+0.31  
LEAD=+1.2SEC

4278A/D-MUP  
X-CORR=-0.70  
LEAD=-1.0SEC

large-scale magnetic field at this time (see Figure 4.15). In contrast to all other observation periods when a phase reversal occurred in either or both micropulsation channels, the H magnetogram does not display the late stages of a bay recovery for this event. In fact, the activity has taken place whilst a small bay is still growing in magnitude. This may indicate that the phase reversal was a very small scale local occurrence, and the lead-lag delays may have been largely governed by chance correlations from out of range of the photometer. The unusual nature of this event, in the light of the points just noted, denies it the right of invalidating the support obtained earlier for the simple E-region current model.

As was shown earlier (refer to Figure 3.14) the H micropulsations generally lead the D, with only a very limited number of true exceptions. For the majority of these occasions the explanation may lie within the framework of the model currents presented here, for they are coincident with the occurrence of one or other of the components undergoing a phase reversal. The remaining situations, where D leads H, involve small values around the sampling rate (0.2s) which are easily forced by simple asymmetry of one or two major pulses, or the chance correlation of a few spurious peaks.

Histograms of the lead-lag times for the micropulsation components, against one another, are produced in Figure 4.16. Three categories are given: H and D of opposite phase, both positive, and both negative. These histograms clearly show that the D component genuinely leads the H when the two files are out of phase.

It appears then, that the small number of reverse correlation events provide an effective means of nailing down the nature of the micropulsation process. The excellent agreement with the predictions of the model presented here, seem to point conclusively, to the H and D micropulsations being generated predominantly by the E-region currents.

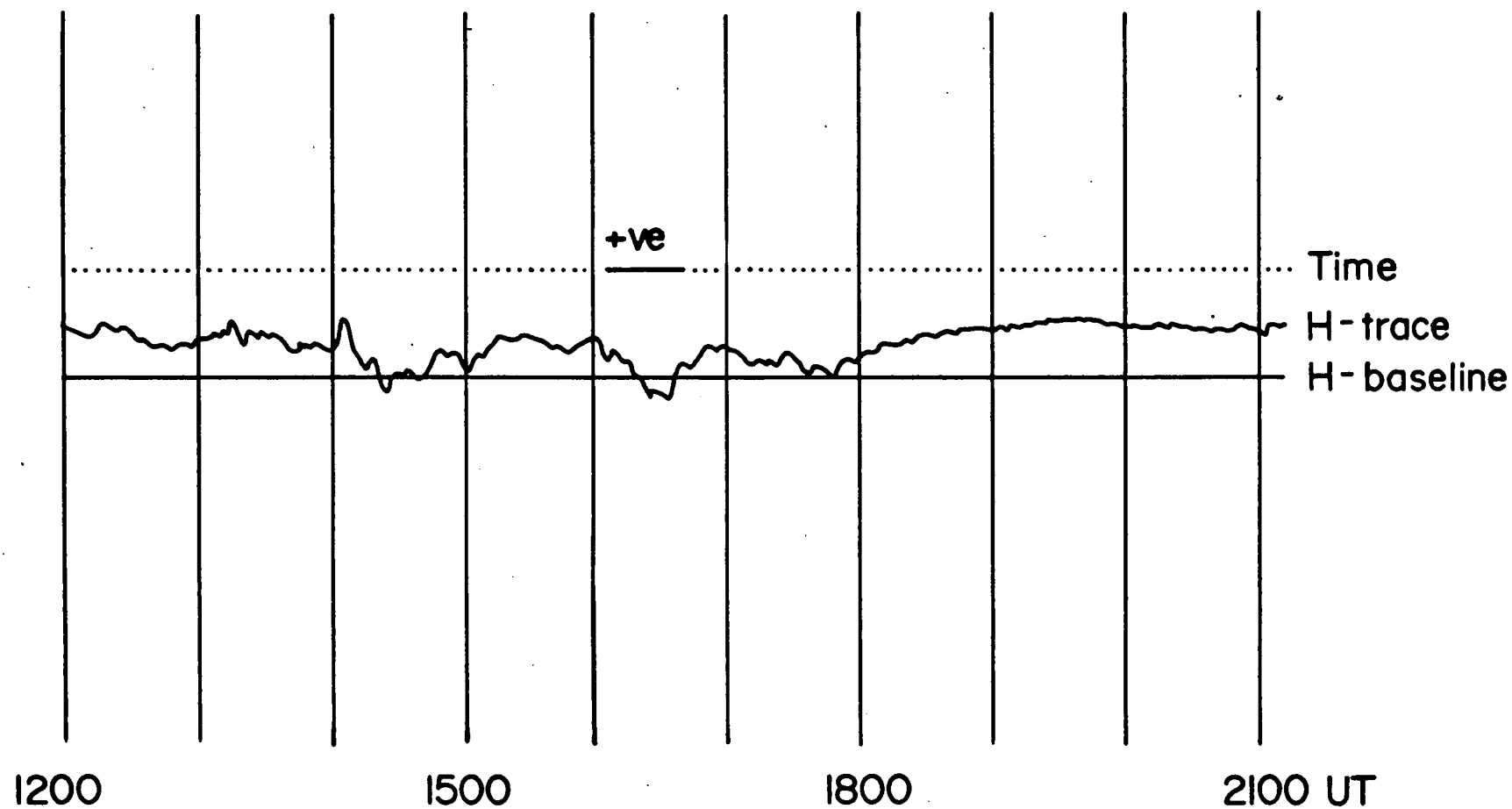


Figure 4.15 Portion of the BMR Macquarie Island magnetogram for the unusual event of 17-September-1983. The H micropulsations produce positive cross-correlations with the optical emission even though the large-scale magnetic field is on the decline.

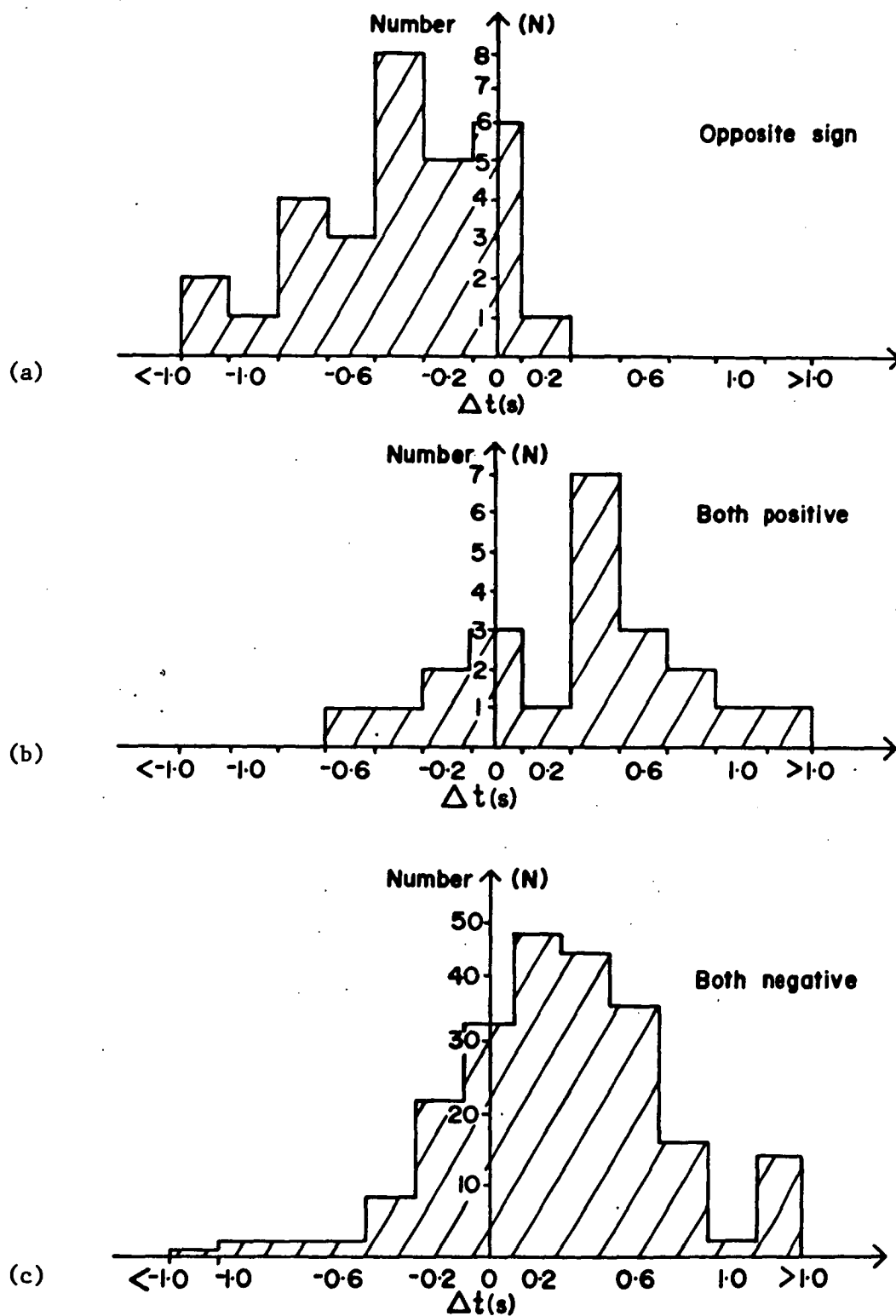


Figure 4.16 Lead-lag histograms depicting H generally leading the D micropulsations ((b) and (c)). In Figure (a), when the optical cross-correlation of the two components are of opposite sign, the D component tends to lead (negative  $\Delta t$ ) as predicted.

In the vast majority of all correlations, the H component is due to an enhancement of Hall conductivity, and hence an electrojet effect, whilst the D micropulsations can be related to equatorward current increases, which are generally slave to Pedersen conductivity variations.

#### 4.5 CURRENT MODELS AND OTHER OBSERVATIONS

The present study has indicated that the electric field seems to adopt orientations other than basically north-south, in the evening and late morning sectors. Precious little of the abundant literature in the field of auroral and geomagnetic phenomena has focussed attention on these observations. However, those articles that do, have their suggestions and ideas borne out completely by the arguments arising from the electric field - current model proposed in Section 4.4.

Heppner (1954) noted that a positive H component disturbance sometimes appeared in the morning hours after the disappearance of the negative H magnetic perturbation, at the auroral site of College, Alaska. He pointed out that this may well be indicative of an eastward current flow above the site in the dawn sector ionosphere.

Rostoker and Hron (1975) appear to be the first to conclusively demonstrate the existence of eastward electrojet flow in the late morning hours, at a latitude normally occupied by the westward convection electrojet. Further to this, they indicated that the eastward current was in fact a Pedersen flux driven by an eastward electric field. Such eastward electric fields have been shown to exist in the dawn sector at auroral latitudes (Mozer and Lucht, 1974). In conclusion, Rostoker and Hron (1975) add that any field-aligned currents which flow, will be closed in the ionosphere by equatorward

Hall currents. Such a system of ionospheric currents would produce positively phased optical/H component micropulsation correlations which lag fractionally, the concurrent negatively phased (in the southern hemisphere) D component, due to the velocity dispersal - altitude dependency effect. Case II of the proposed current models, which seems to be prevalent in the late morning hours, is in perfect accord with these observations. The data obtained in this research, for which the models were formulated, supports the evidence of Rostoker and Hron (1975) totally.

The subtle, but beautiful observation, of a switching of the temporal relationship of the micropulsation components whenever their correlations are oppositely phased, provides a useful tool for monitoring the direction of the ionospheric electric field. This results from a reversal in the emphasis of the Hall and Pedersen conductivities for the two components. Kamide and Brekke (1977) determined the average altitude of the maximum current density, at the peak time of the eastward electrojet, as 119.1 km, and that for the westward electrojet to be 101.6 km. This places the eastward electrojet in the region of peak Pedersen conductivity enhancements, and the westward current in the corresponding Hall conductivity regime. Thus, the micropulsation time-lag analysis provides an alternative method to the incoherent scatter radar measurements adopted by Kamide and Brekke (1977), for determination of the direction of the overhead electric field.

The ionospheric current system may normally consist of eastward electrojet flow equatorward of the omnipresent westward auroral electrojet, near the dawn meridian (Rostoker and Hron, 1975). That its effect is not always detected, may be due to the masking effect



of the strong westward current during periods of moderate to intense magnetospheric activity. At such times, not only may the influence of the westward current overpower the weaker eastward electrojet, but the auroral oval will itself be expanded equatorward, thrusting the eastward current to latitudes lower than that of the particular observation site. It then may be expected that the Case II current system should only be observable at moderate to low substorm activity at such stations. This seems to be confirmed by the occurrence of suitable events exclusively in the late recovery stages of negative magnetic H bays. The conflicting forces of the two electrojets are schematically reproduced in Figure 4.17 (after Rostoker and Hron, 1975).

The high latitude ionosphere exhibits two principal zones of energetic electron precipitation, as shown in Figure 4.18 (after Hartz and Brice, 1967). Wave particle interactions, associated with the hard particle precipitation, produce magnetic variations in the Pi1, Pi2 frequency ranges (Coroniti and Kennel, 1970). These occur predominantly on the equatorward side of the auroral oval. Figure 4.19 displays Pi(c) activity on magnetograms across the latitudinal extent of the eastward electrojet, in the dawn sector. From the present research, and in particular that of Burns (1983), Oguti et al., (1984), it is expected that pulsating aurora would also have been present there at these times.

Further support for the current models presented in Section 4.4 comes from direct observation of complex rotations of the electric field vector. This activity was hinted at by Banks and Doupnik (1975) from their incoherent scatter radar data, and subsequently expanded upon by them in collaboration with Horwitz (1978). They describe counterclockwise rotations from northward, through westward, to southward,

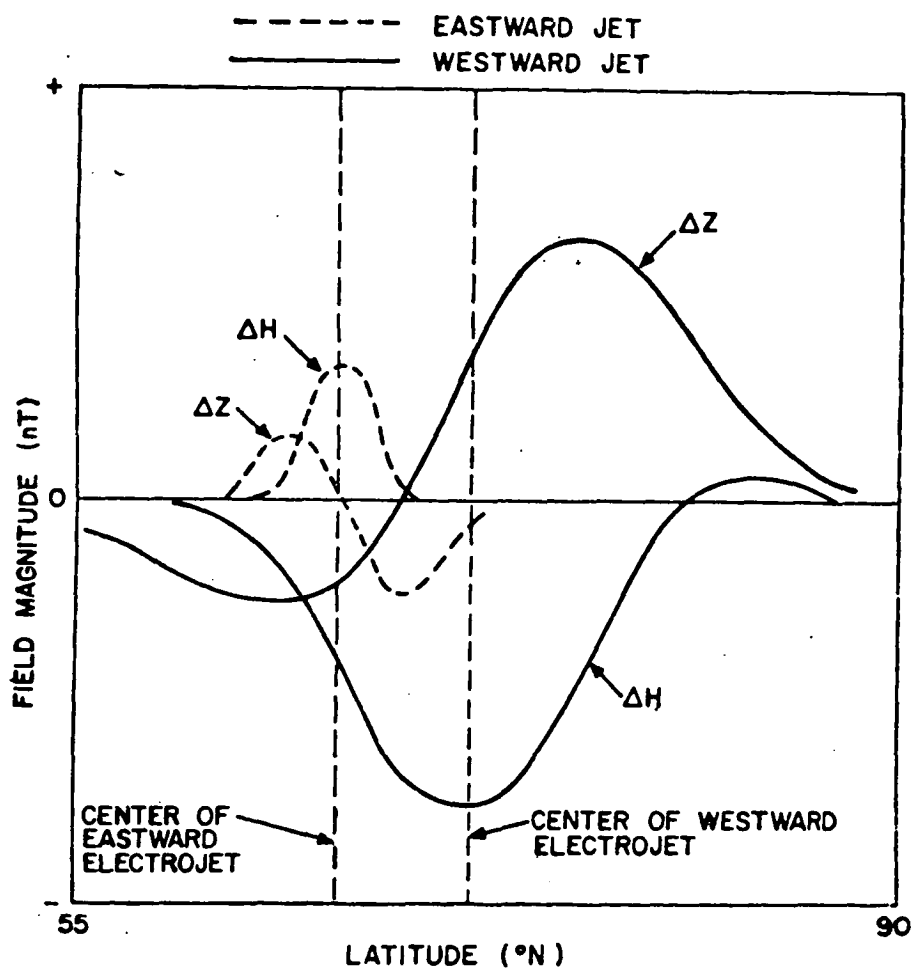


Figure 4.17 Schematic latitude profiles of the contributions to the H and Z component perturbations, from eastward and westward electrojets adjacent to one another, and crossing the same meridian (from Rostoker and Hron, 1975).

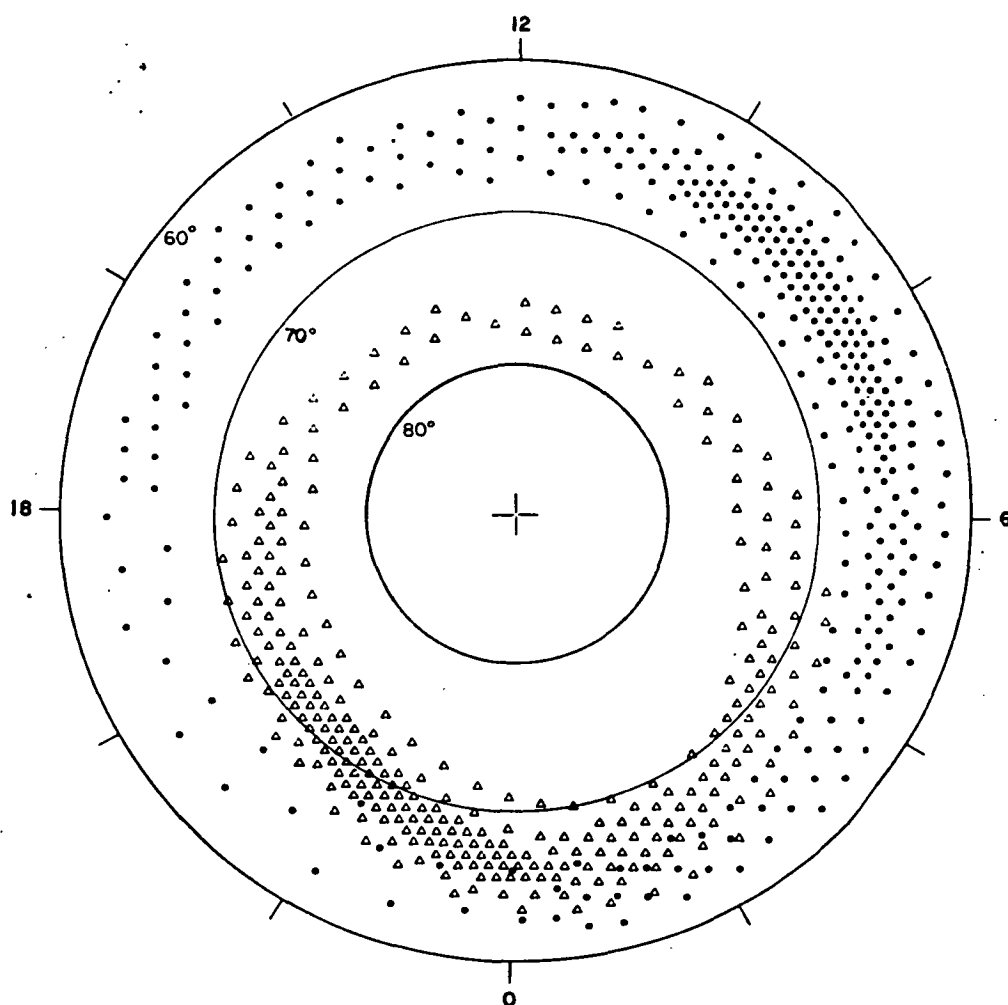


Figure 4.18 Idealized representation of the two main zones of auroral precipitation (northern hemisphere) in geomagnetic latitude and time co-ordinates. The open triangles are for discrete aurora, whilst the dots indicate the diffuse events (and hence the site of pulsating aurora, from Hartz and Brice, 1967).

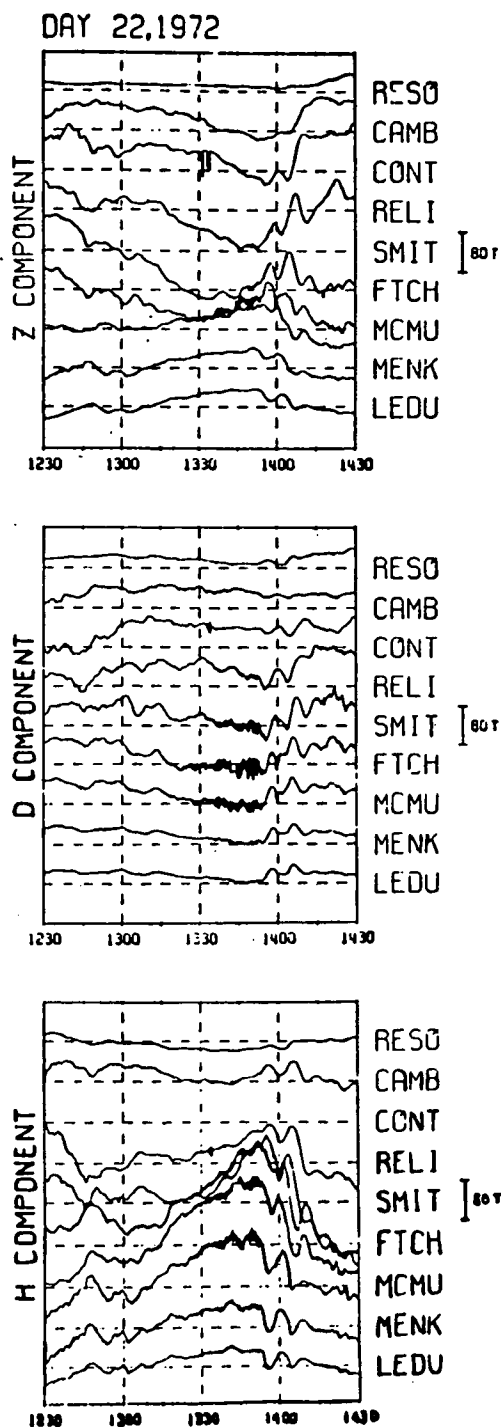


Figure 4.19 Magnetograms from the Alberta station line ( $83.0^{\circ}\text{N}$  to  $60.6^{\circ}\text{N}$ ) on 22-January-1972. Note the positive  $\Delta H$  deflection (eastward electrojet) in association with intense Pi activity (from Rostoker and Hron, 1975).

associated with the Harang discontinuity in the evening sector. Macquarie Island data strongly favours the Case I current model in evening hours, involving such a counterclockwise rotation of the electric field. The rotations commence later in the evening, and are more gradual (approximately 30 minutes as against 3 hours), in the equatorward portions of the oval (Horwitz et al., 1978). This is typical of the relative location of Macquarie Island with respect to the auroral oval, and the pulsating aurora - micropulsation observations thus obtained, support their view. Horwitz et al., (1978) also indicate the existence of small eastward electric field components in the dawn hours, and present evidence for the electric field rotations to occur principally during the recovery phase of a substorm. These conditions applied almost without exception in the Macquarie Island data.

Substorm electric fields and currents have been modelled by Kamide and Matsushita (1979). They adopt field-aligned currents based on recent satellite observations (such as Armstrong and Zmuda, 1970) and conductivity models akin to Chatanika radar observations (such as Brekke et al., 1974). Eastward currents are seen to be produced in the evening sector, and near the equatorward edge of the auroral belt in the morning sector (see Figure 4.20). Kamide and Matsushita (1979) indicate that this morning eastward electrojet is produced by an eastward electric field and Pedersen conductivity as a natural consequence of the calculated morning sector potential peak.

Thus it seems that the existence of an eastward auroral electrojet, in the late morning hours, equatorward of the more prominent westward electrojet current is now well established observationally, and becoming so theoretically. The correlation of pulsating optical aurora with the

# IONOSPHERIC CURRENT VECTORS

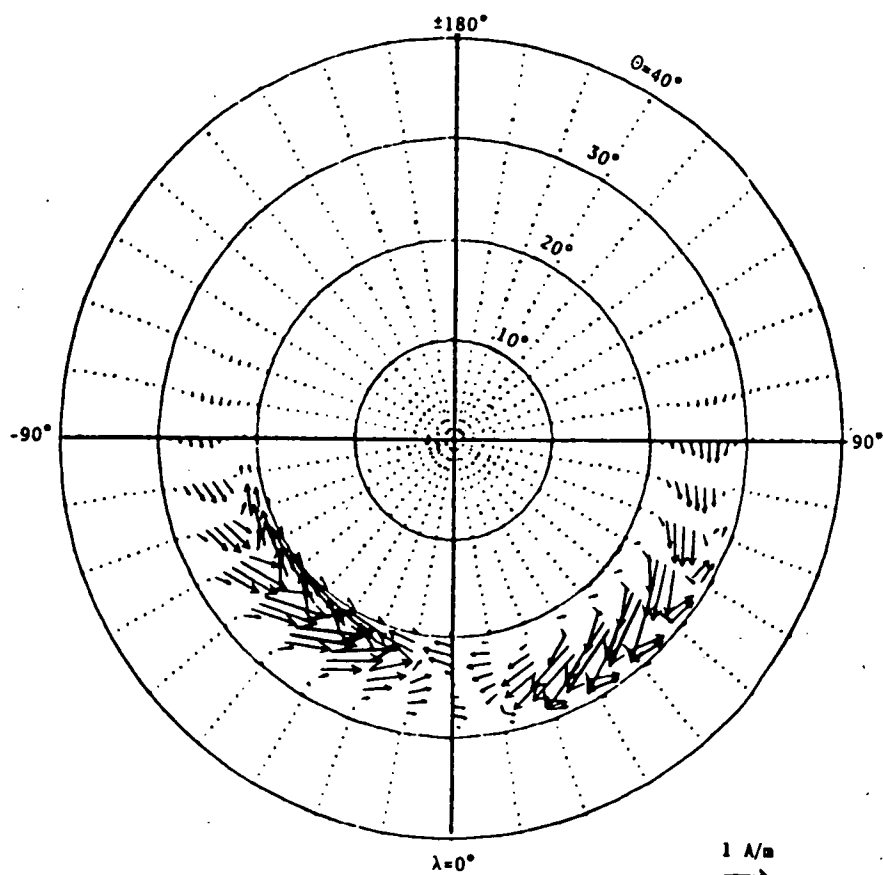


Figure 4.20 The distribution of ionospheric current vectors based on a model by Kamide and Matsushita (1979). Note the strong eastward evening electrojet (in the vicinity of the Harang discontinuity), and the late morning eastward current on the equatorward edge of the auroral oval.

associated Pi(c) micropulsations of the magnetic field, have led to confirmation that the micropulsations are ionospheric conductivity controlled phenomena. Changes in the phase of these correlations, and simultaneous alterations to their temporal relationship, allow efficient determination of the ionospheric electric field orientation at any given time.

#### 4.6 CONCLUSIONS AND FURTHER RESEARCH

The present study concludes that the small scale magnetic Pi(c) pulsations result from precipitation induced conductivity fluctuations within the E-region. These are responsible for variations in the ionospheric currents, giving rise to magnetic perturbations detectable at ground level.

Detailed monitoring of the pulsating aurora and the associated Pi(c) makes it possible to determine the orientation of the overall local ionospheric electric field. The lead-lag relationship between the phenomena, and the phase of the cross-correlations, strongly reflect any changes in the direction of the electric field vector. This is a simple but effective method for such determinations, as an alternative to the backscatter radar techniques generally adopted.

In the main, the pulsating aurora have been found to occur throughout the recovery phase of negative geomagnetic bays. At these times, the H and D component magnetic pulsations result principally from electron precipitation induced conductivity fluctuations in predominantly westward Hall current, and equatorward Pedersen current, respectively. These variations have been shown to be maximized at different altitudes. In combination with fast response riometer measurements of cosmic noise absorption (CNA) pulsations (detected in the lower E-region, 90-100km), this provides a means for studying the recombination rates of electrons

at three altitudes during auroral events. Such research is at present under preparation, to be conducted at Macquarie Island during 1985.

The actual state of the ionosphere itself will be able to be determined at such times as well, as the Ionospheric Prediction Service (IPS) have provided an ionosonde which has been recently installed at Macquarie Island. Such a tool will provide valuable added information about ionization levels within the auroral ionosphere during pulsation activity. Parameters such as  $f_oF_2$  and  $FE_s$  will be examined, to determine if they exert any influence on the lead-lag times between the optical and magnetic pulsation components.

It may also be possible to carry out a calibration of the photometers themselves, allowing absolute measurements of light levels to be determined. The efficiency of the  $4278\text{\AA}$  band in converting incoming electron energy into photons is believed to be reasonably well established (Omholt, 1971). Hence it would be possible to determine the total energy flux dumped into the atmosphere by precipitating electrons during pulsations. Practical problems arise with a wide angle photometer since ground optical measurements necessarily integrate along the line of sight. Strict comparisons are valid for measurements only in the direction along the field lines themselves, but it may be possible to make due allowance for this discrepancy.

A further possibility exists, if absolute measurements do not become available, in the ratio of  $5577\text{\AA}$  to  $4278\text{\AA}$  emission. These may result at slightly different altitudes, and so reflect different electron energies. The relaxation delay time of 0.7s associated with the  $5577\text{\AA}$  emission will be an extra factor to be considered here.

It has been both exciting and interesting to study a phenomenon as visually spectacular as the aurora. To all the many people, especially those close to me, who have provided this stimulating opportunity, my everlasting thanks and deepest appreciation.



## APPENDIX

As discussed in Section 3.5, quiet day curves for the H component were determined for each complete month of data collection. This comprised the period from November 1982 to September 1983 inclusive.

The QDC's were calculated from the Macquarie Island BMR magnetograms, and were produced in situ at the station for data analysis. Since the BMR geophysicist does a complete mean hourly value (MHV) calculation for the entire year, upon return to Australia, it was felt desirable to check those figures with our calculated QDC's. Agreement, as expected, was generally extremely good, though a few discrepancies did arise. For instance, the curves reproduced in Figure 3.19 (see Section 3.5), for September 1983, are those calculated at Macquarie Island. The official BMR mean QDC for the month included the 23 September 1983, as one of the quiet days for the determination, in preference to the 02nd, 03rd. However, on this day, two distinct minor negative magnetic bays appeared in the H magnetogram between 1030-1700Z. These significantly lowered the value during that period by up to 50 nT, and hence biased the QDC by 20% of this, that is 10 nT. Such an effect is certainly not disastrous but it was decided to retain our own QDC figures for use in the research, and consult with BMR MHV's as secondary check. The results were, in the main, very consistent.

Matsushita and Campbell (1965) in their discussion of QDC's, group the annual variation into three sets of equivalent months. They denote November, December, January and February as D months, May, June, July and August as J months, and March, April, September and October as E months. The approximate range of the magnetic daily variation in the H component is of the order of 80 nT for D months, falling through 40 nT for E months, down to only 25 nT during J months.

Figure A1 reproduces the calculated QDC's for November 1982, December, January and February 1983 as determined from Macquarie Island magnetograms. The average of these four traces is plotted with the Matsushita and Campbell D month curve for comparison in Figure A2. The minimum and maximum of the measured average QDC appear to both be slightly delayed with respect to the D month variation. The Macquarie Island curve also has a depression between 0900-1600 UT that does not appear on the extrapolated D month trace.

For the smaller J, and E month fluctuations, Figures A3 and A4 show the comparison between the measured four month averages and the Matsushita and Campbell extrapolations.

The overall agreement is quite satisfactory, recalling the fact that the D, J, and E month curves of Matsushita and Campbell refer to solar minimum (IQSY - International Quiet Sun Year). Measured Macquarie Island curves are for one year only, with the 1982-83 Austral Summer being situated just beyond the 1979-80 maximum of the present solar cycle.

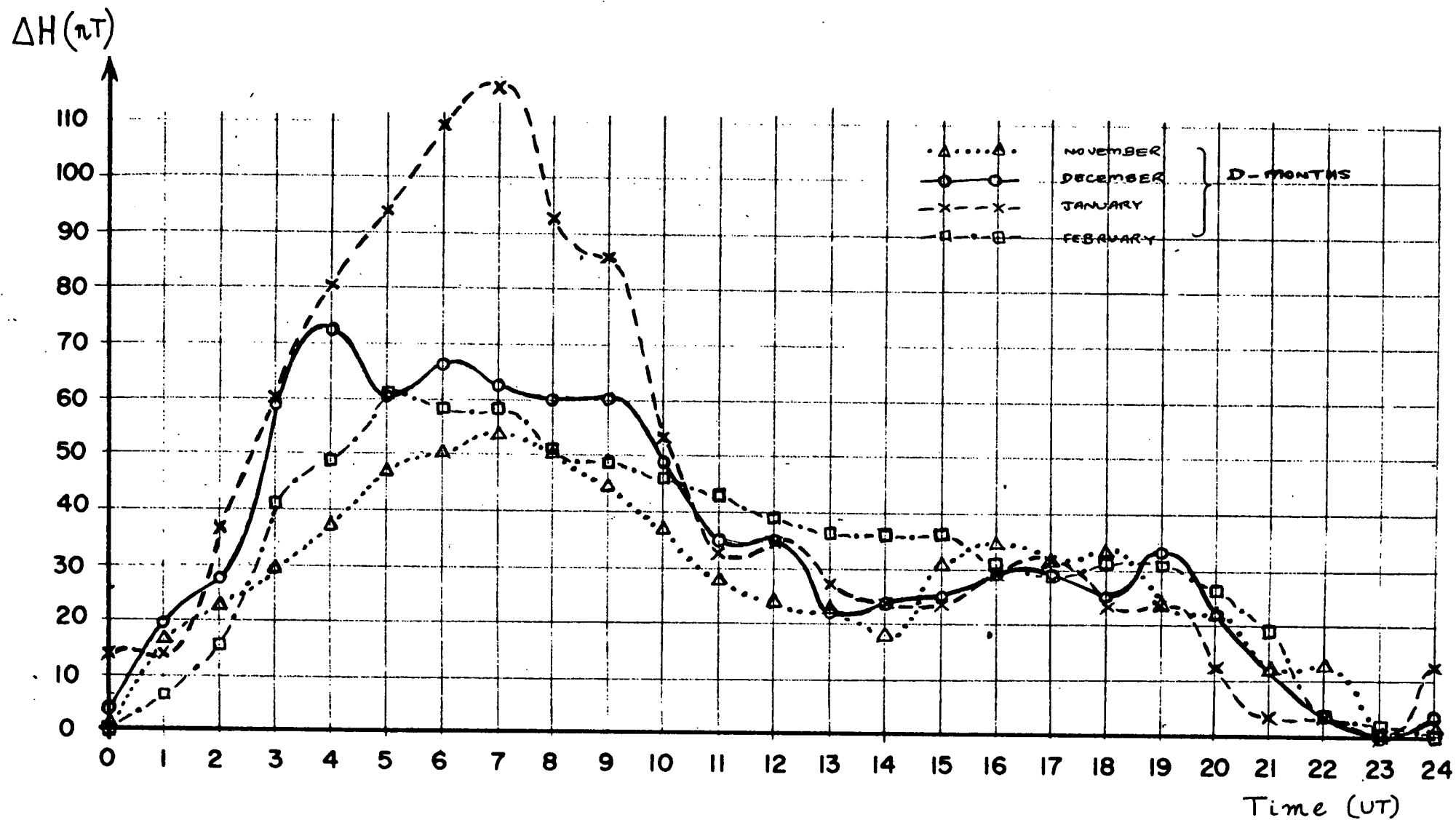


Figure A1. Measured QDC's during the 1982-83 Austral summer for the H component at Macquarie Island

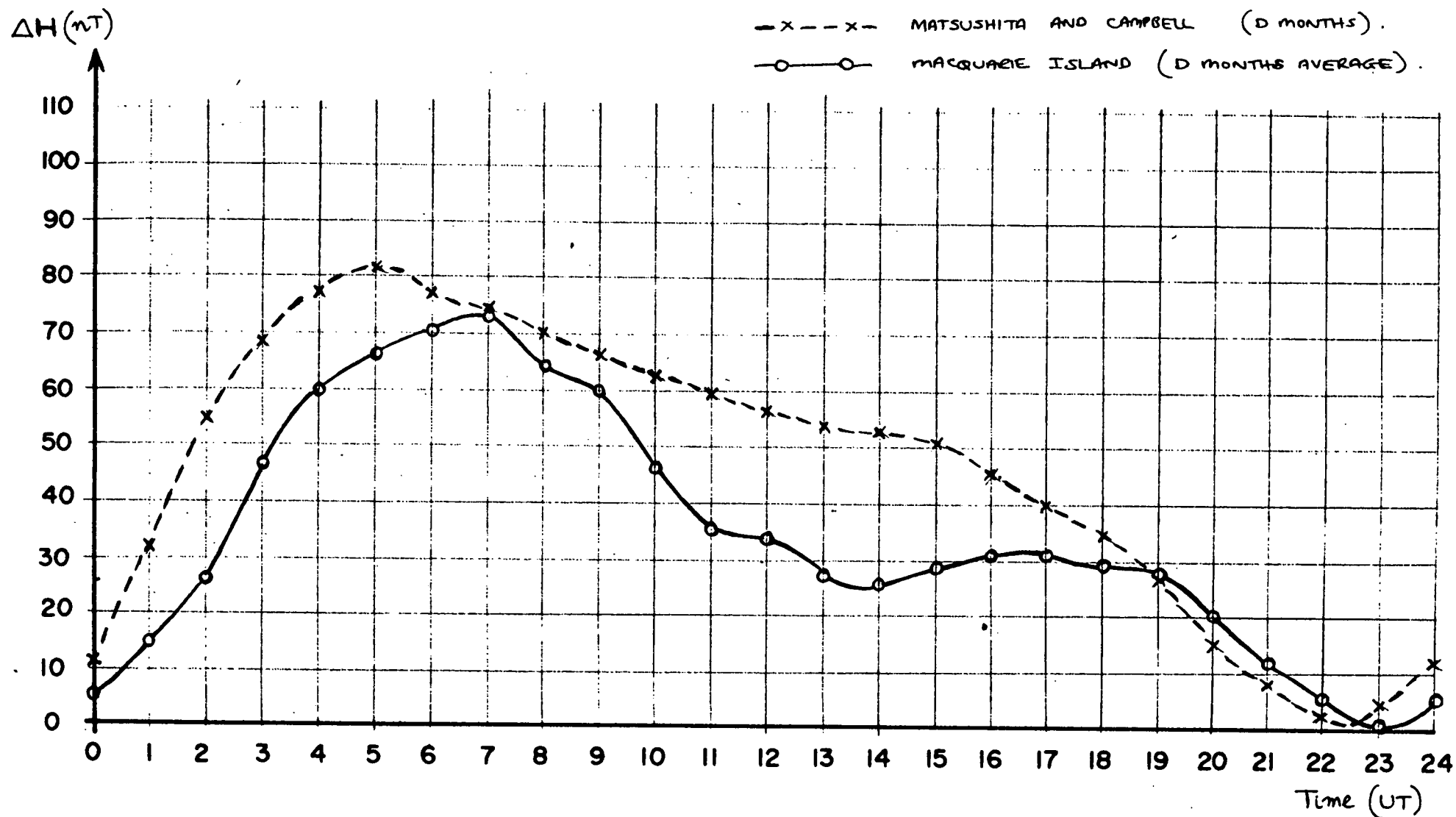


Figure A2 Comparison between the D month predicted QDC of Matsushita and Campbell, and the average of the four curves in Figure A1

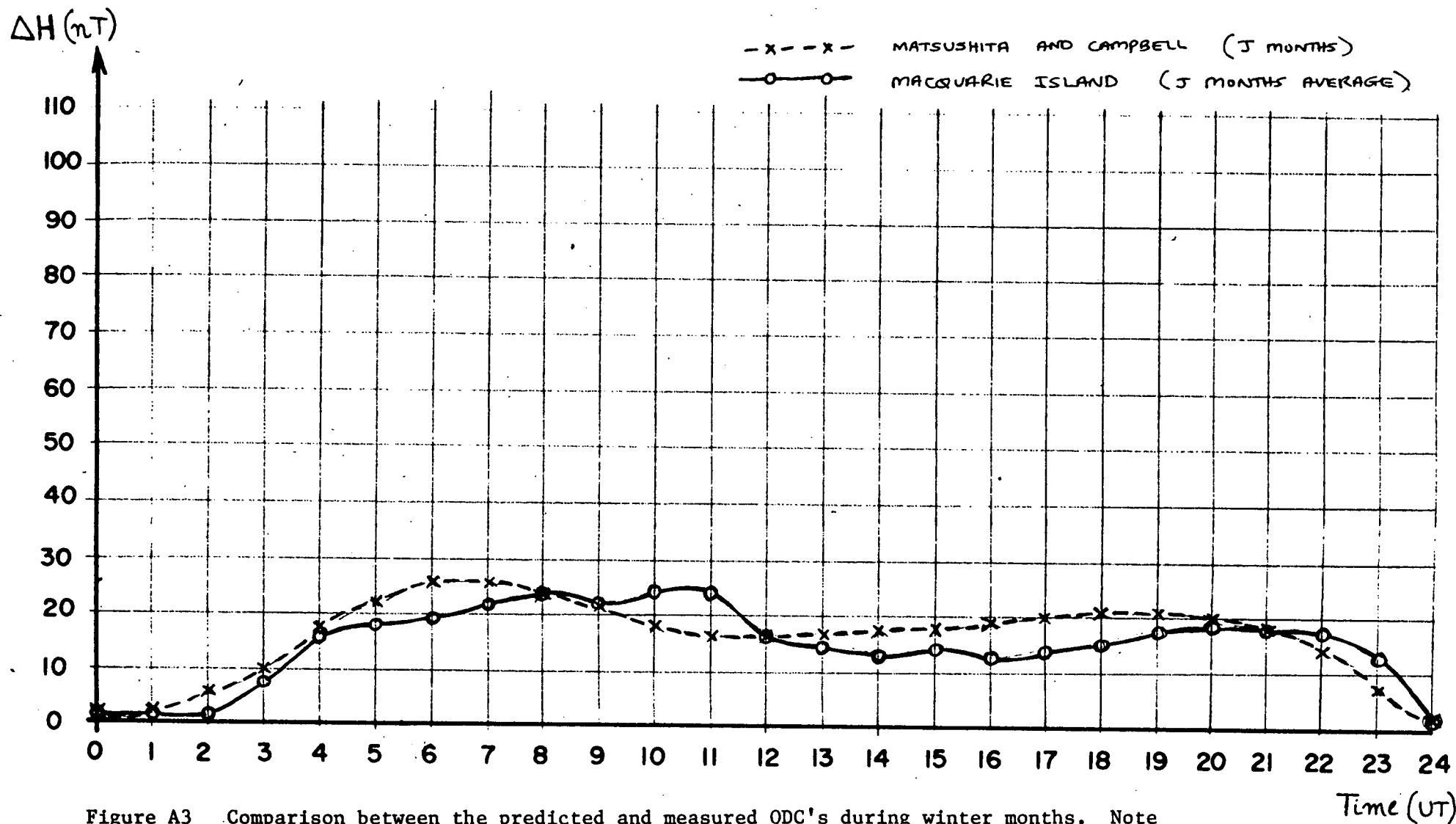


Figure A3 Comparison between the predicted and measured QDC's during winter months. Note the small daily range of only 25 nt.

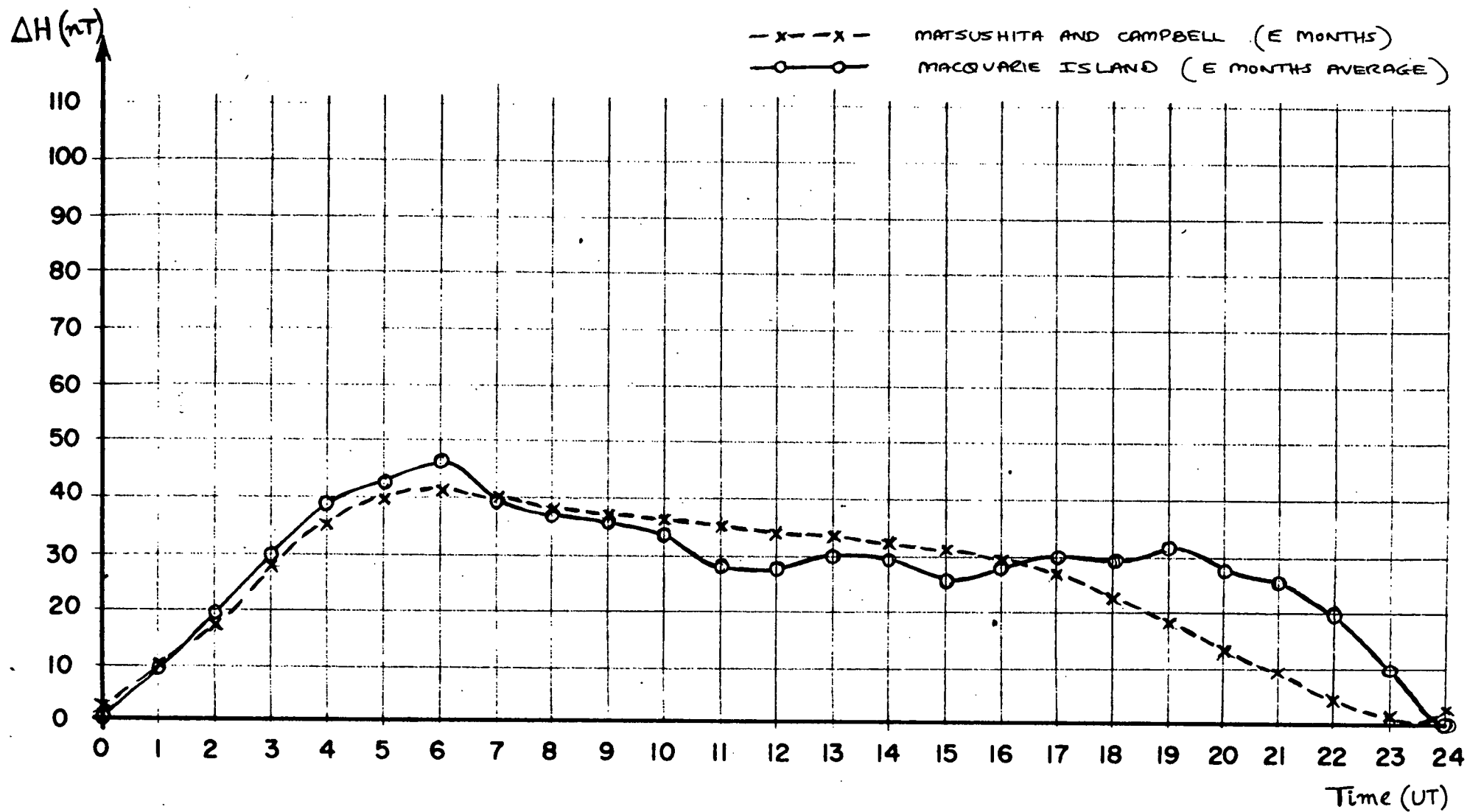


Figure A4 Similar comparison for E (equinoctial) months with a daily range around 45 nt

## REFERENCES

- AKASOFU, S.-I. (1968). Polar and Magnetospheric Substorms.  
D Reidel, Hingham, Dordrecht - Holland.
- ARMSTRONG, J.C. and ZMUDA, A.J. (1970). "Field aligned currents  
at 1100 km in the auroral region measured by satellites",  
J. Geophys. Res., Space Phys., 75:7122.
- ARNOLDY, R.L. (1974). "Auroral particle precipitation and Birkeland  
currents", Rev. Geophys. Space Phys., 12:217.
- ARNOLDY, R.L., DRAGOON, K., CAHILL, L.J., MENDE, S.B., and ROSENBERG, T.J.  
(1982). "Detailed correlations of magnetic field and riometer  
observations at L=4.2 with pulsating aurora", J. Geophys. Res.,  
87: 10449.
- ARTHUR, C.W., MCPHERRON, R.L., and COLEMAN, JR., P.J. (1973).  
"Micropulsations in the morning sector, 1, Ground observations  
of 10-45 second waves, Tungsten, N.W. Territory, Canada",  
J. Geophys. Res., 78: 8180.
- BANKS, P.M. and KOCKARTS, A. (1973). Aeronomy Academic New York.
- BANKS, P.M. and DOUPNIK, J.R. (1975). "A review of auroral zone  
electrodynamics deduced from incoherent scatter radar observations",  
J. Atmos. Terr. Phys., 37:951.
- BANKS, P.M., DOUPNIK, J.R. and AKASOFU, S.-I. (1973). "Electric  
field observations by incoherent scatter radar in the auroral  
zone", J. Geophys. Res., 78:6607.
- BELON, A.E., MAGGS, J.E., DAVIS, T.N., MATHER, K.B., GLASS, N.W., and  
HUGHES, G.F. (1969). "Conjugacy of visual aurora during  
magnetically quiet periods", J. Geophys. Res., 74:1.
- BERKO, F.W. (1973). "Distributions and characteristics of high  
latitude field aligned electron precipitation", J. Geophys. Res.,  
78:1615.
- BIRKELAND, K. (1908). The Norwegian Aurora Polaris Expedition,  
1902-03; Vol. 1, 1st Sec. Aschhoug, Christiania.
- BIRKELAND, K. (1913). The Norwegian Aurora Polaris Expedition,  
1902-03; Vol. 1, 2nd Sec. Aschhoug, Christiania.
- BONNEVIER, B., BÖSTROM, R. and ROSTOKER, G. (1970). "A 3-D model  
current system for polar magnetic substorms", J. Geophys. Res.,  
75:107.
- BÖSTROM, R. (1964). "A model of the auroral electrojets",  
J. Geophys. Res., 69:4983.
- BÖSTROM, R. (1968). "Currents in the ionosphere and magnetosphere",  
Ann. Geophys., 24:681.

- BREKKE, A. (1971). "On the correlation between pulsating aurora and cosmic radio noise absorption", Planet. Space Sci., 19:891.
- BREKKE, A., DOUPNIK, J.R. and BANKS, P.M. (1974). "Incoherent scatter measurement of E-region conductivities and currents in the auroral zone", J. Geophys. Res., 79:3773.
- BROWN, N.B., DAVIS, T.N., HALLINAN, T.J. and STENBAEK-NIELSEN, H.C. (1976). "Altitude of pulsating aurora determined by a new instrumental technique", Geophys. Res. Lett., 3:403.
- BRYANT, D.A., COURTIER, G.M. and JOHNSTONE, A.D. (1969). "Modulation of auroral electrons at large distances from the Earth", J. Atmos. Terr. Phys., 31:579.
- BRYANT, D.A., COURTIER, G.M. and BENNETT, G. (1971). "Equatorial modulation of electrons in a pulsating aurora", J. Atmos. Terr. Phys., 33:859.
- BRYANT, D.A., SMITH, M.F. and COURTIER, G.M. (1975). "Distant modulation of electron intensity during the expansion phase of an auroral substorm", Planet Space Sci., 23:867.
- BURNS, G.B. (1983). "Pulsating aurora: photometer, riometer and micropulsation coil observations", Ph.D thesis, Latrobe University
- BURNS, G.B., COLE, K.D. (1984 - to be published). "Concerning the origin of Pi(c) micropulsations".
- CAMPBELL, W.H. and MATSUSHITA, S. (1962). "Auroral zone geomagnetic micropulsations with periods of 5 to 30 seconds", J. Geophys. Res., 67:555.
- CAMPBELL, W.H. and MATSUSHITA, S. (1967). "Geomagnetic Pulsations" in Physics of Geomagnetic Phenomena Vol. 2, New York Academic Press.
- CAMPBELL, W.H. (1970). "Rapid auroral luminosity fluctuations and geomagnetic field pulsations", J. Geophys. Res., 75:6182.
- CAMPBELL, W.H. (1978). "Highlights in the studies of the relationship of geomagnetic field changes to auroral luminosity", J. Geomagnet. Geoelect., 30:315.
- CHAMBERLAIN, J.W. (1961). Physics of the Aurora and Airglow. Academic Press, New York.
- CHANCE, M.S., CORONITI, F.V. and KENNEL, C.F. (1973). "Auroral micropulsation instability", J. Geophys. Res., 78:7521.
- CHAO, J.K. and HEACOCK, R.R. (1980). "Modulation of type Pi waves by temporal variations in ionospheric conductivity in a 3-D magnetospheric-ionospheric current system", Planet. Space Sci., 28:475.
- CHAPMAN, S. and BARTELS, J. (1940). Geomagnetism Vols. I, II, Oxford at the Clarendon Press, London.



- CHEN, A.J. and ROSTOKER, G. (1974). "Auroral-polar currents during periods of moderate magnetospheric activity", Planet Space Sci., 22:1101.
- COLE, K.D. (1963). "Motions of the aurora and radio aurora and their relationship to ionospheric currents", Planet. Space Sci., 10:129.
- CORONITI, F.V., McPHERRON, R.L. and PARKS, G.K. (1968). "Studies of the magnetospheric substorm, 3, Concept of the magnetospheric substorm and its relation to electron precipitation and micro pulsations", J. Geophys. Res., 73:1715.
- CORONITI, F.V. and KENNEL, C.F. (1970a). "Electron precipitation pulsations", J. Geophys. Res., 75:1279.
- CORONITI, F.V. and KENNEL, C.F. (1970b). "Auroral micropulsation instability", J. Geophys. Res., 75:1863.
- CRESSWELL, G.R. and DAVIS, T.N. (1966). "Observations on pulsating auroras", J. Geophys. Res., 71:3155.
- CUMMINGS, W.D. and DESSLER, A.J. (1967). "Field aligned currents in the magnetosphere", J. Geophys. Res., 72:1007.
- DALGARNO, A. (1961). "Charged particles in the upper atmosphere", Ann. Geophys., 17:16.
- DALGARNO, A. (1964). "Ambipolar diffusion in the F-region", J. Atmos. Terr. Phys., 26:939.
- D'ANGELO, N. (1969). "Role of the universal instability in auroral phenomena", J. Geophys. Res., 74:909.
- DAVIDSON, G.T. (1979). "Self modulated VLF wave electron interactions in the magnetosphere : a cause of auroral pulsations", J. Geophys. Res., 84:6517.
- DAVIS, T.N. (1966). "The application of image orthicon techniques to auroral observations", Space Sci. Rev., 6:222.
- DAVIS, T.N. (1978). "Observed characteristics of auroral forms", Space Sci. Rev., 22:77.
- DONAHUE, T.M., ZIPF, E.C. and PARKINSON, T.D. (1970). "Ion composition and ion chemistry in an aurora", Planet. Space Sci., 18:171.
- DOUPNIK, J.R., BREKKE, A. and BANKS, P.M. (1977). "Incoherent scatter radar observations during three sudden commencements and a Pc5 event on August 4, 1972", J. Geophys. Res., 82:499.
- DUNCAN, C.N. CREUTZBERG, F., GATTINGER, R.L., HARRIS, F.R. and VALLANCE-JONES, A. (1981). "Latitudinal and temporal characteristics of pulsating auroras", Can. J. Phys., 59:1063.
- EATHER, R.H. (1967). "Auroral proton precipitation and hydrogen emissions", Rev. Geophys. Space Phys., 5:207.

- EATHER, R.H. (1968). "Hydrogen emissions in pulsating auroras", Ann. Geophys., 24:525.
- EVANS, J.V. (1975). "Review of F-region dynamics", Rev. Geophys. Space Phys., 13:887.
- FAIRFIELD, D.H. (1970). "The magnetic field of the magnetosphere and tail" in The Polar Ionosphere Magnetospheric Process, ed. G. Skvoli, Gordon and Breach, Sci. Publishers Inc.
- FEJER, J.A. and KAN, J.R. (1969). "A guiding centre Vlasov equation and its application to Alfvén waves", J. Plasma Phys., 3:331.
- FEJER, B.G. and KELLEY, M.C. (1980). "Ionospheric irregularities" Rev. Geophys. Space Sci., 18:401.
- FIELD, E.C. and GREIFINGER, C. (1967). "Geomagnetic fluctuations due to impulse sources with application to high altitude nuclear bursts", J. Geophys. Res., 72:317.
- FRANCIS, W.E. and KARPLUS, R. (1960). "Hydromagnetic waves in the ionosphere", J. Geophys. Res., 65:3593.
- HALDOUPIS, C. and NIELSEN, E. (1983). "Simultaneous geomagnetic and radio auroral observations", J. Atmos. Terr. Phys., 45:543.
- HARTZ, T.R. and BRICE, N.M. (1967). "The general pattern of auroral particle precipitation", Planet. Space Sci., 15:301.
- HASEGAWA, A. and LANZEROTTI, L.J. (1978). "On the orientation of hydromagnetic waves in the magnetosphere", Rev. Geophys. Space Res., 16:263.
- HEACOCK, R.R. (1967a). "Two subtypes of type Pi micropulsations", J. Geophys. Res., 72:399.
- HEACOCK, R.R. (1967b). "Evening micropulsation events with a rising midfrequency characteristic", J. Geophys. Res., 72:3905.
- HEACOCK, R.R. and HUNSUCKER, R.D. (1977a). "A study of concurrent magnetic field and particle precipitation pulsations 0.005 to 0.5 Hz recorded near College, Alaska", J. Atmos. Terr. Phys., 39:487.
- HEACOCK, R.R. (1980). "Simple Pi burst micropulsation events and associated aurora at two sites in Alaska", Planet. Space Sci., 28:907.
- HEACOCK, R.R. and CHAO, J.K. (1980). "Type Pi magnetic field pulsations at very high latitudes, and their relation to plasma convection in the magnetosphere", J. Geophys. Res., 85:1203.
- HEACOCK, R.R. and HUNSUCKER, R.D. (1981). "Type Pi 1-2 magnetic field pulsations", Space Sci. Rev., 28:191.
- HEPPNER, J.P. (1954). "A study of relationships between the aurora borealis and the geomagnetic disturbance caused by electron currents in the ionosphere", Ph.D. thesis. Calif. Inst. of Technology.

- HILLIARD, R.L. and SHEPHERD, E.G. (1968). "Upper Atmospheric temperatures from Doppler line-widths, 4", Planet. Space Sci., 14:383.
- HOFFMAN, R.A. and EVANS, D.S. (1968). "Field aligned electron bursts at high latitudes observed by OGO 4", J. Geophys. Res., 73:6201.
- HORWITZ, J.L., DOUPNIK, J.R. and BANKS, P.M. (1978). "Chatanika radar observations of the latitudinal distributions of auroral zone electric fields, conductivities, and currents", J. Geophys. Res., 83:1463.
- HUGHES, W.J. (1974). "The effect of the atmosphere and ionosphere on long period magnetospheric micropulsations", J. Geophys. Res., 22:1157.
- JACOBS, J.A., KATO, Y., MATSUSHITA, S. and TROITSKAYA, V.A. (1964). "Classification of geomagnetic micropulsations", J. Geophys. Res., 69:180.
- JOHANSEN, O.E. and OMHOLT, A. (1966). "A study of pulsating aurora", Planet. Space Sci., 14:207.
- JOHNSTONE, A.D. (1978). "Pulsating Aurora", Nature, 274:119.
- JONES, R.A. and REES, M.H. (1973). "Time dependent studies of the aurora, I, Ion density and composition", Planet. Space Sci., 21:527.
- KAMIDE, Y.R. and BREKKE, A. (1977). "Altitude of the eastward and westward auroral electrojets", J. Geophys. Res., 82:2851.
- KAMIDE, Y. and ROSTOKER, G. (1977). "The spatial relationships of field aligned currents and auroral electrojets to the distribution of nightside auroras", J. Geophys. Res., 82:5589.
- KAMIDE, Y. and MATSUSHITA, S. (1979). "Simulation studies of ionospheric electric fields and currents in relation to field-aligned currents. 2. Substorms", J. Geophys. Res., 84:4099.
- KAMIDA, Y., RICHMOND, A.D. and MATSUSHITA, S. (1981). "Estimation of ionospheric electric fields, ionospheric currents, and field-aligned currents from ground magnetic records", J. Geophys. Res., 86:801.
- KAMIDE, Y., AHN, B.H., AKASOFU, S.I., BAUMJOHANN, W., FRIIS-CHRISTENSEN, E., KROEHL, H.W., MAURER, H., RICHMOND, A.D., ROSTOKER, G., SPIRO, R.W., WALKER, J.K. and ZAITZEV, A.N. (1982). "Global distribution of ionospheric and field-aligned currents during substorms as determined from six IMS meridian chains of magnetometers : Initial results", J. Geophys. Res., 87:8228.
- KAMIDE, Y., ROBINSON, R.M., AKASOFU, S.-I. and POTEIRA, T.A. (1984). "Aurora and electrojet configuration in the early morning sector", J. Geophys. Res., 89:389.
- KAN, J.R. and HEACOCK, R.R. (1976). "Generation of irregular (Type PiC) pulsations in the plasma sheet during substorms", J. Geophys. Res., 81:2371.

- KAZAK, B.N., ROLDUGIN, V.K and CHERNOUS, S.A. (1972). "Simultaneity of the appearance of geomagnetic and auroral pulsations", Geomag. Aeron., 12:817.
- KENNEL, C.F. and PETSCHKE, H.E. (1966). "Limit on stably trapped particle fluxes", J. Geophys. Res., 71:1.
- KISABETH, J.L. and ROSTOKER, G. (1971). "Development of the polar electrojet during polar magnetic substorms", J. Geophys. Res., 76:6815.
- KLUMPAR, D.M. (1979). "Relationships between auroral particle distributions and magnetic field perturbation associated with field-aligned currents", J. Geophys. Res., 84:6524.
- KVIFTE, G.J. and PETTERSON, H. (1969). "Morphology of the pulsating aurora:", Planet. Space. Sci., 17:1599.
- LANZEROTTI, L.J., MC LENNAN, C.G., and EVANS, C. (1978). Association of ULF magnetic variations and changes in ionospheric conductivity during substorms", J. Geophys. Res., 83:2525.
- LEONINEN, J., KANGAS, J., KUSTOV, A.V., STEPANOV, G.S., USPENSKY, M.V. (1983). "PiC magnetic pulsations and variations of the ionospheric electric field and conductivity", J. Atmos. Terr. Phys., 45:579.
- MAEHLUM, B.N. and O'BRIEN, B.J. (1968). "The mutual effect of precipitated auroral electrons and the auroral electrojet", J. Geophys. Res., 73:1679.
- MAKINO, M. and TAKEDA, M. (1984). "Three-dimensional ionospheric currents and fields generated by the atmospheric global circuit current:", J. Atmos. Terr. Phys., 46:199.
- MATSUSHITA, S. and CAMPBELL, W.H. (1967). Physics of Geomagnetic Phenomena; Vol. 1, Academic Press, New York and London.
- MAYAUD, P.N. (1967). Atlas of Indices K., 1. Text, 2 Figures, IAGA Bulletin #21 International Union of Geodesy and Geophysics.
- MC EWEN, D.J., DUNCAN, C.N. and MONTALBETTI, R. (1981). "Auroral electron energies: Comparisons of in situ measurements with spectroscopically inferred energies", Can. J. Phys., 59:1116.
- MC EWEN, D.J., YEE, E., WHALEN, B.A. and YAU, A.W. (1981). "Electron energy measurements in pulsating aurora", Can. J. Phys., 59:1106.
- MC PHERRON, R.L., PARKS, G.K., CORONITI, F.V. and WARD, S.H. (1968). "Studies of the magnetospheric substorm, 2, Correlated magnetic micropulsations and electron precipitation occurrences", J. Geophys. Res., 73:1697.
- MC PHERRON, R.L. (1970). "Growth phase of magnetospheric substorms", J. Geophys. Res. 75:5592.
- MC PHERRON, R.L. (1980). "Substorm associated micropulsations at synchronous orbit", J. Geomag. Geoelect., 32:57.

- MENDE, S.B., EATHER, R.H., REES, M.H., VONDRAK, R.R. and ROBINSON, R.M. (1984). "Optical mapping of ionospheric conductance", J. Geophys. Res., 89:1755.
- MENG, C.-I., (1978). "Electron precipitations and polar auroras", Space Sci. Rev., 22:223.
- MENG, C.-I., (1984). "Dynamic variation of the auroral oval during intense magnetic storms", J. Geophys. Res., 89:227.
- MILLER, R.E. and ZEITZ, W.M. (1971). "Observations on pulsating auroras", Planet Space Sci., 19:693.
- MOZER, F.S. and LUCHT, P., (1974). "The average auroral zone electric field", J. Geophys. Res., 79:1001.
- NICOLET, M. (1953). "Origin of the emission of the O green line in the airglow", Phys. Rev., 93:633.
- NISHIDA, A. (1964). "Theory of irregular magnetic micropulsations associated with a magnetic bay", J. Geophys. Res., 69:947.
- OGUTI, T. (1976). "Recurrent auroral patterns", J. Geophys. Res., 81:1782.
- OGUTI, T. and WATANABE, T. (1976). "Quasi-periodic poleward propagation of on-off switching aurorae and associated geomagnetic pulsations in the dawn", J. Atmos. Terr. Phys., 38:543.
- OGUTI, T., KOKOBUN, S., HAYASHI, K., TSURUDA, K., MACHIDA, S., KITAMURA, T., SAKA, O. and WATANABE, T. (1981). "Latitudinally propagating on-off switching aurorae and associated geomagnetic pulsations: A case study of an event of February 20, 1980", Can. J. Phys., 59:1131.
- OGUTI, T., MEEK, J.H. and HAYASHI, K. (1984). "Multiple correlation between auroral and magnetic pulsations", J. Geophys. Res., 89:2295.
- OLIVEN, M.N. and GURNETT, D.A. (1968). "Microburst phenomena, 3, An association between microbursts and VLF chorus", J. Geophys. Res., 73:2355.
- OLSON, J.V. and ROSTOKER, G. (1975). "Pi2 pulsations and the auroral electrojet", Planet. Space Sci., 23:1129.
- OLSON, J.V. and ROSTOKER, G. (1977). "Latitudinal variation of the spectral components of auroral zone Pi2", Planet. Space Sci., 25:663.
- OMHOLT, A. (1971). The Optical Aurora., Springer-Verlag, New York.
- PARKS, G.K., CORONITI, F.V., MC PHERRON, R.L. and ANDERSON, K.A. (1968). "Studies of the magnetospheric substorm, 1, Characteristics of modulated energetic electron precipitation occurring during auroral substorms", J. Geophys. Res., 73:1685.
- PARKS, G.K. and WINCKLER, J.R. (1969). "Simultaneous observations of 5- to 15- sec period modulated energetic electron fluxes at the synchronous altitude and the auroral zone", J. Geophys. Res., 74:4003.

- PARTHASARATHY, R. and BERKEY, F.T. (1965). "Auroral zone studies of sudden onset radiowave absorption events using multiple station and multiple frequency data", J. Geophys. Res., 70:89.
- PEMBERTON, E.V. and SHEPHERD, G.G. (1975). "Spatial characteristics of auroral brightness fluctuation spectra", Can. J. Phys., 54:504.
- PETELSKI, E.F., FAHLESON, U. and SHAWHAN, S.D. (1978). "Models for quasi-periodic electric fields and associated electron precipitation in the auroral zone:", J. Geophys. Res., 83:2489.
- PFaff, R.F., KELLY, M.C., FEJER, B.J., KUDEKI, E., CARLSON, C.W., PEDERSEN, A. and HAUSLER, B. (1984). "Electric field and plasma density measurements in the auroral electrojet", J. Geophys. Res., 89:236.
- RAMANATHAN, K.R., BHOMSLE, R.V. and DEKAONKAR, S.S. (1961). "Effect of electron-ion collisions in the F-region of the ionosphere on the absorption of cosmic radio noise at 25Mc/s at Ahmedabad", J. Geophys. Res., 66:2763.
- RANTA, H. and RANTA, A. (1978). "Riometer measurements of ionospheric radio wave absorption", J. Atmos. Terr. Phys., 40:799.
- RATCLIFFE, J.A. (1972). An Introduction to the Ionosphere and Magnetosphere, Cambridge University Press.
- REES, M.H. (1963). "Auroral ionization and excitation by incident energetic electrons", Planet. Space. Sci., 11:1209.
- REES, M.H. and JONES, R.A. (1973). "Time dependent studies of the aurora, 2, Spectroscopic morphology", Planet. Space. Sci., 21:1213.
- REID, J.S. (1967). "Auroral zone cosmic noise absorption pulsations", Nature, 214:1321.
- REID, J.S. and PHILLIPS, J. (1971). "Time lags in the auroral zone ionosphere", Planet Space Sci., 19:1959.
- REID, J.S. (1976). "An ionospheric origin for Pil micropulsations", Planet. Space Sci., 24:705.
- RISHBETH, H. and GARRIOTT, O.K. (1969). Introduction to Ionospheric Physics., pp.130-227, Academic Press, New York.
- ROBERTS, C.S. (1969). "Pitch angle diffusion of electrons in the magnetosphere", Rev. of Geophys., 7:305.
- ROBINSON, R.M. (1984). "Kp dependence of auroral zone field-aligned current intensity", J. Geophys. Res., 89:1743.
- ROBINSON, R.M. and VONDRAK, R.R. (1984). "Measurements of E-region ionization and conductivity produced by solar illumination at high latitudes", J. Geophys. Res., 89:3951.

- ROLDUGIN, V.K. (1967). "Short period pulsations of auroral cosmic noise absorptions", Geomag. Aeron., 7:454.
- ROSTOKER, G. (1972). "Polar magnetic substorms", Rev. Geophys. Space Phys., 10:157.
- ROSTOKER, G. and HRON, M. (1975). "The eastward electrojet in the dawn sector", Planet. Space Sci., 23:1377.
- ROYRVIK, O. and DAVIS, T.N. (1977). "Pulsating aurora : Local and global morphology", J. Geophys. Res., 82:4720.
- SAFLEKOS, N.A. and POTEIRA, T.A. (1980). "The orientation of Birkeland current sheets in the dayside polar region and its relationship to the IMF", J. Geophys. Res., 85:1987.
- SAITO, T. (1961). "Oscillations of the geomagnetic field with the progress of pt-type pulsations", Sci. Rpt. Tohoku Univ. Serial 5 Geophys., 12:105.
- SAITO, T. (1969). "Geomagnetic pulsations", Space Sci. Rev., 10:319.
- SAITO, T., YUMOTO, K. and KOYAMA, Y. (1976). "Magnetic pulsation Pi2 as a sensitive indicator of magnetospheric substorm", Planet. Space Sci., 24:1025.
- SAITO, T. and IIJIMA, T. (1979). "Primary sources of large scale Birkeland currents", Planet. Sci. Rev., 24:347.
- SAKURAI, T. and SAITO, T. (1976). "Magnetic pulsation Pi2 and substorm onset", Planet. Space Sci., 24:573.
- SCOURFIELD, M.W.J. and PARSONS, N.R. (1969). "Auroral pulsations and flaming", Planet. Space Sci., 17:1141.
- SCOURFIELD, M.W.J., CRESSWELL, G.R., PILKINGTON, G.R. and PARSONS, N.R. (1970). "Auroral pulsations - TV image and X-ray correlations", Planet. Space Sci., 18:495.
- SCOURFIELD, M.W.J., KEYS, J.G., NIELSEN, E., GOERTZ, C.K. and COLLIN, H. (1983). "Evidence for the E X B drift of pulsating auroras", J. Geophys. Res., 88:7983.
- SEARS, R.D. and VONDRAK, R.R. (1981). "Optical emission and ionization profiles during an intense pulsating aurora", J. Geophys. Res., 86:6583.
- SENIOR, C., ROBINSON, R.M. and POTEIRA, T.A. (1982). "Relationship between field-aligned currents, diffuse auroral precipitation and the westward auroral electrojet in the early morning sector", J. Geophys. Res., 87:10469.
- SILSBEE, H.C. and VESTINE, E.H. (1942). "Geomagnetic bays, their occurrence frequency and current system", Terr. Magnet. Atmos. Elec., 47:195.
- SMITH, M.J., BRYANT, D.A. and EDWARDS, T. (1980). "Pulsations in auroral electrons and positive ions", J. Atmos. Terr. Phys., 42:167.

- SPIRO, R.W., REIFF, P.H. and MAHER, Jr., L.J. (1982). "Precipitating electron energy flux and auroral zone conductances - An empirical model", J. Geophys. Res., 87:8215.
- SRIVISTAVA, B.N. and MIRZA, I.M. (1968). "Measurements of the electron impact excitation cross-section for  $N_2^+$  first negative bands", Phys. Rev., 176:137.
- SRIVASTAVA, B.N. and MIRZA, I.M. (1969). "Excitation function of the  $N_2^+$  Meinel band by electron impact", Can. J. Phys., 47:475.
- STENBAEK-NIELSEN, H.C. and HALLINAN, T.J. (1979). "Pulsating auroras: Evidence for non-collisional thermalization of precipitating electrons", J. Geophys. Res., 84:3257.
- STENBAEK-NIELSEN, H.C. (1980). "Pulsating aurora: The importance of the ionosphere", Geophys. Res. Lett., 7:353.
- SUGIURA, M. and HEPPNER, J.P. (1965). "The Earth's magnetic field" in Introduction to Space Science., (Ed. W.N. Hess), P.45. Gordon and Breach, New York.
- SWIFT, D.W. and WESCOTT, E.M. (1964). "The effect of small islands on telluric currents", J. Geophys. Res., 69:4149.
- SWIFT, D.W. (1981). "Mechanisms for auroral precipitation: A review", Rev. Geophys. Space Sci., 19:185.
- TEPLEY, L.R., HEACOCK, R.R. and FRASER, B.J. (1965). "Hydromagnetic emissions (Pc1) observed simultaneously in the auroral zone and at low latitudes", J. Geophys. Res., 70:2720.
- TROITSKAYA, V.A. (1961). "Pulsations of the Earth's magnetic field with periods of 1-15s and their connection with phenomena in the high atmosphere", J. Geophys. Res., 66:5.
- TSURUTANI, B.T. and SMITH, E.J. (1974). "Postmidnight chorus: A new substorm phenomenon", J. Geophys. Res., 79:118.
- VASYLIUNAS, V.M. (1975). "Theoretical models of magnetic field line merging (1)". Rev. Geophys. Space Phys., 13:303.
- VESTINE, E.H. and CHAPMAN, S. (1938). "The electric current system of geomagnetic disturbances". Terr. Magnet. Atmos. Elect., 43:351.
- VONDRAK, R.R. and SEARS, R.D. (1978). "Comparison of incoherent scatter radar and photometric measurements of the energy distribution of auroral electrons", J. Geophys. Res., 83:1665.
- WALKER, R.J., ERICKSON, K.N., SWANSON, R.L. and WINCKLER, J.R. (1976). "Substorm-associated particle boundary motion at synchronous orbit". J. Geophys. Res., 81:5541.
- WARD, I.A., LESTER, M. and THOMAS, R.W. (1982). "Pulsing hiss, pulsating aurora, and micropulsations". J. Atmos. Terr. Phys., 44:931.



- WHALEN, B.A., MILLER, J.R. and McDIARMID, I.B. (1971). "Energetic particle measurements in a pulsating aurora". J. Geophys. Res., 76:978.
- WHALEN, B.A. and McDIARMID, I.B. (1973). "Pitch angle diffusion of low energy auroral electrons", J. Geophys. Res., 78:1608.
- WILHELM, K., MUNCH, J.W. and KREMSER, G.(1977). "Fluctuations of the auroral zone current system and geomagnetic pulsations". J. Geophys. Res., 82:2705.
- YAU, A.W., WHALEN, B.A. and McEWEN, D.J. (1981). "Rocket borne measurements of particle pulsation in pulsating aurora". J. Geophys. Res., 86:5673.
- ZMUDA, A.J., MARTIN, J.H. and HEURING, F.T. (1966). "Transverse magnetic disturbance at 1100 km in the auroral regions". J. Geophys. Res., 71: 5033.